

**Novel steroid reductase from *Escherichia coli*: from
identification and characterization towards the
design of a whole-cell biocatalyst**

Inaugural dissertation

for the attainment of the title of doctor
in the Faculty of Mathematics and Natural Sciences
at the Heinrich Heine University Düsseldorf

presented by

Agne Tubeleviciute
from Vilnius

Düsseldorf, June 2014

from the institute for Pharmaceutical and Medicinal Chemistry
at the Heinrich Heine University Düsseldorf

Published by permission of the
Faculty of Mathematics and Natural Sciences at
Heinrich Heine University Düsseldorf

Supervisor: Prof. Dr. Joachim Jose
Co-supervisor: Prof. Dr. Jörg Pietruszka

Date of the oral examination:

TABLE OF CONTENTS

Summary.....	7
Zusammenfassung.....	8
1 Introduction.....	9
1.1 Steroids: structure and biological functions.....	9
1.2 Production of steroid drugs by microbial transformations.....	10
1.3 Microbial reduction of C20 carbonyl of 20-ketosteroids.....	12
1.4 Enzymes catalyzing C20 carbonyl reduction of 20-ketosteroids.....	17
1.4.1 Hydroxysteroid dehydrogenases (HSDs).....	19
1.4.1.1 HSDs with 20-ketosteroid reductase activity in vertebrates.....	19
1.4.1.2 20-HSDs from gut microbiota.....	21
1.4.1.3 Other microbial 20-HSDs.....	22
1.4.2 Miscellaneous enzymes possessing 20-ketosteroid reductase activity.....	23
1.5 Short-chain dehydrogenases/reductases and aldo-keto-reductases.....	24
1.5.1 Short-chain dehydrogenases/reductases (SDRs).....	24
1.5.2 Aldo-keto-reductases (AKRs).....	28
1.6 Examples of applications of 20-ketosteroid reductases in biocatalysis.....	29
1.7 Unidentified 20-ketosteroid reductase in <i>Escherichia coli</i> and a whole-cell biocatalysis.....	29
1.8 Autodisplay.....	31
1.9 Aims of the work.....	35
2 Materials and methods.....	36
2.1 Materials.....	36
2.1.1 Instruments.....	36
2.1.2 Software.....	37
2.1.3 Chemicals and Reagents.....	37
2.1.4 Kits.....	41

2.1.5 Antibodies.....	41
2.1.6 Enzymes and proteins.....	41
2.1.7 Oligonucleotides.....	42
2.1.8 Plasmids.....	43
2.1.9 Bacterial strains.....	44
2.1.10 Media.....	44
2.1.11 Buffers and other solutions.....	45
2.1.12 Protein chromatography media.....	48
2.1.13 Other materials.....	48
2.2 Methods.....	50
2.2.1 Partial purification of <i>E. coli</i> steroid reductase.....	50
2.2.2 Identification of proteins by mass spectrometry.....	51
2.2.3 Enzyme and protein assays.....	52
2.2.4 Analytical HPLC.....	52
2.2.5 Cloning and expression of <i>ydbC</i> gene.....	53
2.2.6 Cloning and expression of <i>kduD</i> , <i>hdhA</i> and <i>uxuB</i> genes.....	54
2.2.7 Whole cell biotransformation assay.....	54
2.2.8 Evaluation of an effect of 11-DOC on the expression level of KduD in <i>E. coli</i>	55
2.2.9 Cloning, expression and affinity purification of KduD.....	55
2.2.10 Determination of pH and temperature optimum.....	55
2.2.11 Determination of substrate specificity.....	56
2.2.12 Evaluation of effect of salts, reducing/oxidizing and denaturing agents.....	57
2.2.13 Kinetic assays.....	57
2.2.14 Construction of pAT002, pAT004, pMATE-AT001 and pMATE-AT002 plasmids	58
2.2.15 Whole-cell activity assays with <i>E. coli</i> cells expressing FP, FPΔβ1, FP1 and FP2	59
2.2.16 Preparation of membrane protein fraction.....	60

2.2.17	Protease assays	61
2.2.17.1	Proteinase K assay	61
2.2.17.2	IgA1 protease assay	61
2.2.18	Immunoblot analysis.....	62
2.2.19	LC-MS analysis of steroid conversions.....	63
2.2.20	DNA sequence analysis	63
2.2.21	Other basic methods	63
3	Results.....	68
3.1	Identification of 11-deoxycorticosterone reductase in <i>Escherichia coli</i>	68
3.1.1	A bioinformatics approach	68
3.1.1.1	Investigation of steroid reductase activity of enzyme encoded by <i>ydbC</i> gene	72
3.1.2	Partial purification of enzyme from <i>E. coli</i> DH5 α	73
3.1.2.1	Ammonium sulfate precipitation step.....	73
3.1.2.2	Column chromatography steps	74
3.1.3	Identification of NADH-dependent oxidoreductases in partially purified enzyme sample.....	81
3.1.3.1	Investigation of 11-DOC reductase activity of NADH-dependent oxidoreductases.....	82
3.2	Characterization of KduD oxidoreductase	84
3.2.1	Purification of KduD and optimization of reaction conditions	84
3.2.2	Determination of the substrate spectrum.....	86
3.2.2.1	Reduction of doxorubicin and doxorubicinone by KduD.....	90
3.2.3	The pH and temperature optimum.....	94
3.2.4	Effect of metal ions, salts and reducing agents	95
3.2.5	Kinetic analysis.....	98
3.3	Investigation of the effect of 11-DOC on the expression level of KduD in <i>Escherichia coli</i>	100
3.4	Autodisplay based on AIDA-I autotransporter	101

3.4.1 Design and expression of fusion protein FP	101
3.4.2 Investigation of the enzyme activity of FP	105
3.4.3 Design and expression of fusion protein FP $\Delta\beta$ 1	107
3.4.4 Investigation of the enzyme activity of FP $\Delta\beta$ 1	109
3.4.5 Digestion of FP with IgA1 protease	110
3.5 Autodisplay based on EhaA autotransporter	114
3.5.1 Design and expression of fusion proteins FP1 and FP2	114
3.5.2 Investigation of the enzyme activity of FP1 and FP2.....	118
4 Discussion	122
4.1 Identification of steroid C20 reductase in <i>Escherichia coli</i>	122
4.2 Novel substrates of KduD	123
4.3 Biological function of KduD in <i>E. coli</i>	124
4.4 KduD is a short-chain dehydrogenase/reductase with a broad substrate spectrum.....	126
4.5 Control of expression of <i>kduD</i> gene in <i>E. coli</i>	128
4.6 Biochemical properties of KduD from <i>E. coli</i>	129
4.7 Design of the KduD whole-cell biocatalyst using Autodisplay	131
4.7.1 Expression	131
4.7.2 Activity	132
5 Conclusions.....	136
6 References.....	137
7 Supplemental material	155
7.1 Abbreviations	155
7.2 Plasmid maps.....	157
7.3 Supplementary tables	159
8 Scientific output.....	161
Acknowledgements.....	163

Summary

In this study a novel steroid C20 reductase which catalyzes the regioselective reduction of 11-deoxycorticosterone (11-DOC) into valuable bioactive 20-hydroxysteroid, 4-pregnen-20,21-diol-3-one, was identified in *Escherichia coli* by protein purification and mass spectrometry. It was demonstrated that a NADH-dependent enzyme encoded by *kduD* gene and previously described as 2-dehydro-3-deoxy-D-gluconate 5-dehydrogenase (KduD), catalyzes a regioselective reduction of 11-DOC. It was found that 11-DOC is not involved in the regulation of expression of *kduD* gene *in vivo*.

A 6xHis-tagged version of KduD was purified to homogeneity and characterized. It was found to reduce several 20-ketosteroid substrates (11-DOC, 11-deoxycortisol, cortisone, cortisol, corticosterone, 21-hydroxypregnenolone) and the anthracycline derivative doxorubicinone. In addition, KduD was found to accept several polyols as substrates including carbohydrate derivatives, D-gluconate and 5-keto-D-gluconate, as well as 1,2-propanediol. KduD oxidoreductase showed higher affinity for steroid substrates than for carbohydrate derivatives *in vitro*. The optimal pH for KduD catalyzed reduction of 11-DOC was found to be pH 7.0, whereas it was 9.5 for oxidation of D-gluconate. The optimal temperature for reduction of 11-DOC was found to be 37 °C. It was shown that KduD does not require metal cofactors for activity. Reducing agents (1 mM 2-ME and 10 mM DTT), fatty acids (1 mM lauric acid and 0.1 mM myristic acid), 10 % ethanol and 0.5 M sodium chloride were found to inhibit the activity of KduD.

KduD was identified as a ‘classical’ short-chain dehydrogenase/reductase (SDR) based on conserved protein sequence motifs. The native form of KduD was proposed to be a homotetramer as indicated by the gel filtration chromatography.

The Autodisplay technology turned out to be unsuitable for the design of a KduD whole-cell biocatalyst in *E. coli* host. The expression of KduD fused to the translocator unit of either AIDA-I or EhaA autotransporter proteins yielded an inactive KduD whole-cell biocatalyst.

Zusammenfassung

In dieser Arbeit wurde mittels Proteinaufreinigung und Massenspektrometrie eine neue Steroid C20 Reduktase in *Escherichia coli* identifiziert, die eine regioselektive, NADH-abhängige Reduktion von 11-Deoxycorticosterone (11-DOC) zum bioaktiven 20-Hydroxysteroid, 4-Pregnen-20,21-diol-3-one, katalysiert. Es wurde gezeigt, dass dieses Enzym durch das *kduD* Gen kodiert wird und früher als 2-dehydro-3-deoxy-D-Gluconat 5-Dehydrogenase (KduD) bekannt war. Es wurde festgestellt, dass die *in vivo* Expression des *kduD* Gens nicht durch 11-DOC beeinflusst wird.

Die 6xHis-markierte KduD Oxidoreduktase wurde bis zur Homogenität aufgereinigt und charakterisiert. Sechs 20-Ketosteroid Substrate (11-DOC, 11-Deoxycortisol, Cortison, Cortisol, Corticosteron, 21-Hydroxypregnenolon) und ein Anthracyclin, Doxorubicinon, wurden von diesem Enzym reduziert. Außerdem wurden drei Polyole, darunter die zwei Zucker D-Gluconat und 5-Keto-D-Gluconat, sowie 1,2-Propandiol als neue Substrate der KduD identifiziert. Die KduD Oxidoreduktase zeigte eine höhere Affinität zu Steroiden als zu Kohlenhydratderivaten *in vitro*. Der optimale pH-Wert für die KduD katalysierte Reduktion von 11-DOC beträgt 7.0, wohingegen für die Oxidation von D-Gluconat ein optimaler pH-Wert von 9.5 bestimmt wurde. Als optimale Temperatur für die Reduktion von 11-DOC wurde 37 °C festgestellt. Es wurde nachgewiesen, dass für die KduD-Aktivität keine Metall-Cofaktoren erforderlich sind. Durch hohe Konzentrationen an Reduktionsmitteln (1 mM 2-ME und 10 mM DTT), Fettsäuren (1 mM Laurinsäure und 0.1 mM Myristinsäure), Ethanol (10 %) oder Natriumchlorid (0.5 M) wurde die Aktivität von KduD gehemmt.

Die KduD Oxidoreduktase wurde als klassische „short-chain“ Dehydrogenase/Reduktase (SDR) auf der Grundlage der konservierten Protein-Sequenzmotive erkannt. Entsprechend den Ergebnissen der Gelfiltration scheint das Enzym als Homotetramer vorzuliegen.

Die Autodisplay-Technologie erwies sich für die Konstruktion eines funktionellen KduD *E. coli* Ganzzellbiokatalysators als ungeeignet. Wenn die KduD Oxidoreduktase als Fusionprotein mit Hilfe der Translokationseinheit von entweder AIDA-I oder EhaA Autotransporter Protein an der Oberfläche von *E. coli* exprimiert wurde, war keine Enzymaktivität nachweisbar.

1 Introduction

1.1 Steroids: structure and biological functions

Steroids constitute a wide variety of organic compounds that represent a separate class of lipids. Typical structure of a steroid compound contains the gonane nucleus of four fused cycloalkane rings (**Fig. 1.1a**). Steroid derivatives vary by the oxidation state of the rings, by the functional groups attached to the four-ring core, and by the configuration of bonds.

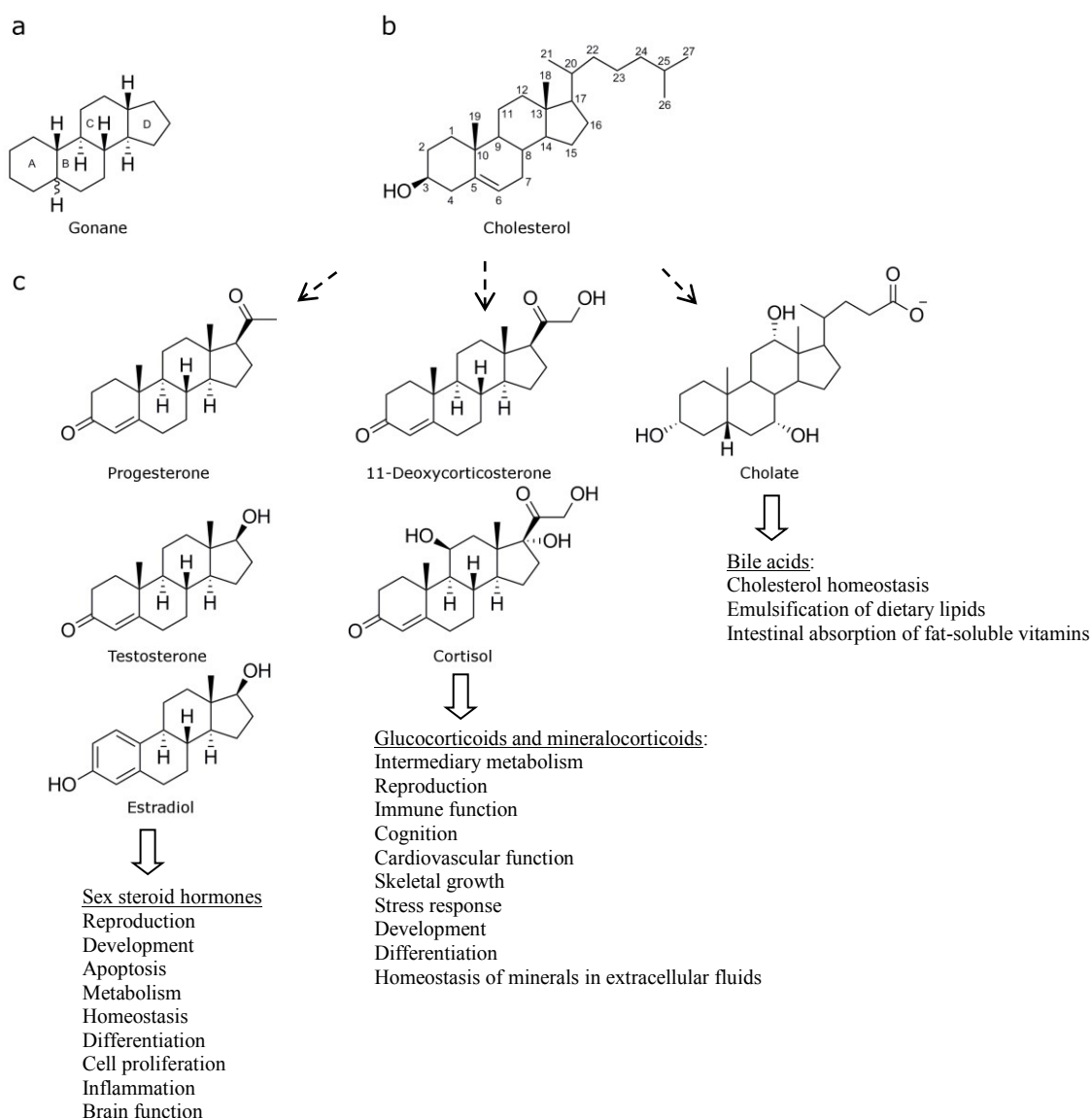


Fig. 1.1 Structure of gonane (**a**), cholesterol (**b**) and examples of several bioactive steroid derivatives (**c**) synthesized from cholesterol in humans. The diverse physiological roles of steroids are summarized according to the reviews (Staels and Fonseca 2009, Edwards 2005, Taves et al. 2011).

Steroid compounds are widespread in nature and have important physiological activities. Steroid derivatives are found in plants, vertebrates, insects and fungi. In animals, all natural

steroids are synthesized from a common precursor, cholesterol (**Fig. 1.1b**). Cholesterol (and its analog phytosterol in plants and ergosterol in fungi) is an important component of eukaryotic cell membrane, and functions as a modulator of membrane flexibility and fluidity. Steroids derived from cholesterol, such as steroid hormones, sex hormones, bile acids, vitamin D and neurosteroids, regulate vital physiological processes in animals, including reproduction, cell signaling, growth and energy homeostasis (**Fig. 1.1c**).

In contrast to eukaryotes, steroids are absent in most prokaryotes. Despite the inability to synthesize eukaryotic-type steroid compounds, prokaryotic microorganisms have enzymes that modify and/or completely degrade these exogenous substances (Ismail and Chiang 2011). The metabolism of eukaryotic steroids is beneficial for prokaryotic microorganisms in several aspects: (i) total degradation of steroid hormones and bile acids provides a carbon source for the growth of certain bacteria (Leu et al. 2011, Horinouchi et al. 2003, Merino et al. 2013); (ii) by transformation of conjugated bile acids bacteria residing in animal intestines acquire several substrates, such as glycine and taurine (Begley et al. 2005); (iii) bacteria can communicate with its eukaryotic host through steroid signaling (García-Gómez et al. 2013).

1.2 Production of steroid drugs by microbial transformations

The use of steroids in medicine has increased dramatically in the second half of the 20th century after the announcement of pharmacological effects of two endogenous steroids, cortisol and progesterone (Fernandes et al. 2003, Hogg 1992). As of 2009 about 300 approved steroid drugs were known and the numbers are expected to continue growing (Donova and Egorova 2012). Steroid pharmaceuticals constitute the second largest group of drugs next to antibiotics (Donova and Egorova 2012). Steroid-based drugs have a broad range of therapeutic purposes, such as anti-inflammatory, anti-microbial, anti-viral, anti-fungal, immunosuppressive, progestational, anabolic, diuretic and contraceptive agents. They have also been administrated for the treatment of several forms of breast and prostate cancer and osteoporosis, in the prevention of coronary heart disease, and prevention and treatment of infection by human immunodeficiency virus (HIV) (Fernandes et al. 2003, Donova and Egorova 2012).

The significant breakthrough in the synthesis of steroids was achieved in 1952, when Peterson and Murray discovered that a fungus *Rhizopus arrhizus* can perform the 11 α -hydroxylation of progesterone, thereby providing a new and cheaper alternative to the challenging multistage chemical synthesis of valuable corticosteroids (Peterson et al. 1952,

Fernandes et al. 2003). Since then, microbial steroid transformations are widely used in the industrial-scale preparation of pharmaceutical steroids (Sedlacek and Smith 1988) as well as a tool for the generation of novel steroid derivatives and potential drug candidates (Donova and Egorova 2012).

Microbial steroid conversions are performed in mild pH, temperature and pressure conditions; they are more ecologically friendly as compared to chemical synthesis. Most importantly, enzymes in microorganisms catalyze reactions with high chemo-, regio- and stereoselectivity, and allow selective one-step functionalization of unactivated C-H bonds of complex molecules, which is hard to achieve by means of chemical catalysis (Godula 2006). In general, in industrial steroid preparation processes whole-cell biocatalysts are preferred to purified enzymes due to high costs associated with isolation, purification and stabilization of enzymes (Donova 2007).

The starting materials for the microbial production of steroid precursors are natural sapogenins and phytosterols from plants as well as cholesterol obtained from animals. Both microbial and chemical conversion steps are combined in transformation of the starting material to the end steroid products (Fernandes et al. 2003).

A great variety of microorganisms is used for the transformation of steroid compounds. Although bacterial and fungal systems are the most prominent ones (Donova 2007, Donova and Egorova 2012), steroid conversions with microalgae (Faramarzi et al. 2008, Abul-Hajj and Qian 1986) and plant cell cultures (Yagen et al. 1978, Shah et al. 2013) were also described.

Microorganisms are capable of catalyzing a wide spectrum of reactions on steroid substrates including hydroxylation, reduction of carbonyl-group, side-chain degradation, isomerization, hydroxyl group oxidation, double-bond introduction, double-bond reduction, bond cleavage and hydrolysis as illustrated by the selected examples in **Fig. 1.2**.

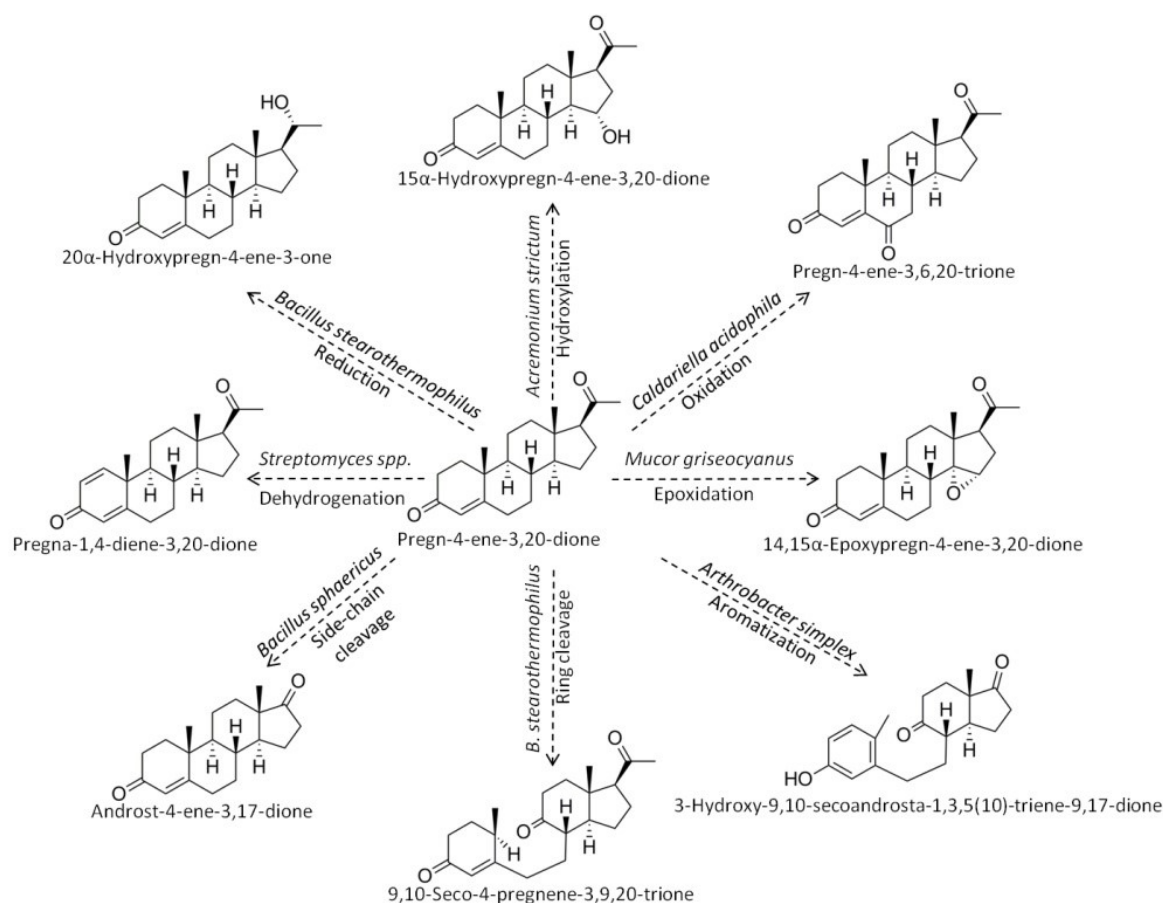


Fig. 1.2 Selected examples of microbial transformations of progesterone (pregn-4-ene-3,20-dione). Several common reactions, including reduction (Al-Awadi et al. 2001), oxidation (De Rosa et al. 1981), hydroxylation (Famarzi et al. 2003), epoxidation (Templeton et al. 1987), dehydrogenation (Atta and Zohri 1995), side-chain cleavage (Wadhwa and Smith 2000), ring cleavage (Al-Awadi et al. 2001) and aromatization (Mahato et al. 1988) of progesterone catalyzed by diverse microorganisms are illustrated.

1.3 Microbial reduction of C20 carbonyl of 20-ketosteroids

Hydroxysteroids have different pharmacological properties in comparison to their ketosteroid counterparts. Various 20-hydroxysteroids show potential for pharmaceutical applications as inhibitors of steroid hormones metabolizing enzymes such as estrone sulfatase, 17β -hydroxysteroid dehydrogenase, 20-ketosteroid reductases (aldo-keto reductases (AKR) 1C1 and 1C3), and 5α -reductase II, for the treatment of breast cancer, endometriosis and prostate diseases in humans (Chetrite et al. 2004, Hannemann et al. 2007, Beranič et al. 2011).

One way to produce valuable bioactive 20-hydroxysteroids is the reduction of the more readily available 20-ketosteroids. The reduction of 20-ketosteroid compounds should be performed in a highly chemo-, regio- and stereo-selective manner because the target

compounds are complex and contain different functional groups on the steroid ring system and more than one prochiral carbonyl group.

Reduction of ketosteroids by chemical approaches is well known from the past. Classical reducing catalysts such as sodium borohydride and lithium aluminium hydride were used for this purpose (Norymberski and Woods 1955, Poos 1955, Caspi 1956, Han and Monder 1982, Han and Monder 1983, Stastná et al. 2010). Chemical reduction of some steroids, however, is a rather complicated and time-consuming process, which requires multiple steps of protection and deblocking of functional groups in order to achieve regioselectivity (Poos 1955, Caspi 1956). In addition, chemical methods often suffer from low stereoselectivity (Poos 1955, Han and Monder 1983, Göndös et al. 1989, Stastná et al. 2010), poor yield (Poos 1955, Göndös and Orr 1982) and relatively harsh reaction conditions.

Reduction of ketosteroids with microorganisms emerged as an alternative and promising technique that overcomes the major limitations of chemical catalysis. Diverse bacteria (members of phylum *Proteobacteria*, *Actinobacteria*, *Cyanobacteria* and *Firmicutes*), fungi and algae were found to catalyze the reduction of C20 keto group of a great variety of pregnane derivatives (C21 steroids) (**Table 1.1**). Microbial cells catalyze reduction of 20-ketosteroids in a stereoselective manner, and thus, produce either 20 α or 20 β hydroxysteroid derivatives. It should be noted here that in series of pregnanes the designation of stereochemistry at C20 position using 20 α /20 β -nomenclature is widely used and continued due to long tradition, however, the *R/S* system is also convenient, nevertheless, used much rarely for C21 steroids (IUPAC commission on the nomenclature of organic chemistry, 1969).

Table 1.1 Examples of microbial transformations of steroids involving C20 carbonyl reduction step

Substrate	Microorganism	Product	Reference	
11 β , 17 α ,21-trihydroxypregn-4-ene-3,20-dione	<i>Acremonium strictum</i> PTCC 5282	11 β ,17 α ,20 β ,21-tetrahydroxypregn-4-en-3-one	(Famararzi et al. 2002)	
	<i>Acremonium strictum</i> PTCC 5282	21-acetoxy-11 β ,17 α ,20-trihydroxypregn-4-en-3-one	(Famararzi et al. 2002)	
	<i>Streptomyces roseochromogenes</i>	11 β ,17 α ,20,21-tetrahydroxypregn-4-en-3-one	(Restaino et al. 2014)	
	<i>Nostoc muscorum</i> PTCC 1636	11 β ,17 α ,20 β ,21-tetrahydroxypregn-4-en-3-one	(Yazdi 2004)	
	<i>Clostridium scindens</i>	11 β ,17 α ,20 α ,21-tetrahydroxypregn-4-en-3-one	(Winter et al. 1984)	
	<i>Cunninghamella blakesleeana</i>	11 β ,17 α ,20,21-tetrahydroxypregn-4-en-3-one	(Garcia-Rodriguez et al. 1978)	
	<i>Cuvularia lunata</i>	11 β ,17 α ,20,21-tetrahydroxypregn-4-en-3-one	(Garcia-Rodriguez et al. 1978)	
	<i>Arthrobacter globiformis</i> 193	11 β ,17 α ,20 β ,21-tetrahydroxypregn-4-en-3-one	(Arinbasarova et al. 1985)	
	<i>Arthrobacter globiformis</i> 193	11 β ,17 α ,20 β ,21-tetrahydroxypregna-1,4-dien-3-one	(Arinbasarova et al. 1985)	
	<i>Eubacterium desmolans</i>	11 β ,17 α ,20 β ,21-tetrahydroxypregn-4-en-3-one	(Bokkenheuser et al. 1986)	
	<i>Clostridium cadavaris</i>	11 β ,17 α ,20 β ,21-tetrahydroxypregn-4-en-3-one	(Bokkenheuser et al. 1986)	
	<i>Bifidobacterium adolescentis</i>	11 β ,17 α ,20,21-tetrahydroxypregn-4-ene-3-one	(Winter et al. 1982)	
	11 β ,17 α -dihydroxypregn-4-ene-3,20-dione	<i>Bifidobacterium adolescentis</i>	11 β ,17 α ,20-trihydroxypregn-4-en-3-one	(Winter et al. 1982)
	11 β ,21-dihydroxypreg-4-ene-3,20-dione 17 α ,21-dihydroxypregn-4-ene-3,11,20-trione	<i>Clostridium scindens</i>	11 β ,20 α ,21-trihydroxypregn-4-en-3-one	(Winter et al. 1984)
<i>Cunninghamella blakesleeana</i>		17 α ,20,21-tryhydroxypregn-4-ene-3,11-dione	(Garcia-Rodriguez et al. 1978)	
<i>Cuvularia lunata</i>		17 α ,20,21-tryhydroxypregn-4-ene-3,11-dione	(Garcia-Rodriguez et al. 1978)	
<i>Clostridium scindens</i>		17 α ,20 α ,21-trihydroxypregn-4-ene-3,11-dione	(Winter et al. 1984)	
17 α ,21-dihydroxypregn-4-ene-3,20-dione	<i>Fusarium oxysporum</i>	17 α ,20,21-trihydroxypregn-4-ene-3,11-dione	(Wilson et al. 1999)	
	<i>Clostridium scindens</i>	17 α ,20 α ,21-trihydroxypregn-4-en-3-one	(Winter et al. 1984)	
	<i>Arthrobacter simplex</i>	pregna-1,4-dien-3-one-17,20 β ,21-triol	(Mahato et al. 1988)	
17 α ,21-dihydroxypregna-1,4-diene-3,11,20-trione	<i>Fusarium oxysporum</i>	17 α ,20,21-trihydroxypregna-1,4-diene-3,11-dione	(Wilson et al. 1999)	

Substrate	Microorganism	Product	Reference
17 α ,21-dihydroxypregna-1,4-diene-3,11,20-trione	<i>Streptomyces roseochromogenes</i> TS79	17 α ,20 β ,21-trihydroxypregna-1,4-diene-3,11-dione	(Zhang et al. 2011)
17 α -hydroxypregn-4-ene-3,11,20-trione	<i>Clostridium scindens</i>	17 α ,20 α -dihydroxypregn-4-ene-3,11-dione	(Winter et al. 1984)
17 α -hydroxypregn-4-ene-3,20-dione	<i>Mucor piriformis</i>	17 α ,20 α -dihydroxypregn-4-en-3-one	(Madyastha 1994)
	<i>Mucor piriformis</i>	6 β ,17 α ,20 α -trihydroxypregn-4-en-3-one	(Madyastha 1994)
	<i>Mucor piriformis</i>	11 α ,17 α ,20 α -trihydroxypregn-4-en-3-one	(Madyastha 1994)
	<i>Nocardia DSM 43298</i>	9,10-seco-3,17 α ,20-trihydroxy-pregna-1,3,5(10)-trien-9-one	(Choudhry et al. 1993)
	<i>Clostridium scindens</i>	17 α ,20 α -dihydroxypregn-4-en-3-one	(Winter et al. 1984)
21-hydroxypregn-4-ene-3,11,20-trione	<i>Clostridium scindens</i>	20 α ,21-dihydroxypregn-4-ene-3,11-dione	(Winter et al. 1984)
21-hydroxypregn-4-ene-3,20-dione	<i>Clostridium scindens</i>	20 α ,21-dihydroxypregn-4-en-3-one	(Winter et al. 1984)
	<i>Bifidobacterium adolescentis</i>	20,21-dihydroxypregn-4-en-3-one	(Winter et al. 1982)
	<i>Escherichia coli</i> E132	20,21-dihydroxypregn-4-en-3-one	(Hannemann et al. 2007)
3 α , 21-dihydroxy-5 β -pregn-20-one	<i>Bifidobacterium adolescentis</i>	5 β -pregnane-3 α ,20,21-triol	(Winter et al. 1982)
3 α ,11 β ,17 α ,21-tetrahydroxy-5 β -pregnan-20-one	<i>Clostridium scindens</i>	5 β -pregnane-3 α ,11 β ,17 α ,20 α ,21-pentol	(Winter et al. 1984)
	<i>Bifidobacterium adolescentis</i>	5 β -pregnane-3 α ,11 β ,17 α ,20,21-pentol	(Winter et al. 1982)
3 α ,11 β ,17 α -trihydroxy-5 β -pregnan-20-one	<i>Bifidobacterium adolescentis</i>	5 β -pregnane-3 α ,11 β ,17 α ,20-tetrol	(Winter et al. 1982)
3 β -acetoxypregn-5-en-20-one	<i>Streptomyces albus</i>	20 α -hydroxypregn-4-en-3-one	(Mukherjee and Mahato 1984)
Pregn-4-ene-3,20-dione	<i>Bacillus stearothermophilus</i>	20 α -hydroxypregn-4-en-3-one	(Al-Awadi et al. 2001)
	<i>Bacillus stearothermophilus</i>	6 α ,20 α -dihydroxyprogesterone	(Al-Awadi et al. 2002)
	<i>Bacillus stearothermophilus</i>	6 β ,20 α -dihydroxyprogesterone	(Al-Awadi et al. 2002)
	<i>Bifidobacterium adolescentis</i>	20-hydroxypregn-4-en-3-one	(Winter et al. 1982)
	<i>Cyanidium caldarium</i>	20 α -hydroxypregn-4-en-3-one	(Pollio et al. 1994)
	<i>Galdieria sulphuraria</i>	20 α -hydroxypregn-4-en-3-one	(Pollio et al. 1994)
	<i>Cyanidioschyzon merolae</i>	20 α -hydroxypregn-4-en-3-one	(Pollio et al. 1994)

Substrate	Microorganism	Product	Reference
Pregn-4-ene-3,20-dione	<i>Schizosaccharomyces pombe</i>	20 α -hydroxypregn-4-en-3-one	(Pajic et al. 1999)
Pregna-4,9(11)-diene-17 α ,21-diol-3,20-dione-17,21-diacetate	<i>Caldariella acidophila</i>	20 α -hydroxypregn-4-en-3-one	(De Rosa et al. 1981)
	<i>Nocardioides simplex</i> VKM Ac-2033D	Pregna-1,4,9(11)-triene-17 α ,20 β ,21-triol-3-one	(Fokina et al. 2003)
Pregna-4,9(11)-diene-17 α ,21-diol-3,20-dione-21-acetate	<i>Nocardioides simplex</i> VKM Ac-2033D	Pregna-1,4,9(11)-triene-17 α ,20 β ,21-triol-3-one	(Fokina et al. 2003)

The reduction of the C20 carbonyl group often accompanies other reactions of steroid transformation by microorganisms. For example, 20 α -reduction of pregnanes was observed along with monohydroxylation at C6 by *Bacillus spp.* (Mahato and Banerjee 1986, Al-Awadi et al. 2002) and monohydroxylation at C6 as well as dihydroxylation at C6 and C11 by *Mucor piriformis* (Madyastha 1994). The reduction of C20 carbonyl group of pregnane derivative was accompanied by 1(2)-dehydrogenation by *Arthrobacter spp.* (Arinbasarova et al. 1985, Mahato et al. 1988), and deacetylation as well as 1(2)-dehydrogenation by *Nocardioides simplex* (Fokina et al. 2003).

Due to the presence of multiple enzymes capable of transforming an exogenous steroid substrate, a mixture of different steroid products is often obtained by whole-cell microbial transformation. Thus, optimization of the whole-cell transformation process is often required when the production of a single steroid metabolite in high yields is desired. Identification and characterization of the enzymes that catalyze steroid transformation reactions in microorganisms can help to achieve this goal. The overexpression of an enzyme that catalyzes a desired reaction and/or knock-out of genes coding for enzymes catalyzing undesired side-reactions can increase the yield of the preferred steroid product.

1.4 Enzymes catalyzing C20 carbonyl reduction of 20-ketosteroids

The terms “20-ketosteroid reductase” or “20-oxosteroid reductase” are often used in the scientific literature to describe an enzyme’s property to catalyze reduction of C20 carbonyl group of steroid molecule into corresponding hydroxyl group. This activity was reported for diverse NAD(P)H-dependent alcohol oxidoreductases (EC 1.1.1.X) (**Table 1.2**). Based on the stereoselectivity of the catalyzed reaction, 20-ketosteroid reductases can be organized into two groups: oxidoreductases that upon reduction of the prochiral C20 carbonyl group produce 20 α -hydroxysteroid and oxidoreductases that produce 20 β -hydroxysteroid. In case the enzyme is capable of catalyzing the corresponding reverse oxidation reaction, it can be named as 20 α -hydroxysteroid dehydrogenase or 20 β -hydroxysteroid dehydrogenase, respectively. Based on the origin of the steroid substrates 20-ketosteroid reductases can be organized into two groups: enzymes that convert endogenous steroids (synthesized by the organism producing the enzyme) and enzymes that convert exogenous steroids (not synthesized by the organism producing the enzyme). Diverse 20-ketosteroid reductases from mammals and lower vertebrates,

such as fishes that synthesize 20-ketosteroids *in vivo*, belong to the first group, whereas the majority of microbial 20-ketosteroid reductases are in the second group. In addition, enzymes with 20-ketosteroid reductase activity can be further classified into substrate-specific and rather substrate-promiscuous enzymes. Most 20-ketosteroid reductases described to date are substrate promiscuous enzymes, which catalyze reduction of the broad range of steroids or convert, in addition to steroids, other substrates such as prostaglandins, carbohydrates, xenobiotics and diverse carbonyl compounds (Maser 1995).

Table 1.2 Selected examples of enzymes that were shown to possess 20-ketosteroid reductase activity

Enzyme name	Organism	Enzyme class*	Reference
20 β -HSD type 2	<i>Danio rerio</i>	(EC=1.1.1.53)	(Tokarz et al. 2012)
Ovarian carbonyl reductase-like 20 β -HSD	<i>Clarias gariepinus</i> <i>Plecoglossus altivelis</i>	(EC=1.1.1.53) Unclassified	(Sreenivasulu and Senthilkumaran 2009) (Tanaka et al. 2002)
Testicular 20 β -HSD	<i>Sus scrofa</i>	EC=1.1.1.53	(Tanaka et al. 1992)
3 α ,20 β -HSD	<i>Streptomyces hydrogenans</i>	EC=1.1.1.53	(Allner and Eggstein 1976)
20-HSD	<i>Gallus gallus</i>	Unclassified	(Bryndova et al. 2006)
Ovarian 20 α -HSD	<i>Rattus norvegicus</i>	EC=1.1.1.149	(Ma and Penning 1999, Mao et al. 1997)
3 β ,20 α -HSD from fetal blood	<i>Ovis aries</i>	(EC=1.1.1.210)	(Chen et al. 1987)
20 α -HSD	<i>Tetrahymena pyriformis</i> <i>Clostridium scindens</i> <i>Streptomyces hydrogenans</i>	EC=1.1.1.149 (EC=1.1.1.149) Unclassified	(Inazu et al. 1994) (Krafft and Hylemon 1989, Ridlon et al. 2013) (Rimsay et al. 1988)
Carbonyl reductase	<i>Cricetulus griseus</i>	EC=1.1.1.184	(Terada et al. 2001)
Testicular aldehyde reductase (20 α -HSD)	<i>Bos taurus</i>	EC=1.1.1.21	(Warren et al. 1993)
Placental estradiol 17 β -dehydrogenase	<i>Homo sapiens</i>	(EC=1.1.1.62)	(Strickler et al. 1981)
Ovarian prostaglandin-E ₂ 9-reductase	<i>Oryctolagus cuniculus</i>	(EC=1.1.1.189)	(Wintergalen et al. 1995)
Liver indanol dehydrogenase	<i>Macaca fuscata</i>	EC=1.1.1.112	(Hara et al. 1989)

*The EC numbers that were not mentioned in the original references were retrieved from BRENDA, UNIPROT or associated databases and are depicted in brackets.

1.4.1 Hydroxysteroid dehydrogenases (HSDs)

HSDs are a group of enzymes widely involved in conversions of steroids. These are NADP(H)-dependent oxidoreductases that catalyze the reversible oxidation of secondary alcohols to ketones on the steroid nucleus and side chain in a regio- and stereoselective manner (Maser 1995). In mammals HSDs can be specific for carbonyl/hydroxyl groups at C3, C11, C17 or C20 position of steroid hormones of androgen (C19 carbons), progestogen (C21 carbons) and estrogen (C18 carbons) series (Penning 2003). HSDs play a pivotal role in interconversion of potent steroid hormone (capable to bind its receptor) into its cognate inactive metabolite (incapable to bind a specific receptor), or vice-versa, thus functioning as molecular switches that turn the steroid hormone receptor occupancy 'on' or 'off' (Penning 2003). In addition, bacteria express multiple HSDs which catalyze reversible reduction of carbonyl groups at C3, C7 and C12 position of bile acids in the intestinal tract of humans (Prabha and Ohri 2006, Ridlon et al. 2006), and thus contribute to the formation of diverse physiologically active derivatives of bile acids.

1.4.1.1 HSDs with 20-ketosteroid reductase activity in vertebrates

20 α -HSD (EC=1.1.1.149) catalyzes the reversible reduction of progesterone into 20 α -hydroxyprogesterone in an NAD(P)H-dependent manner. Initially this enzyme was purified and characterized from rat ovaries (Wiest and Wilcox 1961, Noda et al. 1991, Ma and Penning 1999, Miura et al. 1994) and later was described in other mammals, including human (Zhang et al. 2000), rabbit (Lacy et al. 1993), bovine (Naidansuren et al. 2011), goat (Jayasekara et al. 2004) and pig (Sato et al. 1972). The rat ovarian 20 α -HSD is involved in the control of progesterone homeostasis during the pregnancy. By converting progesterone into its inactive 20 α -hydroxymetabolite this enzyme was proposed to play a key role in the termination of pregnancy and initiation of labor in rats (Penning 1997). Although it is believed that metabolism of progesterone is a key biological function of this enzyme in mammals, in addition to progesterone, 20 α -HSDs show high affinity towards other endogenous and exogenous substrates. The enzyme from rat ovaries was observed to convert also 17 α -hydroxyprogesterone and non-steroidal substrates, such as 9,10-phenanthrenequinone and 4-nitrobenzaldehyde (Ma and Penning 1999). Similarly, 20 α -HSD from rabbit accepts a broad range of substrates. It reduces 3-ketosteroids, 20-ketosteroids, 17-ketosteroids and non-steroidal carbonyl compounds, including xenobiotics as well as endogenous ketones and aldehydes (Endo et al. 2013).

3 α (20 β)-HSDs (EC=1.1.1.53) catalyze NAD(P)H-dependent reversible reduction of 17 β -hydroxyandrostane-3-one into androstane-3 α ,17 β -diol. In addition to the reversible reduction of 3-ketosteroid derivatives into corresponding 3 α / β -hydroxysteroids (Ohno et al. 1991), the enzyme from pig testes was shown to catalyze the reduction of C21 steroids, such as 17 α -hydroxyprogesterone, 17 α -hydroxypregnenolone, progesterone, 11-deoxycortisol, 11-deoxycorticosterone and pregnenolone into respective 20 β -hydroxysteroids (Nakajin et al. 1988). In addition, pig enzyme was found to reduce versatile carbonyl compounds, including quinones and ketoaldehydes (Tanaka et al. 1992), thus, resembling the carbonyl reductases. Carbonyl reductase-like 20 β -HSD with substrate specificities similar to that of pig testicular 20 β -HSD was also found in ovaries of fish (Tanaka et al. 2002, Sreenivasulu and Senthilkumaran 2009), where it plays a key role in the process of final oocyte maturation. By reducing 17 α -hydroxyprogesterone, ovarian 20 β -HSD produces 17 α ,20 β -dihydroxyprogesterone which is an oocyte maturation inducing hormone in most species of fish (Nagahama 1997). In addition, another type of 20 β -HSD, which is very specific for steroid hormone cortisone, was recently found in fish (Tokarz et al. 2012). By reducing cortisone into 20 β -hydroxycortisone this 20 β -HSD is proposed to be involved in the regulation of the stress response in fish (Tokarz et al. 2013).

3 β (20 α)-HSD (EC=1.1.1.210) catalyze a reversible NAD(P)H-dependent reduction of 17 β -hydroxy-5 α -androstane-3-one into 5 α -androstane-3 β ,17 β -diol. The enzyme was isolated and characterized from ovine blood (Chen et al. 1987) as well as erythrocytes of fetal lamb (Chen et al. 1989) and fetal calf (Sharaf and Sweet 1982). In addition to 3-ketosteroid reductase activity, the enzyme also shows 20-ketosteroid reductase activity: it catalyzes the reduction of progesterone to its 20 α -hydroxymetabolite (Sharaf and Sweet 1982, Chen et al. 1989). This activity could be important for the clearance of progesterone produced by the pregnant mother from the blood of the developing fetus (Chen et al. 1989).

Estradiol 17 β -dehydrogenase (EC=1.1.1.62) catalyzes a reversible NAD(P)-dependent reduction of estrone into 17 β -estradiol. Originally, the enzyme was purified from human placenta (Jarabak et al. 1962). The 17 β -dehydrogenase in placenta and ovaries catalyze the final step in the biosynthesis of estrogen by converting estrone (a weak estrogen) into 17 β -estradiol (a potent estrogen) (Penning 1997). The enzyme purified from human placenta was found to catalyze, in addition, a reversible reduction of progesterone into 20 α -hydroxyprogesterone (Strickler et al.

1981). 17 β -HSD/17-ketosteroid reductase and 20 α -HSD/20-ketosteroid reductase activities were shown to reside at the single active site of the enzyme (Strickler et al. 1981). Today multiple isozymes of estradiol 17 β -dehydrogenases are known in humans (Penning 1997), and several of these enzymes were shown to possess 20-ketosteroid reductase and/or 20-HSD activities (Wu et al. 1993, Dufort et al. 1999, Andersson and Moghrabi 1997).

1.4.1.2 20-HSDs from gut microbiota

Gut microbiota is the population of microorganisms living in the gastrointestinal tract (GI) of warm-blooded organisms. In the second part of the 20th century, the first evidence appeared that gut microbiota produces enzymes possessing 20-ketosteroid reductase activity. In 1975 Bokkenheuser *et al.* (1975) showed that *Bacteroides* species isolated from fecal flora of healthy human subjects were able to metabolize 11-deoxycorticosterone into the 20-hydroxysteroid metabolite. Later Winter *et al.* (1982) demonstrated that *Bifidobacterium adolescentis* isolated from fecal flora of rats and humans transformed cortisol into 20 β -dihydrocortisol and *Clostridium scindens* isolated from human feces converted corticosterone into 20 α -dihydrocorticosterone (Winter et al. 1984). Based on these findings it was hypothesized that gut microbiota produces 20-HSDs that might play important roles in the metabolism of steroid hormones of the host.

The number of studies dealing with the identification and characterization of the enzymes possessing 20-HSD activity in the gut microbiota is, however, very limited. The best-known example is 20 α -HSD from *Clostridium scindens*. The characteristics of 20 α -HSD from *C. scindens*, such as spectrum of substrates and requirement for cofactors, were first described in the crude cell extract (Krafft et al. 1987) and only later the properties of homogenous enzyme preparation were investigated (Krafft and Hylemon 1989). It was found that 20 α -HSD is a NADH-dependent oxidoreductase that efficiently reduces steroid substrates such as cortisone, cortisol, 11-deoxycortisol and 5 β -dihydrocortisol (Krafft and Hylemon 1989). The determined amino-terminal sequence of the purified enzyme suggested that this enzyme might belong to glyceraldehyde 3-phosphate dehydrogenase gene family (Krafft and Hylemon 1989). More than a decade later a gene encoding 20 α -HSD from *C. scindens* was finally identified (Ridlon et al. 2013). It was shown that the *desC* gene (GenBank accession number EDS07887.1) encodes 20 α -HSD of *C. scindens* that has characteristics of previously purified enzyme (Krafft and

Hylemon 1989) and belongs to the zinc-containing alcohol dehydrogenase family (Ridlon et al. 2013).

1.4.1.3 Other microbial 20-HSDs

A 20 β -HSD was purified from a gram-positive soil bacterium *Streptomyces hydrogenans* (Hubener et al. 1959). It was shown to reduce C20 carbonyl group of various 20-ketosteroids to the corresponding 20 β -hydroxysteroid compounds in a NADH-dependent manner (Allner and Eggstein 1976). The biosynthesis of steroids is not known to occur in *S. hydrogenans*, but the exogenous steroids such as 11-deoxycortisol were found to induce the expression of 20 β -HSD (Hubener et al. 1959) in this microorganism. The physiological role of 20 β -HSD is not clear and the natural endogenous substrates of this enzyme remain to be found. Despite that, 20 β -HSD catalyzed conversions of steroids gained a lot of attention and were extensively studied by enzymologists. In addition to the C20 carbonyl position, the enzyme was found to catalyze reversible reduction of C3 carbonyl groups of 5 α -androstane and 5 α -pregnane compounds producing 3 α -hydroxysteroids (Gibb and Jeffery 1973). It was proposed that the same active site is responsible for the bifunctional activity of the enzyme (Sweet and Samant 1980). It was suggested that the 20 β and 3 α -HSD activities of the enzyme might be due to the alternative binding of the steroid substrates at the same active site of the enzyme (Sweet and Samant 1980). The native form of 20 β -HSD was shown to be a tetramer (Blomquist 1973) and the formation of tetramers was found to be essential for enzyme's activity (Pasta et al. 1980, Carrea et al. 1989). The crystal structure of the native tetramer of 20 β -HSD from *S. hydrogenans* was solved by Ghosh *et al.* (1991, 1994). It was the first described three-dimensional structure of dehydrogenase belonging to the short-chain dehydrogenase/reductase protein superfamily.

In addition to 20 β -HSD, 20 α -HSD was also found in *S. hydrogenans* (Rimsay et al. 1988). The partially purified enzyme with the MW of 48 kDa was shown to catalyze the NADH-dependent reduction of progesterone, cortisone and cortisol to the corresponding 20 α -hydroxysteroids (Rimsay et al. 1988). The gene encoding this enzyme, however, remains to be identified.

The 20 α -HSD was purified from eukaryotic microorganism *Tetrahymena pyriformis*. The enzyme with the MW of 68 kDa was shown to catalyze the NADPH-dependent reduction of 17 α -hydroxyprogesterone into 17 α ,20 α -dihydroxypregn-4-en-3-one (Inazu et al. 1994). In addition, the enzyme catalyzed the reduction of various non-steroidal aldehydes and ketones

(such as isatin, D-glyceraldehyde, phenylglyoxal); thus, authors concluded that it resembles pluripotent carbonyl reductases (EC=1.1.1.184) and might be responsible for the detoxification of xenobiotic chemicals in this organism (Inazu et al. 1994). Although *Tetrahymena* does not contain endogenous steroid hormones, the exogenously supplied steroid hormones affect the growth, phagocytic capacity, and chemotaxis of this organism (Csaba 2012). Based on the determined N-terminal sequence of the enzyme it was suggested that it might belong to the aldo-keto-reductase protein superfamily (Inazu et al. 1994).

1.4.2 Miscellaneous enzymes possessing 20-ketosteroid reductase activity

In addition to HSDs, 20-ketosteroid reductase activity was also reported for other enzymes. Carbonyl reductases are enzymes which catalyze the reduction of various carbonyl compounds including aldehydes, ketones, and quinones, in the presence of NAD(P)H. Carbonyl reductases reduce xenobiotic carbonyl compounds such as drugs and environmental chemicals as well as endogenous prostaglandins, steroids and retinoids (Oppermann 2007). Reduction of xenobiotic carbonyls produces more soluble compounds, which can be conjugated and excreted (Oppermann 2007). Several carbonyl reductases (EC=1.1.1.184) from Chinese hamster were shown to possess detectable 20-ketosteroid reductase activity against 5 β -pregnan-3 α -ol-20-one (Terada et al. 2001, Terada et al. 2003). Similarly, multiple aldo-keto reductases were cloned recently from rabbit and were discovered to catalyze C20 carbonyl reduction of ketosteroids, in addition to the reduction of a broad spectrum of xenobiotic carbonyl compounds (Endo et al. 2014).

An aldehyde reductase (EC=1.1.1.21) from bull testis was shown to be capable of reducing 17 α -hydroxyprogesterone at C20 position into 20 α -hydroxymetabolite, in addition to reducing classical aldehyde reductase substrates including benzaldehyde, glyceraldehyde and glucose (Warren et al. 1993). Moreover, a prostaglandin-E₂ 9 reductase was purified from rabbit and was shown to reduce progesterone into 20 α -hydroxyprogesterone as well as prostaglandin E₂, methylglyoxal, DL-glyceraldehyde and quinones (Wintergalen et al. 1995).

Indanol dehydrogenase (EC=1.1.1.112) purified from monkey liver was shown to possess 20-ketosteroid reductase activity in addition to 1-indanol dehydrogenase, 3 α /20 α -HSD and 3-ketosteroid reductase activities. This enzyme was shown to reduce 5 β -pregnan-3 α -ol-20-one into 5 β -pregnan-3 α ,20 α -diol (Hara et al. 1989).

1.5 Short-chain dehydrogenases/reductases and aldo-keto-reductases

The majority of enzymes that possess 20-ketosteroid reductase activity can be classified into one of the two big protein superfamilies, namely, short-chain dehydrogenases/reductases (SDRs) and aldo-keto-reductases (AKRs).

1.5.1 Short-chain dehydrogenases/reductases (SDRs)

Historically the short-chain dehydrogenase/reductase protein superfamily was established based on the discovery that insect alcohol dehydrogenases (Thatcher 1980) are different from mammalian alcohol dehydrogenases, such as horse liver alcohol dehydrogenase (Brändén et al. 1973, Jörnvall et al. 1981). In contrast to mammalian classical Zn-containing alcohol dehydrogenases, which are now grouped into the protein superfamily of the medium-chain alcohol dehydrogenases/reductases (MDR) (Persson et al. 2008), the enzymes from *Drosophila melanogaster* were found to be smaller in size and not dependent on metal cofactors (Thatcher 1980, Persson et al. 1991).

As of 2010, the SDR protein superfamily contained over 47,000 primary structures and more than 300 crystal structures (Kallberg et al. 2010). SDR proteins are found in all three domains of life (Kallberg et al. 2010). The majority of SDR members have quite low pairwise sequence identity (around 25 %) (Persson et al. 1991) but their three-dimensional structures are highly homologous (Oppermann et al. 2003). The majority of the members of SDR superfamily were classified into 314 different families (Kallberg et al. 2010). Based on these families a nomenclature system for SDRs was proposed (Persson et al. 2009).

A typical SDR is a one-domain NAD(P)H-dependent enzyme of about 250-350 residues. The cofactor binding region is located at the N-terminal part of the polypeptide, whereas the substrate-binding part is located at the C-terminal part of the sequence (Ghosh et al. 1994). SDRs may have transmembrane domains or signal peptides, or be a part of multienzyme complexes (Kallberg et al. 2002). Most SDRs function as homodimers or homotetramers (Ghosh et al. 1994, Ghosh et al. 1995, Tanaka et al. 1996). The substrate spectrum of SDRs includes alcohols, prostaglandins, steroids, sugars, xenobiotics, and aromatic compounds. The majority of SDRs are oxidoreductases (EC=1.x.x.x), however, several isomerases (EC=5.x.x.x) and lyases (EC=4.x.x.x) were also found to belong to SDR superfamily (Persson et al. 2003).

Based on conserved sequence motifs, SDR proteins were grouped into five families: ‘classical’, ‘extended’, ‘intermediate’, ‘divergent’ and ‘complex’ (Persson et al. 2003). The members of the ‘classical’ SDR family contain conserved cofactor binding motif sequence composed of TGxxx[AG]xG and the conserved active site motif sequence YxxxK, where x depicts any amino acid residue and residues shown in the brackets might be present or absent (Kavanagh et al. 2008). The members of other four SDR families have slight variations in the conserved sequence of cofactor binding motif and/or active site motif in comparison to the ‘classical’ SDRs (Kavanagh et al. 2008). Most of the members of the ‘classical’ SDR family are oxidoreductases (EC=1.x.x.x) (Persson et al. 2003).

The first crystal structure of SDR was solved by Ghosh *et al.* in 1991. It was shown that 20 β (3 α)-HSD from *S. hydrogenans* is composed of four identical subunits that adopt a single-domain globular α/β structure (Ghosh et al. 1991). After the crystal structures became available for many other SDR enzymes it turned out that the three-dimensional folds of SDR enzymes are highly homologous and can be superimposed, except for the C-terminal region (Favia et al. 2008, Nobeli et al. 2009). The variable loops at the C-terminal region account for the shape and size of the substrate-binding cleft of different SDRs, explaining the wide substrate spectrum of this enzyme superfamily (Kallberg et al. 2010). In most of SDR enzymes, a substrate binding loop is formed by more than 20 residues which are located at the C-terminal part of the enzyme. This loop covers the active site and becomes well ordered after substrate binding (Hwang et al. 2013, Tanaka et al. 1996). The substrate binding loop is often found to be disordered in SDR crystal structures without bound substrate (Yamazawa et al. 2011).

The N-terminal part of SDR adopts a ‘Rossmann-fold’ dinucleotide cofactor binding motif. The Rossmann-fold structural element is composed of a central, twisted parallel β -sheet consisting of 6-7 β -strands flanked by 3-4 α -helices from each side (Kavanagh et al. 2008). The cofactor binding region has a variable glycine-rich motif (GxxxGxG) which enables the binding of the pyrophosphate portion of a cofactor molecule and is critical for structural integrity (Kavanagh et al. 2008).

It was proposed that SDR reaction proceeds through an ordered ‘bi-bi’ mechanism with a cofactor molecule binding first and leaving last (Betz and Warren 1968, Ueda et al. 2004). Three conserved catalytic residues: Tyr, Lys, and Ser were identified in the active site of SDR enzymes

(Ghosh et al. 1994, Tanaka et al. 1996). The Tyr residue acts as a catalytic acid/base and donates/abstracts a proton to/from the substrate molecule (Tanaka et al. 1996). The adjacent Lys residue lowers the pKa of the hydroxyl group of catalytic Tyr (Tanaka et al. 1996). The ϵ -amino group of lysine binds nicotinamid ribose and the active site serine stabilizes and polarizes the carbonyl group of the substrate molecule. The simplified reaction mechanism of SDR oxidoreductase is shown in **Fig. 1.3**. In addition to the conserved catalytic triad, recently an additional catalytic residue (Asn) was identified in several SDRs (Filling 2002, Carius et al. 2010).

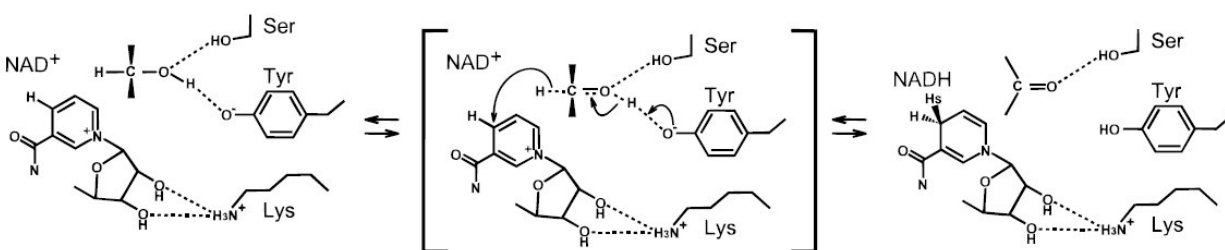


Fig. 1.3 A reaction mechanism of dehydrogenase of SDR protein superfamily. The part of a substrate which is modified by the enzyme, the catalytic residues (Ser, Tyr and Lys), and the nicotinamide nucleoside moiety of NAD⁺ (or NADH) are shown. The figure was adapted from publication of Tanaka *et al.* (1996).

The vast majority of SDRs do not need a metal cofactor. However, several SDRs, such as galactitol dehydrogenase from *Rhodobacter sphaeroides D* and R-alcohol dehydrogenase from *Lactobacillus brevis* (Schneider et al. 1995, Niefind et al. 2003) were found to require divalent metal ions for the activity. A Ca²⁺ ion was found at the active site of D-gluconate 5-dehydrogenase from *Streptococcus suis* (Zhang et al. 2009). It was proposed that bound Ca²⁺ ion may contribute to the formation of the active site of an enzyme by retaining and orienting both the nicotinamid ring of cofactor molecule and molecule of substrate D-gluconate (Zhang et al. 2009). In the crystal structure of homotetramer of galactitol dehydrogenase from *R. sphaeroides D*, two Mg²⁺ ions were found to be coordinated each by the two opposing C-termini (Carius et al. 2010), and, therefore, might be involved in the stabilization of an active tetrameric form of an enzyme. Similarly, two ‘structural’ Mg²⁺ ions were found in the homotetramer of R-alcohol dehydrogenase from *L. brevis* (Niefind et al. 2003).

The analysis of the three-dimensional structure of a homotetrameric 20 β -HSD from *S. hydrogenans* (Ghosh et al. 1994) revealed the structural motifs that are involved in the subunit

association of tetrameric SDR enzymes (Tanaka et al. 1996) (**Fig. 1.4a-c**). The oligomerization of subunits of 20 β -HSD occurs across the three axes. One type of oligomerization that is strictly conserved among SDRs (Ghosh and Vihko 2001) occurs across a so-called Q-axis and involves association of α -helix E and α -helix F of each of the two subunits resulting in the formation of a bundle of four helices. This type of association involves extensive hydrophobic interactions, and is important for the formation of the active site cleft (Ghosh and Vihko 2001), and activity of the enzyme (Puranen et al. 1997, Hoffmann and Maser 2007). The second type of monomer association occurs across the so-called P-axis by an antiparallel association of β -strand G and α -helix G of each subunit (Ghosh et al. 1994, Tanaka et al. 1996). This type of oligomerization involves less hydrophobic interactions in comparison to Q-axis interface. The third type of monomer association is across the R-axis. The R-axis interface is created by the 1.5 α -helical turns of each subunit. The interaction across the R-axis is the weakest of the three (Ghosh et al. 1994) and is not observed in some tetrameric SDRs (Tanaka et al. 1996).

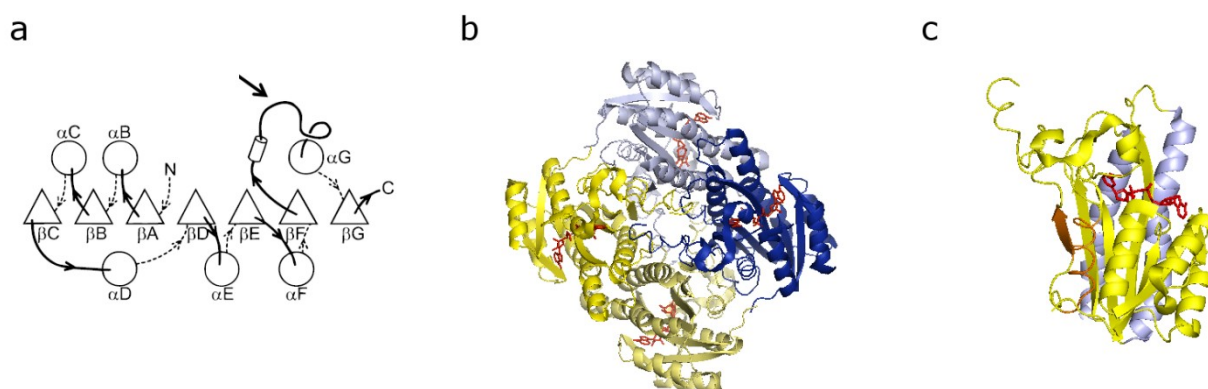


Fig. 1.4 Structure of a 20 β -HSD from *Streptomyces hydrogenans*. **(a)** Folding topology of 20 β -HSD. α -Helices are shown as circles and β -strands as triangles, cylinder represents a short α -helix. The region between the α G-helix and the β F-strand forms a substrate-binding loop (indicated with an arrow). The illustration was adapted from publication of Tanaka *et al.* (1996). **(b)** The structure of a homotetramer of the 20 β -HSD. The individual subunits are colored in yellow, light yellow, blue and light blue, the bound cofactor molecule NAD⁺ is shown in red. **(c)** The structure of a subunit of the 20 β -HSD with depicted conserved structural elements involved in oligomerization. α E and α F helices involved in oligomerization across Q-axis interface are depicted in light blue, whereas the β G-strand and α G-helix, involved in the oligomerization across the P-axis interface, are depicted in orange. The bound cofactor molecule NAD⁺ is shown in red. Illustrations were produced with PyMOL program using 2HSD PDB file of crystal structure of 20 β -HSD from *S. hydrogenans* (Ghosh et al. 1994).

1.5.2 Aldo-keto-reductases (AKRs)

Aldo-keto-reductases (AKRs) are a group of structurally related proteins of common ancestry, expressed in prokaryotes and eukaryotes (Barski et al. 2008, Penning 2004). Most AKRs convert carbonyl and aldehyde compounds into secondary and primary alcohols, respectively. AKRs have a broad spectrum of substrates that overlaps with the substrates of SDRs. In addition to endogenous substrates, such as sugar aldehydes, steroid hormones, prostaglandins and lipid-derived aldehydes, AKRs also convert exogenous substrates, such as drugs and other xenobiotic compounds (Jin and Penning 2007).

Typically AKRs are monomeric NAD(P)H-dependent oxidoreductases with a size of 34-37 kDa (Jin and Penning 2007). Several dimeric (Kozma 2002, Kavanagh et al. 2002) AKRs were also described. The number of AKRs is considerably lower in comparison to SDRs: as of 2009 there are over 150 AKRs that are grouped into 15 families based on the amino acid comparison (Mindnich and Penning 2009).

From the available crystal structures of AKRs it is clear that all AKRs adopt a conserved $(\alpha/\beta)_8$ -barrel structure with three large associated loops (Jez et al. 1997). In the $(\alpha/\beta)_8$ -barrel structure α -helix and β -strand repeats itself eight times in alternating manner (Penning 2004). The β -strands form the core of the barrel, whereas α -helices surround the core structure. The substrate binding cavity is formed by the residues in the loops at the back of the barrel. The size and shape of a substrate binding pocket is defined by these variable loops, explaining the observed broad substrate selectivity of AKR superfamily proteins (Jez et al. 1997). The cofactor binding site and active site are highly conserved across AKR superfamily. In contrast to SDR superfamily, AKRs bind cofactor without the 'Rossmann fold' structural motif.

Similarly to SDRs, reactions of AKRs follow an ordered 'bi-bi' mechanism in which cofactor binds first and leaves last (Mindnich and Penning 2009, Askonas et al. 1991). At the active site AKRs contain a catalytic tetrad: Tyr, Asp, Lys, and His. Tyr residue functions as a general acid/base catalyst, whereas Asp and Lys lowers pKa of catalytic Tyr (Schlegel et al. 1997). In contrast to SDRs, AKRs catalyze the transfer of '4-pro-R' hydride from the NAD(P)H cofactor to the carbonyl of substrate (Askonas et al. 1991, Jez et al. 1997).

1.6 Examples of applications of 20-ketosteroid reductases in biocatalysis

The use of 20 β -HSD from *S. hydrogenans* for the large-scale biocatalytic preparation of 20 β -hydroxysteroids was first described by Cremonesi *et al.* in 1975. In order to overcome the problem of low steroid solubility in water, Cremonesi *et al.* (1975) used two-phase water/organic solvent system, for an efficient reduction of cortisone, prednisone, cortisol, deoxycorticosterone, and prednisolone to respective 20 β -hydroxysteroids. The selective enzymatic reductions of 20-ketosteroids were coupled with the alcohol dehydrogenase-catalyzed dehydrogenation of ethanol for an efficient regeneration of NADH (Cremonesi *et al.* 1975).

In addition, De Amici *et al.* (1991) described the use of 20 β -HSD from *S. hydrogenans* in the chemoenzymatic synthesis of several muscarines, which are agonists of a physiological neurotransmitter acetylcholine. Moreover, previously this enzyme was used for the gram-scale enantioselective reduction of a series of bicycloheptenones, which are widely used synthons in organic chemistry (Davies *et al.* 1986).

Naumann *et al.* (2010) produced human 20 α -HSD whole-cell biocatalyst by overexpressing human 20 α -HSD in fission yeast *Schizosaccharomyces pombe*. The obtained recombinant strain was used for reduction of progesterone to 20 α -hydroxyprogesterone and dydrogesterone, to 20 α -hydroxydydrogesterone (Naumann *et al.* 2010, Naumann *et al.* 2011). Biocatalytically produced steroid metabolites are important for toxicity studies and development of drugs (Naumann *et al.* 2010).

1.7 Unidentified 20-ketosteroid reductase in *Escherichia coli* and a whole-cell biocatalysis

Escherichia coli is a gram-negative bacterium originally discovered by Theodor Escherich and found in the lower intestine of warm-blooded organisms. Hannemann *et al.* (2007) showed that a laboratory strain of *E. coli* can transform 11-deoxycorticosterone (11-DOC) into 4-pregnen-20,21-diol-3-one (Fig. 1.5). The molecular structure of the produced steroid compound (4-pregnen-20,21-diol-3-one) was solved using mass spectrometry and carbon-13 nuclear magnetic resonance (NMR) method. It clearly indicated that the cells of *E. coli* transform 11-DOC by catalyzing a selective reduction of carbonyl group at C20 position of 11-DOC. The 20-ketosteroid reductase activity was observed in *E. coli* for the first time and it suggested that *E. coli* contains a 20-ketosteroid reductase which remains to be identified and characterized (Hannemann *et al.* 2007).

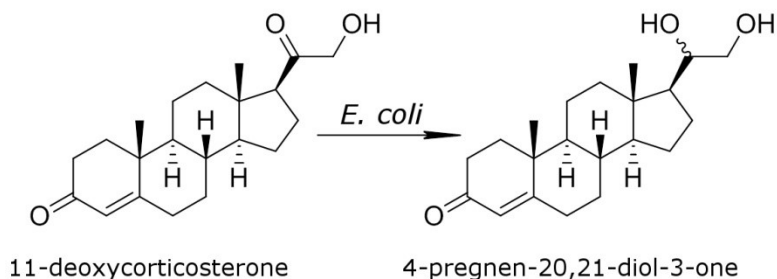


Fig. 1.5 Transformation of 11-deoxycorticosterone with *E. coli* cells as described by Hannemann *et al.* (2007).

E. coli, like most of prokaryotic microorganisms does not produce mammalian steroid hormones such as 11-DOC, but it is able to transform them. Yoshimoto *et al* (1991) purified and characterized a 7α -hydroxysteroid dehydrogenase (7α -HSD) which is the only *E. coli* oxidoreductase that was shown to metabolize eukaryotic steroids so far (Yoshimoto *et al.* 1991). This enzyme catalyzes a reversible stereoselective reduction of carbonyl group at C7 position of bile acids and plays an important role in the bile acid metabolism in the human intestinal tract (Ridlon *et al.* 2006). In contrast to 7α -HSD, the role of 20-ketosteroid reductase activity in *E. coli* and other prokaryotic microorganisms remains to be obscure. In order to find out if *E. coli* 20-ketosteroid reductase could be involved in the metabolism of 20-ketosteroids in the intestinal tract of human host, it would be important to identify the enzyme possessing 20-ketosteroid reductase activity in this microorganism and determine its affinity towards eukaryotic 20-ketosteroids.

Despite the unknown biological function of *E. coli* 20-ketosteroid reductase, this enzyme might have high potential for biotechnological applications. Most of the enzymes possessing 20-ketosteroid reductase activity such as hydroxysteroid dehydrogenases and carbonyl reductases are substrate promiscuous enzymes (Maser 1995). The enzyme's property to convert a broad range of substrates could be used in organic chemistry for the synthesis of building blocks as well as for the production of novel drug derivatives.

Hannemann *et al.* (2007) used cells of *E. coli* containing unidentified 20-ketosteroid reductase as a whole-cell biocatalyst for the efficient conversion of 11-DOC into 4-pregnen-20,21-diol-3-one, which was found to be a potent and selective inhibitor of human 5α -reductase type II, a drug target for the treatment of prostate diseases in men. The half maximal inhibitory concentration

(IC₅₀) of produced 20-hydroxysteroid derivative for the human 5 α -reductase type II was determined to be 1.56 μ M. The 20-ketosteroid reductase activity was detected in the cytosolic fraction of *E. coli* suggesting that the unidentified reductase is a soluble cytosolic enzyme (Hannemann et al. 2007). The transformation of 11-DOC into 4-pregnen-20,21-diol-3-one was thus possible with whole *E. coli* cells because the substrate and product molecules due to their lipophilic nature were able to pass the cell envelope of *E. coli*. Outer membranes of various Gram-negative bacteria including *E. coli* were found to be quite permeable to very hydrophobic steroid molecules (Plesiat and Nikaido 1992). Diffusion of these molecules occurs mainly through the lipid bilayer regions of the membrane (Plesiat and Nikaido 1992). In contrast, charged steroids penetrate the bacterial cell much slower in comparison to uncharged steroid compounds (Plesiat and Nikaido 1992). In addition, recently it was shown that several multiple-drug efflux (MDE) pump proteins are involved in the efflux of mammalian steroid hormones such as estradiol and progesterone in *E. coli* (Elkins and Mullis 2006). In the efflux-deficient *E. coli* that contains mutations in several MDE pumps, steroid hormone-dependent growth suppression is observed (Elkins and Mullis 2006). Thus, it was proposed that MDE pumps are essential for the survival of *E. coli* under conditions where steroids are present, such as in the gastrointestinal tract (Elkins and Mullis 2006).

A limited uptake and active efflux of steroid substrates by *E. coli* cells might significantly decrease the efficiency of *E. coli* whole-cell biocatalysts that utilize intracellularly expressed enzymes for the transformation of the steroid substrate molecule into desired steroid product. One way to overcome this problem is to use alternative whole-cell biocatalysts that are based on the expression of the enzyme of interest on the surface of *E. coli* cell (Jose *et al.* 2012).

1.8 Autodisplay

Autodisplay is the recombinant surface display of proteins or peptides by means of an autotransporter protein in any Gram-negative bacterium (Jose and Meyer 2007). Autotransporter proteins represent a large protein superfamily with over 1500 members identified in genomes of diverse Gram-negative bacteria (Celik et al. 2012). These proteins play important roles in the pathogenesis of invasive Gram-negative bacteria as well as survival of non-invasive environmental bacterial species (van Ulsen et al. 2013). Gram-negative bacteria use several well-characterized secretion systems (I-VI) to excrete molecules across the barrier of the cell

wall, which is composed of the inner-membrane, periplasm with peptidoglycan layer, and the outer membrane (Filloux 2013, Desvaux et al. 2009). Classical monomeric autotransporters, which were classified as type V secretion system, represent one of the simplest secretion systems in Gram-negative bacteria (Benz and Schmidt 2011).

The autotransporter secretion system is used by bacteria to transport proteins to the surface of a cell or secrete proteins to the extracellular space (Jose and Meyer 2007). The autotransporter secretion pathway was first described for IgA1 protease from *Neisseria gonorrhoeae* (Pohlner et al. 1987). Proteins transported by this pathway have similar structural organization. As proposed for the IgA1 autotransporter (Pohlner et al. 1987), a classical autotransporter is synthesized in the cytoplasm as a precursor protein, which is composed of an N-terminal signal peptide, followed by an N-terminal passenger domain, a linker region, and a C-terminal translocator domain. The signal peptide directs the translocation of the precursor protein across the inner membrane. Upon arrival at the periplasm, the signal peptide is removed by the specific proteases and the C-terminus of the precursor protein forms a porin-like structure, called β -barrel, within the outer membrane. The N-terminal passenger domain is then translocated to the cell surface across the outer membrane. A linker region is required for an efficient exposure of the passenger domain on the surface of the cell. A simplified mechanism for secretion of classical autotransporter is illustrated in **Fig. 1.6**.

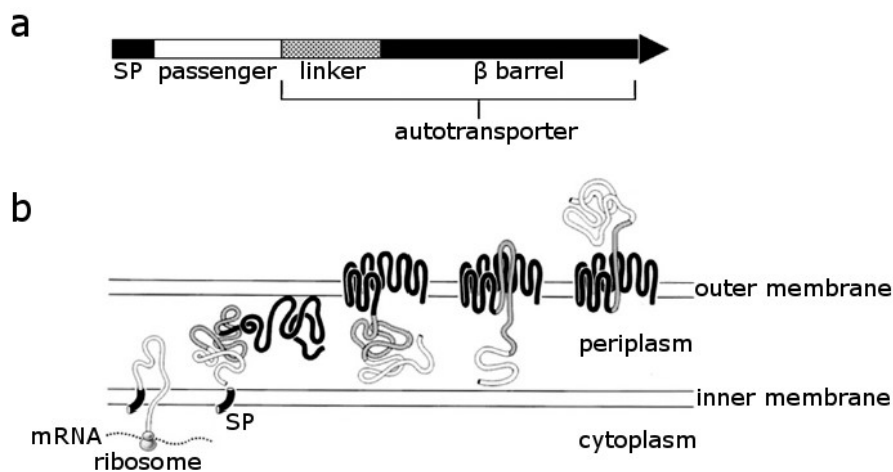


Fig. 1.6 Secretion mechanism of a classical autotransporter. **(a)** The structure of a precursor protein synthesized in the cytoplasm of the cell of a Gram-negative bacterium. **(b)** The transport of a passenger domain to the surface of the cell. The N-terminal signal peptide (SP) directs the translocation of the precursor protein across the inner membrane. After the cleavage of the signal peptide in the periplasm, the C-terminal part of the protein folds into β -barrel into the outer membrane. The passenger domain is translocated across the outer membrane with the aid of the β -barrel in unfolded state. Surface translocation is supported by the folding of the passenger domain on the surface of the cell. The illustration was adapted from the publication of Jose *et al.* (2012).

The secretion of autotransporter proteins is not autonomous as it was previously thought, but is rather dependent on the action of other proteins (Leyton *et al.* 2012). The translocation of classical autotransporter precursor proteins through the inner membrane is dependent on the Sec machinery (Benz and Schmidt 2011). The incorporation of the β -barrel into the outer membrane is assisted by the Bam complex (β -barrel assembly machinery) (Rossiter *et al.* 2011). Moreover, periplasmic chaperones, such as Skp, SurA, and DegP were also shown to be important for the secretion of the autotransporters (Purdy *et al.* 2007). The exact translocation mechanism of the passenger domain across the outer membrane is still not well understood at the molecular level (Gawarzewski *et al.* 2013). Currently a so-called alternative model mechanism for the passenger translocation across the outer membrane was proposed (Gawarzewski *et al.* 2013). According to this model, the autotransporter forms a stable intermediate in the periplasm by interacting with periplasmic chaperone Skp. This intermediate with the linker domain incorporated in the pore of the prefolded β -barrel is targeted to the outer membrane with a help of assisting proteins. The prefolded β -barrel is integrated into the outer membrane and the passenger domain is transferred across the outer membrane with the help of assisting proteins. Upon arrival at the cell surface passenger domain adopts its fully folded conformation (Gawarzewski *et al.* 2013).

An *E. coli* autotransporter protein AIDA-I (the adhesin involved in diffuse adherence of enteropathogenic *E. coli*) (Benz and Schmidt 1989) was used for the development of the Autodisplay technology in the *E. coli* host (Jose and Meyer 2007). The AIDA-I-based Autodisplay technology uses the linker and a β -barrel region of AIDA-I autotransporter, whereas the natural passenger domain of AIDA-I is replaced by the protein/peptide of interest, and the signal peptide is most often originating from the cholera toxin B subunit (CtxB) (Jose and Meyer 2007).

The AIDA-I-based Autodisplay technology allows the expression of more than 10^5 molecules of a recombinant protein on the surface of a single *E. coli* cell (Jose et al. 2001, Jose and von Schwichow 2004). Due to the motility of the β -barrel domain within the outer membrane, the dimerization (Jose et al. 2001, Jose and von Schwichow 2004) and multimerization (Detzel et al. 2013) of the recombinant passenger proteins can easily occur.

The AIDA-I based Autodisplay technology was used for successful recombinant expression of numerous functional enzymes, such as nitrilase (Detzel et al. 2013), organophosphate hydrolase (Li et al. 2008), cytochrome P450 monooxygenases (Schumacher et al. 2012, Schumacher and Jose 2012), lipase (Kranen et al. 2014), sorbitol dehydrogenase (Jose and von Schwichow 2004), and esterases (Schultheiss et al. 2002, Schultheiss et al. 2008). Each of these functional whole-cell biocatalysts can be used in specific applications, such as synthesis of fine chemicals and building blocks, degradation of environmental pollutants, or in the studies of drug metabolism.

The autotransporter based Autodisplay technology offers several advantages, which make it an attractive alternative for the use of pure enzymes in biocatalysis. The Autodisplay technology provides a protein immobilization platform, which may stabilize and, therefore, increase the activity of the enzyme. The whole-cell biocatalyst can be reused without a significant loss of activity. The biocatalyst can be removed from the reaction mixture by a simple centrifugation step, which simplifies the downstream processes associated with the isolation of the product (Jose and Meyer 2007, Jose *et al.* 2012).

In addition, Autodisplay based whole-cell biocatalysts offer several advantages over alternative whole-cell systems, which are based on the intracellular expression of a recombinant enzyme.

The Autodisplay based biocatalyst can be used to catalyze the transformations of a broader spectrum of substrates, such as compounds or polymers, which are not able to pass the cell wall barrier. In this case, undesirable side-reactions, which arise from the enzymatic activities within the cell and can modify the substrate or the product, could also be avoided.

1.9 Aims of the work

The cells of *Escherichia coli* are able to transform the eukaryotic-type steroid hormone 11-deoxycorticosterone (11-DOC) into valuable bioactive steroid derivative, 4-pregnen-20,21-diol-3-one (**Fig. 1.5**), which was previously found to selectively inhibit the human 5α -reductase type II with a half maximal inhibitory concentration (IC₅₀) of 1.56 μ M (Hannemann et al. 2007). The observed 20-ketosteroid reductase activity, however, was not annotated to any gene product of *E. coli*.

The current work aimed to:

- identify the gene encoding 20-ketosteroid reductase in *E. coli*;
- characterize the biochemical properties of the enzyme;
- investigate the applicability of Autodisplay technology for the design of *E. coli* 20-ketosteroid reductase whole-cell biocatalyst for efficient regioselective reduction of steroids and related compounds.

2 Materials and methods

2.1 Materials

2.1.1 Instruments

Instrument	Source
1-D protein electrophoresis system (Mini-Protean Tetra Cell)	Bio-Rad Laboratories GmbH, München, Germany
ÄKTA FPLC (UPC-900, P920)	GE Healthcare Europe GmbH, Freiburg, Germany
Analytical balance (CP124S)	Sartorius AG, Göttingen, Germany
Autoclave (VX-95)	Systec GmbH, Wettenberg, Germany
Balance (BP1200)	Sartorius AG, Göttingen, Germany
Centrifuge 5417R	Eppendorf, Hamburg, Germany
Chemiluminescence imaging system (ChemoCam imager)	INTAS Science Imaging Instruments GmbH, Göttingen, Germany
Cooling centrifuge (Sorvall RC-5C Plus)	Thermo Fisher Scientific, Waltham, MA, USA
Cooling centrifuge (Universal 320R)	Andreas Hettich GmbH & Co.KG, Tuttlingen, Germany
Cooling microcentrifuge (Mikro 200R)	Andreas Hettich GmbH & Co.KG, Tuttlingen, Germany
Electroporator (Eporator)	Eppendorf, Hamburg, Germany
Eppendorf Biospectrometer Kinetics	Eppendorf, Hamburg, Germany
Freezer (Forma 900 Series)	Fisher Scientific GmbH, Schwerte, Germany
Gel documentation system (Gel Imager)	INTAS Science Imaging Instruments GmbH, Göttingen, Germany
Horizontal DNA gel electrophoresis system (Sub System 150)	Labnet, Edison, NY, USA
HPLC-System Hitachi LaChrom Elite (organizer, diode array detector L-2455, pump L-2130, autosampler L-2200, column oven L-2300)	VWR, Radnor, PA, USA
Ice flaker (Scotsman AF 100)	Hubbard Ice Systems, Ipswich, UK
Incubation shaker (Infors HT Minitron)	Infors AG, Basel, Switzerland
Incubator (Heratherm)	Fisher Scientific GmbH, Schwerte, Germany
Microcentrifuge (MiniSpin)	Eppendorf, Hamburg, Germany
Microplate reader Mithras LB 940	Berthold Technologies GmbH & Co. KG, Bad Wildbach, Germany
Milli-Q academic water purification system	EMD Millipore, Billerica, MA, USA

Nanophotometer (Pearl)	Implen Gmb
pH-Meter (inoLab)	WTW GmbH, Weilheim, Germany
Pipettes (Pipetman P2, P10, P20, P200, P1000)	Gilson, Middleton, WI, USA
Power supply (Power Pac HC)	Bio-Rad Laboratories GmbH, München, Germany
Rotors (SS-34, SLA-1500, Sorvall)	Thermo Fisher Scientific, Waltham, MA, USA
Spectrophotometer (Genesys 10S UV-Vis)	Thermo Fisher Scientific, Waltham, MA, USA
Thermocycler (Mastercycler Gradient)	Eppendorf, Hamburg, Germany
Thermomixer	Eppendorf, Hamburg, Germany
Ultrasonic processor UP200S	Hielscher Ultrasound Technology
Ultrasonic unit (Transsonic 420)	Elma Hans Schmidbauer GmbH & Co. KG, Singen, Germany
Vacuum pump	ABM Greiffenberger, Marktredwitz, Germany
Vortex mixer (Vortex Genie 2)	Scientific Industries, Bohemia, NY, USA

2.1.2 Software

Name	Source
EzChrom elite	Agilent Technologies, Santa Clara, CA, USA
GraphPad Prism 6	GraphPad Software, Inc., La Jolla, CA, USA
Unicorn V4.00.16	GE Healthcare Europe GmbH, Freiburg, Germany

2.1.3 Chemicals and Reagents

Name	Source
1,2-Propanediol	Merck, Darmstadt, Germany
1,4-Dithiothreitol (DTT)	Applichem GmbH, Darmstadt, Germany
11-Deoxycorticosterone (11-DOC)	Sigma-Aldrich, St. Louis, MO, USA
11-Deoxycortisol (RSS)	Sigma-Aldrich, St. Louis, MO, USA
2,5-Hexanedione	Alfa Aesar GmbH & Co KG, Karlsruhe, Germany
21-Hydroxypregnenolone	Sigma-Aldrich, St. Louis, MO, USA
2-Hydroxyacetophenone	Sigma-Aldrich, St. Louis, MO, USA
2-Mercaptoethanol (2-ME)	Roth, Karlsruhe, Germany
2-Propanol	Sigma-Aldrich, St. Louis, MO, USA

3,4-Hexanedione	Alfa Aesar GmbH & Co KG, Karlsruhe, Germany
3-Bromopyruvic acid	Fisher Scientific GmbH, Nidderau, Germany
5-Bromo-4-chloro-3-indolyl phosphate/Nitro blue tetrazolium (BCIP/NBT)	Sigma-Aldrich, St. Louis, MO, USA
Acetic acid	Fisher Scientific GmbH, Schwerte, Germany
Acetonitrile, chromasolv gradient-grade	Sigma-Aldrich, St. Louis, MO, USA
Acetylacetone	Sigma-Aldrich, St. Louis, MO, USA
Agar	Roth, Karlsruhe, Germany
Agarose	Roth, Karlsruhe, Germany
Ammonium chloride	Grüssing GmbH Analytika, Filsum, Germany
Ammonium persulfate (APS)	Merck, Darmstadt, Germany
Ammonium sulfate	Honeywell Speciality Chemicals Seelze GmbH, Seelze, Germany
Calcium chloride dehydrate	Sigma-Aldrich, St. Louis, MO, USA
Carbenicillin disodium salt	Roth, Karlsruhe, Germany
Casamino acids (N-Z Amine A)	Sigma-Aldrich, St. Louis, MO, USA
Chloroform	Sigma-Aldrich, St. Louis, MO, USA
Coomassie brilliant blue R250	Serva, Heidelberg, Germany
Corticosterone	Sigma-Aldrich, St. Louis, MO, USA
Cortisol	Sigma-Aldrich, St. Louis, MO, USA
Cortisone acetate	Sigma-Aldrich, St. Louis, MO, USA
D-fructose	Sigma-Aldrich, St. Louis, MO, USA
D-galactose	Merck, Darmstadt, Germany
D-glucose	Sigma-Aldrich, St. Louis, MO, USA
D-mannitol	Sigma-Aldrich, St. Louis, MO, USA
D-mannose	Merck, Darmstadt, Germany
Doxorubicin	Applichem GmbH, Darmstadt, Germany
D-sorbitol	Merck, Darmstadt, Germany
Ethanol	VWR Prolabo, Dublin, Ireland
Ethylenediaminetetraacetic acid (EDTA)	Applichem GmbH, Darmstadt, Germany
Glutathione, oxidized (GSSG)	Sigma-Aldrich, St. Louis, MO, USA

Glutathione, reduced (GSH)	Sigma-Aldrich, St. Louis, MO, USA
Glycerol	Applichem GmbH, Darmstadt, Germany
Glycine	Roth, Karlsruhe, Germany
Glyoxal	Sigma-Aldrich, St. Louis, MO, USA
HEPES (4-(2-Hydroxyethyl)piperazine-1-ethanesulfonic acid)	Applichem GmbH, Darmstadt, Germany
Hydrochloric acid, concentrated	Sigma-Aldrich, St. Louis, MO, USA
Hydroxyacetone	Alfa Aesar GmbH & Co KG, Karlsruhe, Germany
Imidazole	Sigma-Aldrich, St. Louis, MO, USA
Inositol	Applichem GmbH, Darmstadt, Germany
Isopropyl β -D-1-thiogalactopyranoside (IPTG)	Fisher Scientific GmbH, Schwerte, Germany
Kanamycin sulfate	Roth, Karlsruhe, Germany
L-arabinose	Roth, Karlsruhe, Germany
Lauric acid	Sigma-Aldrich, St. Louis, MO, USA
Lithium dihydroxyacetone phosphate	Sigma-Aldrich, St. Louis, MO, USA
Luminol reagent	Santa Cruz Biotechnology, Heidelberg, Germany
Magnesium chloride	Sigma-Aldrich, St. Louis, MO, USA
Magnesium sulfate	Sigma-Aldrich, St. Louis, MO, USA
Manganese (II) chloride tetrahydrate	Sigma-Aldrich, St. Louis, MO, USA
Methanol	Sigma-Aldrich, St. Louis, MO, USA
Methanol, chromasolv gradient-grade	Sigma-Aldrich, St. Louis, MO, USA
Myristic acid	Sigma-Aldrich, St. Louis, MO, USA
Oxaloacetic acid	Sigma-Aldrich, St. Louis, MO, USA
Peptone/tryptone from casein	Roth, Karlsruhe, Germany
Phenylmethanesulfonyl fluoride (PMSF)	Sigma-Aldrich, St. Louis, MO, USA
Potassium 5-keto-D gluconate	Sigma-Aldrich, St. Louis, MO, USA
Potassium hydroxide	Sigma-Aldrich, St. Louis, MO, USA
Potassium phosphate dibasic	Merck, Darmstadt, Germany
Potassium phosphate monobasic	Merck, Darmstadt, Germany
Potassium chloride	Merck, Darmstadt, Germany
Pregnenolone	Sigma-Aldrich, St. Louis, MO, USA

Progesterone	Sigma-Aldrich, St. Louis, MO, USA
Protease-peptone	Becton Dickinson, Heidelberg, Germany
Rotiphorese acrylamide gel 30 (37.5:1)	Roth, Karlsruhe, Germany
Roti-Quant reagent	Roth, Karlsruhe, Germany
Rubidium chloride	Sigma-Aldrich, St. Louis, MO, USA
Sodium dodecyl sulfate (SDS)	Serva Electrophoresis GmbH, Heidelberg, Germany
Sodium acetate	Sigma-Aldrich, St. Louis, MO, USA
Sodium chloride	Sigma-Aldrich, St. Louis, MO, USA
Sodium D-gluconate	Applichem GmbH, Darmstadt, Germany
Sodium hydroxide	Sigma-Aldrich, St. Louis, MO, USA
Sodium phosphate dibasic anhydrous	Merck, Darmstadt, Germany
Sodium phosphate dibasic heptahydrate	Merck, Darmstadt, Germany
Sodium phosphate monobasic	Merck, Darmstadt, Germany
Sodium pyruvate	Boehringer Mannheim, Mannheim, Germany
Sodium 2-oxobutyrate	Sigma-Aldrich, St. Louis, MO, USA
Sucrose	Merck, Darmstadt, Germany
Tetramethylethylenediamine (TEMED)	Roth, Karlsruhe, Germany
Testosterone propionate	Sigma-Aldrich, St. Louis, MO, USA
Trifluoroacetic acid, HPLC grade	Applichem GmbH, Darmstadt, Germany
Tris base	Roth, Karlsruhe, Germany
Tris-HCl	Roth, Karlsruhe, Germany
Triton X-100	Applichem GmbH, Darmstadt, Germany
Tween 20	Roth, Karlsruhe, Germany
Urea	Merck, Darmstadt, Germany
Yeast extract	Roth, Karlsruhe, Germany
Zinc chloride	Merck, Darmstadt, Germany
Zulkowsky starch	Merck, Darmstadt, Germany
β -Nicotinamide adenine dinucleotide (NAD ⁺)	Applichem GmbH, Darmstadt, Germany
β -Nicotinamide adenine dinucleotide reduced disodium salt (NADH)	Applichem GmbH, Darmstadt, Germany

2.1.4 Kits

Name	Source
Low molecular weight gel filtration calibration kit	GE Healthcare Europe GmbH, Freiburg, Germany
High molecular weight gel filtration calibration kit	GE Healthcare Europe GmbH, Freiburg, Germany
GeneJET Genomic DNA Purification kit	Fisher Scientific GmbH, Schwerte, Germany
In-Fusion HD EcoDry cloning kit	Clontech, Saint-Germain-en-Laye, France
Topo TA cloning kit (pCR2.1)	Life Technologies GmbH, Darmstadt, Germany
QIAquick PCR purification kit	Qiagen, Hilden, Germany
QIAquick gel extraction kit	Qiagen, Hilden, Germany
QIAprep Spin Miniprep Kit	Qiagen, Hilden, Germany

2.1.5 Antibodies

Name	Source
6xHIS epitope tag mouse monoclonal antibody	Fisher Scientific GmbH, Schwerte, Germany
Goat anti-mouse IgG (H+L) antibody labeled with the alkaline phosphatase	KPL, Gaithersburg, USA
PEYFK epitope tag mouse monoclonal antibody	Produced by hybridoma technology in our lab
Rabbit anti-mouse IgG (H+L) antibody conjugated with the horseradish peroxidase	Antibodies-online GmbH, Aachen, Germany

2.1.6 Enzymes and proteins

Name	Source
Aprotinin	Roth, Karlsruhe, Germany
BamHI restriction endonuclease	NEB, Ipswich, USA
BglII Fast Digest restriction endonuclease	Fisher Scientific Germany GmbH, Schwerte, Germany
Bovine serum albumin (BSA)	Roth, Karlsruhe, Germany
BspHI restriction endonuclease	NEB, Ipswich, USA
DNase I	Roth, Karlsruhe, Germany
IgA1 protease	Mobitech GmbH, Göttingen, Germany
KOD DNA polymerase	Merck KGaA, Darmstadt, Germany
Lysozyme from chicken egg white	Roth, Karlsruhe, Germany
Milk powder	Roth, Karlsruhe, Germany

NcoI restriction endonuclease	NEB, Ipswich, USA
PageRuler prestained protein ladder	Fisher Scientific Germany GmbH, Schwerte, Germany
PageRuler unstained protein ladder	Fisher Scientific Germany GmbH, Schwerte, Germany
Phusion High-Fidelity DNA polymerase	NEB, Ipswich, USA
Proteinase K from <i>Tritirachium album</i>	Sigma-Aldrich, St. Louis, MO, USA
T4 DNA ligase	NEB, Ipswich, USA
Taq DNA polymerase	Fisher Scientific Germany GmbH, Schwerte, Germany
XbaI Fast Digest restriction endonuclease	Fisher Scientific Germany GmbH, Schwerte, Germany

2.1.7 Oligonucleotides

DNA oligonucleotides were synthesized by Eurofins MGW Operon (Ebersberg, Germany).

Table 2.1 Oligonucleotide sequences

Name	Sequence (5'→3')
AT001	AGA AGG AGA TAT ACC ATG ATT TTA AGT GCA T
AT002	TAG CAG CCG GAT CCG TTA ACG CGC CAG CCA AC
AT003	AGA AGG AGA TAT ACC ATG TTT AAT TCT GAC A
AT004	TAG CAG CCG GAT CCG TTA ATT GAG CTC CTG T
AT009	GGT ATA TCT CCT TCT TAA AGT TAA ACA AAA TT
AT010	CGG ATC CGG CTG CTA ACA AAG CCC GAA AGG A
AT011	AGA AGG AGA TAT ACC ATG ACT ACT ATT GTT G
AT012	TAG CAG CCG GAT CCG TTA CAG CGC AGC CAC A
AT018	GGT GAT GTT CTG CGG AGT ACC GTG AGC GTA AGC AGA GG
AT019	ATT GAG GGC CGC ATC CCG GAA TAC TTT AAA CTG AC
AT020	CCG CAG AAC ATC ACC CAC CAC CAT CAC CAT CAT ATG ATT TTA AGT GCA TTT TCT CTC GA
AT021	GAT GCG GCC CTC AAT ACG CGC CAG CCA ACC GCC ATC C
AT023	CAT CAC CAT CAT ATG ATT TTA AGT GCA TTT TC
AT024	CAT ATG ATG GTG ATG GTG GTG CAT GGT ATA TCT CCT TC
AT025	AGA AGG AGA TCT AGA ATG CAC CAC CAT C
AT027	CCG CCA GAA CCA CCA CCA CCA GCA CGA CGA GCA CGC GCC AGC C
AT028	TGG TGG TTC TGG CGG TGG CGG TTC CGG CGG CGG CGG CAG CAT TGA GGG CCG C
AT029	GAA ATA TTC AGG AGA TCT ACG CGC CAG CCA AC
AT030	AGA TCG TGG AGA AGG TGG ACC TTT G
AT031	CCT TCT CCA CGA TCT CTT CCC ACA TCT GAT AC
ATseq2	AAG GGG TTA TGC TAG TTA TTG CTC
DB010	CCT CCC ATA ATC CCT AAG GTA AAA TCA CCC AGT TG
E132_for	GGC AGG GTG TCA TGA GCA GCA ATA CA
E132_rev	CCT TTT GTA GGA TCC TTA TTC TCG CGA

FB001	AAA AAT AGG CGT ATC ACG AGG
MT013	CTT ACC GTC AAC GTG GAT CAA C
MT014	CGC CTT TCA CCG TAT TAT CG
pTF	CTC GAA AAT AAT AAA GGG AAA ATC AG
pTR	TGG TAG TGT GGG GAC TC
SH002	CAC CAC CAG ACG GTC CGT AAG TG
SH011	CAG CAT ATG CAC ATG GAA CAC C
T7 promoter	TAA TAC GAC TCA CTA TAG GG

Table 2.2 Oligonucleotides used for DNA sequence analysis of plasmids.

Plasmid	Sequencing primers*
pET-11d-ydbC	T7 promoter, FB001
pET-11d-kduD, pET-11d-His-kduD, pET-11d-hdhA, pET-11d-uxuB	T7 promoter, ATseq2
pAT002	SH002, SH011
pAT004	T7 promoter, ATseq2, DB010
pMATE-AT001, pMATE-AT002	pTF, pTR, MT013, MT014

* - The sequence of the oligonucleotide is provided in the Table 2.1 above.

2.1.8 Plasmids

Name	Antibiotic resistance	Source
pET-11d	Carbenicillin	Merck KGaA, Darmstadt, Germany
pET-SH3-SDH08	Carbenicillin	(Jose and von Schwichow 2004)
pMT005	Kanamycin	(Teese et al., unpublished)
pET-11d-ydbC	Carbenicillin	This study
pET-11d-kduD	Carbenicillin	This study
pET-11d-His-kduD	Carbenicillin	This study
pET-11d-hdhA	Carbenicillin	This study
pET-11d-uxuB	Carbenicillin	This study
pAT002	Carbenicillin	This study
pAT004	Carbenicillin	This study
pMATE-AT001	Kanamycin	This study
pMATE-AT002	Kanamycin	This study

2.1.9 Bacterial strains

<i>Escherichia coli</i> strain	Genetic markers	Reference/Source
BL21 (DE3)	<i>B, F⁻, dcm, ompT, lon, hsdS(rB⁻ mB⁻), gal, λ(DE3)</i>	(Studier and Moffatt 1986)
BL21	<i>B, F⁻, dcm, ompT, lon, hsdS(rB⁻ mB⁻), gal</i>	(Studier and Moffatt 1986)
ClearColi™ BL21 (DE3)	<i>F⁻ ompT hsdSB (rB⁻ mB⁻) gal dcm lon λ(DE3 [lacI lacUV5-T7 gene 1 ind1 sam7 nin5]) msbA148 ΔgutQΔkdsDΔlpxLΔlpxMΔpagPΔlpxPΔeptA</i>	Lucigen, Middleton, USA
DH5α	<i>F⁻, φ80dlacZΔM15, Δ(lacZYA-argF)U169, deoR, recA1, endA1, hsdR17(rK⁻mK⁺), phoA, supE44, λ-, thi-1, gyrA96, relA1</i>	(Bethesda Research Labs, 1986)
F470	<i>F⁻, met⁻, his⁻, pro⁻, mtl⁻, (Str^r)</i>	(Schmidt et al. 1970)
F515	<i>F⁻, met⁻, his⁻, pro⁻, mtl⁻, (Str^r)</i>	(Schmidt et al. 1970)
JK321 (DE3)	<i>ΔompT, proC, leu-6, trpE38, entA, zih12::Tn10, dsbA::kan λ(DE3) lysogen</i>	(Jose et al. 1996, Handel 2003)
Stellar™	<i>F⁻, ara, Δ(lac-proAB) [Φ80d lacZΔM15], rpsL(str), thi, Δ(mrr-hsdRMS-mcrBC), ΔmcrA, dam, dcm</i>	Clontech, Saint-Germain-en-Laye, France
Top10	<i>F⁻ mcrA Δ(mrr-hsdRMS-mcrBC) φ80lacZΔM15 ΔlacX74 recA1 araD139 Δ(ara-leu)7697 galU galK rpsL (Str^R) endA1 nupG</i>	Life Technologies GmbH, Darmstadt, Germany
UT5600 (DE3)	<i>F⁻, ara-14, leuB6, secA6, lacY1, proC14, tsx-67, Δ(ompT-fepC)266, entA403, trpE38, rfbD1, rpsL109(Str^r), xyl-5, mtl-1, thi-1, λ(DE3)</i>	(Earhart et al. 1979, Jose and von Schwichow 2004)
UT5600	<i>F⁻, ara-14, leuB6, secA6, lacY1, proC14, tsx-67, Δ(ompT-fepC)266, entA403, trpE38, rfbD1, rpsL109(Str^r), xyl-5, mtl-1, thi-1</i>	(Earhart et al. 1979)

2.1.10 Media

Media used for the cultivation and storage of *E. coli* as well as buffers used for the preparation of competent *E. coli* cells were sterilized by autoclaving (121 °C, 20 min). The heat-labile components, such as antibiotics, as well as glucose were filter-sterilized.

LB medium: 5 g/l yeast extract, 10 g/l tryptone, 10 g/l NaCl, pH 7.0.

LB agar: 5 g/l yeast extract, 10 g/l tryptone, 10 g/l NaCl, 16 g/l agar, pH 7.0.

M9 medium: 6 g/l Na₂HPO₄, 3 g/l KH₂PO₄, 0.5 g/l NaCl, 1 g/l NH₄Cl, 0.6 % glucose (w/v), 2 mM MgSO₄, 0.1 mM CaCl₂, pH 7.0.

M9Cas medium: 12.8 g/l Na₂HPO₄·7H₂O, 3 g/l KH₂PO₄, 0.5 g/l NaCl, 1 g/l NH₄Cl, 2 g/l casamino acids, 0.4 % glucose (w/v), 2 mM MgSO₄, 0.1 mM CaCl₂, pH 7.0.

SOC medium: 20 g/l tryptone, 5 g/l yeast extract, 0.5 g/l NaCl, 2.5 mM KCl, 20 mM D-glucose, 10 mM MgCl₂, pH 7.0.

PPM medium: 15 g/l Proteose-peptone, 5 g/l NaCl, 1 g/l Zulkowsky starch, 1 g/l KH₂PO₄, 0.8 g/l K₂HPO₄, 25 % glycerol (w/v).

2xYT medium: 16 g/l tryptone, 10 g/l yeast extract, 5 g/l NaCl, pH 7.0.

2.1.11 Buffers and other solutions

Buffers for preparation of competent E. coli cells

TMF buffer: 100 mM CaCl₂, 50 mM RbCl, 40 mM MnCl₂.

Mg²⁺-solution: 0.5 M MgCl₂, 0.5 M MgSO₄.

10 % glycerol solution: 10 % glycerol (v/v).

KduD purification buffers

Buffer A: 20 mM Tris-HCl pH 8.0, 1 mM EDTA.

Buffer B: 1 M NaCl in buffer A.

Buffer C: 50 mM potassium phosphate pH 7.0.

Buffer D: 5 mM NADH in buffer C.

Buffer E: 20 mM sodium phosphate pH 6.6.

Buffer F: 1 M NaCl in buffer E.

Buffer G: 20 mM Tris-HCl, 150 mM NaCl, pH 8.0.

Buffer H: 50 mM NaH₂PO₄ pH 0.8, 300 mM NaCl, 10 mM imidazole, pH 8.0.

KduD storage buffer: 20 mM Tris-HCl, 2 mM DTT, pH 8.0.

TE buffer: 10 mM Tris-HCl, pH 8.0, 1 mM EDTA.

Buffers for DNA electrophoresis

TAE buffer: 40 mM Tris, 20 mM acetic acid, 1 mM EDTA (pH 8.0).

6x DNA loading dye (Fisher Scientific GmbH, Schwerte, Germany): 10 mM Tris-HCl (pH 7.6), 0.03% bromophenol blue, 0.03% xylene cyanol FF, 60% glycerol, 60 mM EDTA.

DNA staining solution: GelGreen dye (10,000x, Biotium, Hayward, CA, USA) diluted in water to the final concentration of 1x.

Buffers for SDS-PAGE

2x protein electrophoresis sample buffer: 100 mM Tris-HCl, pH 6.8, 4 % SDS, 0.2 % bromophenol blue, 0.2 M DTT, 20 % glycerol.

SDS-running buffer: 3 g/l Tris-base, 18.8 g/l glycine, 1 g/l SDS.

Acrylamide solution: 30 % acrylamide, 0.8 % bisacrylamide (Roth, Karlsruhe, Germany).

4x Stacking gel solution: 6.06 g/100 ml Tris-base, 0.4 g/100 ml SDS, 0.4 g/100 ml tetramethylethylenediamine (TEMED), pH 6.8.

4x Separating gel solution: 18.17 g/100 ml Tris-base, 0.4 g/100 ml SDS, 0.4 g/100 ml TEMED, pH 8.8.

Ammonium persulfate (APS) solution: 10 % APS (w/v).

Protein staining solution: 2 g Coomassie Brilliant blue G-250, dissolved in 500 ml methanol, 100 ml acetic acid, 400 ml H₂O.

Gel destaining solution: 10 % acetic acid (v/v).

Western blot buffers

Transfer buffer: 25 mM Tris-base, 192 mM glycine, 20 % methanol (v/v), pH 8.3-8.4.

TBS buffer (1x): 25 mM Tris-base, 140 mM NaCl, 2.7 mM KCl, pH 7.4.

Membrane protein isolation buffers and solutions

Tris-HCl buffer: 0.2 M Tris-HCl, pH 8.0.

Sucrose solution: 1 M sucrose.

EDTA solution: 10 mM EDTA, pH 8.0.

Lysozyme solution: 10 mg/ml lysozyme.

Phenylmethanesulfonyl fluoride solution (PMSF): 100 mM PMSF in isopropanol.

Aprotinin solution: 10 mg/ml aprotinin dissolved in 10 mM 4-(2-hydroxyethyl)-1-piperazineethanesulfonic acid (HEPES) buffer (pH 8.0).

DNase I solution: 1 mg/ml DNase I.

Proteinase K solution: 5 mg/ml proteinase K.

Fetal calf serum (FCS) solution: 10 % FCS.

Extraction buffer: 50 mM Tris-HCl, 10 mM MgCl₂, 2 % Triton-X-100, pH 8.0.

PCR buffers and solutions

Phusion DNA polymerase buffer: 5x Phusion HF buffer (NEB, Ipswich, USA).

10x KOD polymerase buffer (Merck, Darmstadt, Germany): 1.2 M Tris-HCl, 100 mM KCl, 60 mM (NH₄)₂SO₄, 1 % Triton X-100, 0.01 % BSA, pH 8.0.

10x Taq DNA polymerase buffer (Fisher Scientific Germany GmbH, Schwerte, Germany): 100 mM Tris-HCl (pH 8.8), 500 mM KCl, 0.8 % Nonidet P40 (v/v).

25 mM MgCl₂ (Merck, Darmstadt, Germany).

dNTP mix solution: 10 mM each dNTP (Fisher Scientific – Germany GmbH, Schwerte, Germany).

DNA ligation buffer

10x T4 DNA ligase reaction buffer (NEB, Ipswich, USA): 500 mM Tris-HCl, 100 mM MgCl₂, 10 mM ATP, 100 mM DTT, pH 7.5.

DNA digestion buffers

10x Fast Digest Green buffer (Fisher Scientific GmbH, Schwerte, Germany).

10x NeBuffer 4 (NEB, Ipswich, USA): 500 mM potassium acetate, 200 mM Tris-acetate, 100 mM magnesium acetate, 10 mM DTT, pH 7.9.

IgA1 protease reaction buffer

IgA1 protease reaction buffer: 50 mM Tris-HCl, 100 mM NaCl, 1 mM EDTA, pH 7.5.

Other buffers

Sodium acetate buffers: 1 M pH 5.0 and pH 5.5.

Potassium phosphate buffers: 1 M pH 6.1, pH 7.0, pH 8.0.

Tris-HCl buffers: 1 M pH 8.5, pH 9.0.

Glycine-NaOH buffers: 1 M pH 9.0, pH 9.5, pH 10.0, pH 10.5.

2.1.12 Protein chromatography media

Name	Source
Blue sepharose 6 fast flow	GE Healthcare Europe GmbH, Freiburg, Germany
Ni-NTA agarose	Qiagen GmbH, Hilden, Germany
Poros HS 20	Applied Biosystems, Foster City, USA
Q-sepharose fast flow	GE Healthcare Europe GmbH, Freiburg, Germany
Superdex 200	GE Healthcare Europe GmbH, Freiburg, Germany

2.1.13 Other materials

Name	Source
96 Well microplate, PS, F-bottom	Greiner Bio-One GmbH, Frickenhausen, Germany
Amicon molecular weight cut-off (MWCO) columns Ultracel 10k	Merck KGaA, Darmstadt, Germany
Centrifugal tubes (15 and 50 ml)	Sarstedt, Nümbrecht, Germany
Cryovials	VWR International GmbH, Darmstadt, Germany
Disposable cuvettes for OD measurements	GML alfaplast, München, Germany
Durapore membrane filters (HVLP, pore size 0.45 µm)	Merck Darmstadt, Germany
Glass beads	Marienfeld-Superior, Lauda-Königshofen, Germany
LiChrosphere 60 RP-select B HPLC column	Merck Darmstadt, Germany
Microtubes (0.2, 1.5 and 2 ml)	Sarstedt, Nümbrecht, Germany
Minicolumn (Econocolumn)	Bio-Rad Laboratories GmbH, München, Germany
Petri dishes	Greiner Bio-One GmbH, Frickenhausen, Germany
Pipette tips (10 µl)	Gilson, Middleton, WI, USA
Pipette tips (200 and 1000 µl)	Sarstedt, Nümbrecht, Germany
Polyvinylidene fluoride (PVDF) membrane	Macherey-Nagel, Düren, Germany
Protein dialysis clips	Spectrum Europe, Breda, Netherlands
Quartz suprasil (QS, 200-2500 nm) absorption cell, 10 mm	Hellma GmbH & Co. KG, Muellheim, Germany
Syringe filter units (Millex-GP, 0.22 µm)	Merck KGaA, Darmstadt, Germany
Syringes (Omniflix 10 and 20 ml)	B. Braun medical Inc., Bethlehem, PA, USA

Vacuum filtering apparatus	Duran Group GmbH, Wertheim, Germany
Visking Dialysis Tubing (MWCO 12,000-14,000, pore diameter 25 Å)	Serva Electrophoresis GmbH, Heidelberg, Germany

2.2 Methods

2.2.1 Partial purification of *E. coli* steroid reductase

E. coli DH5 α cells were grown in two liters of LB medium (4 x 2 l flasks with 500 ml of LB medium) at 37 °C overnight with vigorous shaking. Bacterial cells were collected by centrifugation (10 min, 4,300 g, 4 °C). All protein purification steps including cell disruption, centrifugation and column chromatography were conducted at 4 °C. Chromatography steps were carried out with an ÄKTA FPLC, using flow rates recommended by the manufacturer for each appropriate media and fraction volumes of 0.4 to 5 ml.

Preparation of cell-free extract

Wet cell biomass (11 g) was resuspended in 11 ml of buffer A containing 1 mM PMSF and disrupted by sonication (6 cycles of 20 s on and 20 s off, amplitude 60%, UP200S Hielscher Ultrasound Technology). The cell debris was removed by centrifugation (14,000 g, 30 min). In total 12.5 ml of cell-free extract were obtained.

Ammonium sulfate precipitation

Ammonium sulfate was added to the 12.5 ml of cell-free extract to a final concentration of 40% (w/v). After one hour incubation at 4°C, the precipitate was removed by centrifugation (14,000 g, 30 min). Ammonium sulfate was then added to the supernatant to a final concentration of 80% (w/v). After one hour incubation at 4°C the sample was centrifuged and the protein pellet resuspended in buffer A. This sample was dialyzed against buffer A overnight to remove salts before anion exchange chromatography.

Anion exchange chromatography

The enzyme solution was loaded on a Q sepharose fast flow column (1.2 x 28 cm), equilibrated with buffer A. The enzyme was eluted with linear gradient (0-100%) of buffer B. All fractions were tested for 11-DOC C-20 carbonyl reductase activity using the HPLC assay described below. The active fractions were combined and concentrated to 10 ml with molecular weight cut-off (MWCO) columns (Ultracel 10k, Amicon), and dialyzed against buffer C.

Blue sepharose chromatography

Blue sepharose chromatography media can be used to purify NADH-dependent enzymes. The enzyme solution was loaded on a Blue sepharose 6 fast flow column (1.2 x 7.7 cm), equilibrated with buffer C. Proteins were eluted with linear gradient (0-100%) of buffer D. The fractions containing 11-DOC reductase activity were mostly found in the flowthrough, suggesting that the enzyme responsible did not bind the media. These fractions were combined and proteins concentrated to 12 ml with MWCO columns as described above, and dialyzed against buffer E.

Cation exchange chromatography

The enzyme solution was loaded on a Poros HS 20 column (1.2 x 7.7 cm), equilibrated with buffer E. Proteins were eluted with linear gradient (0-100%) of buffer F. The fractions containing 11-DOC C20 reductase activity were mostly found in the flowthrough, suggesting that the enzyme responsible did not bind the media. These fractions were combined and concentrated to 0.55 ml with MWCO columns as described above.

Size exclusion chromatography

A Superdex 200 column (1.0 x 30 cm) was equilibrated with buffer G. The enzyme was loaded and proteins separated with a constant flow rate of 0.4 ml min⁻¹ buffer G. The fractions containing 11-DOC C20 reductase activity were concentrated to 0.15 ml with MWCO columns as described above. Ferritin (Mw 440 kDa), conalbumin (Mw 75 kDa) and aprotinin (Mw 6.5 kDa) were used as molecular weight standards.

2.2.2 Identification of proteins by mass spectrometry

The partially purified 11-DOC C20 carbonyl reductase after size exclusion chromatography was digested with trypsin and analyzed by the Core Unit Integrated Functional Genomics of the Interdisciplinary Center for Clinical Research of the Medical Faculty of the University of Münster. Tryptic peptides were separated with C18 reversed phase chromatography, and nanoUPLC-MS/MS and MS^E was conducted as previously described (Pakkianathan et al. 2012) with a Q-TOF Premier (Waters Corporation). Data were searched against all *E. coli* sequences in public databases. Stringent validation settings were applied. Only proteins identified with high confidence were considered.

2.2.3 Enzyme and protein assays

The assay mixture for steroid reductase activity comprised, in 0.1 ml, 100 mM potassium phosphate buffer (pH 7.0), 0.4 mM NADH, 0.4 mM 11-DOC (from 100 mM stock solution in methanol) and an appropriate amount of enzyme (0.020-0.376 mg ml⁻¹ of protein). Samples were incubated at 37 °C for 2 hours, then heated at 99 °C for two minutes and cooled on ice. After addition of 0.15 mM of 11-deoxycortisol (internal standard, 10 mM stock solution in methanol), steroid compounds were extracted with an equal amount of chloroform. Extracted compounds were dissolved in 50 µl of acetonitrile and were analyzed by HPLC as described below (2.2.4). One unit of enzyme activity was defined as the amount of enzyme catalyzing the reduction of 1 µmol of 11-DOC per minute under the assay conditions.

In order to investigate cofactor specificity, 29.1 mg of partially purified enzyme (after purification with Poros Sepharose) was incubated in 0.2 ml of 100 mM potassium phosphate buffer (pH 7.0) with 0.4 mM 11-DOC for 24 hours at 30 °C. These samples contained either 0.4 mM NADH, 0.4 mM NADPH or 0.4 mM NADH+20 mM EDTA. After incubation, the steroid products were extracted and analyzed as described above.

Protein concentration was measured with a Bradford assay (Roti-Quant reagent) calibrated with bovine serum albumin as a standard.

2.2.4 Analytical HPLC

Reaction products were analyzed with VWR HPLC-System LaChrom Elite equipped with a diode array detector L-2455. A reversed phase column (125 mm x 4 mm internal diameter), filled with LiChrosphere 60 RP-select B 5 µm diameter particles) was used to separate 11-DOC conversion products, which were detected at 240 nm. A flow rate of 1 ml min⁻¹, a constant column temperature (22 °C) and a mobile phase consisting of water and acetonitrile (60:40, v/v) were used. The areas under the peaks were calculated with the associated software (EzChrom elite). The concentration of products was calculated using a standard curve of 11-DOC.

All other steroids were analyzed as described above with a few modifications. Conversion products of 11-deoxycortisol (RSS), corticosterone, testosterone propionate, progesterone, cortisone acetate and cortisone were detected at 240 nm, of pregnenolone and 21-hydroxypregnenolone at 196 nm, and of cortisol at 245 nm. The isocratic mobile phase

consisted of water and acetonitrile (v/v) 70:30 for separation of conversion products of RSS, corticosterone and pregnenolone, 60:40 for 21-hydroxypregnenolone, 40:60 for testosterone propionate, 50:50 for progesterone and 65:35 for cortisone acetate and cortisone. In the case of cortisol a gradient of water and acetonitrile (v/v) from 85:15 to 50:50 was used.

Doxorubicin and its metabolites were detected at 480 nm, using a mobile phase consisting of water (+0.1 % trifluoroacetic acid) and acetonitrile (77:23, v/v).

2.2.5 Cloning and expression of *ydbC* gene

The ORF of *ydbC* was amplified by polymerase chain reaction (PCR) from genomic DNA of *E. coli* DH5 α (whole-cells were used in PCR as a DNA template) with high-fidelity KOD DNA polymerase using a pair of primers: E132_for and E132_rev containing BspHI and BamHI restriction endonuclease recognition sites, respectively (**Table 2.1**). The PCR fragment was subcloned into PCR2.1-TopoTA vector using TopoTA cloning kit, then excised with BspHI and BamHI and cloned into the NcoI/BamHI-digested pET-11d using T4 DNA ligase. Recombinant proteins were overexpressed in *E. coli* strain BL21 (DE3). Cells were grown in LB medium with 0.05 mg ml⁻¹ carbenicillin at 37 °C until the OD₆₀₀ reached 0.6-0.8. Protein expression was then induced by the addition of 1 mM IPTG. The induced cells were cultured at 30 °C for a further two hours. Afterwards, cells were collected by centrifugation (4 °C, 3,880 g, 5 min), concentrated in the fresh LB medium to the final concentration of OD₆₀₀=10, and were used directly in a whole cell biotransformation assay. After addition of 11-DOC (50 mg ml⁻¹ stock solution in ethanol) to the final concentration of 1.5 mM, 700 μ l of concentrated cell suspensions were incubated at 30 °C for 20 h. Then, steroids were extracted with an equal amount of chloroform. Extracted compounds were dissolved in 700 μ l of acetonitrile and analyzed by HPLC as described above (**2.2.4**).

Recombinant overexpression of the YdbC oxidoreductase in *E. coli* BL21 (DE3) cells was monitored by sodium dodecyl sulfate polyacrylamide gel electrophoresis (SDS-PAGE) of proteins from whole cells. *E. coli* cell suspensions with an OD₆₀₀=10 in TE buffer were mixed with an equal volume of 2x protein electrophoresis sample buffer, boiled for 5 min, and analyzed on 10 % polyacrylamide gels.

2.2.6 Cloning and expression of *kduD*, *hdhA* and *uxuB* genes

To determine which of the three oxidoreductases from DH5 α (*KduD*, *HdhA* and *UxuB*) was responsible for the C20 ketosteroid reductase activity, all three were cloned and overexpressed in *E. coli* with their native start and stop codons. Genomic DNA of *E. coli* strain DH5 α was isolated using GeneJET Genomic DNA Purification Kit. The ORFs of *kduD*, *hdhA* and *uxuB* were amplified by PCR with Phusion High-Fidelity DNA polymerase from genomic DNA of *E. coli* DH5 α using the following pairs of primers: AT001 and AT002 for *kduD*, AT003 and AT004 for *hdhA*, and AT011 and AT012 for *uxuB* (**Table 2.1**). The backbone of the pET-11d vector was amplified with the primers AT009 and AT010 (**Table 2.1**). The two PCR products (the amplified *kduD*, *hdhA* or *uxuB* gene, and amplified vector backbone) were combined to form a plasmid using In-Fusion HD EcoDry cloning kit as per the manufacturer's instructions.

Recombinant proteins were overexpressed in *E. coli* strain UT5600 (DE3). Cells were grown in LB medium with 0.1 mg ml⁻¹ carbenicillin at 37 °C until the OD₆₀₀ reached 0.6-0.8. Protein expression was then induced by the addition of 1 mM IPTG. The induced cells were cultured at 30 °C for a further three hours. Afterwards, cells were collected by centrifugation (4 °C, 3,880 g, 5 min), concentrated in the fresh LB medium to OD₆₀₀ = 25, and were used directly in a whole cell biotransformation assay.

Recombinant overexpression of the three NADH-dependent oxidoreductases in *E. coli* UT5600 (DE3) cells was monitored by SDS-PAGE of proteins from whole cells. *E. coli* cell suspensions with an OD₆₀₀=10 in TE buffer were mixed with an equal volume of 2x protein electrophoresis sample buffer, boiled for 5 min, and analyzed on 10 % polyacrylamide gels.

2.2.7 Whole cell biotransformation assay

Concentrated cell suspensions (200 μ l) of *E. coli* UT5600 (DE3) expressing the oxidoreductase were incubated with 0.4 mM of 11-DOC (10 mM stock solution in methanol) 14 h at 30 °C, followed by heating at 99 °C for one minute. An internal standard (11-deoxycortisol, 10 mM stock solution in methanol) was added to a final concentration of 0.15 mM and steroids were extracted with an equal amount of chloroform. Extracted compounds were dissolved in 50 μ l of acetonitrile and analyzed by HPLC as described above (**2.2.4**).

2.2.8 Evaluation of an effect of 11-DOC on the expression level of KduD in *E. coli*

E. coli DH5 α and *E. coli* UT5600 (DE3) cells were grown in LB medium at 37 °C until the OD₆₀₀ reached 0.5-0.6. Then, 0.1 % (v/v) of 11-DOC (100 mM solution in methanol) or pure methanol was added and cells were cultured at 37 °C overnight. The cell-free extracts were prepared from 100 ml of overnight cell cultures as described in previous section (2.2.1). Enzyme and protein assays were performed as described in previous section (2.2.3).

2.2.9 Cloning, expression and affinity purification of KduD

In order to obtain pure protein, KduD was overexpressed in *E. coli* UT5600 (DE3) with an N-terminal 6xHis tag and purified by affinity chromatography. To insert the 6xHis, the *kduD* gene was amplified from pET-11d-kduD by PCR with the primers AT023 and AT002 (Table 2.1). The backbone of pET-11d vector was amplified with the primers: AT024 and AT010 (Table 2.1). The two PCR products were combined to form a plasmid using In-Fusion HD EcoDry cloning kit (Clontech). Recombinant 6xHis-KduD was overexpressed in *E. coli* UT5600 (DE3). Cells were grown in 500 ml of LB medium with 0.1 mg ml⁻¹ of carbenicillin at 37 °C with vigorous shaking (200 rpm) until the OD₆₀₀ reached 0.6-0.8. Protein expression was then induced by the addition of 1 mM IPTG. The induced cells were cultured at 30 °C for a further two hours. Afterwards, cells were collected by centrifugation (4 °C, 3,880 g, 10 min). The cells (0.72 g of wet cell biomass) were resuspended in 7 ml of buffer H containing 1 mM PMSF and 10 mM imidazole. Cells were sonicated and cell debris was removed by centrifugation as described above. The obtained supernatant was loaded on minicolumn filled with 1 ml of Ni-NTA agarose pre-equilibrated with buffer H. The column was then washed with buffer H containing 20 mM imidazole to remove unbound proteins. The recombinant enzyme was eluted from the column with buffer H containing 250 mM imidazole. The purified enzyme was dialyzed against the KduD storage buffer. SDS-PAGE and assays of protein concentration and steroid reductase activity were conducted as described above.

2.2.10 Determination of pH and temperature optimum

The optimal temperature and pH was examined using 0.02 mg ml⁻¹ of purified 6xHis-KduD. The optimal pH for the reduction reaction was determined with 0.4 mM 11-DOC as a substrate in 100 mM sodium acetate, potassium phosphate, Tris-HCl or sodium glycine buffer containing

0.6 mM NADH. The samples were incubated at 37 °C for 40 minutes and product formation analyzed by HPLC as described above (2.2.4).

The optimal pH for oxidation reaction was determined with 100 mM D-gluconate as a substrate in 100 mM buffers containing 1 mM NAD⁺. The reaction was monitored spectrophotometrically with a reaction volume of 1 ml. The reaction was started by the addition of enzyme. The absorbance of reaction mixtures at 340 nm were recorded for three minutes at 37 °C using a spectrophotometer (Eppendorf Biospectrometer Kinetics). For calculation of initial velocities, the molar extinction coefficient of NADH (6,220 M⁻¹ cm⁻¹) was used. The optimum temperature was determined with 0.4 mM 11-DOC as substrate in 100 mM potassium phosphate buffer pH 7.0 with 0.6 mM NADH. Samples were incubated one hour with shaking at temperatures ranging from 4 to 55 °C (Thermomixer, Eppendorf) and product formation measured by HPLC as described above (2.2.4).

2.2.11 Determination of substrate specificity

The purified 6xHis-KduD was used as the enzyme source at a final concentration of 0.02 mg ml⁻¹. The reduction reactions were carried out in 100 mM potassium phosphate buffer pH 7.0, previously described as an optimal buffer for a closely related enzyme (Condemine et al. 1984). The oxidation reactions were performed in 100 mM glycine-NaOH buffer pH 9.3, previously described as an optimal buffer for the oxidation reaction of 2-keto-3-deoxy-D-gluconate (KDG) into 2,5-diketo-3-deoxygluconate (DKII) by *E. coli* KduD (Hantz 1977). Steroid compounds were dissolved in methanol to produce 10 mM stock solutions. Cortisone was prepared from commercial cortisone acetate by alkaline hydrolysis with 0.5 mM KOH at 25°C for 12 minutes followed by extraction with chloroform. The yield of cortisone was 55.7 %. Due to low solubility in methanol, pregnenolone and cortisone acetate were dissolved in methanol/chloroform mixture (80:20, v/v). The enzyme was incubated with 0.4 mM of steroid compound in buffer containing 0.6 mM of NADH for 2 hours at 37 °C. Product formation was measured by HPLC as described above (2.2.4). For pregnenolone and cortisone acetate, extracted steroids were dissolved in a mixture of acetonitrile/chloroform (80:20, v/v).

Partially hydrolyzed doxorubicin sample (hDox) was prepared by incubating 3.4 mM doxorubicin (dissolved in water) with 0.5 M HCl at 37° C for four hours. KduD activities against prepared hDox and doxorubicin were investigated by incubating 0.02 mg ml⁻¹ of KduD in 100 mM potassium phosphate buffer (pH 7.0) with 0.6 mM NADH and 0.15 mM hDOX (or

0.4 mM doxorubicin) at 37° C for 16 hours. The samples of hDox conversions were analyzed by HPLC as described above (2.2.4). The samples of doxorubicin conversions were mixed with the equal volume of chloroform and the aqueous phases were subjected to HPLC analysis as specified above (2.2.4).

A spectrophotometric assay was used to detect oxidation or reduction of non-steroid compounds. The final substrate concentration was typically 0.4 mM in buffer containing 0.6 mM NADH or 1 mM NAD⁺. Absorbance was measured at 340 nm with a microplate reader or spectrophotometer at 37 °C.

2.2.12 Evaluation of effect of salts, reducing/oxidizing and denaturing agents

An effect of various agents on the activity of KduD was tested for the D-gluconate oxidation reaction. The initial velocity of D-gluconate oxidation with KduD without an agent and in the presence of an agent was compared. The sample was composed of 100 mM glycine-NaOH buffer pH 9.3, 200 mM D-gluconate, 2 mM NAD⁺, 0.02 mg ml⁻¹ KduD and variable concentration of effector molecules (1-100 mM of divalent metal ion salts (ZnCl₂, MgSO₄, CaCl₂, MnCl₂), 0.01-10 mM of 2-ME and DTT, 0.07-0.7 mM of GSH and GSSG, 0.03-0.2 M of urea, 0.01-1 mM of fatty acids, 1-10 % (v/v) of ethanol). Sample without a cofactor was pre-incubated at 37 °C for three minutes, then, reaction was started by addition of NAD⁺. The absorbance of reaction mixture at 340 nm was recorded for two minutes at 37 °C using a spectrophotometer (Eppendorf Biospectrometer Kinetics). For calculation of initial velocities, the molar extinction coefficient of NADH (6,220 M⁻¹ cm⁻¹) was used. For evaluation of EDTA effect, 1.75 mg ml⁻¹ of KduD was incubated in 100 mM potassium-phosphate buffer pH 7.0 with 100 mM of EDTA at 4° C for three and a half hours. Afterwards, enzyme's activity was measured as described above.

2.2.13 Kinetic assays

Oxidation of D-gluconate and 1,2-propanediol and reduction of 5-keto-D-gluconate and NAD⁺ were measured at 37 °C at 340 nm with a spectrophotometer for at least three minutes. For calculation of initial rates the molar extinction coefficient of NADH (6,220 M⁻¹ cm⁻¹) was used. For reduction reactions 100 mM potassium phosphate buffer pH 7.0, 0.25 mM NADH and 0.02 mg ml⁻¹ of purified enzyme were used. A typical oxidation reaction mixture was composed of 100 mM glycine-NaOH buffer pH 9.5, 1 mM NAD⁺ and 0.02 mg ml⁻¹ of the purified enzyme.

Kinetic parameters were obtained from initial-rate data measured at several constant levels of substrate: D-gluconate (10-450 mM), 1,2-propanediol (0.45-6.7 M), and 5-keto-D-gluconate (10-100 mM). Kinetic parameters for reduction of NAD⁺ were obtained at five constant levels of NAD⁺ (0.1-10 mM) in the presence of 100 mM of D-gluconate.

Reduction of 11-DOC and RSS and oxidation of NADH were measured at 37 °C. The reduction reaction contained 100 mM potassium phosphate buffer pH 7.0, 0.6 mM NADH and 0.02 mg ml⁻¹ of purified enzyme. The reactions were always started by addition of enzyme to the pre-heated reaction mixture. Reactions were stopped by heating the samples at 99 °C for two minutes, followed by rapid cooling to 4 °C and addition of equal volume of chloroform for extraction of steroids as described above (2.2.3). Initial-rate data was obtained by measuring the amount of product produced after one, two, six and eight minutes of reaction time using HPLC as described above (2.2.4). The data was obtained at several constant levels of substrate: 11-DOC (0.01-0.8 mM) and RSS (0.01-0.5 mM). The data for oxidation of NADH was obtained at eight constant levels of NADH (0.02-4.8 mM) in the presence of 0.4 mM of 11-DOC.

The kinetic data was analyzed with GraphPad Prism 6 using Michaelis-Menten equation, ($v = v_{\max} * [S] / (K_M + [S])$), where v is a reaction velocity, v_{\max} – maximal velocity of reaction at saturating substrate concentrations, K_M – Michaelis-Menten constant, and $[S]$ concentration of the substrate. The turnover value (k_{cat} expressed in min⁻¹) for 6xHis-KduD was calculated on the basis of a molecular mass of 28 kDa using the following equation $k_{\text{cat}} = v_{\max} / [E]_0$, where $[E]_0$ is the enzyme concentration.

2.2.14 Construction of pAT002, pAT004, pMATE-AT001 and pMATE-AT002 plasmids

DNA fragment encoding N-terminally 6xHis-tagged KduD oxidoreductase was amplified by PCR with a Phusion high-fidelity DNA polymerase from pET-11d-His-KduD plasmid with primers AT025 and AT029 containing XbaI and BglII restriction endonuclease cleavage sites, respectively (Table 2.1). The amplified DNA fragment was digested with XbaI and BglII restriction endonucleases and cloned into XbaI/BglII-digested pET-SH3-SDH08 plasmid backbone using T4 DNA ligase. The correct DNA sequence of the resulting plasmid pAT002, encoding FP protein, was confirmed by DNA sequence analysis.

The deletion of DNA fragment encoding a β 1-domain of AIDA-I autotransporter was introduced in pAT002 plasmid using In-Fusion cloning. Briefly, a DNA fragment was amplified by PCR

with the Phusion high-fidelity DNA polymerase from the pAT002 plasmid using the pair of primers AT030 and AT031 (**Table 2.1**). The amplified DNA fragment (~7.5 kb) was self-circulated using In-Fusion HD EcoDry cloning kit and a protocol provided by the manufacturer. The correct DNA sequence of the constructed plasmid pAT004, encoding FPΔβ1 fusion protein, was confirmed by DNA sequence analysis.

The DNA fragment encoding KduD oxidoreductase was amplified by PCR with the Phusion high-fidelity DNA polymerase from the pET-11d-kduD plasmid and the pair of primers AT020 and AT021 (**Table 2.1**). The backbone of pMT005 plasmid encoding CtxB signal peptide, the linker region and the β-barrel of EhaA autotransporter (Wells et al. 2008) (codon-optimized for expression in an *E. coli* host), was amplified by PCR with the Phusion high-fidelity DNA polymerase and the pair of primers AT018 and AT019 (**Table 2.1**). Two PCR fragments were combined to form a plasmid using In-Fusion HD EcoDry cloning kit. The resulting plasmid pMATE-AT001, coding for FP1 protein, was subjected to DNA sequence analysis and was confirmed to contain a correct DNA sequence.

For construction of pMATE-AT002 plasmid, the backbone of the pMATE-AT001 plasmid was amplified by PCR with the Phusion high-fidelity DNA polymerase and the pair of primers AT027 and AT028 (**Table 2.1**). The amplified DNA fragment (~6.4 kb) was self-circulated using In-Fusion HD EcoDry cloning kit and a protocol provided by the manufacturer. The correct DNA sequence of the constructed plasmid pMATE-AT002, encoding FP2 fusion protein, was confirmed by DNA sequence analysis.

2.2.15 Whole-cell activity assays with *E. coli* cells expressing FP, FPΔβ1, FP1 and FP2

The recombinant *E. coli* strains carrying the plasmid pAT002, pAT004, pMATE-AT001 or pMATE-AT002 encoding FP, FPΔβ1, FP1 or FP2 fusion protein, respectively, were cultured routinely at 37 °C in LB medium supplemented with 30 μg ml⁻¹ of kanamycin or 50 μg ml⁻¹ of carbenicillin (**2.1.8**). Cells were grown until optical density OD₅₇₈ of 0.5-0.6 was reached. The protein expression was induced by adding IPTG to a final concentration of 1 mM and cells were cultured at 30 °C for up to three hours or at 25 °C for 20 hours. The *E. coli* BL21 and BL21 (DE3) strains carrying the expression plasmid were cultured at 37 °C in M9 medium supplemented with 30 μg ml⁻¹ of kanamycin or 50 μg ml⁻¹ of carbenicillin (**2.1.8**). Cells were grown until optical density OD₅₇₈ of 0.5-0.6 was reached. The protein expression was induced by

adding IPTG to a final concentration of 1 mM and cells were cultured at 30 °C for another 16 hours.

For the whole-cell steroid transformation assays, *E. coli* cells were harvested by centrifugation (5 min, 3,850 g, 4 °C), washed two times with 100 mM potassium phosphate buffer pH 7.0, and resuspended in the same buffer to the final optical density $OD_{578}=1, 10, 20$ or 25. After addition of steroid substrate (11-DOC or RSS) and NADH to the final concentration of 0.4 mM and 0.6 mM, respectively, cells were incubated at 37 °C for two or 16 hours. Then, steroids were extracted with chloroform and analyzed by HPLC as described above (2.2.4).

When D-gluconate substrate was used in the whole-cell activity assays, harvested *E. coli* cells were washed twice with 100 mM glycine-NaOH buffer pH 9.3 and resuspended in the same buffer to the final optical density $OD_{578}=20$. After addition of D-gluconate and NAD^+ to the final concentration of 200 mM and 1 mM, respectively, cells were incubated at 37 °C for 0, 15, 30, 45 and 60 min. At each time point cells were removed by centrifugation (3 min, 8,000 g, 4 °C) and the absorbance of supernatants was measured at 340 nm using spectrophotometer.

2.2.16 Preparation of membrane protein fraction

The recombinant *E. coli* strains carrying the plasmid pAT002, pAT004, pMATE-AT001 or pMATE-AT002 encoding FP, $FP\Delta\beta 1$, FP1 or FP2 fusion protein, respectively, were cultured routinely at 37 °C in LB medium supplemented with 30 $\mu\text{g ml}^{-1}$ of kanamycin or 50 $\mu\text{g ml}^{-1}$ of carbenicillin (2.1.8) and with 10 mM β -ME and 10 μM EDTA or without these additives. Cells were grown until optical density OD_{578} of 0.5-0.6 was reached. The protein expression was induced by adding IPTG to a final concentration of 1 mM and cells were cultured at 30 °C for up to three hours or at 25 °C for 20 hours.

Cells were harvested by centrifugation (10 min, 3,850 g, 4 °C, from 40 ml of cell culture), washed twice with 0.2 M Tris-HCl, pH 8.0, and subjected to rapid outer membrane protein isolation as described by Hantke (1981), except for few modifications. Briefly, cells were kept on ice and resuspended in 0.5 ml 0.2 M Tris-HCl pH 8.0. The following solutions were added in sequence and gently mixed with the cells: 1 ml 0.2 M Tris-HCl pH 8.0; 0.1 ml 1 M sucrose; 0.1 ml 10 mM EDTA pH 8.0; 0.1 ml 10 mg ml^{-1} lysozyme; 3.2 ml H_2O . The cells were kept 10 min at room temperature to allow the formation of spheroplasts. Then, the following solutions

were added in sequence: 50 μ l 100 mM PMSF, 10 μ l 10 mg ml⁻¹ aprotinin; 5 ml extraction buffer (2 % Triton X-100, 10 mM MgCl₂, 50 mM Tris-HCl pH 8.0) and 100 μ l 1 mg ml⁻¹ DNase I. The solution was mixed thoroughly and kept for 20-30 min on ice until it was no longer viscous. Then, the solution was centrifuged (5 min, 3,120 g, +4 °C) to remove intact cells and large debris. The clarified bacterial lysate was centrifuged (10 min, 38,700 g, +4 °C) and the supernatant containing soluble proteins was discarded. The resulting protein pellets were resuspended in 10 ml of water and centrifuged as above (10 min, 38,700 g, +4 °C). This washing step was repeated, then, pellets were resuspended in 1 ml of H₂O, transferred to an Eppendorf tube and centrifuged again (10 min, 15,000 g, +4 °C). The protein pellet was resuspended in water (5-50 μ l), mixed with an equal volume of 2x protein electrophoresis sample buffer, boiled for 15 min, and analyzed on 10 % polyacrylamide gels by SDS-PAGE. Proteins were stained with Coomassie brilliant blue R250 or analyzed by immunoblot analysis as described below (2.2.18).

2.2.17 Protease assays

2.2.17.1 Proteinase K assay

E. coli cells were cultured as described above (2.2.16). Cells were harvested by centrifugation (10 min, 3,850 g, 4 °C, from 40 ml of cell culture), washed twice with 0.2 M Tris-HCl, pH 8.0, and resuspended in 1 ml Tris-HCl pH 8.0 buffer. After addition of proteinase K to a final concentration of 0.0625 mg ml⁻¹, cells were incubated at 37 °C for one hour. In order to stop the reaction, cells were transferred on ice, 5 ml of 0.2 M Tris-HCl pH 8.0 with 10 % fetal calf serum (FCS) were added, cells were pelleted by centrifugation (5 min, 3,850 g, 4 °C) and washed three times with 0.2 M Tris-HCl pH 8.0, then, subjected to the membrane protein isolation as described above (2.2.16).

2.2.17.2 IgA1 protease assay

The recombinant *E. coli* JK321 (DE3) cells carrying the plasmid pAT002, encoding FP, were grown at 37 °C in M9Cas medium supplemented with 30 μ g ml⁻¹ of kanamycin and 50 μ g ml⁻¹ of carbenicillin. The *E. coli* JK321 (DE3) cells without a plasmid were grown in M9Cas medium supplemented with 30 μ g ml⁻¹ of kanamycin under the same conditions. Cells were grown until optical density OD₅₇₈ of 0.5-0.6 was reached. The protein expression was induced by adding IPTG to a final concentration of 1 mM and cells were cultured at 30 °C for up to three hours.

Cells were harvested by centrifugation (10 min, 3,850 g, 4 °C), washed twice with an IgA1 protease reaction buffer (50 mM Tris-HCl pH 7.5, 100 mM NaCl, 1 mM EDTA) and resuspended in the same buffer to the final optical density $OD_{578}=20$. After addition of IgA1 protease to a final concentration of $0.01 \mu\text{g } \mu\text{l}^{-1}$ or $0.05 \mu\text{g } \mu\text{l}^{-1}$ (total sample volume 50 μl), cells were incubated for 60 hours at 20 °C with a gentle shaking. Afterwards, samples were centrifuged (5 min, 10,000 g, +4 °C), supernatants were transferred to new Eppendorf tubes, and cell pellets were resuspended in the 50 μl of the same buffer as above. Samples of supernatants and cell pellets were mixed with an equal volume of 2x protein electrophoresis sample buffer, boiled for 20 min, and analyzed on 10 % polyacrylamide gels by SDS-PAGE. Proteins were stained with Coomassie brilliant blue R250 or analyzed by immunoblot analysis as described below (2.2.18).

2.2.18 Immunoblot analysis

For immunoblot analysis, proteins separated on SDS-PAGE gels were transferred on polyvinylidene fluoride (PVDF) membranes using standard electroblotting technique. Afterwards, the membranes were blocked in TBS buffer (25 mM Tris-base pH 7.4, 140 mM NaCl, 2.7 mM KCl) with 0.1 % Tween 20 and 5 % milk powder for an hour at room temperature, followed by washing step in TBS buffer for five minutes. For immune detection, membranes were incubated overnight at +4 °C with the primary anti-PEYFK mouse monoclonal antibody diluted 1:50 in TBS buffer with 0.1 % Tween 20 and 3 % BSA. Then, membranes were rinsed three times in TBS buffer with 0.1 % Tween 20 and 3 % BSA. Afterwards, membranes were incubated for two hours at room temperature with a secondary antibody, goat anti-mouse IgG (H+L) conjugated with alkaline phosphatase, diluted 1:5000 in TBS buffer with 0.1 % Tween 20 and 3 % BSA. Then, membranes were rinsed once in TBS buffer with 0.1 % Tween 20 and twice in TBS buffer. Antigen-antibody conjugates were visualized by a color reaction with BCIP/NBT reagent.

A slightly different protocol was used for detection of anti-6xHis-tag. Briefly, the membranes were blocked in TBS buffer with 5 % milk powder for an hour at room temperature. For immune detection, membranes were incubated overnight at +4 °C with the primary anti-6xHis mouse monoclonal antibody diluted 1:1500 in TBS buffer. Then, membranes were rinsed three times in TBS buffer with 0.1 % Tween 20. Afterwards, membranes were incubated for two hours at room

temperature with a secondary antibody, rabbit anti-mouse IgG (H+L) conjugated with a horseradish peroxidase (HRP), diluted 1:5000 in TBS buffer. Then, membranes were rinsed once in TBS buffer with 0.1 % Tween 20 and twice in TBS buffer. Afterwards, the membranes were treated with Luminol reagent and the antigen-antibody conjugates were detected with chemiluminescence imaging system (Intas). When the secondary antibody, goat anti-mouse IgG (H+L) conjugated with alkaline phosphatase (diluted 1:5000 in TBS buffer) was used, the antigen-antibody conjugates were visualized by a color reaction with BCIP/NBT reagent.

2.2.19 LC-MS analysis of steroid conversions

The steroid conversions were analyzed using micrOTOF-Q-II (Bruker Daltonics) coupled to Ultimate 3000 RS Dionex LC system (Dionex Softron).

2.2.20 DNA sequence analysis

The DNA sequences of the new plasmids, constructed in this study, were verified by SeqLab (Göttingen, Germany) and BMFZ (Biological-Medical Research Center, Heinrich-Heine University, Düsseldorf) using Sanger DNA sequencing method.

2.2.21 Other basic methods

DNA electrophoresis

DNA samples were mixed with a 6x DNA loading dye and separated in 1 % TAE agarose gels in 1xTAE electrophoresis buffer applying the voltage of 10 V/cm. Separated DNA was stained with 1x GelGreen dye solution and was visualized with gel documentation system (Intas).

Protein SDS-PAGE

Protein samples were mixed with an equal volume of 2x protein electrophoresis sample buffer, boiled for 5-20 min, and ran on 10 % or 12.5 % polyacrylamide gels in 1x SDS-running buffer applying voltage of 120 V. Proteins were stained with Coomassie brilliant blue R250 solution for up to one hour, then, gels were destained with 10 % acetic acid solution.

Polymerase-chain reaction (PCR)

The standard PCR mixture with Phusion DNA polymerase contained: 1x Phusion HF buffer, 0.2 mM dNTP mix, 0.5 μ M forward primer, 0.5 μ M reverse primer, template DNA (0.02 ng/ μ l

plasmid DNA or 2 ng μl^{-1} genomic DNA), 0.02 u μl^{-1} Phusion DNA polymerase. The standard thermocycling conditions were as follows: 98 °C 30 s, [98 °C 10 s, T_A 15 s, 72 °C 20 s/1 kilobase]_{25 cycles}, 72 °C 10 min, where T_A stands for a primer annealing temperature.

The standard PCR mixture with KOD DNA polymerase contained: 1x KOD DNA polymerase buffer, 1.5 mM MgCl_2 , 0.2 mM dNTP mix, 0.5 μM forward primer, 0.5 μM reverse primer, template DNA (0.02 ng μl^{-1} plasmid DNA or 2 ng μl^{-1} genomic DNA), 0.02 u μl^{-1} KOD DNA polymerase. The standard thermocycling conditions were as follows: 95 °C 5 min, [95 °C 30 s, T_A 30 s, 72 °C 1 min/1 kilobase]_{30 cycles}, 72 °C 5 min, where T_A stands for a primer annealing temperature.

A colony PCR was used routinely to screen for the recombinant *E. coli* clones containing the correctly cloned plasmid. A typical colony PCR mixture contained in 20 μl : 1x Taq DNA polymerase buffer, 1.5 mM MgCl_2 , 0.2 mM dNTP mix, 0.5 μM forward primer, 0.5 μM reverse primer, biomass from a single *E. coli* clone (as a source of a template plasmid DNA), 0.025 u μl^{-1} Taq DNA polymerase. The standard thermocycling conditions were as follows: 95 °C 5 min, [95 °C 30 s, T_A 30 s, 72 °C 1 min/1 kilobase]_{33 cycles}, where T_A stands for a primer annealing temperature.

Purification of plasmids, genomic DNA and PCR products

Plasmids were routinely purified from 5 ml of recombinant *E. coli* overnight cultures (grown in LB medium at 37 °C for 16 hours under vigorous shaking) using QIAprep Spin Miniprep Kit (Qiagen) and the protocol provided by the manufacturer. Genomic DNA was purified from 5 ml of *E. coli* DH5 α overnight cell culture using GeneJET Genomic DNA Purification kit (Thermo Fisher Scientific) and the protocol provided by the manufacturer.

QIAquick PCR purification kit (Qiagen) and QIAquick gel extraction kit (Qiagen) were used routinely to purify PCR products from the PCR mixtures and DNA fragments separated in agarose gels, respectively.

DNA ligation reaction and In-Fusion cloning

The typical ligation reaction mixture contained in 20 μl : 1x T4 DNA ligase buffer, 70 ng of purified DNA vector fragment, insert DNA fragment (3:1 molar ratio over vector fragment), 1 u

of T4 DNA ligase. The reaction mixture was incubated at room temperature (~22 °C) for up to one hour. Then, up to 5 µl of reaction mixture were used for transformation of chemically competent *E. coli* cells.

In-Fusion cloning was performed using In-Fusion HD EcoDry cloning kit and protocol provided by the manufacturer.

DNA digestion with restriction endonucleases

The standard reaction with FastDigest restriction endonucleases contained in 50 µl: 1x FastDigest green buffer, DNA (2.5 µg of plasmid or 0.33 µg of purified PCR product) and 2.5 u of FastDigest restriction endonuclease. The reaction was performed at 37 °C for up to 25 minutes.

The standard reaction with conventional restriction endonucleases contained in 50 µl: 1x NEBuffer 4, 1 µg of DNA and 10 u of conventional restriction endonuclease. The reaction was performed at 37 °C for one hour.

Preparation of competent *E. coli* cells

Preparation of chemically competent cells

E. coli cells were grown in LB medium overnight at 37 °C with vigorous shaking. The 0.4 ml of overnight cell culture were transferred to 40 ml of fresh LB medium supplemented with 0.8 ml of Mg²⁺-solution and cells were cultivated until an optical density of OD₅₇₈=0.5-0.8 was reached. Then, cells were transferred on ice and all following steps were performed at +4 °C, using chilled solutions. Cells were harvested by centrifugation (5 min, 3,850 g, 4 °C) and resuspended in 4 ml of TMF buffer. After addition of 1 ml of glycerol, cells were aliquoted and frozen using dry ice and ethanol bath. Cells were stored at -80 °C.

Preparation of electrocompetent cells

E. coli cells were grown in 25 ml of LB medium overnight at 37 °C with vigorous shaking. The 25 ml of overnight cell culture were transferred to 500 ml of 2x YT medium and cells were cultivated at 37 °C until an optical density OD₅₇₈=0.35 was reached. Cells were stored on ice for 20 minutes and all following steps were performed at +4° using chilled solutions. Cells were

harvested by centrifugation (1,000 g, 15 min, 4 °C), resuspended in 100 ml of sterile cold water and centrifuged again (1,000 g, 20 min, 4 °C). Afterwards, cells were resuspended in 100 ml of 10 % glycerol solution and centrifuged as above. Then, cells were resuspended in 10 ml of 10 % glycerol solution and centrifuged as above. After final centrifugation step, cells were resuspended in 1 ml of 10 % glycerol solution and were aliquoted and frozen using dry ice and ethanol bath. Cells were stored at -80 °C.

Transformation of *E. coli* cells

Protocol for chemically competent cells

Transformation of commercial chemically competent *E. coli* cells (Top10, Stellar) was performed according to the protocols provided by the manufacturer.

The aliquot of chemically competent *E. coli* cells (100 µl) was thawed on ice, then, 50-100 ng of plasmid DNA (0.5-2 µl) or ligation mixture (up to 5 µl) were added and cells were incubated on ice for 15 min. Afterwards, cells were transferred to 42 °C heating block for 90 seconds, then, kept on ice for up to 60 seconds. Afterwards, 900 µl of LB medium were added and cells were incubated at 37 °C for one hour under vigorous shaking. The 100 µl of cell suspension were spread on LB agar plate containing appropriate selection antibiotic and plates were incubated at 37 °C overnight.

Protocol for electrocompetent cells

Transformation of commercial electrocompetent *E. coli* cells (BL21 ClearColi (DE3)) was performed according to the protocol provided by the manufacturer.

The aliquot of electrocompetent *E. coli* cells (50 µl) was thawed on ice, then, 1 ng of plasmid DNA (0.5-1 µl) was added and cells were transferred to cooled electroporation cuvette (0.1 cm gap between electrodes). The cuvette was transferred to the electroporator and was pulsed at 1800 V for several milliseconds (4-6 ms). Afterwards, 450 µl of warm SOC medium (37 °C) were added, cells were mixed gently by pipetting up and down and were transferred to the eppendorf tube and incubated for one hour at 37 °C under vigorous shaking. Afterwards, 100 µl of diluted cells (10-1000x in LB medium) were spread on LB agar plates containing appropriate antibiotic. Plates were incubated at 37 °C overnight.

Storage of recombinant *E. coli* strains

The recombinant *E. coli* cells were cultured in LB medium for 16 hours at 37 °C under vigorous shaking. Cells were harvested from 5 ml of overnight culture by centrifugation (5 min, 3,850 g, 4 °C) and resuspended in 1 ml of PPM medium. Cells were transferred to sterile cryovials filled with glass beads and were frozen using dry ice and ethanol bath. Recombinant *E. coli* strains were stored at -80 °C.

3 Results

3.1 Identification of 11-deoxycorticosterone reductase in *Escherichia coli*

3.1.1 A bioinformatics approach

The reaction catalyzed by an unidentified reductase from *Escherichia coli* DH5 α , 11-DOC reduction into 4-pregnen-20,21-diol-3-one (Hannemann et al. 2007), was previously shown to be also performed by two hydroxysteroid dehydrogenases isolated from other organisms, 3 α ,20 β -hydroxysteroid dehydrogenase (20 β -HSD) from microorganism *Streptomyces hydrogenans* (Allner and Eggstein 1976) and 20 α -hydroxysteroid dehydrogenase (20 α -HSD) from mammal *Mus musculus* (Hershkovitz et al. 2007). The protein sequences of these enzymes were used to search for homologous enzymes in the proteome database of *E. coli*. The genome sequence of *E. coli* DH5 α , which is a derivative of *E. coli* K-12, is not available. Therefore, the search was performed against the proteome database of closely related *E. coli* K-12 strain derivative DH10B using the resources (HAMAP) of the Swiss Institute of Bioinformatics (SIB) and the BLAST network service (Altschul et al. 1997, Pedruzzi et al. 2013). In addition, the search was conducted against a proteome database of *E. coli* B strain derivative BL21(DE3) which was found to be incapable of converting 11-DOC into the 4-pregnen-20,21-diol-3-one (**Fig. 3.1**).

In the proteome of *E. coli* DH10B in total eight aldo-keto reductases (AKRs) were found that share significant but low protein amino acid sequence identity (22-34 %) with 20 α -HSD from *M. musculus* (**Table 3.1**). Seven out of these eight *E. coli* DH10B AKRs were found to be conserved in *E. coli* BL21 (DE3), sharing 99-100 % amino acid sequence identity with the respective homologous AKR in *E. coli* BL21 (DE3). One out of the eight AKRs of *E. coli* DH10B had no homolog in *E. coli* BL21 (DE3). (UniProt accession no. B1XDB9, **Table 3.1**).

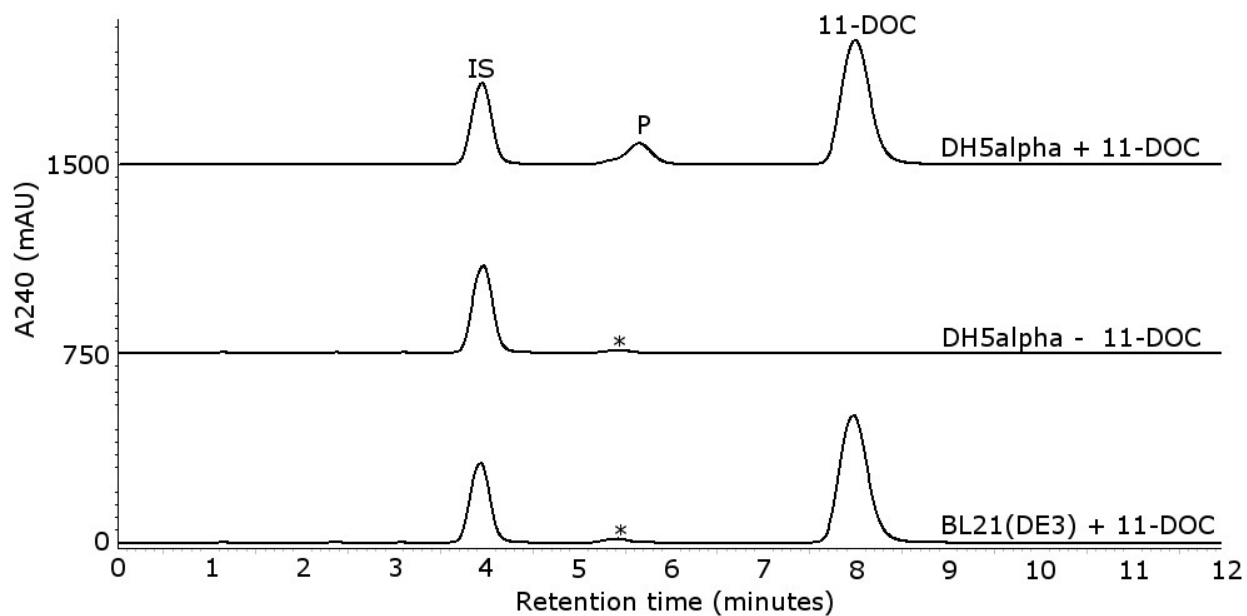


Fig. 3.1 Investigation of 11-DOC reduction with whole cells of *E. coli* DH5 α and *E. coli* BL21 (DE3). Peaks depicted with an asterisk (*) represent natural bacterial compounds that were co-extracted and absorbed at 240 nm but had maximum absorbance at 220 and 270 nm, IS – internal standard (RSS), 11-DOC – 11-deoxycorticosterone (maximum absorbance at 240 nm), P – 4-pregnen-20,21-diol-3-one (maximum absorbance at 240 nm). *E. coli* DH5 α and BL21 (DE3) cells were cultured in LB medium at 37 °C for 16 h. Whole-cell biotransformations were performed with concentrated cell suspensions ($OD_{600}=10$) in 100 mM potassium phosphate buffer pH 7.0 in presence of 0.4 mM of 11-DOC at 37 °C for 18 hours.

A BLAST search with the protein sequence of 20 β -HSD from *S. hydrogenans* in the proteome of *E. coli* DH10B revealed in total 16 short-chain dehydrogenases/reductases (SDRs) that share significant but low amino acid sequence identity (25-40 %) with dehydrogenase from *S. hydrogenans* (**Table 3.2**). In comparison to the search results in the proteome of *E. coli* DH10B, in addition to these 16 conserved homologous enzymes (sequence identity 95-100 %) *E. coli* BL21 (DE3) also contained an additional putative dehydrogenase not present in *E. coli* DH10B (UniProt accession no. C6ECE0, **Table 3.2**).

Table 3.1 AKRs from *E. coli* DH10B and *E. coli* BL21 (DE3) that share protein sequence similarity with 20 α -HSD from *M. musculus* (UniProt accession no. Q8K023).

Protein name	DH10B			BL21(DE3)		
	Accession No.*	E-value**	Identity with Q8K023 (%)	Accession No.*	E-value**	Identity with Q8K023 (%)
2,5-diketo-D-gluconate reductase A	B1XFG4	7e-40	34	C6EHY2	9e-40	34
2,5-diketo-D-gluconate reductase B	B1XD71	7e-30	29	C6EA83	4e-30	29
Predicted oxidoreductase	B1XGP1	3e-18	26	C6EC48	3e-18	26
Aldo-keto reductase	B1XFF5	1e-07	23	C6EHZ1	1e-07	23
Predicted oxidoreductase, NAD(P)-binding	B1XF07	2e-07	22	C6ELG5	2e-07	22
Predicted oxidoreductase	B1XGN2	4e-06	22	C6ECI6	2e-06	23
Predicted oxidoreductase, NAD(P)-binding	B1XDB9	2e-05	24	-	-	-
Predicted oxidoreductase	B1XFV8	5e-05	28	C6EDJ8	5e-05	28

* - UniProt accession number,

** - the expect value (E) shows the number of hits expected to be found by chance when searching a database of a particular size.

Table 3.2 SDRs from *E. coli* DH10B and *E. coli* BL21 (DE3) that share protein sequence similarity with 20 β -HSD from *S. hydrogenans* (UniProt accession no. P19992).

Protein name	DH10B			BL21(DE3)		
	Accession No.*	E-value**	Identity with P19992 (%)	Accession No.*	E-value**	Identity with P19992 (%)
3-oxoacyl-[acyl-carrier-protein] reductase	B1XA03	5e-26	38	C6EHC1	3e-26	38
Predicted oxidoreductase with NAD(P)-binding Rossmann-fold domain	B1X7M6	4e-20	34	C6EAH4	5e-20	34
Predicted oxidoreductase, sulfate metabolism protein	B1XA97	4e-20	37	C6EL51	1e-19	36
Predicted NAD(P)-binding oxidoreductase with NAD(P) domain	B1XEI9	2e-19	40	C6EIK6	2e-19	40
2-deoxy-D-gluconate 3-dehydrogenase	B1XED6	3e-18	36	C5W8E6***	9e-11	36
5-keto-D-gluconate-5-reductase	B1XEP5	5e-18	32	C6EC85	6e-18	32
Predicted deoxygluconate dehydrogenase	B1XDI5	7e-18	32	C6EJ99	1e-18	32
7-alpha-hydroxysteroid dehydrogenase, NAD-dependent	B1XF84	1e-17	32	C6EDM8	1e-17	32
2,3-dihydro-2,3-dihydroxybenzoate dehydrogenase	B1X5Z3	3e-15	30	C6EK98	1e-14	31
L-allo-threonine dehydrogenase, NAD(P)-binding	B1XEC6	4e-15	30	C6EDU7	5e-15	30
Sorbitol-6-phosphate dehydrogenase	B1XCN2	7e-12	30	C6EJS6	8e-12	30
Predicted oxoacyl-(Acyl carrier protein) reductase	B1XBM0	2e-11	25	C6EFW6	2e-11	25
Predicted glutathionylspermidine synthase, with NAD(P)-binding domain	B1XFF7	3e-10	29	C6EHY9	3e-10	29
Predicted oxidoreductase with NAD(P)-binding Rossmann-fold domain	B1XEM9	7e-09	29	C6ECA1	1e-08	29
3-phenylpropionate-dihydrodiol/cinnamic acid-dihydrodiol dehydrogenase	B1XB16	5e-08	32	C6EKG6	6e-08	32
Predicted oxidoreductase with NAD(P)-binding Rossmann-fold domain	B1XFT0	3e-07	29	C5W0E9****	4e-07	29
Putative oxoacyl reductase	-	-	-	C6ECE0	2e-07	28

* - UniProt accession number

** - the expect value (E) shows the number of hits expected to be found by chance when searching a database of a particular size.

*** - a protein in BL21 (DE3) has a C-terminal truncation of 55 amino acids in comparison to homolog (B1XED6) in DH10B

**** - an additional truncated protein form is found in BL21 (DE3) (accession no. C6EKX1, 13 amino acid truncation in comparison to C5W0E9)

3.1.1.1 Investigation of steroid reductase activity of enzyme encoded by *ydbC* gene

In order to investigate if a putative uncharacterized oxidoreductase, which was found to be present only in *E. coli* DH10B but not in BL21 (DE3) (**Table 3.1**, UniProt accession no. B1XDB9), could be responsible for 11-DOC conversion into 4-pregnen-20,21-diol-3-one, a gene encoding this enzyme (*ydbC*) was amplified from the genomic DNA of *E. coli* DH5 α and cloned for expression in *E. coli* BL21 (DE3). The apparent MW of overexpressed recombinant YdbC oxidoreductase in the SDS-PAGE gel was found to be a few kDa lower than the expected theoretical MW of this enzyme (30.7 kDa) (**Fig. 3.2**). Analysis of protein sequence of YdbC with SignalP 4.1 tool (Petersen et al. 2011) revealed that YdbC does not contain any signal peptide.

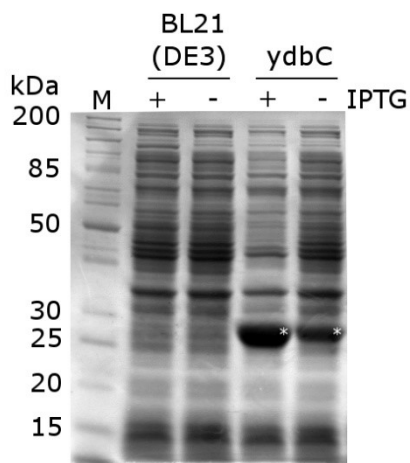


Fig. 3.2 SDS-PAGE of *E. coli* BL21 (DE3) whole cells overexpressing YdbC oxidoreductase of *E. coli* DH5 α . BL21 (DE3): whole-cell protein extract from *E. coli* BL21 (DE3) without expression plasmid, *ydbC*: whole-cell protein extract from *E. coli* BL21 (DE3) cells transformed with pET-11d-*ydbC* plasmid encoding YdbC enzyme under control of T7 promoter. The protein expression was induced with IPTG (+) at 30 °C for two hours or not induced (-). The theoretical molecular mass of the protein encoded by *ydbC* gene is 30.7 kDa. The protein band corresponding to YdbC oxidoreductase is depicted with an asterisk.

The activity of YdbC against 11-DOC was tested in whole-cell 11-DOC biotransformation assay. When BL21 (DE3) cells overexpressing YdbC oxidoreductase were incubated with 11-DOC, the formation of 4-pregnen-20,21-diol-3-one was not detectable (**Table 3.3**). It was a strong indication that this enzyme is not responsible for 11-DOC reduction in *E. coli* DH5 α .

Table 3.3 11-DOC conversion into 4-pregnen-20,21-diol-3-one with whole cells of *E. coli*.

<i>E. coli</i> strain	Substrate conversion* (%)
DH5 α	78.4
BL21 (DE3)	0
BL21 (DE3)/pET-11d-ydbC (-IPTG)	0
BL21 (DE3)/pET-11d-ydbC (+IPTG)**	0

* - Conversion of 11-DOC into 4-pregnen-20,21-diol-3-one was calculated based on the areas under the substrate and product peaks in the HPLC chromatograms. The mean value of two experiments is shown. Whole-cell biotransformations were performed with concentrated cell suspensions (OD₆₀₀=10) in LB medium in the presence of 1.5 mM 11-DOC at 30 °C for 20 hours. ** - the expression of YdbC oxidoreductase was induced with IPTG at 30 °C for two hours.

3.1.2 Partial purification of enzyme from *E. coli* DH5 α

The identification of 20-ketosteroid reductase in *E. coli* DH5 α using bioinformatics approach was not successful. Thus, an attempt to purify the enzyme from *E. coli* DH5 α has been undertaken. The purification of native 11-DOC reductase from *E. coli* DH5 α was performed using traditional protein purification techniques. Active protein fractions were identified by monitoring 11-DOC reduction into 4-pregnen-20,21-diol-3-one using HPLC-based assay.

3.1.2.1 Ammonium sulfate precipitation step

Crude extract of soluble proteins of *E. coli* DH5 α were fractionated using ammonium sulfate precipitation. The highest 11-DOC reductase activity was observed in 40-60 % saturated ammonium sulfate fraction (**Fig. 3.3**).

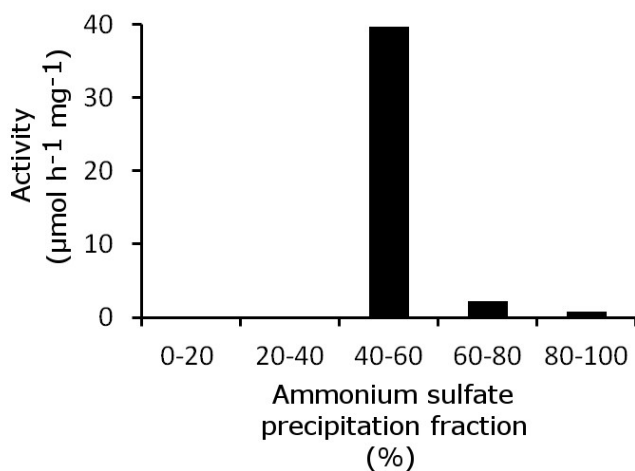
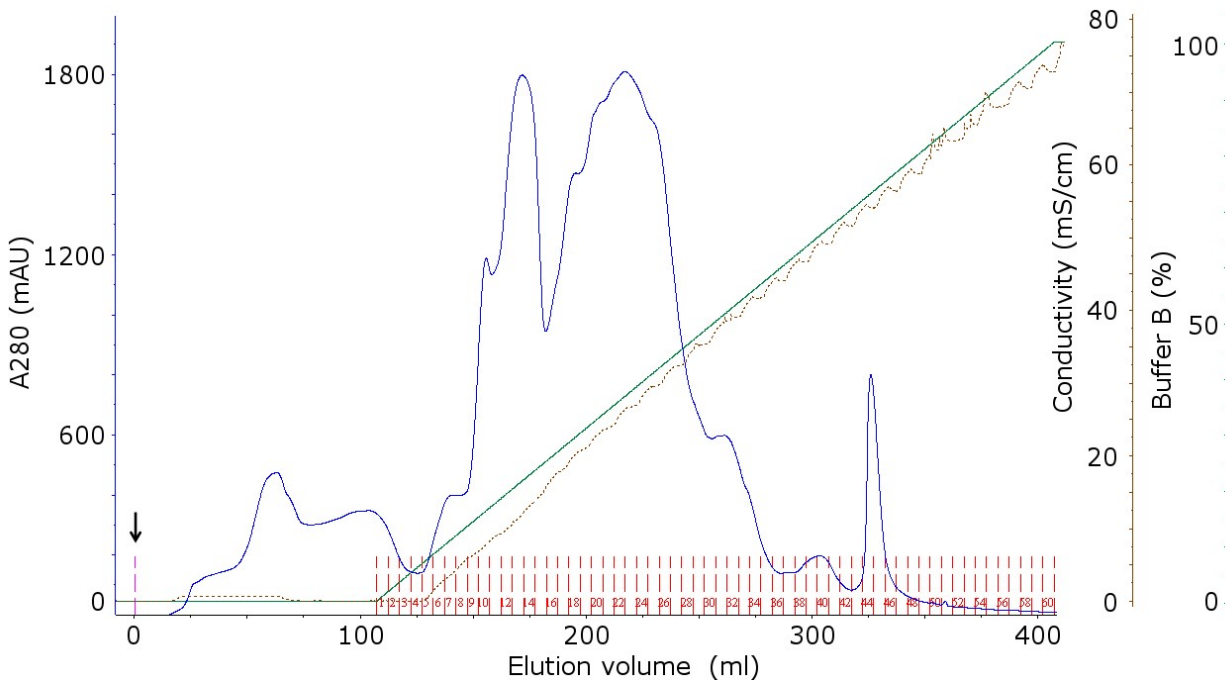


Fig. 3.3 Steroid reductase activity in ammonium sulfate fractions of soluble DH5 α cytosolic extract. Protein fractions were incubated in 100 mM potassium phosphate buffer (pH 7.0) with 1 mM of 11-DOC and 0.4 mM NADH for six hours at 30 °C. The amount of formed product (4-pregnen-20,21-diol-3-one) was quantified using HPLC assay. The 11-DOC reductase activity was expressed as μmol of product formed by one milligram of protein per one hour.

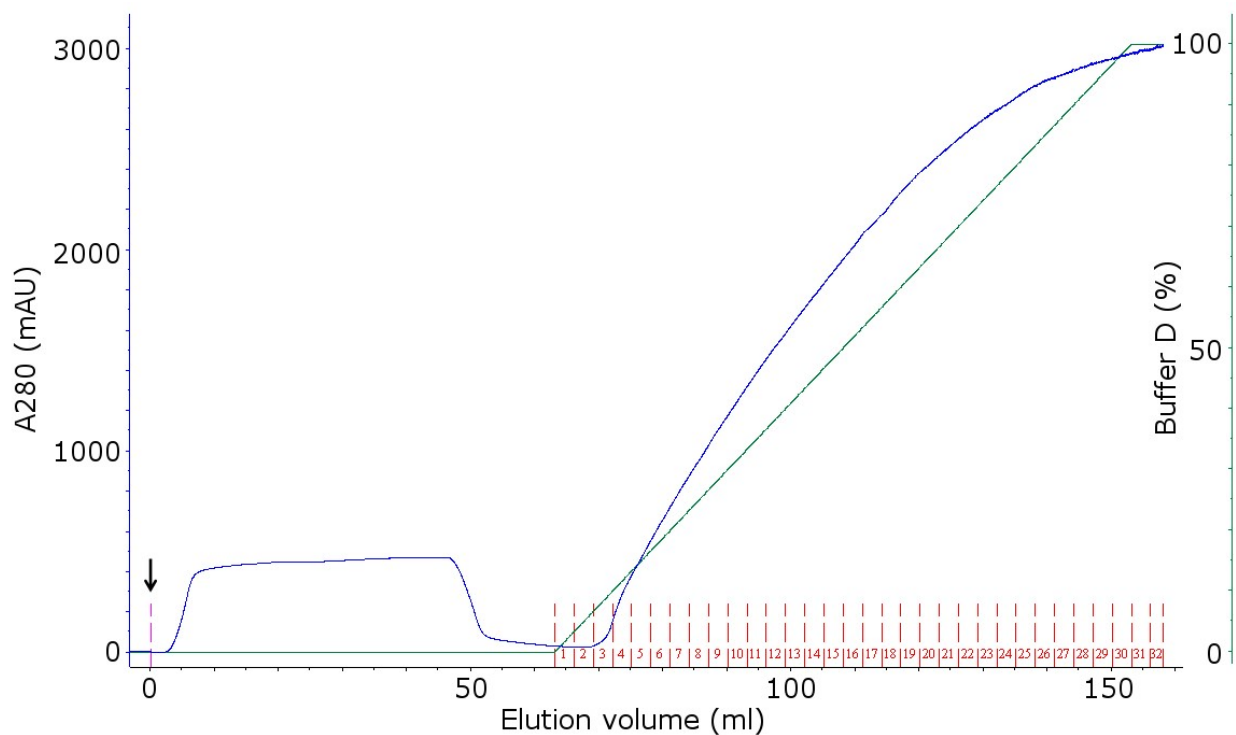
3.1.2.2 Column chromatography steps

The 40-60 % ammonium sulfate precipitation fraction was subjected to four column chromatography steps: strong anion-exchange (**Fig. 3.4**), affinity (**Fig. 3.5**), strong cation-exchange (**Fig. 3.6**) and size-exclusion (**Fig. 3.7**).



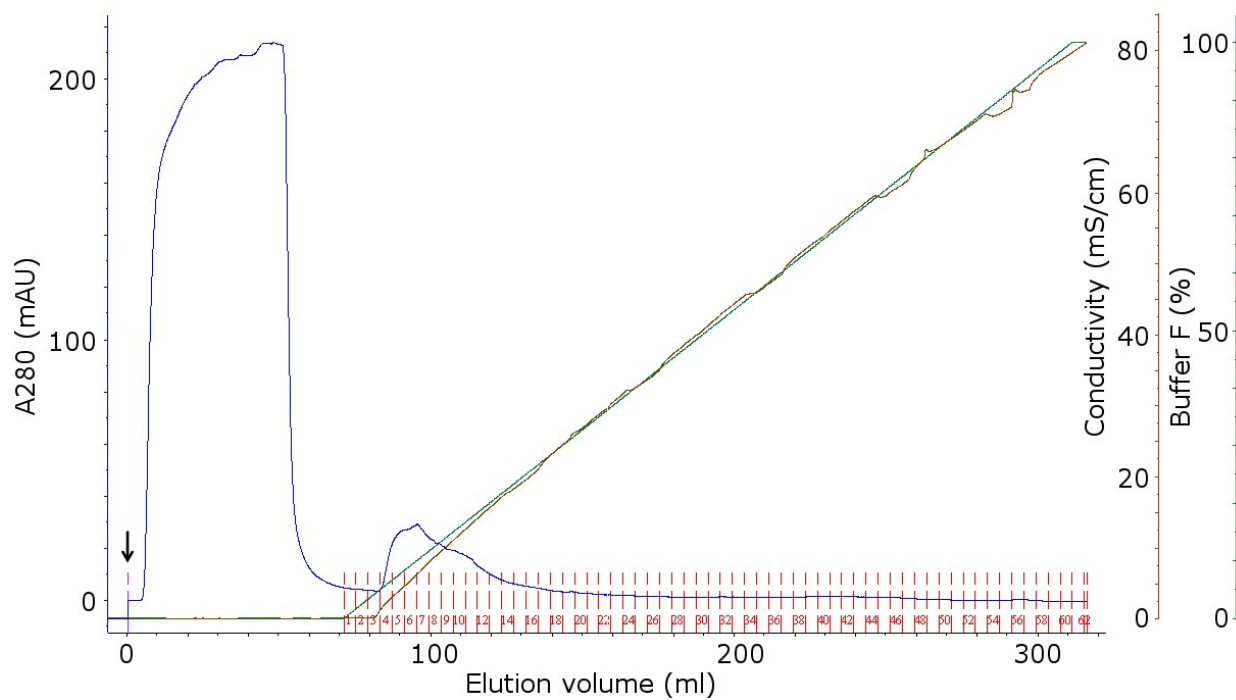
Protein fraction	[1-18]	[19-24]	[25-28]	[29-34]	[35-60]
Activity ($\mu\text{mol h}^{-1} \text{mg}^{-1}$)	0	21.6	36.5	1.9	0

Fig. 3.4 FPLC profile of Q-sepharose chromatography step and 11-DOC reductase activity of protein fractions. Absorbance at 280 nm (blue curve), conductivity (brown curve), and gradient of buffer B (green curve) are shown; protein injection is marked with an arrow, and collected protein fractions are shown in red. Steroid reductase activity of collected fractions was measured in 100 mM potassium phosphate buffer (pH 7.0) in the presence of 0.4 mM NADH and 1 mM 11-DOC at 30 °C for 20 hours. The amount of formed product (4-pregnen-20,21-diol-3-one) was quantified using HPLC assay. The 11-DOC reductase activity was expressed as μmol of product formed by one milligram of protein per one hour. Protein fractions with the highest 11-DOC reductase activity (19-28) were subjected to the Blue sepharose step (Fig. 3.5).



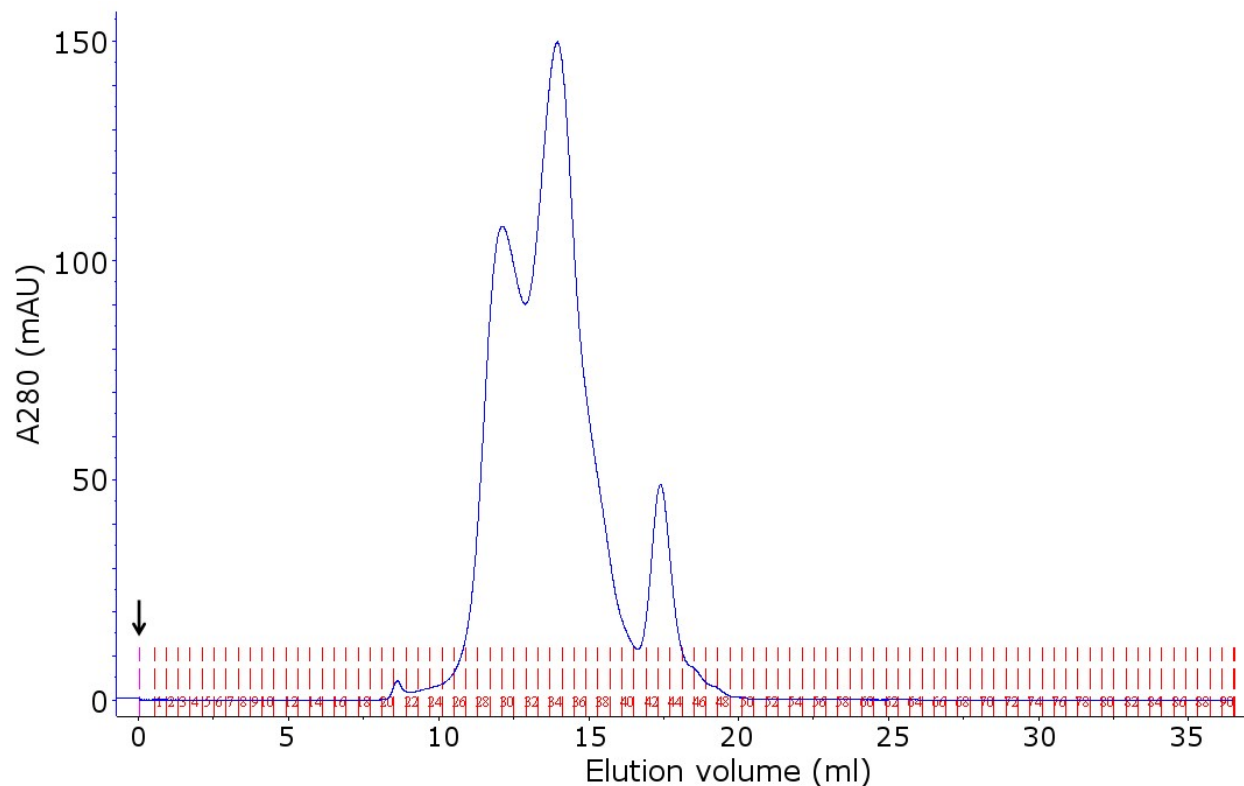
Protein fraction	Flowthrough (injection)	Flowthrough (wash)	[1-6]	[7-12]	[13-18]	[19-24]	[25-30]
Activity ($\mu\text{mol h}^{-1} \text{mg}^{-1}$)	36.0	38.0	29.2	29.6	16.7	6.3	6.0

Fig. 3.5 FPLC profile of Blue sepharose chromatography step and 11-DOC reductase activity of protein fractions. Absorbance at 280 nm (blue curve) and gradient of buffer D (green curve) are shown; protein injection is marked with an arrow, and collected protein fractions are shown in red. Steroid reductase activity of collected fractions was measured in 100 mM potassium phosphate buffer (pH 7.0) in the presence of 0.4 mM NADH and 1 mM 11-DOC at 30 °C for 24 hours. The amount of formed product (4-pregnen-20,21-diol-3-one) was quantified using HPLC assay. The 11-DOC reductase activity was expressed as μmol of product formed by one milligram of protein per one hour. An unbound protein fraction and protein fractions comprising 1-12, which had the highest steroid reductase activity, were subjected to the Poros sepharose step (Fig. 3.6).



Protein fraction	Flowthrough (injection)	Flowthrough (wash)	[1-62]
Activity ($\mu\text{mol h}^{-1} \text{mg}^{-1}$)	29.4	58.5	0

Fig. 3.6 FPLC profile of Poros sepharose chromatography step and 11-DOC reductase activity of protein fractions. Absorbance at 280 nm (blue curve), conductivity (brown curve), and gradient of buffer F (green curve) are shown; protein injection is marked with an arrow, and collected protein fractions are shown in red. Steroid reductase activity of collected fractions was measured in 100 mM potassium phosphate buffer (pH 7.0) in the presence of 0.4 mM NADH and 1 mM 11-DOC at 30 °C for 18 hours. The amount of formed product (4-pregnen-20,21-diol-3-one) was quantified using HPLC assay. The 11-DOC reductase activity was expressed as μmol of product formed by one milligram of protein per one hour. The highest steroid reductase activity was found in an unbound protein fraction. This fraction was subjected to the Superdex 200 sepharose step (Fig. 3.7).



Protein fraction	[1-32]	[33]	[34]	[35]	[36]	[37]	[38-42]
Activity, $\mu\text{mol h}^{-1} \text{mg}^{-1}$	0	8.3	101.5	144.8	200.0	137.6	37.3

Fig. 3.7 FPLC profile of size-exclusion chromatography step and 11-DOC reductase activity of protein fractions. Absorbance at 280 nm (blue curve) is shown; protein injection is marked with an arrow, and collected protein fractions are shown in red. Steroid reductase activity of collected fractions was measured same as described in the caption of Fig. 3.6. The 11-DOC reductase activity was expressed as μmol of product (4-pregnen-20,21-diol-3-one) formed by one milligram of protein per one hour. The highest steroid reductase activity was found in fraction 36.

After ammonium sulfate precipitation and four column chromatography steps, 11-DOC reductase activity was increased by only 9.9-fold from the cytosolic protein fraction of *E. coli* DH5 α (**Table 3.4**). Only low fold purification was achieved because the enzyme did not interact with the two of the four protein chromatography columns that were used in this work (**Fig. 3.5**, **Fig. 3.6**).

Table 3.4 Summary of purification of 11-DOC reductase from *E. coli* DH5 α .

Purification step	Total protein (mg)	Total activity (10^{-3} U)	Specific activity* (10^{-3} U mg $^{-1}$)	Yield (%)	Purification (fold)
Crude extract	669.6	310.8	0.46	100.0	1.0
Ammonium sulfate	376.1	253.2	0.67	81.5	1.5
Q-Sepharose	91.6	121.9	1.33	39.2	2.9
Blue Sepharose	49.2	69.0	1.40	22.2	3.0
Poros Sepharose	9.0	24.2	2.69	7.8	5.8
Superdex 200	0.4	2.0	4.61	0.6	9.9

* - One unit (U) of enzyme activity was defined as the amount of enzyme catalyzing the reduction of 1 μ mol of 11-DOC per minute under the assay conditions. Steroid reductase activity was measured in 100 mM potassium phosphate buffer (pH 7.0) in the presence of 0.4 mM NADH and 0.4 mM 11-DOC at 37 °C for two hours. The amount of formed product (4-pregnen-20,21-diol-3-one) was quantified using HPLC assay.

The steroid reductase activity in crude protein extracts could only be detected in the presence of NADH. No activity was detectable when NADH was replaced with NADPH (**Fig. 3.8**) and the activity of the enzyme was not decreased in the presence of 20 mM EDTA (**Fig. 3.8**). This provided strong evidence that the 11-DOC reductase from *E. coli* DH5 α was a NADH-dependent enzyme that did not require divalent metal-ions for activity.

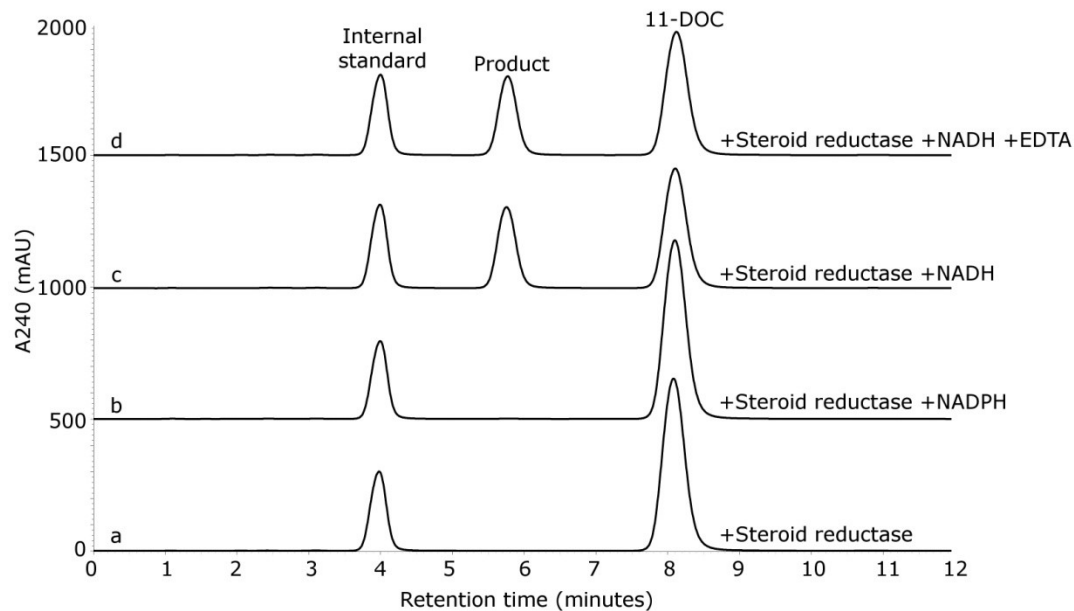


Fig. 3.8 Effect of NADH, NADPH and EDTA on 11-DOC reductase activity. The partially purified steroid reductase from *E. coli* DH5 α (after the Poros sepharose chromatography step) was incubated for 24 hours at 30 °C in 100 mM potassium phosphate buffer (pH 7.0) in the presence of 0.4 mM 11-DOC steroid substrate. (a): without a cofactor; (b): with 0.4 mM NADPH; (c): with 0.4 mM NADH; and (d): with 0.4 mM NADH and 20 mM EDTA.

The size-exclusion chromatography was performed with a calibrated Superdex 200 chromatography column in order to determine the molecular weight of native *E. coli* DH5 α steroid reductase. The steroid reductase activity was found in fractions corresponding to a molecular weight of 100 kDa (**Fig. 3.9**).

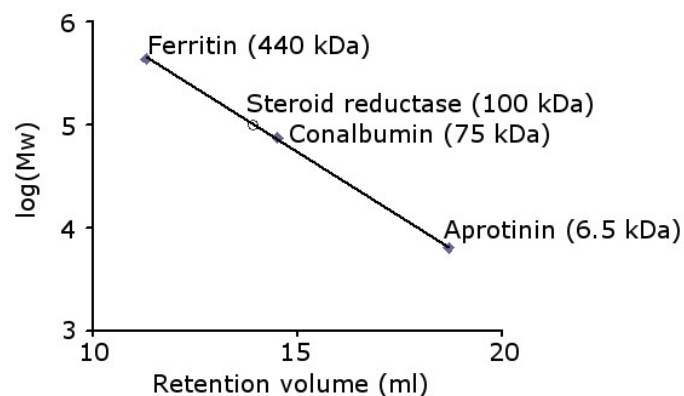


Fig. 3.9 Determination of molecular weight of native *E. coli* DH5 α steroid reductase by gel filtration with calibrated Superdex 200 chromatography column.

3.1.3 Identification of NADH-dependent oxidoreductases in partially purified enzyme sample

Protein mass spectrometry was used to identify the proteins within the partially purified sample of the steroid reductase obtained after the final size exclusion chromatography step (**Fig. 3.7**, protein fraction 36). As the *E. coli* DH5 α genome was unavailable, the mass spectrometry data was searched against the *E. coli* K-12 protein database. In total 59 *E. coli* proteins were identified from the sample (summary is provided in **Table 3.5**, a list of all proteins is provided in the supplemental material **Table S1**).

Table 3.5 Proteins identified by mass spectrometry in partially purified 11-DOC reductase sample

Number of proteins matched to <i>Escherichia coli</i> K-12: 59			
Enzymes:	51	Other proteins:	8
Transferases	18	Elongation factors	4
Lyases	10	DNA repair proteins	1
Ligases	2	Chaperones	3
Hydrolases	5		
Isomerases	7		
Oxidoreductases:			
NADH-dependent	3		
NADPH-dependent	4		
Other	2		

Nine of these were putative oxidoreductases that could have been responsible for the steroid reductase activity. To determine which of these 59 sequences in this list encoded the steroid reductase, candidates for overexpression in *E. coli* were chosen. As described above it could be shown that the 11-DOC reductase was NADH dependent (**Fig. 3.8**). The list contained three putative NADH-dependent oxidoreductases, namely 7 α -hydroxysteroid dehydrogenase (HdhA), D-mannonate oxidoreductase (UxuB) and 2-dehydro-3-deoxy-D-gluconate 5-dehydrogenase (KduD). Functional studies have been carried out on all of these enzymes before (Yoshimoto et al. 1991, Hickman and Ashwell 1960, Hantz 1970), however, none of these enzymes were described to use 11-DOC as a substrate.

3.1.3.1 Investigation of 11-DOC reductase activity of NADH-dependent oxidoreductases

In order to test which of the three putative NADH-dependent oxidoreductases can reduce 11-DOC, *kduD*, *hdhA* and *uxuB* genes were amplified from the genomic DNA of *E. coli* DH5 α and cloned for expression in *E. coli* UT5600 (DE3) (**Fig. 3.10**).

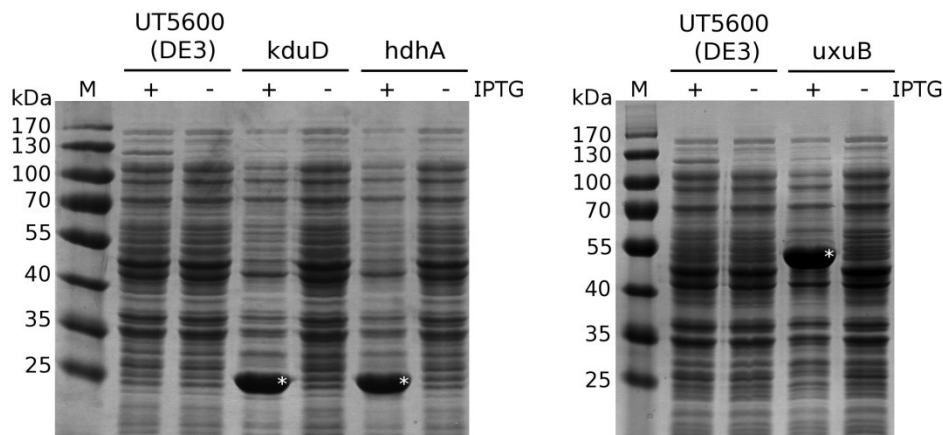


Fig. 3.10 SDS-PAGE of *E. coli* UT5600 (DE3) whole cells overexpressing putative NADH-dependent oxidoreductases from *E. coli* DH5 α . UT5600 (DE3): whole-cell protein extract of UT5600 (DE3) without expression plasmid; *kduD*, *hdhA* and *uxuB*: whole-cell protein extract of UT5600 (DE3) transformed with expression plasmid encoding KduD (27 kDa), HdhA (26.8 kDa) or UxuB (53.6 kDa) oxidoreductases, respectively. The protein expression was induced with IPTG (+) or not induced (-). The protein bands corresponding to overexpressed putative oxidoreductases are depicted with asterisks.

E. coli expressing KduD, HdhA and UxuB were subjected to the whole-cell 11-DOC reductase assay. Only *E. coli* cells expressing KduD converted 11-DOC. The product of this conversion had the same retention time during HPLC as the product obtained with the native cells of *E. coli* DH5 α (**Fig. 3.11**). The cells of *E. coli* UT5600 (DE3) host strain itself did not convert 11-DOC into the product (**Fig. 3.11**).

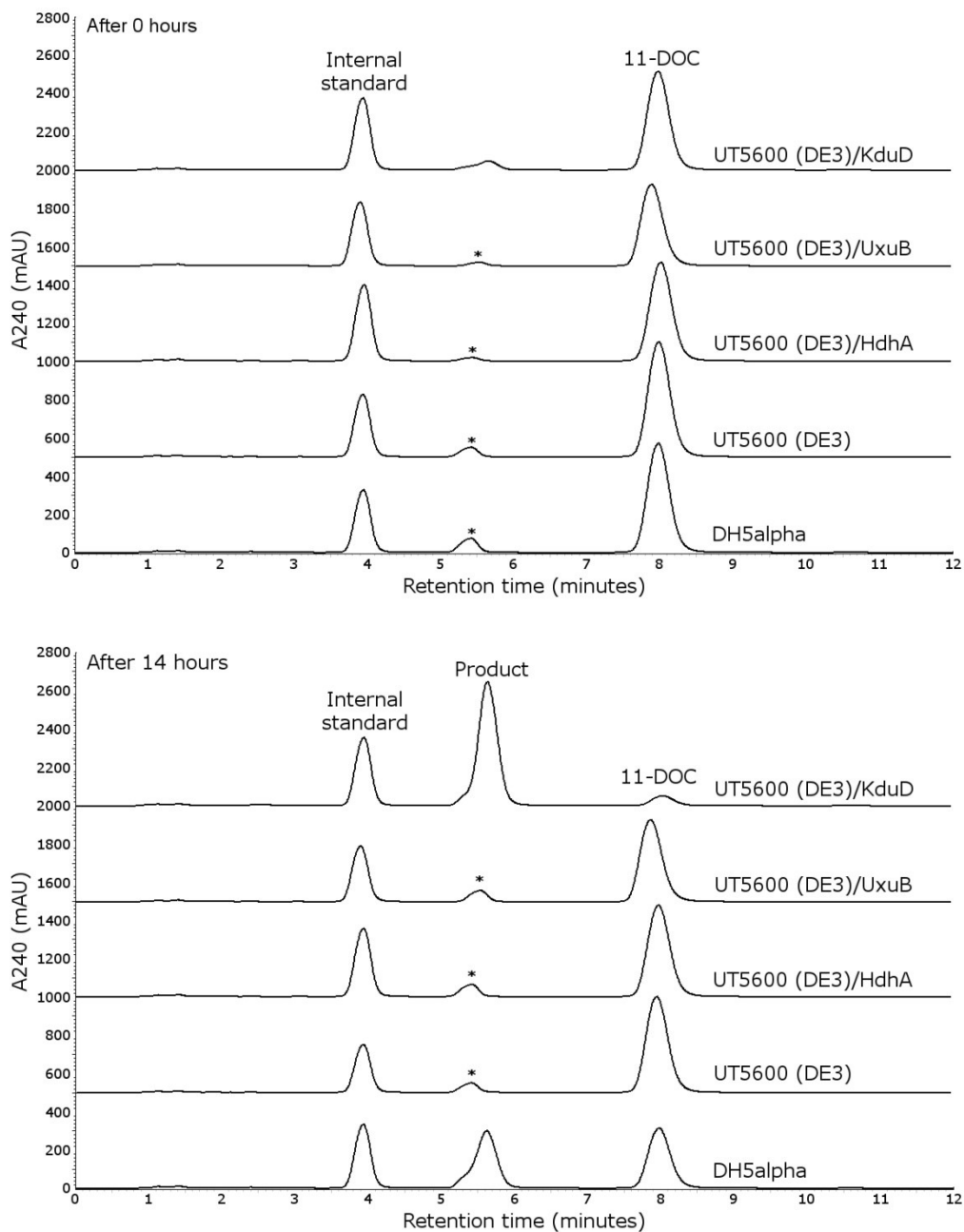


Fig. 3.11 Whole cell 11-DOC reduction assays with *E. coli* overexpressing KduD, HdhA and UxuB, to determine which gene encoded the steroid reductase from *E. coli* DH5 α . *E. coli* UT5600 (DE3) whole-cells overexpressing putative NADH-dependent oxidoreductases as well as *E. coli* DH5 α and UT5600 (DE3) cells not carrying the expression plasmid were concentrated in LB medium to the final OD₆₀₀=25. After addition of 11-DOC (0.4 mM), cells were incubated at 30 °C for 14 hours. Products of the reaction were analyzed by HPLC. Peaks depicted with asterisk (*) represent natural bacterial compounds that were co-extracted and absorbed at 240 nm.

11-DOC transformation with *E. coli* DH5 α cells in LB medium resulted in relatively high yield of 4-pregnen-20,21-diol-3-one (**Fig. 3.11**), in contrast to 11-DOC transformation with *E. coli* DH5 α cells in 100 mM potassium phosphate buffer (pH 7.0) (**Fig. 3.1**). The observed higher conversion of 11-DOC in LB medium than in potassium phosphate buffer could be due to the more efficient intracellular generation of NADH in *E. coli* DH5 α cells incubated in the medium containing carbon source (LB). However, other factors such as higher concentration of *E. coli* DH5 α cells used in 11-DOC transformation assay (OD₆₀₀=25 in **Fig. 3.11** and OD₆₀₀=10 in **Fig. 3.1**) as well as lower reaction temperature (30 °C in **Fig. 3.11** and 37 °C in **Fig. 3.1**) might have influenced the overall yield of the product.

3.2 Characterization of KduD oxidoreductase

3.2.1 Purification of KduD and optimization of reaction conditions

In order to characterize KduD oxidoreductase, an N-terminal 6xHis version of the enzyme was overexpressed in *E. coli* UT5600 (DE3). The recombinant enzyme (28 kDa) was purified using Ni-NTA affinity chromatography to a purity of more than 99 % (**Fig. 3.12**).

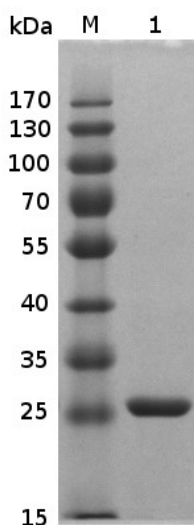


Fig. 3.12 Denaturing SDS-PAGE of the purified recombinant KduD. M: protein molecular weight marker, 1: purified KduD (4.4 μ g) with an N-terminal 6xHis tag.

In total 21 mg of recombinant enzyme were purified from 0.72 g of wet recombinant *E. coli* biomass. A protein concentration of purified enzyme sample was 17.46 mg/ml, specific activity was determined to be - 0.0598 U/mg.

In order to select the reaction conditions for characterization of recombinant KduD, the effects of enzyme, substrate (11-DOC) and cofactor (NADH) concentrations on the amount of formed reaction product (4-pregnen-20,21-diol-3-one) were investigated. A linear relationship between the amount of formed product and the concentration of enzyme in the reaction mixture was observed with up to $0.0218 \text{ mg ml}^{-1}$ of KduD (**Fig. 3.13a**). In the range of 0.1-0.4 mM of 11-DOC the increasing amount of product was formed, however, in the presence of high concentration of substrate, such as 1 mM of 11-DOC, an inhibition of KduD was observed (**Fig. 3.13b**). The saturation of product formation was achieved in the presence of 0.4 mM of NADH, but no inhibition of KduD was observed with up to 1.2 mM of NADH in the presence of 0.4 mM of 11-DOC (**Fig. 3.13c**).

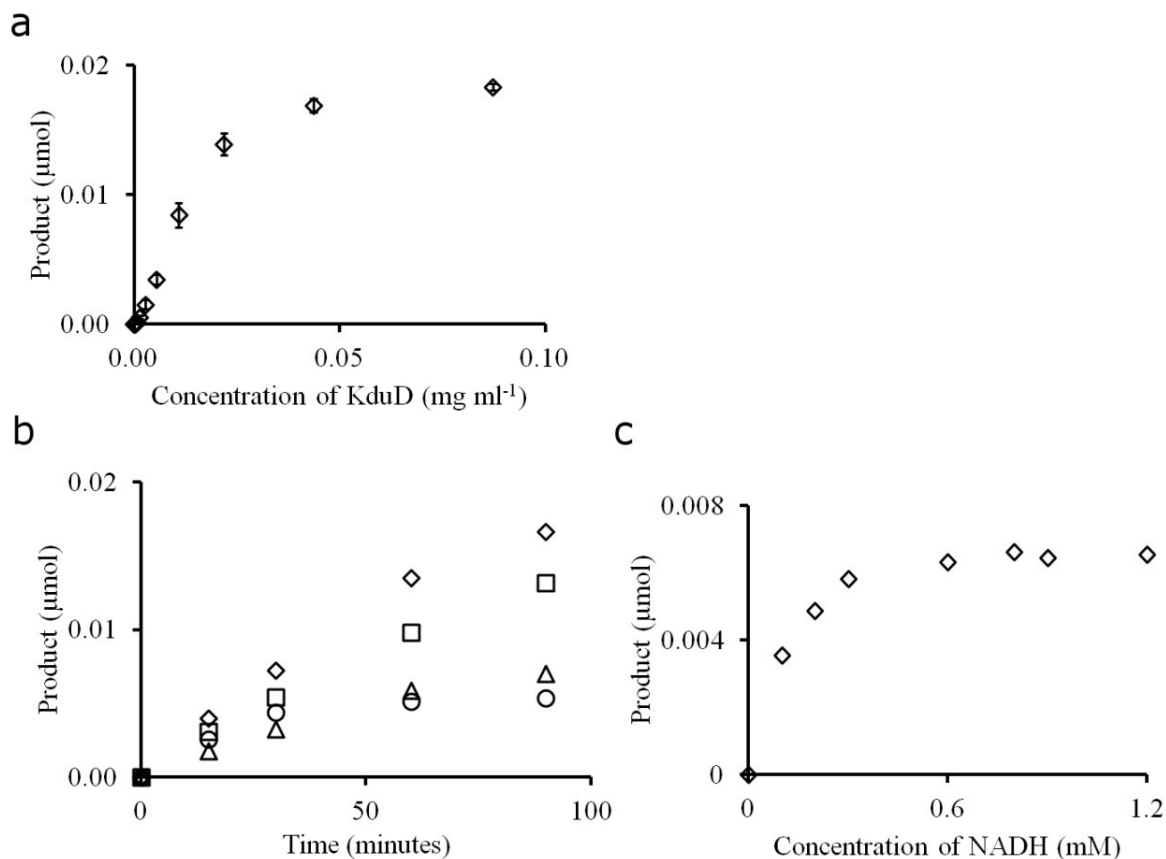


Fig. 3.13 Effect of reaction conditions on amount of produced 4-pregnen-20,21-diol-3-one with recombinant KduD. Effect of enzyme concentration (a): various amounts of KduD were incubated in 100 mM potassium phosphate buffer (pH 7.0) with 0.4 mM of 11-DOC and 0.4 mM of NADH for two hours at 37° C. The mean values \pm SD of three experiments are shown. Effect of substrate concentration (b): KduD (0.02 mg ml⁻¹) was incubated in 100 mM potassium phosphate buffer (pH 7.0) with 0.4 mM of NADH and various amounts of 11-DOC: 0.1 mM (Δ), 0.2 mM (\square), 0.4 mM (\diamond) or 1 mM (\circ), for 90 minutes at 37° C. Effect of cofactor concentration (c): KduD (0.02 mg ml⁻¹) was incubated in 100 mM potassium phosphate buffer (pH 7.0) with 0.4 mM of 11-DOC and various concentrations of NADH for 30 minutes at 37° C. Formed product was quantified using HPLC assay as described in Materials and Methods.

3.2.2 Determination of the substrate spectrum

The activity of purified KduD was tested against a total of 9 potential steroid substrates, 10 potential sugar substrates, and 12 other non-steroidal compounds. All sugar and non-steroid substrates were tested by a continuous spectrophotometric assay for NADH oxidation (or NAD⁺ reduction) for 30 minutes at 37°C. Turnover of steroid substrates was tested using HPLC assays, after incubation for up to two hours at 37°C. In addition to 11-DOC, five other steroid compounds (11-deoxycortisol, cortisol, corticosterone, cortisone and 21-hydroxypregnenolone)

were reduced by KduD (**Fig. 3.14**). In contrast, the turnover of pregnenolone, testosterone propionate, cortisone acetate, or progesterone was not detectable. The molecular masses of the steroid substrates and the products formed by KduD were confirmed by LC-MS. The obtained molecular masses were found to match the expected theoretical masses of the steroid substrates (20-ketosteroids) and their respective reduced forms (20-hydroxysteroids). Hannemann *et al.* (2007) showed that *E. coli* 11-DOC reductase, which was identified as KduD in this work, is a regioselective enzyme which catalyzes the reduction of only C20 carbonyl group of 11-DOC producing respective 20-hydroxysteroid (4-pregnen-20,21-diol-3-one). Results of mass spectrometry and carbon-13 nuclear magnetic resonance (NMR) clearly indicated that carbonyl group at C3 position and the double bond at C4-C5 position of 11-DOC were not reduced by *E. coli* 11-DOC reductase (Hannemann *et al.* 2007). Thus, based on the previous findings of Hannemann *et al.* (2007), KduD should reduce its 20-ketosteroid substrates only at C20 position producing respective 20-hydroxysteroid products.

11-deoxycortisol served as the best substrate for KduD, whereas conversion of cortisol, 11-DOC and 21-hydroxypregnenolone by KduD was about two and a half fold lower in comparison to 11-deoxycortisol (**Fig. 3.14**). In contrast, the activity of KduD against corticosterone was relatively low (only 6.3 % substrate conversion in two hours, **Fig. 3.14**). Steroid compounds that lack C21 hydroxyl group next to C20 carbonyl group (pregnenolone and progesterone) were not reduced by KduD (**Fig. 3.14**). In addition, cortisone acetate, which has the C21 hydroxyl group blocked with an acetyl group, was also not converted by KduD (**Fig. 3.14**).

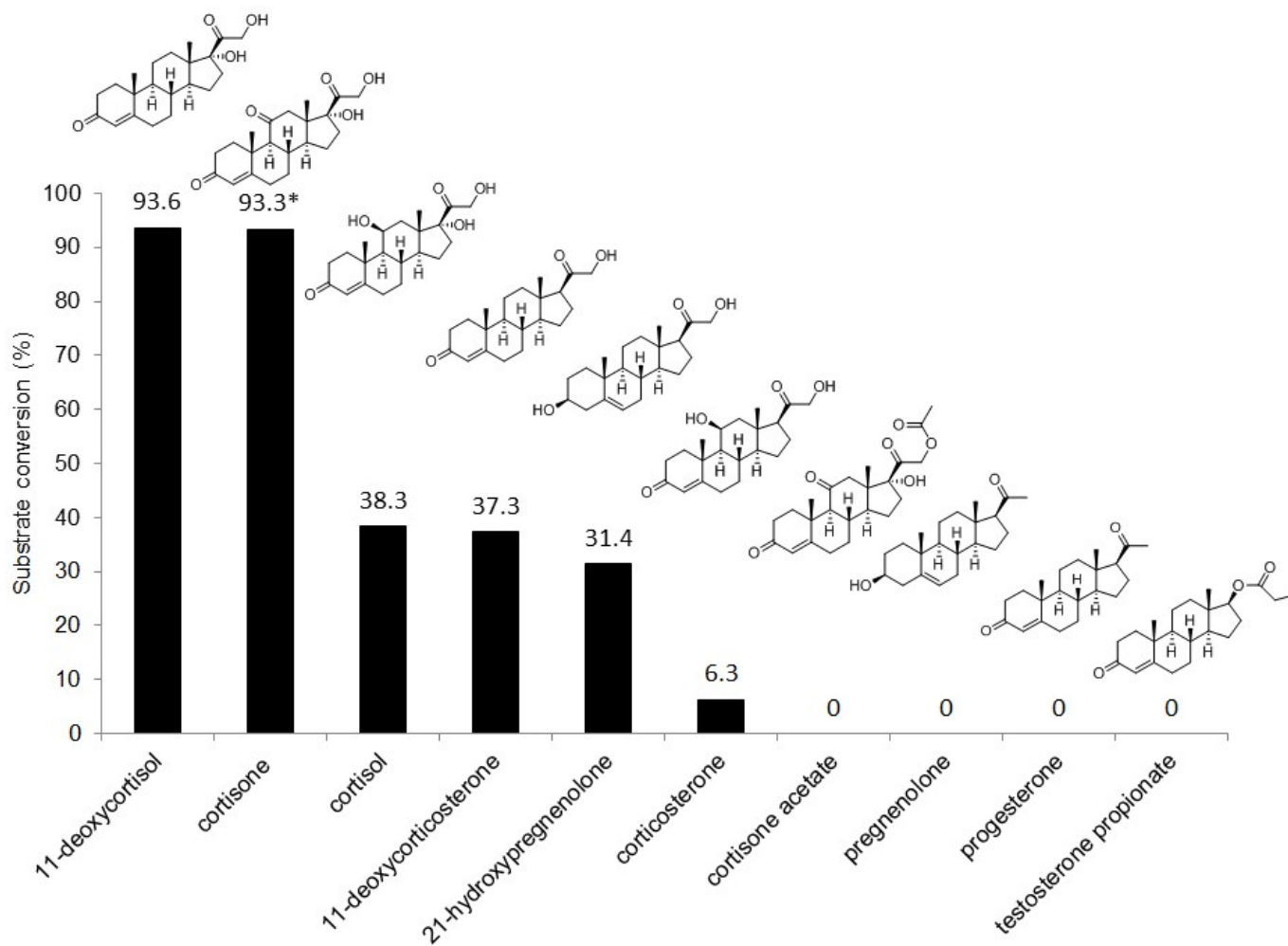


Fig. 3.14 Reduction of steroid substrates by KduD. The amount of the substrate (in %) that is converted into the product by the recombinant enzyme after two hours (* five hours) incubation time is shown below the structure of the steroid substrate. Substrate conversion was calculated based on the areas under the substrate and product peaks in the HPLC chromatograms. The reaction was performed in 100 mM potassium phosphate buffer (pH 7.0) with 0.02 mg ml⁻¹ KduD, 0.6 mM NADH and 0.4 mM of steroid substrate at 37 °C for two hours (* five hours).

It was found that KduD can also reduce 5-keto-D-gluconate (tested at the concentrations of 88 mM) and oxidize D-gluconate and 1,2-propanediol (both tested at the concentration of 100 mM) (Fig. 3.15).

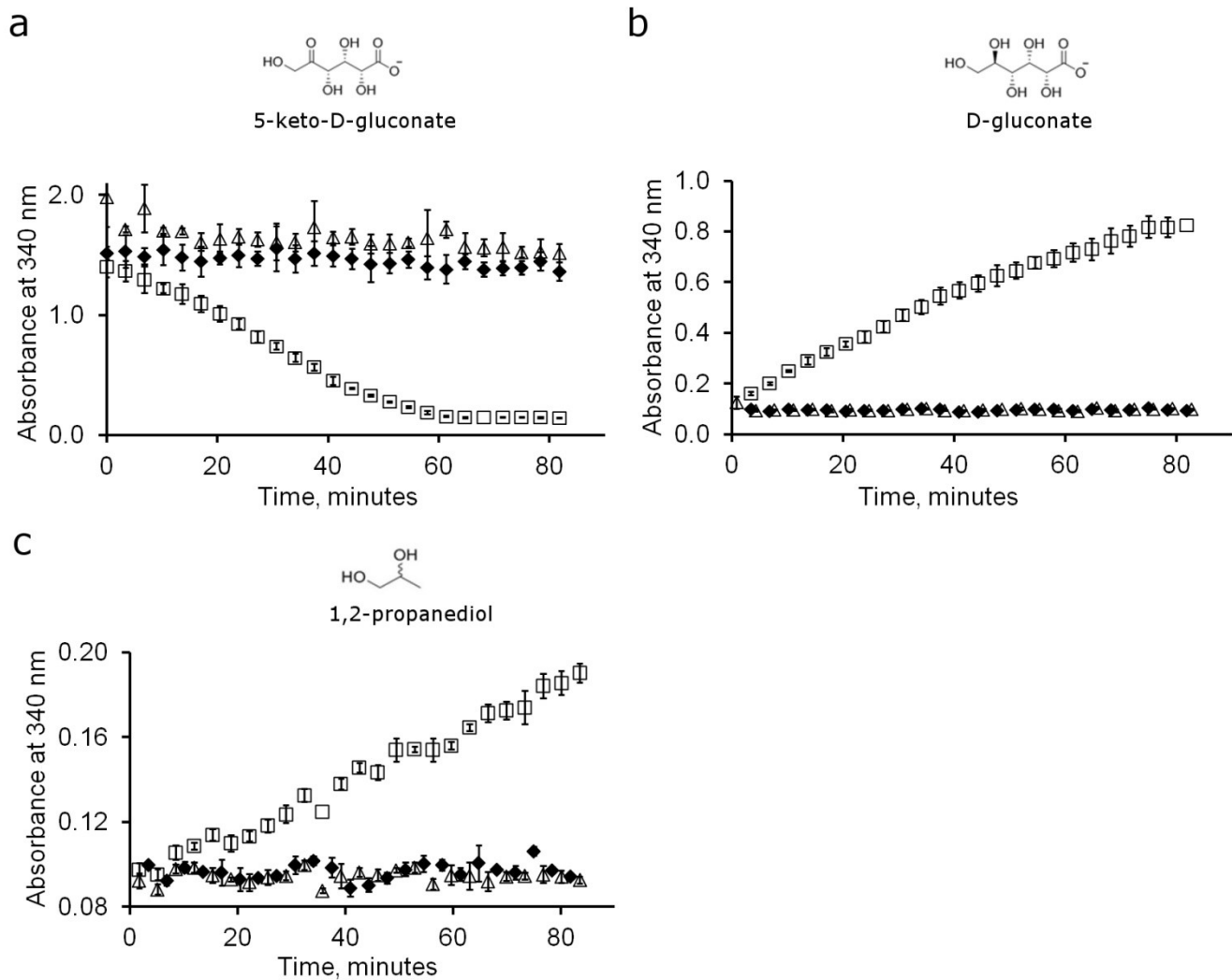


Fig. 3.15 Novel polyol substrates of KduD. KduD catalyzed reduction of 5-keto-D-gluconate (**a**), oxidation of D-gluconate (**b**) and oxidation of 1,2-propanediol (**c**) was measured using spectrophotometric microplate assay. The presented data are means \pm SD from three measurements. The following reactions are shown: with enzyme and without a substrate (\blacklozenge), with enzyme and with substrate (\square), with substrate and without an enzyme (\triangle). Reduction reaction was performed at 37 °C with 0.02 mg ml⁻¹ of KduD in 100 mM potassium phosphate buffer (pH 7.0) in presence of 0.6 mM of NADH and 88 mM of 5-keto-D-gluconate (**a**); oxidation reactions were performed at 37 °C with 0.02 mg ml⁻¹ of KduD in 100 mM glycine-NaOH buffer (pH 9.3) in presence of 1 mM NAD⁺, and 100 mM D-gluconate (**b**) or 1,2-propanediol (**c**).

KduD did not show any detectable reduction of the following compounds: pyruvate, glyoxal, oxaloacetic acid, dihydroxyacetone phosphate, 2-oxobutyrate, 3-bromopyruvic acid, acetylacetone, 3,4-hexanedione, 2,5-hexanedione, D-gluconate (tested at the concentration of 0.4 mM), D-(-)-fructose and hydroxyacetone (tested at the concentrations of 0.4-100 mM),

2-hydroxyacetophenone (tested at the concentrations of 1-100 mM). KduD did not show any detectable oxidation of the following compounds: D-(+)-glucose, D-(-)-fructose, L-(+)-arabinose, D-mannitol, inositol, D-(+)-galactose, D-mannose, D-sorbitol, 5-keto-D-gluconate and glycerol when tested at the concentration of 20 mM at 37 °C.

3.2.2.1 Reduction of doxorubicin and doxorubicinone by KduD

Recent high-throughput protein-protein interaction studies suggested that KduD from *E. coli* K-12 interacts with NuoG protein (NADH-quinone oxidoreductase subunit G) *in vivo* (Arifuzzaman 2006). NuoG is a component of a multisubunit respiratory electron transport complex I, which is found in bacteria, archaea, mitochondria of eukaryotes, and chloroplasts of plants (Friedrich and Scheide 2000). In addition, another recent study showed that NADH dehydrogenase component (consisting of subunits nuoE, nuoF and nuoG) of respiratory complex I is involved in inactivation of anticancer drug doxorubicin in *Streptomyces* WAC04685 (Westman et al. 2012). The doxorubicin inactivation pathway described by Westman *et al.* (2012) involves reductive deglycosylation of doxorubicin into 7-deoxydoxorubicinolone and subsequent reduction of 7-deoxydoxorubicinolone to 7-deoxydoxorubicinol by unidentified cytoplasmic carbonyl reductase as illustrated in **Fig. 3.16**.

Molecules of doxorubicin and 7-deoxydoxorubicinolone share a common structural feature with steroid substrates of KduD. Both molecules have a carbonyl group at C13 position (equivalent to C20 carbonyl group of KduD substrate 11-DOC) and hydroxyl group at adjacent C14 position (equivalent to hydroxyl group at C21 position of 11-DOC). As a result, doxorubicin, 7-deoxydoxorubicinolone and related compounds were predicted to be substrates of KduD.

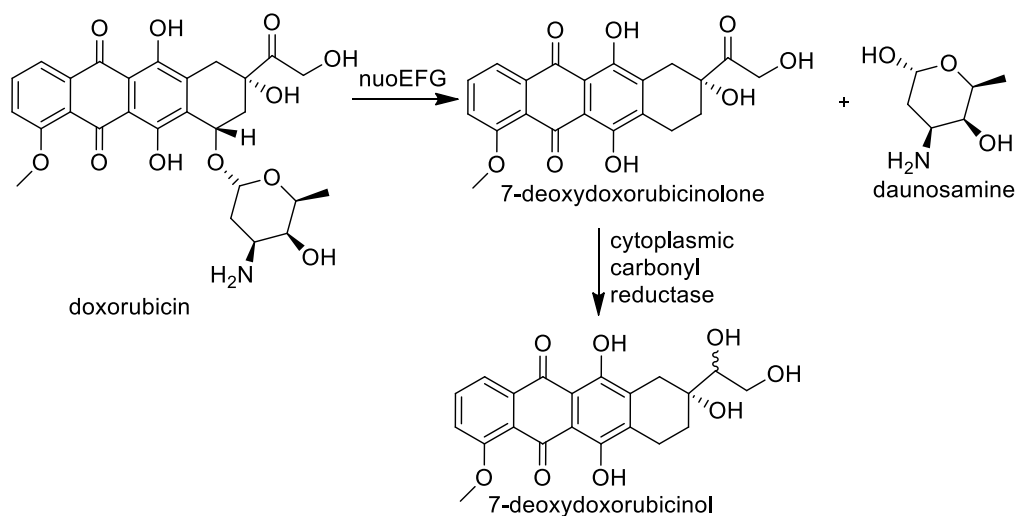


Fig. 3.16 Doxorubicin inactivation in *Streptomyces* WAC04685. Scheme was adapted from the publication of Westman *et al.* (2012).

The activity of KduD against doxorubicin was investigated under the same conditions as for steroids. Incubation of doxorubicin with KduD resulted in formation of a very small amount of a new product (**Fig. 3.17**, RT=6.5 min). It was assumed that doxorubicin is not an optimal substrate for KduD because of the bulky carbohydrate moiety present at the C7 position of doxorubicin molecule.

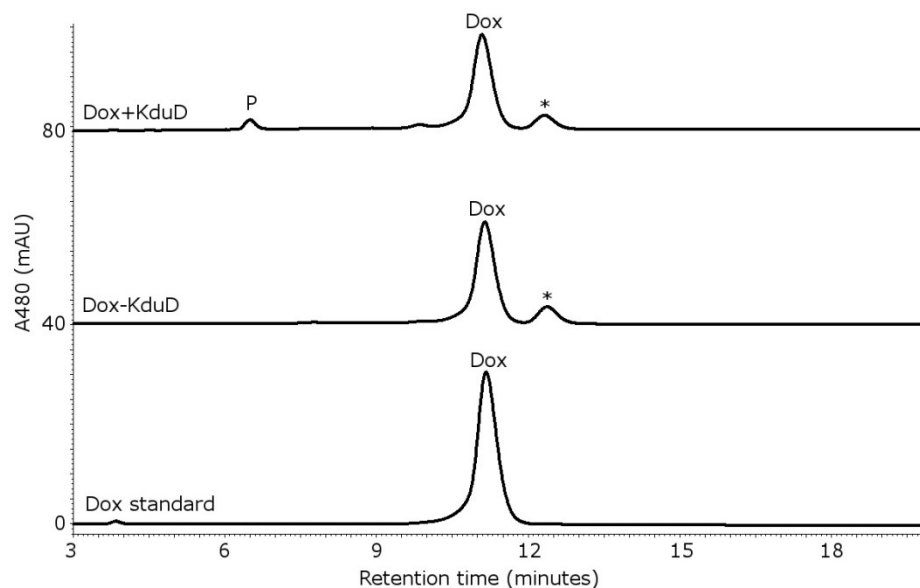


Fig. 3.17 HPLC chromatograms of doxorubicin conversions with KduD. Dox standard: doxorubicin standard, Dox-KduD: doxorubicin incubated without KduD in 100 mM potassium phosphate buffer (pH 7.0) in presence of NADH, Dox+KduD: doxorubicin incubated with KduD in 100 mM potassium phosphate buffer (pH 7.0) in presence of NADH. All samples, except Dox standard, were incubated at 37 °C for 16 hours. Reaction was performed in 100 mM potassium phosphate buffer (pH 7.0) with 0.02 mg ml⁻¹ KduD, 0.6 mM NADH and 0.4 mM of doxorubicin. P: new product, Dox: doxorubicin, *: unidentified compound resulting from spontaneous degradation of doxorubicin.

In order to test the hypothesis that the carbohydrate moiety in doxorubicin prevents KduD from reducing this compound, the activity of KduD against a doxorubicinone, a deglycosylated derivative of doxorubicin, was tested. Doxorubicinone was produced by the mild acidic hydrolysis of doxorubicin. Under these conditions, only approximately 1/3 of doxorubicin was deglycosylated into doxorubicinone (**Fig. 3.18**, RT=18.2 min) and 2/3 were left intact in the sample (**Fig. 3.18**, RT=11.0 min). When partially hydrolyzed doxorubicin sample was incubated with KduD oxidoreductase in the presence of NADH, a complete reduction of doxorubicinone into the new product (**Fig. 3.18**, RT=9.8 min) was observed. In addition to that, formation of a small amount of a second product (**Fig. 3.18**, RT=6.5 min), which was also previously detected in the sample of pure doxorubicin incubated with KduD (**Fig. 3.17**), was also observed. The LC-MS measurements showed that the new product that has a retention time of 9.8 min is produced by KduD catalyzed reduction of doxorubicinone, whereas the product that has a retention time of 6.5 min is generated by KduD catalyzed reduction of doxorubicin (**Table 3.6**).

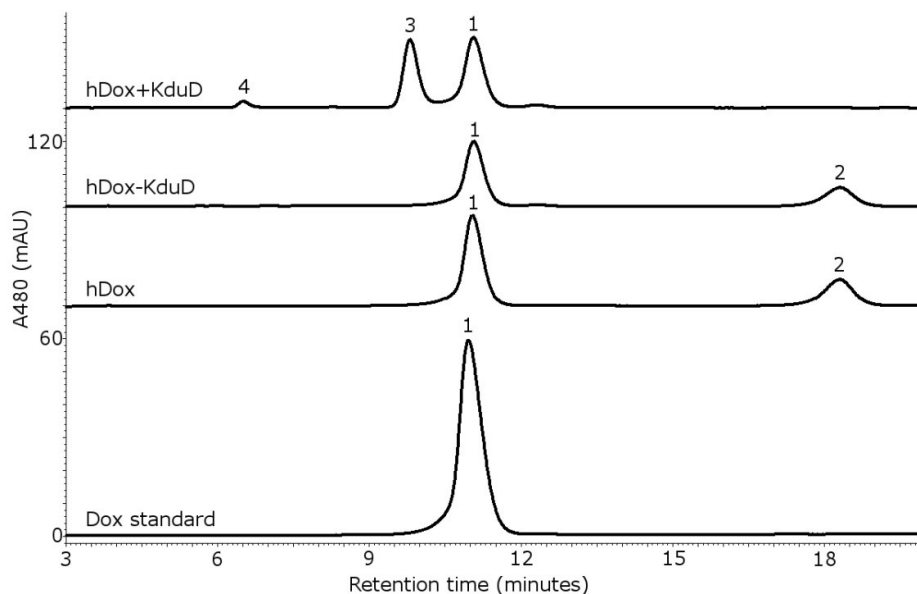
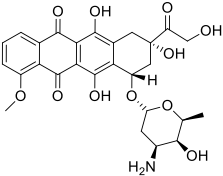
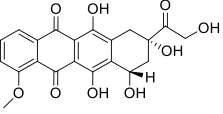
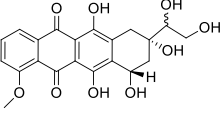
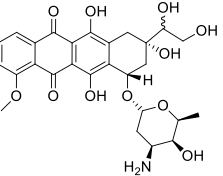


Fig. 3.18 HPLC chromatograms of doxorubicinone conversion with KduD. Dox standard: doxorubicin standard, hDox: partially hydrolyzed doxorubicin sample obtained after mild acidic hydrolysis of doxorubicin, hDox-KduD: partially hydrolyzed doxorubicin sample incubated without KduD in 100 mM potassium phosphate buffer (pH 7.0) in presence of NADH, hDox+KduD: partially hydrolyzed doxorubicin sample incubated with KduD in 100 mM potassium phosphate buffer (pH 7.0) in presence of NADH. All samples, except Dox standard and hDox, were incubated at 37 °C for 16 hours. Reaction was performed in 100 mM potassium phosphate buffer (pH 7.0) with 0.02 mg ml⁻¹ KduD, 0.6 mM NADH and 0.15 mM of hydrolyzed doxorubicin. Peak 1: doxorubicin, 2: doxorubicinone, 3: doxorubicinolone (predicted), 4: doxorubicinol (predicted). Identities of HPLC peaks were further investigated by LC-MS as summarized in Table 3.6.

Table 3.6 Summary of LC-MS analysis of samples of hDox conversion by KduD.

Peak number	1	2	3	4
Retention time (minutes)	11.0	18.2	9.8	6.5
Expected compound	Doxorubicin	Doxorubicinone	Doxorubicinolone	Doxorubicinol
Structure				
Molecular mass	543.52	414.36	416.38	545.52
Ions detected by LC-MS	[M+H] ⁺ =544.19	[M+H] ⁺ =415.12 [M+H] ⁺ -H ₂ O=397.11 [2M+Na] ⁺ =851.20	[M+H] ⁺ =417.12 [M+H] ⁺ -H ₂ O=399.11 [2M+Na] ⁺ =855.22	[M+H] ⁺ =546.2

3.2.3 The pH and temperature optimum

The pH optimum of KduD was tested for the reduction of 11-DOC and oxidation of D-gluconate. For the reduction reaction, the enzyme showed the highest activity at pH 7.0 in 100 mM potassium phosphate buffer (**Fig. 3.19a**). In contrast, the oxidation reaction showed the highest activity at pH 9.5, in sodium-glycine buffer (**Fig. 3.19b**). The optimal temperature for the reduction of 11-DOC was found to be 37 °C (**Fig. 3.19c**).

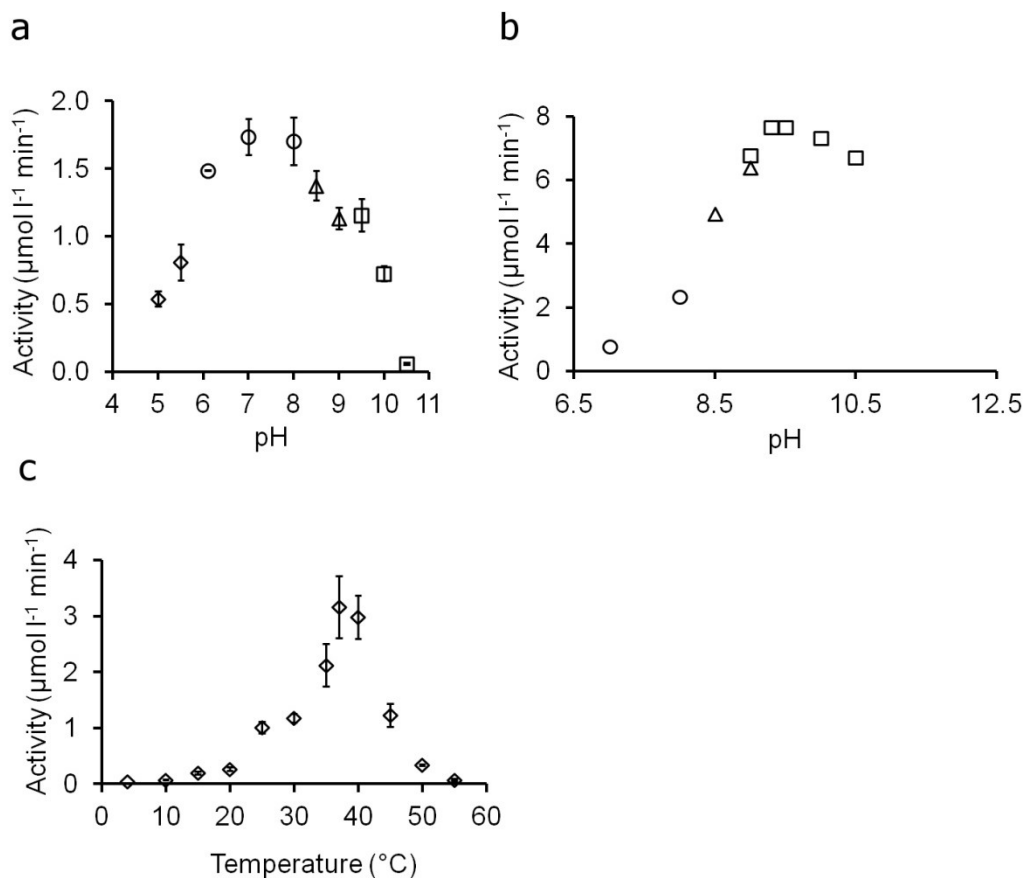


Fig. 3.19 pH and temperature optimum of KduD. (a) Reduction of 11-DOC at various pH values at 37°C. Reaction was performed with 0.02 mg ml⁻¹ of KduD in the presence of 0.4 mM 11-DOC and 0.6 mM NADH in various buffers (100 mM): sodium acetate pH 5.0-5.5 (\diamond), potassium phosphate pH 6.1-8.0 (\circ), Tris-HCl pH 8.5-9.0 (Δ) and glycine-NaOH pH 9.5-10.5 (\square) for 40 minutes. The amount of formed product (4-pregnen-20,21-diol-3-one) was quantified using HPLC. The activity is expressed as μM of product formed by KduD per one minute. (b) Oxidation of D-gluconate at various pH values at 37°C. The initial reaction velocity was monitored by the detection of formed NADH using spectrophotometer. Reaction was performed with 0.02 mg ml⁻¹ of KduD in the presence of 100 mM D-gluconate and 1 mM NAD⁺ in various buffers (100 mM): potassium phosphate pH 7.0-8.0 (\circ), Tris-HCl pH 8.5-9.0 (Δ) and glycine-NaOH pH 9.0-10.5 (\square). The activity is expressed as an initial reaction velocity, which was calculated using molar extinction coefficient of NADH. (c) Reduction of 11-DOC at various temperatures. Reaction

was performed with 0.02 mg ml⁻¹ of KduD in the presence of 0.4 mM 11-DOC and 0.6 mM NADH in 100 mM potassium phosphate buffer (pH 7.0) for 60 minutes. The amount of formed product (4-pregnen-20,21-diol-3-one) was quantified using HPLC. The activity is expressed as μM of product formed by KduD per one minute. In (a) and (c) data are shown as means ± SD of three experiments.

3.2.4 Effect of metal ions, salts and reducing agents

An effect of various agents (divalent metal ions, EDTA, reducing, oxidizing compounds) on the activity of KduD was tested for the D-gluconate oxidation reaction. The initial velocity of D-gluconate oxidation with KduD without an effector and in the presence of an effector was compared. Divalent metal ions Zn²⁺, Mg²⁺, Ca²⁺ and Mn²⁺ at concentration of 1 mM did not show any significant stimulating effect on the activity of KduD. In contrast, at high concentrations of divalent metal ions (100 mM) the activity of KduD was reduced ~50-60 % (Mg²⁺, Ca²⁺) or inhibited completely (Zn²⁺) (Fig. 3.20). Preincubation of KduD with 100 mM of EDTA for three hours did not decrease the activity of KduD (Fig. 3.20).

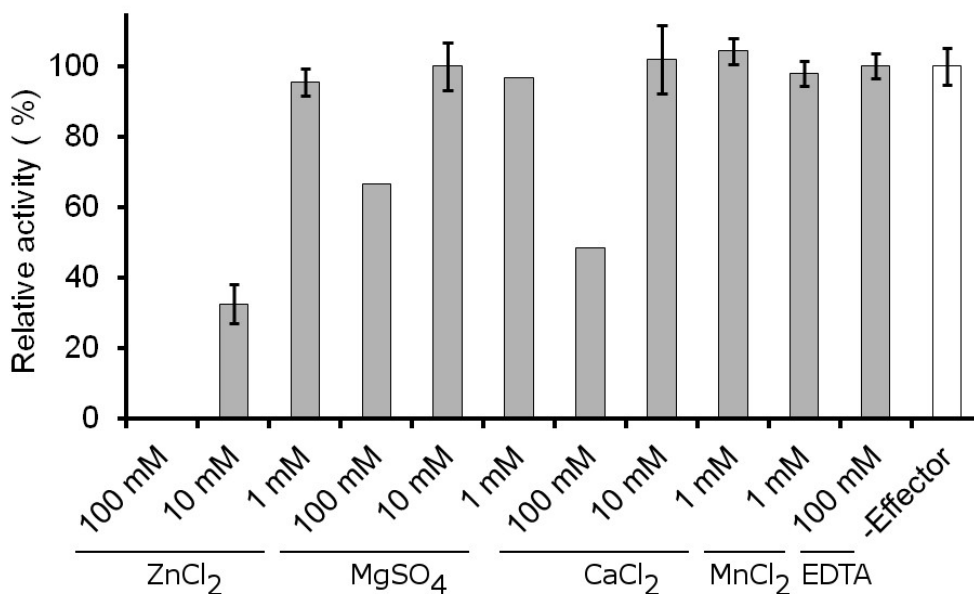


Fig. 3.20 The effect of divalent metal ions and EDTA on the activity of KduD. The initial velocity of oxidation of D-gluconate catalyzed by KduD was monitored by measuring the absorbance of formed NADH. The activity of KduD was expressed in % as a ratio of initial velocity of reaction with effector and initial velocity of reaction without an effector. The data shown are means of 2-3 experiments. Standard deviations (indicated by error bars) were calculated only for the data obtained from three experiments.

The inhibition of the activity of KduD was observed with NaCl at concentrations higher than 10 mM (**Fig. 3.21**). In the presence of NaCl at concentrations higher than 0.5 M, the activity of KduD was inhibited completely (**Fig. 3.21**). The activity of KduD was investigated in the presence of various disulfide bonds reducing agents (dithiothreitol (DTT), 2-mercaptoethanol (2-ME) and glutathione (GSH)) and cysteines oxidizing agent glutathione disulfide (GSSG). At concentrations 0.01-0.1 mM DTT had no effect on the activity of KduD. It showed a slight inhibition at 1 mM and up to 50 % inhibition at 10 mM. Likewise, 2-ME showed inhibitory effect at 0.1 mM and higher concentrations. A 100 % inhibition of KduD activity was observed in the presence of 10 mM 2-ME. The GSH had no strong stimulating effect on the activity of KduD at concentration of 0.7 mM and showed slight inhibition at 7 mM. Similar results were obtained with GSSG, which also showed inhibitory effect on the activity of KduD (**Fig. 3.22**) at higher concentrations (7 mM).

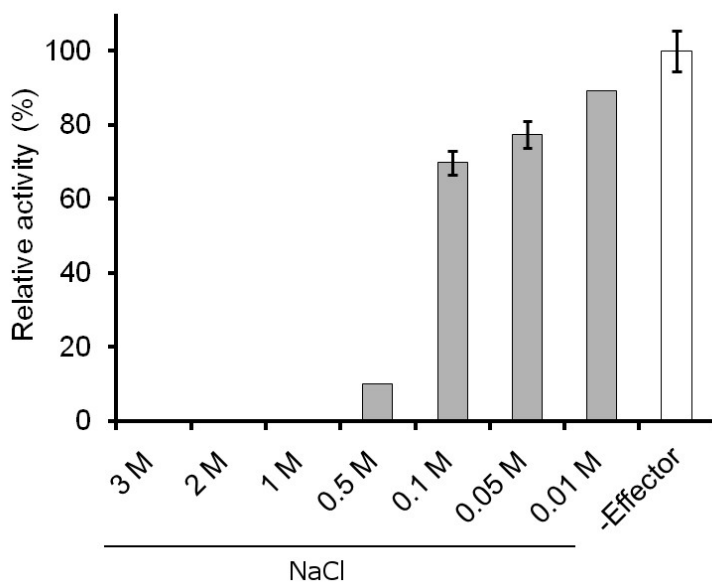


Fig. 3.21 The effect of NaCl on the activity of KduD. The initial velocity of oxidation of D-gluconate catalyzed by KduD was monitored by measuring the absorbance of formed NADH. The activity of KduD was expressed in % as a ratio of initial velocity of reaction with NaCl and initial velocity of reaction without NaCl. The data shown are means of 2-3 experiments. Standard deviations (indicated by error bars) were calculated only for the data obtained from three experiments.

KduD oxidoreductase was found to be sensitive to common protein denaturing agents, ethanol and urea, and long-chain fatty acids (**Fig. 3.23**). The enzyme was completely deactivated in the

presence of 10 % of ethanol in reaction mixture (**Fig. 3.23a**). A decrease of activity of KduD with increasing concentrations of urea was observed. In the presence of 0.2 M of urea KduD activity decreased by approximately 30 % (**Fig. 3.23a**). Furthermore, no activity of KduD could be measured in the presence of 1 mM of lauric or myristic acids (**Fig. 3.23b**).

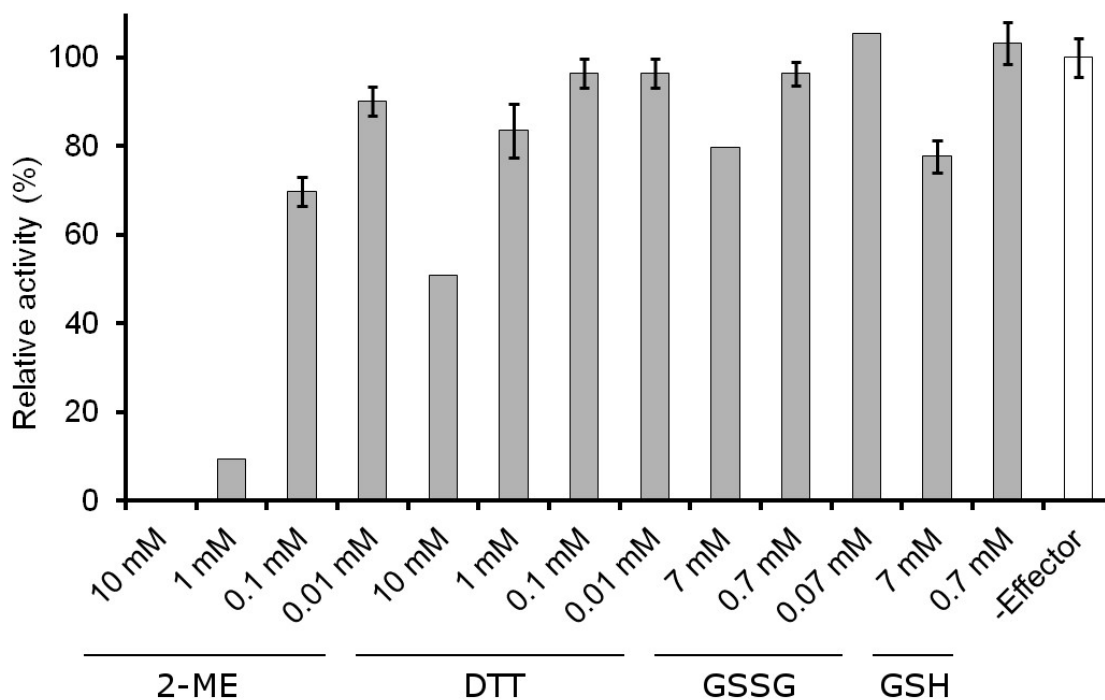


Fig. 3.22 The effect of reducing and oxidizing agents on the activity of KduD. The initial velocity of oxidation of D-gluconate catalyzed by KduD was monitored by measuring the absorbance of formed NADH. The activity of KduD was expressed in % as a ratio of initial velocity of reaction with effector (2-ME: 2-mercaptoethanol, DTT: dithiothreitol, GSSG: glutathione disulfide, GSH: glutathione) and initial velocity of reaction without an effector. The data shown are means of 2-3 experiments. Standard deviations (indicated by error bars) were calculated only for the data obtained from three experiments.

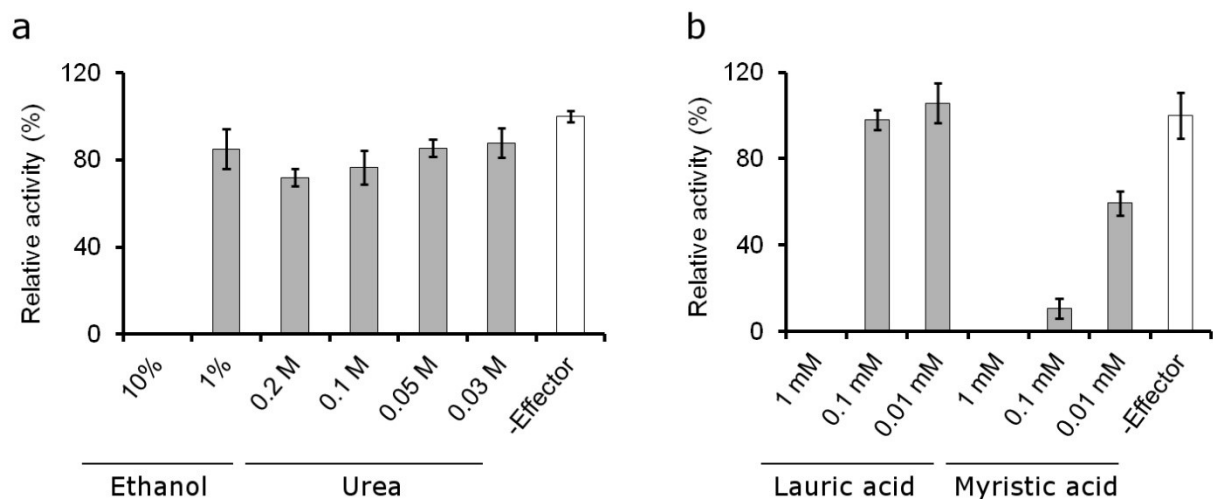


Fig. 3.23 Effect of ethanol, urea, and fatty acids on the activity of KduD. The initial velocity of oxidation of D-gluconate catalyzed by KduD was monitored by measuring the absorbance of formed NADH. **(a)** Activity of KduD in the presence of ethanol and urea. The activity of KduD was expressed in % as a ratio of initial velocity of reaction with effector (ethanol or urea) and initial velocity of reaction without an effector. **(b)** Activity of KduD in the presence of fatty acids. The activity of KduD was expressed in % as a ratio of initial velocity of reaction with effector (lauric acid or myristic acid which were dissolved in ethanol and added to the reaction mixture to obtain the final ethanol concentration of 1 %) and initial velocity of reaction with 1 % of ethanol (without an effector). Data shown are means \pm SD of three experiments.

3.2.5 Kinetic analysis

The kinetic constants for the KduD catalyzed reactions were calculated by plotting the initial reaction rate against the substrate concentration and using nonlinear regression of Michaelis-Menten equation as illustrated for 11-DOC reduction reaction in **Fig. 3.24**.

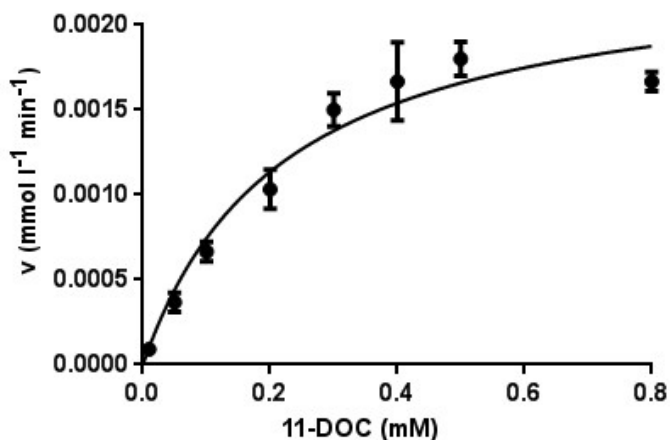


Fig. 3.24 Relationship between an initial reaction rate (v) and the concentration of the substrate of the reduction reaction of 11-DOC catalyzed by the KduD. The error bars represent the standard deviation obtained from three independent experiments. The data points were fitted into Michaelis-Menten equation using nonlinear regression in GraphPad Prism 6.

The calculated kinetic constants are summarized in **Table 3.7**. In a reduction reaction, the KduD showed a ~802-971-fold higher K_M towards the sugar substrate 5-keto-D-gluconate (184.5 mM, **Table 3.7**) than towards the two steroid substrates tested 11-DOC and RSS (0.230 and 0.190 mM, respectively, **Table 3.7**). In the oxidation reaction, the K_M of KduD towards D-gluconate and 1,2-propanediol was $\sim 10^3$ - 10^4 -fold higher than towards the steroid substrates. The K_M value for the cofactor of the enzyme in the reduction reaction (NADH) was determined with the substrate 11-DOC and was found to be 0.037 mM (**Table 3.7**). The K_M of KduD towards D-gluconate and 1,2-propanediol in the oxidation reaction was in the same high millimolar range as for the reduction of 5-keto-D-gluconate, rather than the sub-millimolar range seen for the 11-DOC and RSS. The K_M value for the cofactor of the enzyme in the oxidation reaction (NAD⁺) was determined with the substrate D-gluconate and was found to be 0.285 mM (**Table 3.7**), around 8-fold higher than the K_M towards NADH. The k_{cat} of KduD towards the sugar substrates (31-58 min⁻¹) and 1,2-propanediol (18 min⁻¹) was in approximately the same range as the k_{cat} towards the steroid RSS (17 min⁻¹), and only ~10-19-fold higher than the k_{cat} towards 11-DOC (3.1 min⁻¹). Due the lower K_M values measured for the steroid substrates, the “specificity constant” (k_{cat}/K_M) was over ~81- 1.5×10^4 -fold higher for the steroid substrates than for the sugars or 1,2-propanediol (**Table 3.7**).

Table 3.7 Calculated kinetic constants of KduD.

Compound	v_{\max} (10^{-3} mM min $^{-1}$)	K_M (mM)	k_{cat} (min $^{-1}$)	k_{cat}/K_M (min $^{-1}$ mM $^{-1}$)
11-DOC ^{a)}	2.4 ± 0.1	0.230 ± 0.055	3.1	13.5
RSS ^{a)}	12.9 ± 0.7	0.190 ± 0.019	16.6	87.6
D-gluconate ^{b)}	45.4 ± 7.7	544.8 ± 143.4	58.3	0.107
5-keto-D-gluconate ^{b)}	23.9 ± 2.9	184.5 ± 23.2	30.7	0.166
1,2-propanediol ^{b)}	14.2 ± 1.3	3,231 ± 305	18.3	0.006
NADH ^{a), c)}	1.3 ± 0.1	0.037 ± 0.009	1.7	46.4
NAD ^{+b), d)}	9.8 ± 0.2	0.285 ± 0.020	12.6	44.2

^{a)} the kinetics of the reaction was followed using HPLC-based assay, ^{b)} the kinetics of the reaction was followed using spectrophotometric assay, ^{c)} the kinetic constants were determined with 11-DOC as a substrate, ^{d)} the kinetic constants were determined with D-gluconate as a substrate. The v_{\max} , K_M and k_{cat} data are the means ± standard deviations.

3.3 Investigation of the effect of 11-DOC on the expression level of KduD in *Escherichia coli*

The specific steroid C-20 reductase activity was measured and compared in cell-free extracts of *E. coli* DH5 α and UT5600 (DE3) cells cultivated in LB medium with 11-DOC and without this steroid compound. Comparable specific activities of 20-ketosteroid reductase in the cell-free extracts of *E. coli* DH5 α cells that were cultured in LB medium in the presence of 11-DOC and in the absence of this steroid were measured (**Table 3.8**). Moreover, the specific steroid reductase activity was not detected in the cell-free extracts of *E. coli* UT5600 (DE3) cells that were grown in LB medium with 11-DOC or without it (**Table 3.8**).

Table 3.8 Comparison of specific steroid reductase activities in *E. coli* DH5 α and UT5600 (DE3) cultured with and without 11-DOC**.

<i>E. coli</i> strain	Cultivation conditions	Specific activity (10^{-3} U mg $^{-1}$)
DH5 α	-	0.18 ± 0.01
	+MeOH	0.17 ± 0.04
	+11-DOC	0.15 ± 0.03
UT5600 (DE3)	-	0*
	+MeOH	0*
	+11-DOC	0*

**Cells were cultured under various conditions: in LB medium without 11-DOC or methanol (-), in LB medium supplemented with methanol (+MeOH), in LB medium supplemented with 11-DOC (+11-DOC). The specific activity data was obtained from three experiments (mean ± standard deviation), * - no product detectable under conditions as described in *Materials and Methods*.

3.4 Autodisplay based on AIDA-I autotransporter

3.4.1 Design and expression of fusion protein FP

For the surface expression of KduD oxidoreductase in *E. coli* host, the plasmid pAT002 was designed as described in *Materials and Methods*. The pAT002 plasmid codes for the fusion protein FP, which consists of N-terminal signal peptide, 6xHis-tagged KduD oxidoreductase and the translocator unit (linker region and β -barrel) of AIDA-I autotransporter protein as shown in **Fig. 3.25**.

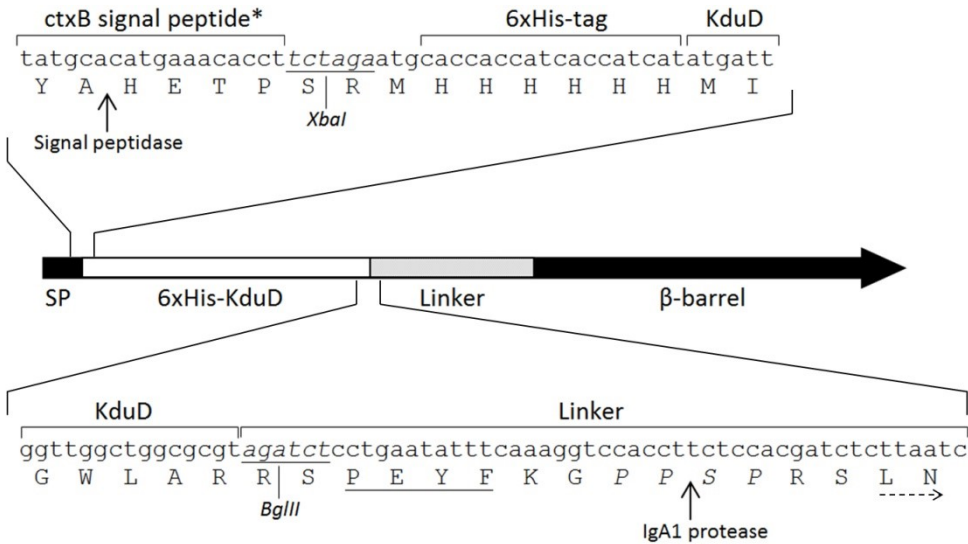


Fig. 3.25 The domain structure of FP fusion protein encoded by pAT002 plasmid. A gene encoding KduD oxidoreductase fused to N-terminal 6xHis-tag was amplified by PCR and inserted into pET-SH3-SDH08 plasmid using *XbaI* and *BglIII* restriction endonuclease cleavage sites (shown in italics and underlined in DNA sequence) as described in *Materials and Methods*. In the protein sequence PEYFK-tag is underlined and IgA1 protease cleavage site is shown in italics. * - mutated signal peptide (SP) of cholera toxin B subunit (ctxB). In comparison to wild-type ctxB protein sequence (GenBank AED88285.1) mutated ctxB contains two point mutations: I2V and G21E (numbering according to the GenBank AED88285.1). Signal peptidase cleavage site was predicted by SignalP 4.1 (Petersen et al. 2011). A start of a protein sequence derived from *E. coli* AIDA-I autotransporter (GenBank: Q03155.1, amino acids: 840-1286) is depicted with a broken arrow. In comparison to sequence of wild-type *E. coli* AIDA-I, the following point amino acid mutations are present in the linker and β -barrel region of pAT002 plasmid-encoded fusion protein: A975T, K1008R, I1013R, R1210E, R1212S (numbering according to the GenBank: Q03155.1).

The FP fusion protein encoded by pAT002 plasmid was expressed in *E. coli* JK321 (DE3) (*ompT*⁻, *dsbA*⁻) that has a knock-out of genes encoding outer membrane protease T (OmpT) and

thiol-disulfide interchange protein DsbA. This strain was previously described as a suitable host for the autotransporter protein mediated surface expression of recombinant passengers containing cysteine residues (Jose et al. 1996). The sequence analysis of KduD protein revealed that KduD oxidoreductase contains two cysteine residues (Cys18 and Cys35), which are unlikely to form the intramolecular disulfide bond as predicted by the DISULFIND server (Ceroni et al. 2006).

The expression of a FP fusion protein with an expected MW of 78.6 kDa was observed in a membrane protein preparation from *E. coli* JK321 (DE3) cells transformed with a pAT002 plasmid and induced with IPTG (**Fig. 3.26**). Only a single fusion protein band could be detected by SDS-PAGE and immunoblot analysis (**Fig. 3.26**). If an observed fusion protein band represents an unprocessed form (with unremoved signal peptide) or a fully-processed form (without a signal peptide) could not be judged from the given results due to a very small difference in MW of processed (78.6 kDa) and unprocessed (80.6 kDa) forms of the fusion protein.

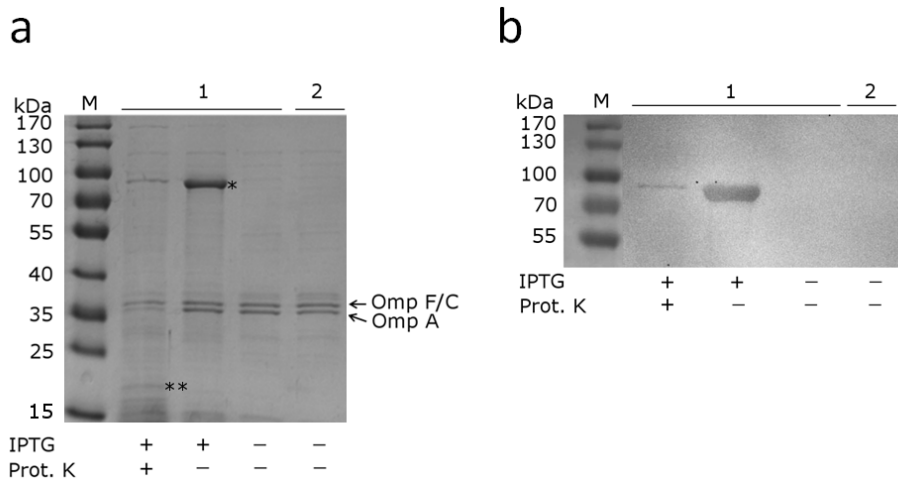


Fig. 3.26 Expression of a FP fusion protein in *E. coli* JK321 (DE3). SDS-PAGE (**a**) and anti-6xHis-tag immunoblot analysis (**b**) of membrane protein preparation from *E. coli* JK321 (DE3) transformed with pAT002 plasmid (1) and *E. coli* JK321 (DE3) (2). A recombinant protein expression was induced (+) or not induced (-) with 1 mM IPTG at 30° C for one hour in the presence of 10 mM β -ME and 10 μ M EDTA in LB medium. Cells were treated (+) or not treated (-) with protease K before the isolation of membrane protein fraction as described in *Materials and Methods*. Expected fusion protein is depicted with asterisk (*), 19 kDa OmpA degradation product is marked with double asterisk (**) and intact outer membrane proteins Omp F/C and Omp A are shown with arrows in SDS-PAGE gel. M - protein molecular weight marker.

The protease K accessibility test can be used for the investigation of the surface exposure of proteins in *E. coli* cells. Because the outer membrane of *E. coli* cells is not permeable to externally added protease K (28.9 kDa), degradation of a protein by protease indicates surface exposure of a protein (Maurer et al. 1997) on condition that *E. coli* cells are intact. The outer membrane protein A (OmpA) can be used as an indicator for the integrity of the outer membrane of the *E. coli* cells (Maurer et al. 1997). OmpA (35 kDa) has an N-terminal transmembrane domain (19 kDa) and a C-terminal globular periplasmic domain (16 kDa) (Ried et al. 1994, Arora et al. 2001). If the periplasm is accessible for externally added protease, the size of OmpA should decrease owing to the degradation of the periplasmic C-terminus and thus the amount of the full-size OmpA protein should decrease in comparison to the control cells not treated with the protease. When recombinant JK321 (DE3) *E. coli* cells overexpressing FP were treated with protease K before the isolation of membrane protein fraction, the disappearance of the FP band was observed in comparison to the membrane protein fraction isolated from recombinant *E. coli* cells, which were not treated with the protease (**Fig. 3.26**). In the membrane protein preparation from the cells overexpressing FP and treated with protease the OmpA protein band (35 kDa) could be detected in SDS-PAGE gel, though in much lower amounts than in the sample not treated with the protease (**Fig. 3.26**). In addition, only in the sample that was treated with protease K an additional band of ~19 kDa appeared; most likely corresponding to the membrane domain (19 kDa) of degraded OmpA, which is resistant to digestion with protease K (**Fig. 3.26**). Thus, these results suggest that the membrane of *E. coli* cells was not integral, and therefore, the degradation of OmpA and FP from the periplasmic side of the outer membrane could have occurred.

The fusion protein FP encoded by pAT002 plasmid was also successfully expressed in *E. coli* BL21 ClearColi (DE3) strain that has a genetically modified lipopolysaccharide (LPS). The LPS of *E. coli* BL21 ClearColi (DE3) cells is composed of only lipid IV_A and does not contain a complex polysaccharide that is typically attached to the lipid A in the natural LPS of *E. coli* cell.

The expression of a fusion protein with an expected MW of 78.6 kDa was observed in a membrane protein preparation from *E. coli* BL21 ClearColi (DE3) cells transformed with a pAT002 plasmid (**Fig. 3.27**). Only a single fusion protein band could be detected by SDS-PAGE and immunoblot analysis (**Fig. 3.27**), same as in case of expression in *E. coli* JK321 (DE3) cells

(Fig. 3.26). The small amount of FP was also expressed in BL21 ClearColi (DE3) cells transformed with pAT002 plasmid but not induced with IPTG as detected by the Western-Blot analysis (Fig. 3.27b). In the pAT002 plasmid the expression of a target gene encoding FP is under control of T7 RNA polymerase promoter. The expression cassette of T7 RNA polymerase is integrated into genome of *E. coli* BL21 ClearColi under control of lacI regulated lacUV5 promoter, which is known to allow a basal level transcription of T7 RNA polymerase in uninduced *E. coli* cells (Dubendorf and Studier 1991).

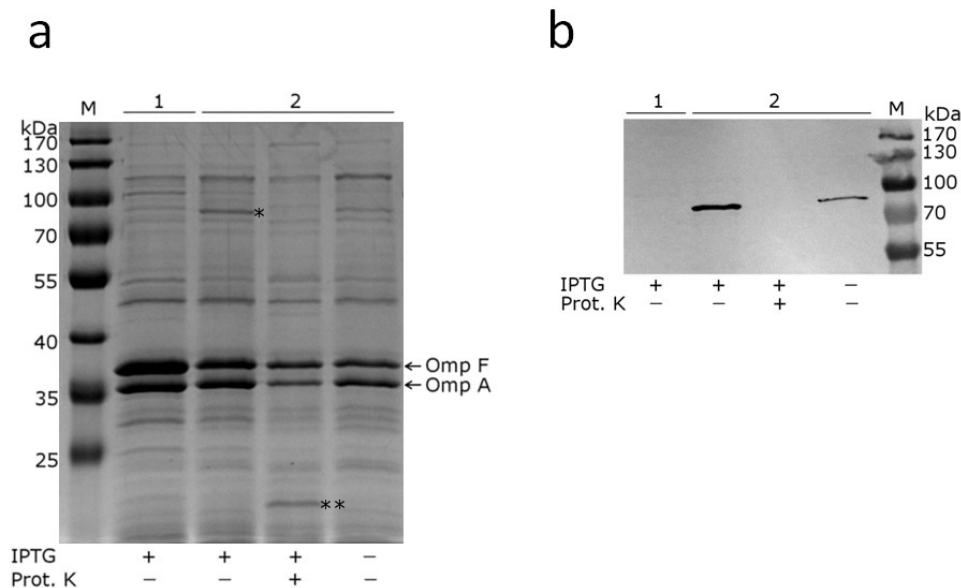


Fig. 3.27 Expression of a FP fusion protein in *E. coli* BL21 ClearColi (DE3). SDS-PAGE (a) and anti-PEYFK-tag immunoblot analysis (b) of membrane protein preparation from *E. coli* BL21 ClearColi (DE3) transformed with pAT002 plasmid (2) and *E. coli* BL21 ClearColi (DE3) (1). A recombinant protein expression was induced (+) or not induced (-) with 1 mM IPTG for 20 hours at 25 °C in LB medium. Cells were treated (+) or not treated (-) with protease K before the isolation of membrane protein fraction as described in *Materials and Methods*. Expected fusion protein is depicted with asterisk (*), 19 kDa OmpA degradation product is marked with double asterisk (**) and intact outer membrane proteins Omp F and Omp A are shown with arrows in SDS-PAGE gel (a). M - protein molecular weight marker.

When recombinant *E. coli* BL21 ClearColi (DE3) cells overexpressing FP were treated with protease K before the isolation of membrane protein fraction, the complete degradation of the FP was observed in comparison to the membrane protein fraction isolated from recombinant *E. coli* cells, which were not treated with the protease (Fig. 3.27). This could be a hint that FP protein was exposed to the cell surface. A slight degradation of OmpA was however observed in the

membrane protein fraction isolated from *E. coli* BL21 ClearColi (DE3) expressing FP and treated with protease (**Fig. 3.27**). Moreover, an additional band of ~19 kDa appeared only in the sample that was treated with protease K, most likely corresponding to the membrane domain (19 kDa) of degraded OmpA, which is resistant to digestion with protease K (**Fig. 3.27**). This result indicates that not all recombinant *E. coli* cells had an integral outer membrane. Thus, the possibility that the degradation of FP occurred from the periplasmic side of the cell outer membrane should not be excluded.

3.4.2 Investigation of the enzyme activity of FP

Recombinant *E. coli* cells overexpressing FP protein were subjected to the whole-cell 11-DOC reduction assay in order to investigate if KduD oxidoreductase was expressed in its active form when fused to the translocator unit of the AIDA-I autotransporter protein.

The expression of FP protein was induced in *E. coli* JK321 (DE3) cells with 1 mM IPTG at 30° C for one hour in LB medium in the absence of EDTA and 2-ME. Then, cells were incubated at 37° C for 24 h in 100 mM potassium phosphate buffer (pH 7.0) with KduD substrate (11-DOC) in the presence of NADH. As shown in **Fig. 3.28** the formation of the product was not observed with *E. coli* cells expressing FP. In contrast, under the same reaction conditions, the purified soluble KduD oxidoreductase reduced 11-DOC into the 4-pregnen-20,21-diol-3-one (**Fig. 3.28**).

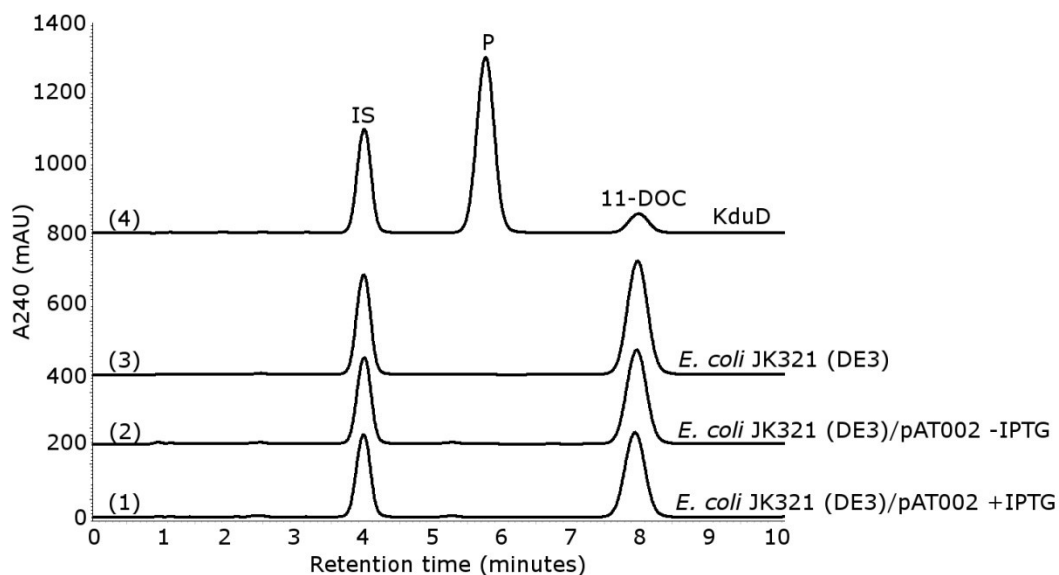


Fig. 3.28 Investigation of a steroid reductase activity of *E. coli* JK321 (DE3) cells overexpressing FP by HPLC-based assay. (1) – *E. coli* JK321 (DE3) transformed with pAT002 and induced with IPTG, (2) – *E. coli* JK321 (DE3) transformed with pAT002 and not induced with IPTG, (3) – *E. coli* JK321 (DE3), (4) – reaction with pure KduD enzyme. FP expression was induced with 1 mM of IPTG in LB medium at 30 °C for one hour, whole-cell transformations were performed at 37° C for 24 hours in 100 mM potassium-phosphate buffer (pH 7.0) and a final concentration of cells corresponding to an $OD_{578}=1$ (or 0.02 mg ml⁻¹ of pure KduD in case of sample 4) in the presence of 0.4 mM 11-DOC and 0.6 mM NADH. In the HPLC chromatograms the peaks of 11-DOC, 4-pregnen-20,21-diol-3-one (P) and internal standard (IS) are depicted.

When higher densities of *E. coli* JK321 (DE3) cells expressing FP were used in the activity assay (OD_{578} up to 25), steroid reductase activity of KduD was also not detectable (data not shown). In addition, when different protein expression conditions were tested, such as expression at lower temperatures (23 °C), expression for short (one hour) and longer times (up to three hours), as well as expression in LB medium supplemented with reducing agent (2-ME) and metalloprotease inhibitor (EDTA), an active KduD whole-cell biocatalyst was not obtained (data not shown).

Similarly, inactive FP was also expressed in *E. coli* BL21ClearColi (DE3) cells (**Fig. 3.29**). In addition, expression of FP in *E. coli* BL21 (DE3) strain in the minimal medium M9 with 1 mM IPTG at 30° C for 16 hours did not yield any active KduD whole-cell biocatalyst as tested in the standard 11-DOC reduction assay using high cell concentration ($OD_{578}=10$) (data not shown).

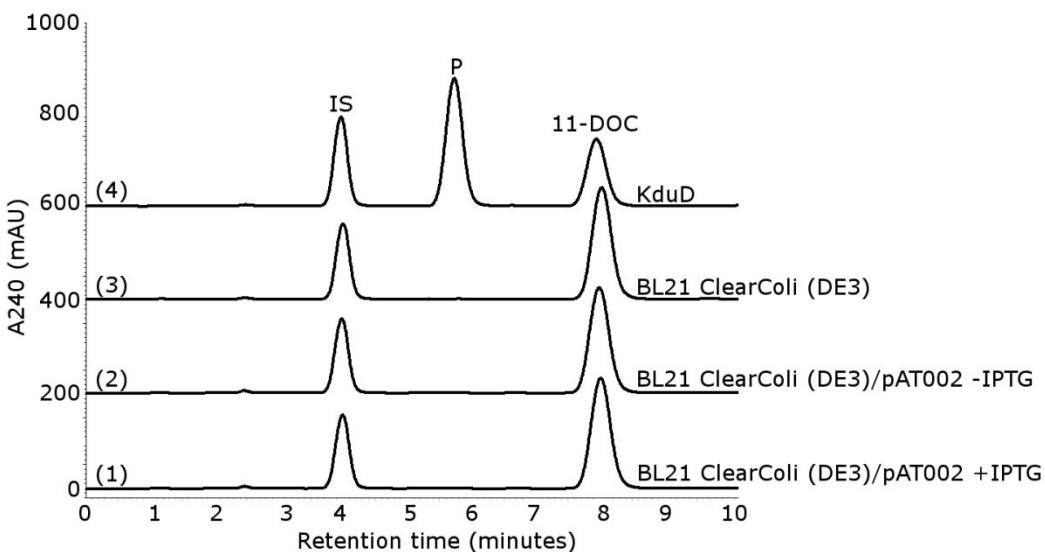


Fig. 3.29 Investigation of a steroid reductase activity of *E. coli* BL21 ClearColi (DE3) cells overexpressing FP by HPLC-based assay. (1) – *E. coli* BL21 ClearColi (DE3) transformed with pAT002 and induced with IPTG, (2) – *E. coli* BL21 ClearColi (DE3) transformed with pAT002 and not induced with IPTG, (3) – *E. coli* BL21 ClearColi (DE3), (4) – reaction with pure KduD enzyme. FP expression was induced with 1 mM of IPTG in LB medium at 25 °C for 20 hours, whole-cell transformations were performed at 37° C for 2 hours in 100 mM potassium-phosphate buffer (pH 7.0) and a final concentration of cells corresponding to an $OD_{578}=20$ (or 0.02 mg ml^{-1} of pure KduD in case of sample 4) in the presence of 0.4 mM 11-DOC and 0.6 mM NADH. In the HPLC chromatograms the peaks of 11-DOC, 4-pregnen-20,21-diol-3-one (P) and internal standard (IS) are depicted.

3.4.3 Design and expression of fusion protein FP $\Delta\beta$ 1

AIDA-I translocator unit (linker and β -barrel, 847-1286 aa, according to the numbering of wild-type AIDA-I, GenBank: Q03155.1) has a two-domain organization: an N-terminal β 1-domain (847-950 aa) and a C-terminal β 2-domain (951-1286 aa) (Konieczny et al. 2001). The β 2-domain forms a β -barrel that is embedded into the outer membrane of the cell, and a hydrophilic α -helix (965-980 aa) that resides within a pore of the β -barrel (Gawarzewski 2013). It was predicted that a β 1-domain, which is exposed to the outside of the outer membrane, interacts with an extracellular side of a β 2-domain (Gawarzewski 2013).

Based on the knowledge of the structure of AIDA-I translocator unit (Gawarzewski 2013), the hypothesis was made that β 1-domain might interfere with an assembly of a functional tetramer of the KduD passenger. It was previously shown that a modified AIDA-I translocator unit with

deleted β 1-domain is capable of transporting a passenger domain to the surface of the *E. coli* cell and is the minimal essential transport unit of AIDA-I autotransporter (Maurer et al. 1999).

The linker region corresponding to the β 1-domain was deleted from pAT002 plasmid using In-Fusion cloning technique as described in *Materials and Methods*. The schematic structure of modified fusion protein (FP $\Delta\beta$ 1) encoded by designed pAT004 plasmid is shown in **Fig. 3.30**.

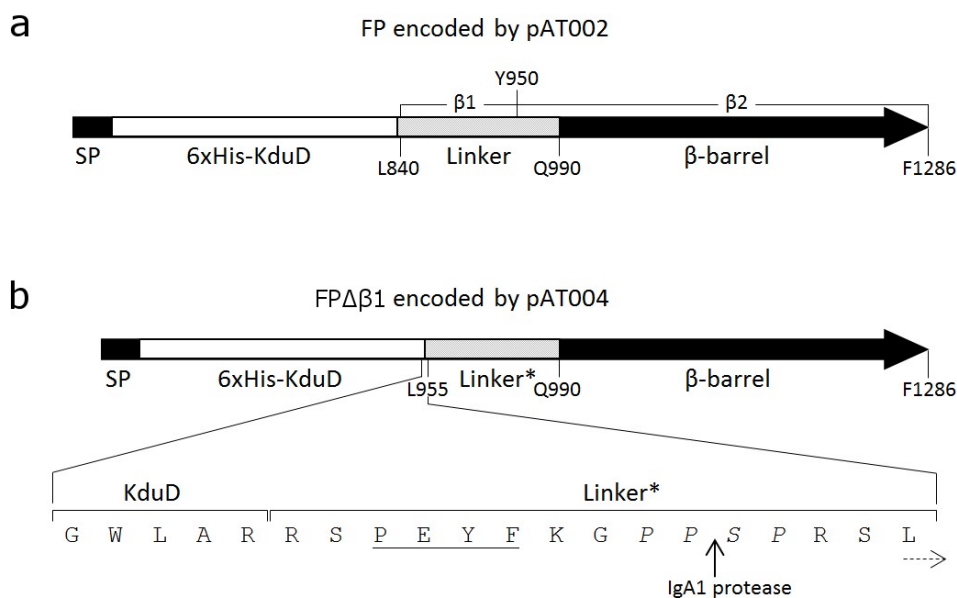


Fig. 3.30 Comparison of a fusion protein (FP) encoded by pAT002 plasmid (**a**) and a modified fusion protein (FP $\Delta\beta$ 1) encoded by pAT004 plasmid (**b**). pAT004 plasmid encoding FP $\Delta\beta$ 1 that has a deletion of β 1-domain within a linker (*) was constructed from pAT002 plasmid as described in *Materials and Methods*. Amino acid numbering is according to the protein sequence of *E. coli* AIDA-I autotransporter (GenBank: Q03155.1). In a protein sequence of a linker region of FP $\Delta\beta$ 1 a PEYFK-tag is underlined and an IgA1 protease cleavage site is shown in italics. SP - signal peptide of mutated cholera toxin B subunit (ctxB) as described in Fig. 3.25. A start of a protein sequence derived from *E. coli* AIDA-I autotransporter (GenBank: Q03155.1, amino acids: 955-1286) is depicted with a broken arrow in the protein sequence of FP $\Delta\beta$ 1.

The expression of FP $\Delta\beta$ 1 with an expected MW of 66.6 kDa (fully processed form, after removal of a signal peptide) was observed in a membrane protein preparation from *E. coli* JK321 (DE3) cells transformed with a pAT004 plasmid. After an induction time of two hours in LB medium with 1 mM IPTG at 30 °C only a small amount of FP $\Delta\beta$ 1 was produced (**Fig. 3.31a-b**). In contrast, when induction time was increased to three hours, a strong expression of FP $\Delta\beta$ 1 was observed (**Fig. 3.31c**).

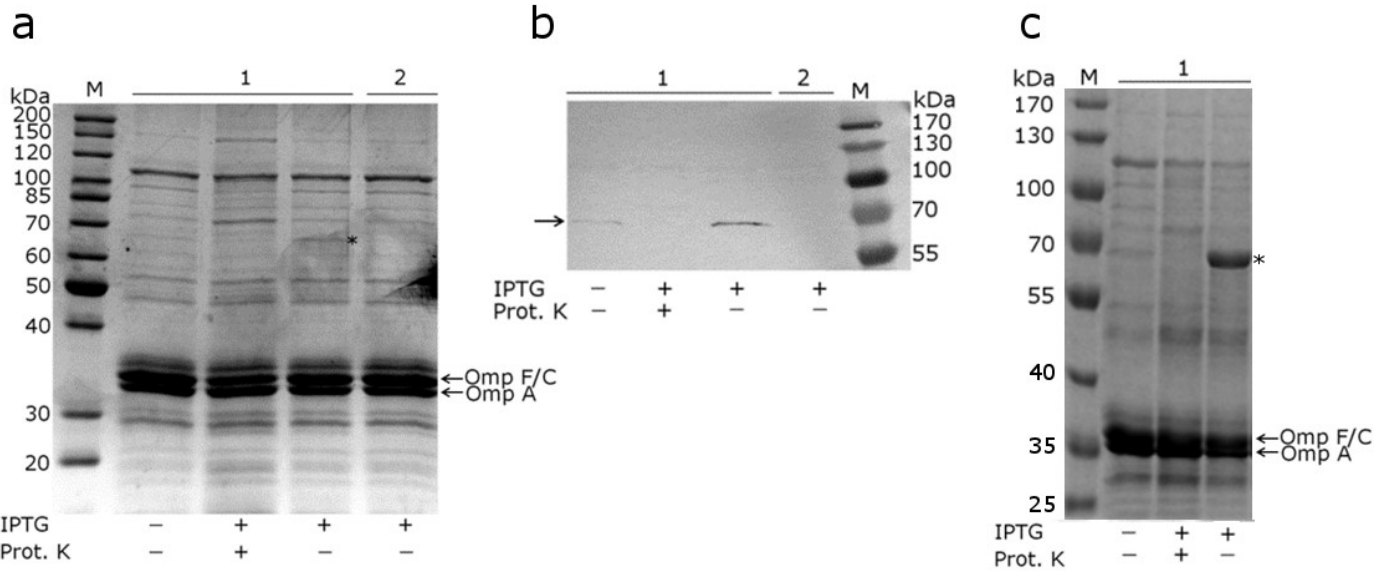


Fig. 3.31 Expression of FPA β 1 in *E. coli* JK321 (DE3). SDS-PAGE (**a** and **c**) and anti-PEYFK-tag immunoblot analysis (**b**) of membrane protein preparation from *E. coli* JK321 (DE3) transformed with pAT004 plasmid (1) and *E. coli* JK321 (DE3) (2). A recombinant protein expression was induced (+) or not induced (-) by 1 mM of IPTG at 30 °C for two hours (**a** and **b**) or three hours (**c**) in LB medium. Cells were treated (+) or not treated (-) with protease K before the isolation of membrane protein fraction as described in *Materials and Methods*. Expected fusion protein band is depicted with asterisk (*) in SDS-PAGE gels (**a** and **c**) and with an arrow in immunoblot analysis (**b**); arrows in SDS-PAGE gels (**a** and **c**) indicate outer membrane proteins Omp F/C and Omp A. M - protein molecular weight marker.

In order to investigate if FPA β 1 was exposed to the cell surface, protease K accessibility assay was performed. When recombinant *E. coli* JK321 (DE3) cells overexpressing FPA β 1 were treated with protease K, a complete degradation of the FPA β 1 was observed (**Fig. 3.31a** and **c**) in comparison to the cells that were not treated with the protease K (**Fig. 3.31a** and **c**). *E. coli* cells were intact as judged by the equal amount of the OmpA protein present in the membrane protein fractions isolated from the cells that were treated with the protease, and the cells that were not incubated with the proteolytic enzyme. Thus, this result is a strong indication that FPA β 1 was successfully translocated to the outer membrane of an *E. coli* cell and it was degraded by protease K from the outer surface of the cell.

3.4.4 Investigation of the enzyme activity of FPA β 1

Recombinant *E. coli* JK321 (DE3) cells overexpressing FPA β 1 protein were subjected to the whole-cell 11-DOC reduction assay in order to investigate if KduD oxidoreductase was

expressed in its active form when fused to the translocator unit of the AIDA-I autotransporter protein that contained the truncated linker region.

The expression of FP $\Delta\beta$ 1 protein was induced in *E. coli* JK321 (DE3) cells in LB medium with 1 mM IPTG at 30° C for one hour. Then, cells were incubated at 37° C for 24 h in 100 mM potassium phosphate buffer (pH 7.0) with KduD substrate (11-DOC) in the presence of NADH. As shown in **Fig. 3.32**, in contrast to purified soluble KduD reductase, the formation of the product was not observed with *E. coli* cells expressing FP $\Delta\beta$ 1.

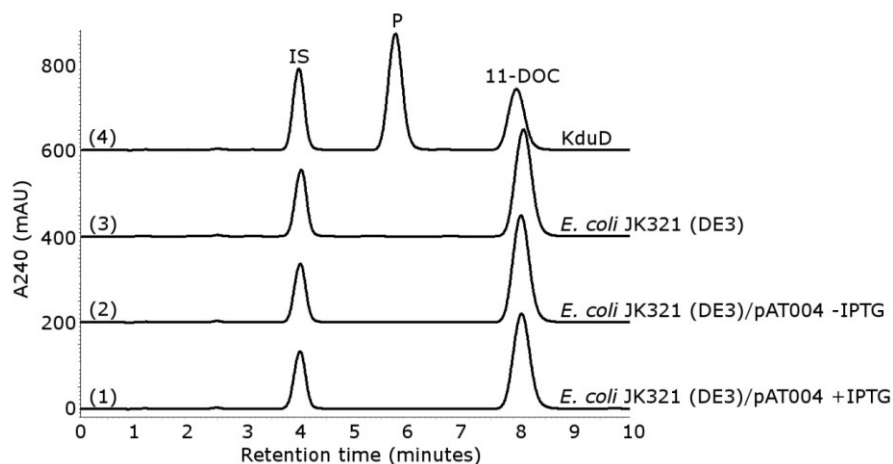


Fig. 3.32 Investigation of a steroid reductase activity of *E. coli* JK321 (DE3) overexpressing FP $\Delta\beta$ 1 by HPLC-based assay. (1) – *E. coli* JK321 (DE3) transformed with pAT004 and induced with IPTG, (2) - *E. coli* JK321 (DE3) transformed with pAT004 and not induced with IPTG, (3) - *E. coli* JK321 (DE3), (4) – reaction with pure KduD enzyme. FP $\Delta\beta$ 1 expression was induced with 1 mM of IPTG in LB medium at 30° C for two hours, whole-cell transformations were performed at 37° C for 2 hours in 100 mM potassium-phosphate buffer (pH 7.0) and a final concentration of cells corresponding to an OD₅₇₈=20 (or 0.02 mg ml⁻¹ of pure KduD in case of sample 4) in the presence of 0.4 mM 11-DOC and 0.6 mM NADH. In the HPLC chromatograms the peak of 11-DOC, 4-pregnen-20,21-diol-3-one (P) and internal standard (IS) are depicted.

3.4.5 Digestion of FP with IgA1 protease

IgA1 from *Neisseria gonorrhoeae* is a specific protease that cleaves a protein within a proline-rich sequence (PPXP, where X=T, S or A). This cleavage site is not commonly found in natural proteins except for a natural substrate of this protease immunoglobulin A1. The IgA1 protease cleavage site (PPSP) was introduced into the linker region of FP protein encoded by pAT002 plasmid by genetic manipulation (**Fig. 3.25**) in order to investigate a specific protease mediated release of passenger domains (KduD) from the surface of *E. coli* cells.

The membrane protein preparation from *E. coli* JK321 (DE3) cells overexpressing FP was used as IgA1 protease substrate in order to optimize the conditions for a cleavage reaction. The cleavage of FP by IgA1 protease should result in a formation of 29.9 kDa and 48.7 kDa protein fragments if FP was fully processed (removed signal peptide). Otherwise, 32.0 kDa and 48.7 kDa FP fragments should be produced by IgA1 cleavage of unprocessed FP (with a signal peptide). A shorter protein fragment contains an N-terminal 6xHis-tag and a C-terminal PEYFK-tag and thus can be detected by immunoblot analysis.

The digestion of FP with IgA1 protease resulted in formation of small amounts of expected protein fragments of about 30 kDa and 50 kDa in size (**Fig. 3.33**). Moreover, a band corresponding to a shorter fragment of FP (~30 kDa) was detected in immunoblot analysis using antibodies directed against an anti-6xHis-tag and anti-PEYFK-tag (**Fig. 3.33b and Fig. 3.34**). Only a single band of a shorter fragment of FP was detected with an apparent MW of about 30 kDa rather than 32 kDa. Thus, it was a strong indication that FP was overexpressed in JK321 (DE3) cells in a fully processed form (with removed signal peptide).

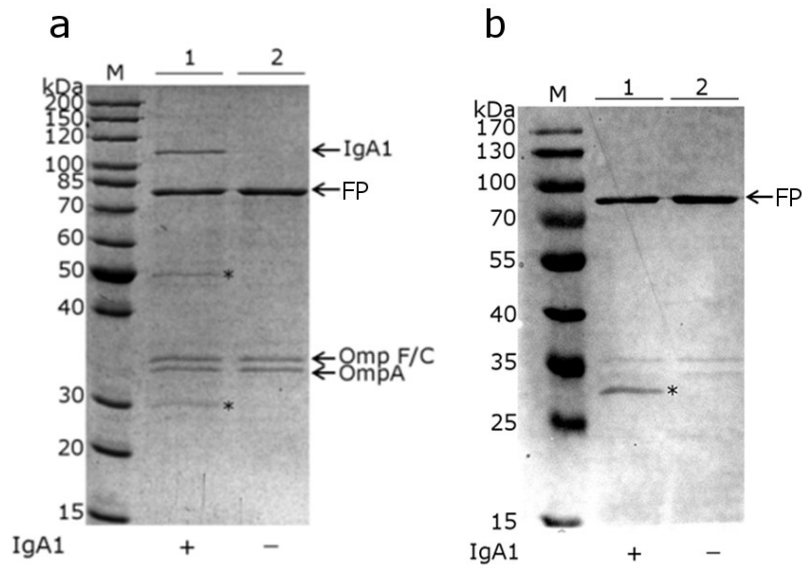


Fig. 3.33 Digestion of FP with IgA1 protease. SDS-PAGE (a) and anti-6xHis-tag immunoblot analysis (b) of membrane protein preparation from recombinant *E. coli* JK321 (DE3) overexpressing FP. (1) - membrane protein preparation was incubated with IgA1 (+), (2) – membrane protein preparation was incubated without IgA1 (-). FP (78.6 kDa), a substrate of IgA1 protease, M - protein molecular weight marker. Protein bands corresponding to IgA1 protease (106 kDa), Omp F/C and Omp A outer membrane proteins are depicted with arrows; two protein bands resulting from IgA1-cleaved FP (48.7 and 29.9 kDa in size) are depicted with asterisks in SDS-PAGE gel (a), an anti-6xHis-tag-containing protein band (29.9 kDa) resulting from FP cleavage by IgA1 is depicted with asterisk in immunoblot analysis (b). FP was incubated at 20° C with 0.01 $\mu\text{g } \mu\text{l}^{-1}$ of IgA1 protease in optimal buffer for 76 hours as described in *Materials and Methods*.

Higher amounts of cleaved FP could be obtained when higher concentrations of IgA1 protease were used in the assay (Fig. 3.34), however, a full digestion of FP was not observed with a concentration of IgA1 protease as high as 0.05 $\mu\text{g } \mu\text{l}^{-1}$ and long incubation times (60 hours at 20° C) (Fig. 3.34).

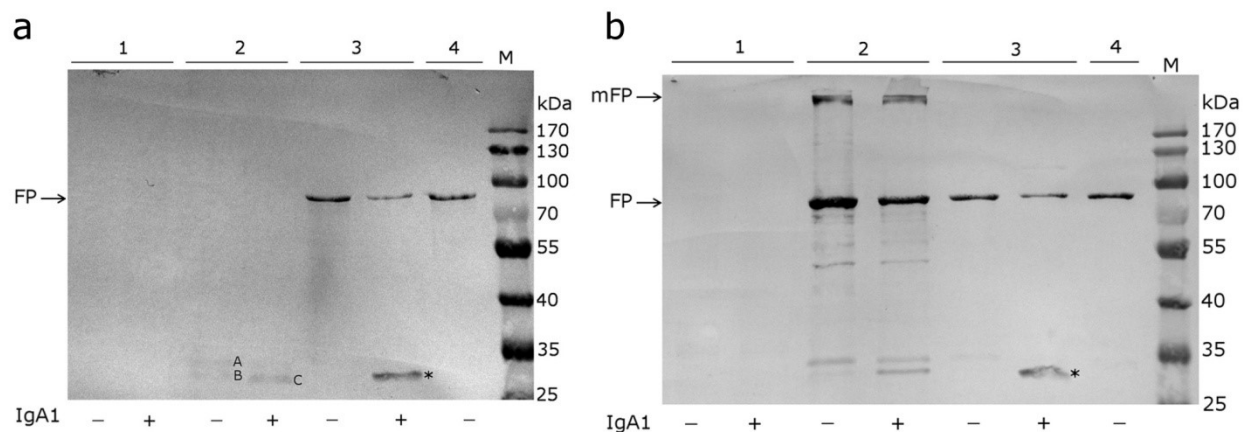


Fig. 3.34 Incubation of whole *E. coli* cells with IgA1 protease. Anti-PEYFK-tag immunoblot analysis of supernatants (a) and cell pellets (b) of *E. coli* cell suspensions incubated with (+) and without (-) IgA1 protease. (1) *E. coli* JK321 (DE3) cells, (2) *E. coli* JK321 (DE3) cells transformed with pAT002 plasmid and expressing FP, (3) membrane protein preparation of FP from *E. coli* JK321 (DE3) expressing FP, (4) membrane protein preparation of FP from *E. coli* JK321 (DE3) expressing FP which was not incubated with IgA1 in order to evaluate possible unspecific degradation of FP over prolonged incubation times as described in *Materials and Methods*. FP – fusion protein, mFP – multimers of fusion protein. An expected 29.9 kDa anti-PEYFK-tag-containing FP fragment cleaved off by IgA1 protease is depicted with an asterisk, protein bands depicted with A, B and C are fragments of FP containing PEYFK-tag, M – protein molecular weight marker. Membrane protein preparation of FP, JK321 (DE3) cells and JK321 (DE3) cells overexpressing FP were incubated at 20° C with 0.05 $\mu\text{g } \mu\text{l}^{-1}$ of IgA1 protease in optimal buffer for 60 hours as described in *Materials and Methods*.

In order to investigate if *E. coli* JK321 (DE3) cells transformed with pAT002 plasmid overexpress FP in the outer membrane with a passenger domain (KduD) displayed on the surface of the cell, whole *E. coli* cells expressing FP were treated with IgA1 protease. If KduD is located on the surface of *E. coli* cells, the release of 29.9 kDa N-terminal fragment of FP should be detected in the supernatant of the cell suspension incubated with IgA1 protease.

In contrast to control *E. coli* JK321 (DE3) cells, in the supernatant of recombinant *E. coli* JK321 (DE3) cells overexpressing FP and incubated with IgA1 protease a protein band with an apparent MW of around the size of the expected FP N-terminal fragment (29.9 kDa) could be detected by immunoblot analysis with antibody directed against the anti-PEYFK-tag (**Fig. 3.34a** band C). Surprisingly, two protein bands were detected in supernatant of cell suspension of *E. coli* JK321 (DE3) cells overexpressing FP but not treated with IgA1 protease (**Fig. 3.34a** protein bands A and B). These FP protein fragments (A and B) had a slightly higher apparent

MW than the protein fragment C detected in supernatant of the cell sample treated with IgA1 protease, suggesting that FP is cleaved by unidentified *E. coli* proteases. Two protein fragments with the apparent MW similar to MW of protein fragments A and B were also detected in cell pellets obtained from suspensions of FP expressing *E. coli* JK321 (DE3) cells that were incubated with and without IgA1 protease (**Fig. 3.34b**). However, in the cell pellet obtained from the cell suspension that was incubated with IgA1 protease a much higher amount of a protein with the apparent MW similar to MW of fragment B (~31 kDa) was detected in comparison to cells not treated with IgA1 protease. This protein fragment could have resulted from a specific IgA1 protease mediated cleavage of FP on the surface of *E. coli* cell, however, due to unknown reasons it remained associated with the cell pellet and also migrated in SDS-PAGE gel with slightly higher apparent MW in comparison to expected 29.9 kDa N-terminal FP fragment (depicted with an asterisk in **Fig. 3.34b**). Most of the FP protein was, however, left intact by IgA1 protease as the thick protein band corresponding to the full length of FP protein (~80 kDa) and a protein band corresponding to the multimers of FP was detected in the cell pellet of JK321 (DE3) cells overexpressing FP and treated with IgA1 protease (**Fig. 3.34b**). The native form of KduD was shown to be a tetramer (**Fig. 3.9**). It is very likely that observed multimers of FP resulted from the dimerization or tetramerization of KduD molecules exposed to the surface of *E. coli* cell in a fully folded form. However, the expected efficient IgA1 protease catalyzed release of KduD passenger domains from the surface of *E. coli* JK321 (DE3) cells expressing FP protein was not observed, most likely due to the limited access of IgA1 protease to its cleavage site, which is located in the linker region of FP.

3.5 Autodisplay based on EhaA autotransporter

3.5.1 Design and expression of fusion proteins FP1 and FP2

Plasmids pMATE-AT001 and pMATE-AT002 encoding recombinant fusion proteins FP1 and FP2, respectively, (**Fig. 3.35a-b**) were constructed using In-Fusion cloning technique as described in *Materials and Methods*. In both plasmids, the expression of recombinant fusion proteins is under control of a strong IPTG-inducible T5 promoter. In the pMATE-AT001-encoded FP1 protein at the N-terminus 6x-His-(N)-tagged KduD oxidoreductase is fused to a Sec signal peptide derived from CtxB protein, and at the C-terminus to a linker and a β -barrel region of EhaA autotransporter (**Fig. 3.35a**). In between the C-terminus

of KduD and N-terminus of the linker region of the EhaA autotransporter, two additional sequences, a specific protease factor Xa cleavage site and a PEYFK epitope, were inserted (**Fig. 3.35a**). In contrast, in the pMATE-AT002-encoded FP2 protein this region contains OmpT protease cleavage site, flexible glycine-serine (GGGGS)₃ linker, factor Xa cleavage site and a PEYFK epitope (**Fig. 3.35b**).

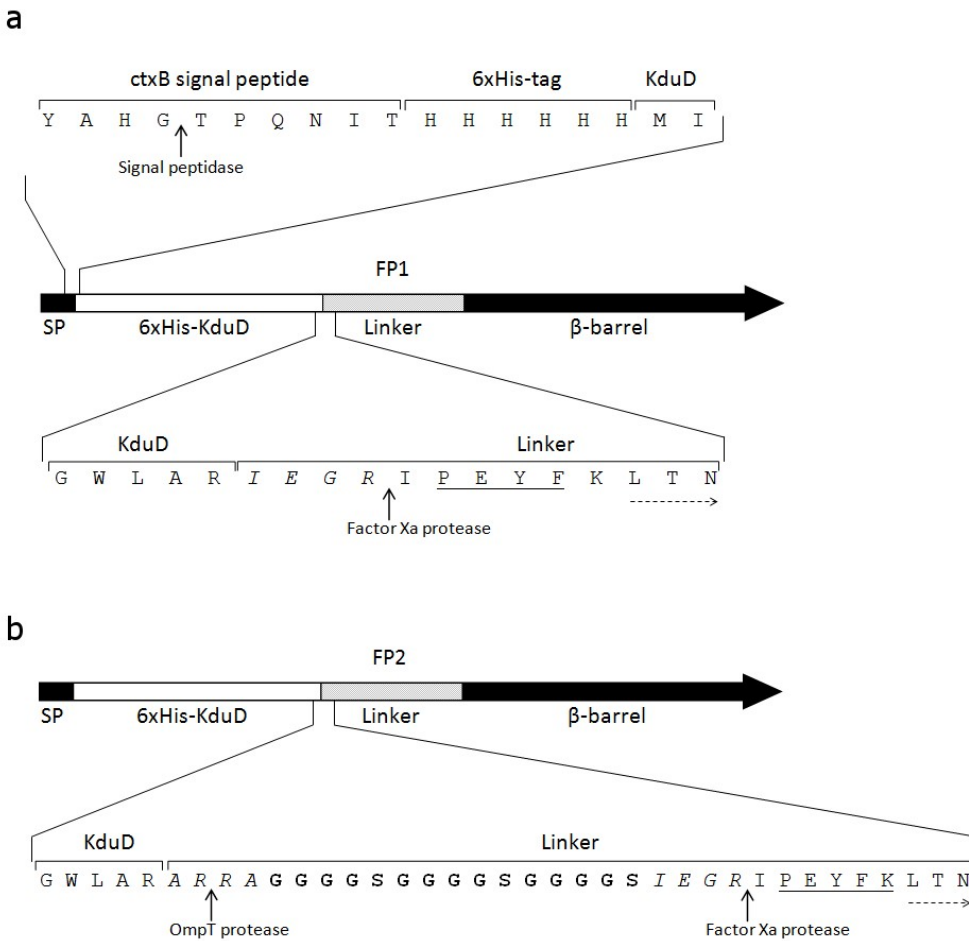


Fig. 3.35 Schematic representation of fusion proteins. Scheme of FP1 encoded by pMATE-AT001 (**a**) and scheme of FP2 encoded by pMATE-AT002 (**b**). SP – signal peptide of cholera toxin B subunit (ctxB, GenBank AED88285.1). OmpT protease and factor Xa protease recognition sites are depicted in italics and cleavage sites are shown with the arrows. A flexible glycine-serine linker is shown in bold and PEYFK-tag is underlined. A start of a protein sequence derived from *E. coli* EhaA autotransporter (GenBank: AAG54657.1, amino acids: 862-1349) is depicted with a broken arrow. The DNA sequence encoding signal peptide of ctxB and linker and β -barrel region of EhaA autotransporter were codon optimized for an efficient overexpression in *E. coli* (Teese *et al.* unpublished data).

The fusion protein FP1 encoded by pMATE-AT001 plasmid was expressed in *E. coli* UT5600, F470 and F515 strains. The expression of the fusion protein that has an apparent molecular mass of less than 100 kDa was observed in membrane protein preparations from all three *E. coli* strains transformed with the pMATE-AT001 plasmid and induced with IPTG (**Fig. 3.36a-c**). The apparent molecular mass of the FP1 protein was higher as judged from the SDS-PAGE gel in comparison to the expected theoretical molecular mass, which is 82.9 kDa for processed FP1 protein and 85.2 kDa for the unprocessed form. The anomalous migration of membrane proteins in SDS-PAGE gels is a common phenomenon (Rath et al. 2009).

overexpressing FP1 fusion protein were treated with protease K before the isolation of membrane protein fraction, a decrease of the protein band corresponding to FP1 was observed in comparison to the membrane protein fraction isolated from recombinant *E. coli* cells, which were not treated with the protease (**Fig. 3.36a-c**). The membrane protein preparation from the cells overexpressing FP1 and treated with protease contained similar amounts of OmpA protein in comparison to the cells that were not treated with the protease. Thus, this result suggests that *E. coli* cells were intact and some of FP1 molecules were exposed to the cell surface. The observed incomplete digestion of FP1 might be an indication that not all FP1 molecules were displayed on the surface of *E. coli* cells (**Fig. 3.36a-c**).

The fusion protein FP2 encoded by pMATE-AT002 plasmid was expressed in *E. coli* F515 strain (**Fig. 3.36c**). The expression of the fusion protein with an apparent molecular mass of less than 100 kDa was observed in the membrane protein preparations from *E. coli* F515 transformed with the pMATE-AT002 plasmid and induced with an IPTG (**Fig. 3.36c**). An apparent molecular mass of the FP2 protein (**Fig. 3.36c**) was higher than the expected theoretical molecular mass, which is 84.2 kDa for processed FP2 protein and 86.6 kDa for unprocessed form. The FP2 migrated in SDS-PAGE gel also anomalously like FP1.

The protease accessibility test was performed with *E. coli* F515 cells overexpressing FP2 protein. Similarly to FP1, the incomplete digestion of FP2 with protease K was observed suggesting that not all molecules of FP2 were translocated to the outer membrane of the cell (**Fig. 3.36c**).

3.5.2 Investigation of the enzyme activity of FP1 and FP2

Recombinant *E. coli* UT5600 cells overexpressing FP1 protein were subjected to the whole-cell 11-DOC reduction assay in order to investigate if KduD oxidoreductase was expressed in its active form when fused to the translocator unit of the EhaA autotransporter protein.

The expression of FP1 protein was induced in *E. coli* UT5600 cells in LB medium with 1 mM IPTG at 30° C for two hours. Then, cells were incubated at 37° C for 16 hours in 100 mM potassium phosphate buffer (pH 7.0) with KduD substrate (11-DOC) in the presence of NADH. As shown in **Fig. 3.37** the formation of the product was not observed with *E. coli* cells expressing FP1. In contrast, under the same reaction conditions, the purified soluble KduD oxidoreductase reduced 11-DOC into the 4-pregnen-20,21-diol-3-one (**Fig. 3.37**).

Modification of protein expression conditions, such as performing protein expression at lower temperatures, expression in LB medium supplemented with reducing agent (2-ME), and metalloprotease inhibitor (EDTA) did not yield an active KduD whole-cell biocatalyst (data not shown).

Under several different reaction conditions that have been tested, the activity of KduD oxidoreductase could not be detected in the UT5600 cells overexpressing FP1 protein. No oxidoreductase activity was measured when concentration of the substrate, cofactor, and cells was varied in the activity assay (data not shown). In addition, the whole-cell biocatalyst was inactive against various KduD substrates (11-DOC, RSS, D-gluconate) as well as under different pH and temperature conditions tested (pH=7.0, 7.5, 8.0, 9.3, T=30° C, 37° C, 45° C) (data not shown).

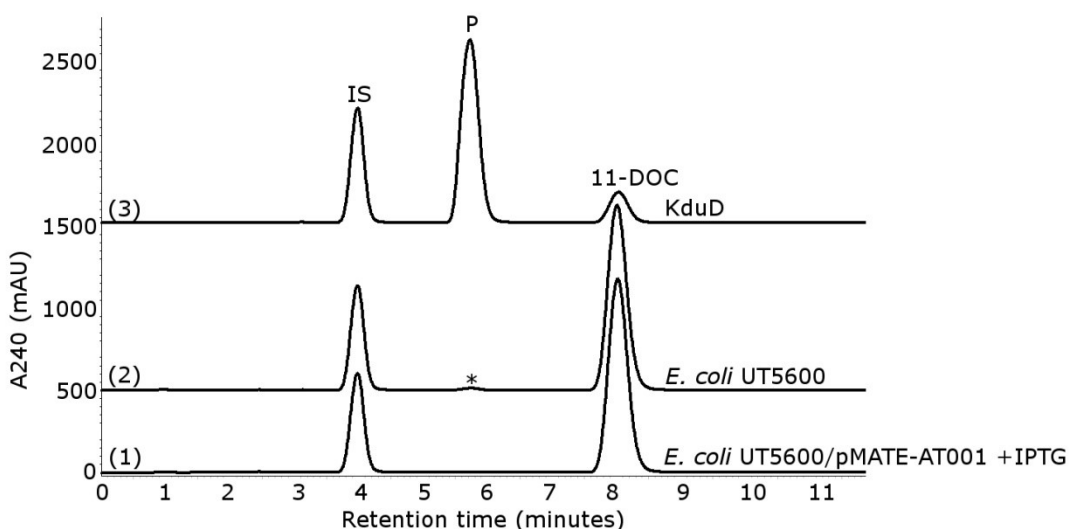


Fig. 3.37 Investigation of a steroid reductase activity of *E. coli* UT5600 cells overexpressing FP1 by HPLC-based assay. (1) – *E. coli* UT5600 transformed with pMATE-AT001 and induced with IPTG, (2) - *E. coli* UT5600, (3) - reaction with pure KduD enzyme. Expression of FP1 was induced with 1 mM of IPTG in LB medium at 30 °C for two hours, whole-cell transformations were performed at 37° C for 16 hours in 100 mM potassium-phosphate buffer (pH 7.0) and a final concentration of cells corresponding to an OD₅₇₈=10 (or 0.02 mg ml⁻¹ of pure KduD in case of sample 3) in the presence of 0.4 mM 11-DOC and 0.6 mM NADH. In the HPLC chromatograms the peaks of 11-DOC, 4-pregnen-20,21-diol-3-one (P) and internal standard (IS) are depicted, (*)-depicts bacterial compounds which copurified with steroids and absorbed at 240 nm, but had an absorbance maximum at 220 nm.

Similarly, *E. coli* F470 cells and *E. coli* F515 cells overexpressing FP1 protein were inactive, when tested for reductase and dehydrogenase activities against KduD substrates, RSS and D-gluconate, respectively (**Fig. 3.38** and **Fig. 3.39a**).

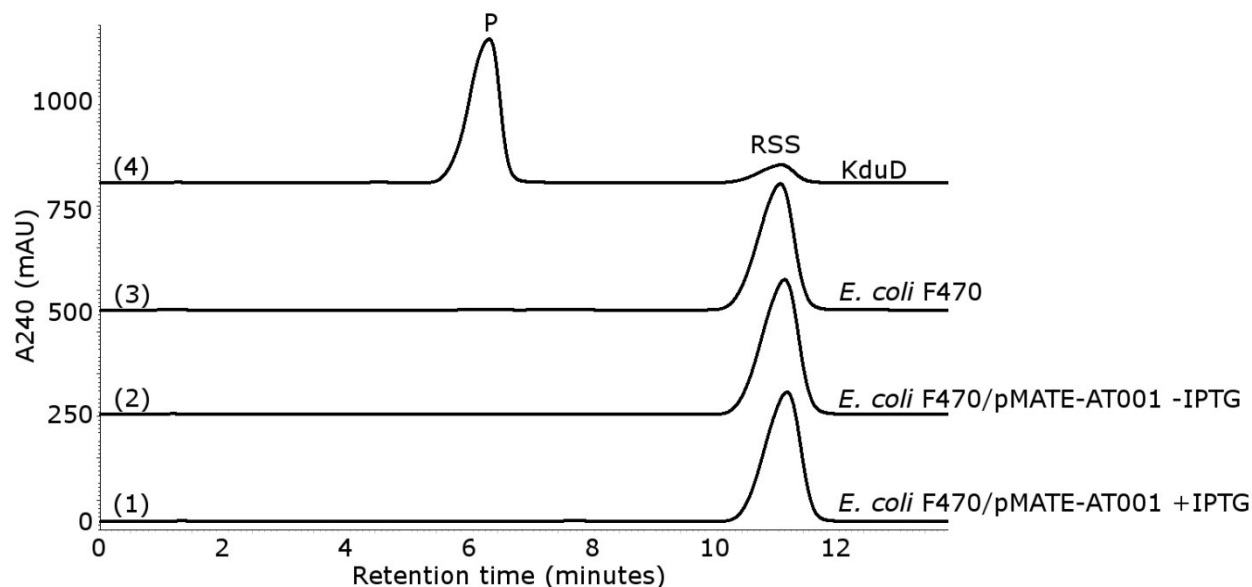


Fig. 3.38 Investigation of a steroid reductase activity of *E. coli* F470 cells overexpressing FP1 by HPLC-based assay. (1) – *E. coli* F470 transformed with pMATE-AT001 and induced with IPTG, (2) – *E. coli* F470 transformed with pMATE-AT001 and not induced with IPTG, (3) – *E. coli* F470, (4) – reaction with pure KduD enzyme. Expression of FP1 was induced with 1 mM IPTG in LB medium at 30 °C for one hour, whole-cell transformations were performed at 37° C for two hours in 100 mM potassium-phosphate buffer (pH 7.0) and a final concentration of cells corresponding to an $OD_{578}=10$. (or 0.02 mg ml⁻¹ of pure KduD in case of sample 4) in the presence of 0.4 mM RSS and 0.6 mM NADH. In the HPLC chromatograms the peaks of 11-deoxycortisol (RSS) and 4-pregnen-17,20,21-triol-3-one (P) are depicted.

Recombinant *E. coli* F515 cells overexpressing FP2 protein were subjected to the whole-cell D-gluconate oxidation assay in order to investigate if KduD oxidoreductase was expressed in its active form when fused to the translocator unit of the EhaA autotransporter protein via glycine-serine (GGGGS)₃ linker. As it is shown in **Fig. 3.39b**, in contrast to the pure soluble KduD oxidoreductase, whole *E. coli* F515 cells overexpressing FP2 protein were not able to oxidize KduD substrate D-gluconate.

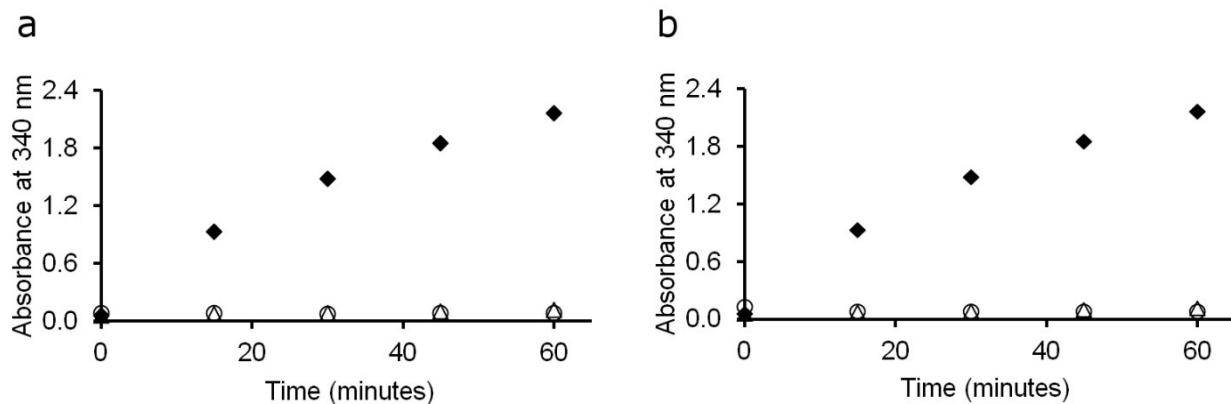


Fig. 3.39 Investigation of activity of recombinant *E. coli* F515 cells expressing FP1 or FP2. **(a)** Investigation of oxidation of D-gluconate with *E. coli* F515 cells expressing FP1 by NADH-absorbance assay: *E. coli* F515 transformed with pMATE-AT001 plasmid and induced by IPTG (○), *E. coli* F515 (Δ), pure KduD enzyme (◆). **(b)** Investigation of oxidation of D-gluconate with *E. coli* F515 cells expressing FP2 by NADH-absorbance assay: *E. coli* F515 transformed with pMATE-AT002 plasmid and induced by IPTG (○), *E. coli* F515 (Δ), pure KduD enzyme (◆). Data points are means of two experiments The expression of FP1 and FP2 was induced with 1 mM of IPTG in LB medium at 30 °C for 2.5 hours, whole-cell transformations were performed at 37° C in 100 mM glycine-NaOH buffer (pH 9.3) in presence of 0.2 M of D-gluconate, 1 mM of NAD⁺ and a final concentration of cells corresponding to an OD₅₇₈=20 (or 0.02 mg ml⁻¹ of pure KduD).

Moreover, expression of FP1 and FP2 proteins in *E. coli* BL21 strain in the minimal medium M9 with 1 mM IPTG at 30° C for 16 hours did not yield an active KduD whole-cell biocatalyst as tested in the standard 11-DOC reduction assay using high cell concentration (OD₅₇₈=10) (data not shown).

4 Discussion

4.1 Identification of steroid C20 reductase in *Escherichia coli*

A BLAST search of homologs of characterized 20-hydroxysteroid dehydrogenases of mammalian or microbial origin against the genome of *E. coli* revealed a great number (8 aldoketo reductases (AKRs) and 17 short-chain dehydrogenases/reductases (SDRs)) of relatively low similarity hits (25-40 %). Among the identified proteins, many experimentally annotated enzymes were found next to the uncharacterized putative oxidoreductases. The biological roles of functionally annotated enzymes, however, were not related to the metabolism of steroids, except for 7 α -hydroxysteroid dehydrogenase. This enzyme was previously purified from *E. coli* and was shown to catalyze a reversible reduction of C7 carbonyl group of several bile acids (Yoshimoto et al. 1991), but has never been reported to catalyze the reversible reduction of C20 carbonyl group of other steroid compounds.

Annotation of 20-HSDs in bacteria using bioinformatics approaches remains to be a difficult task as recently reported by Kisiela *et al.* (2012). The bioinformatics models developed by the authors were not able to provide sensitive and specific tool for sequence based identification of 20 α -HSD and 20 β -HSD in bacteria (Kisiela et al. 2012).

Oxidoreductases belonging to the protein superfamilies of AKR or SDR are known to catalyze oxidation-reduction reactions on a broad spectrum of substrates. Prediction of the substrate specificity of AKRs and SDRs solely based on the amino acid sequence of enzyme remains to be a great challenge. Therefore, identification of 11-DOC reductase in *E. coli* by bioinformatics approach would have required cloning and functional testing of all putative and annotated enzymes encoding genes identified by the BLAST search in this study (in total 25 genes).

Based on the knowledge that 20-keto steroid reductase activity was found in *E. coli* K-12 derivative DH5 α and not in *E. coli* BL21 (DE3) it was hypothesized that a gene encoding 11-DOC reductase was not present in *E. coli* BL21 (DE3). Indeed the comparison of oxidoreductases in *E. coli* DH10B (a K-12 derivative closely related to DH5 α) and *E. coli* BL21 (DE3) revealed an *ydbC* gene-encoded putative AKR (YdbC oxidoreductase) that is present only in the genome of *E. coli* DH10B and not in BL21 (DE3). Recent studies showed that YdbC oxidoreductase can catalyze the oxidative breakdown of the synthetic compound

5-nitrobenzisoxazole (Khersonsky et al. 2011), but the natural substrates of this enzyme are unknown. In the present study, the activity of YdbC oxidoreductase was investigated against the steroid substrate 11-DOC. The YdbC oxidoreductase, however, did not have detectable reductase activity against 11-DOC.

Comparison of SDRs from *E. coli* DH10B and BL21 (DE3) revealed that the enzyme encoded by *kduD* gene was truncated in the *E. coli* BL21 (DE3) strain. The *kduD* gene, therefore, codes for 2-dehydro-3-deoxy-D-gluconate 5-dehydrogenase (KduD oxidoreductase), which lacks part of the substrate binding loop in *E. coli* BL21 (DE3) strain. Because of this truncation, the KduD oxidoreductase is most likely inactive in *E. coli* BL21 (DE3) strain. The functional KduD oxidoreductase was purified from *E. coli* K-12 strain by Hantz (1977) and was shown to catalyze the conversion of carbohydrate derivative 2-keto-3-deoxygluconate (KDG) into 2,5-diketo-3-deoxygluconate (DKII) (**Fig. 4.1a**). The substrate specificity studies performed by Hantz (1977) revealed that this enzyme is a narrow substrate oxidoreductase capable of converting only KDG and DKII, likewise, KduD orthologs characterized in other microorganisms, *Erwinia chrysanthemi* (Condemine et al. 1984) and *Pseudomonas sp.* (Preiss and Ashwell 1963).

The protein mass spectrometry analysis of partially purified 11-DOC reductase from *E. coli* DH5 α strain gave a clue that KduD oxidoreductase is the candidate responsible for the steroid C20 reductase activity in *E. coli*. By cloning the *kduD* gene from *E. coli* DH5 α , and investigating reductase activity of purified recombinant KduD oxidoreductase against 11-DOC, it was possible to show unequivocally that *kduD* gene encodes the steroid C20 reductase previously identified in *E. coli* (Hannemann et al. 2007).

4.2 Novel substrates of KduD

KduD from *E. coli* catalyzed the reduction of the carbonyl group at C20 position of six C21 steroids. The substrate range of the enzyme was limited to the steroid compounds that have a hydroxyl group at C21 position (11-DOC, RSS, corticosterone, cortisol, cortisone, 21-hydroxypregnenolone). Steroids lacking this hydroxyl group (pregnenolone, progesterone, testosterone propionate, and cortisone acetate) were not converted. This suggests that C21 hydroxyl group plays a crucial role in the binding and orientation of the substrate molecule within the active site of the enzyme. The carbonyl group at C3 position and unsaturated bond at

C4-C5 within the ring A of the steroid molecule does not appear to be critical for the substrate recognition by KduD, as judged by the efficient conversion of 21-hydroxypregnenolone. The spectrum of steroid substrates of KduD is similar to 20 α -HSD of *Clostridium scindens* (Krafft and Hylemon 1989) and 20 β -HSD of *Streptomyces hydrogenans* (Allner and Eggstein 1989) which were also demonstrated to reduce C20 carbonyl group of RSS, cortisol and cortisone. In contrast to the enzyme from *S. hydrogenans*, the 20-HSD from *C. scindens* like *E. coli* KduD oxidoreductase is not able to convert substrates without C21 hydroxyl group (Ridlon et al. 2013). However, in contrast to KduD oxidoreductase, the 20 α -HSD from *C. scindens* is not active against steroid substrates lacking 17 α -hydroxyl group (Ridlon et al. 2013). KduD from *E. coli* shows much lower affinity towards steroid substrates in comparison to the enzymes with 20-ketosteroid reductase activity isolated from other microorganisms (Inazu et al. 1994, Krafft and Hylemon 1989) and higher eukaryotes (Ma and Penning 1999). However, these 20-ketosteroid reductases share a very low protein sequence identity (only 9-13 %) with KduD from *E. coli*.

4.3 Biological function of KduD in *E. coli*

Although KduD was found in *E. coli* K-12 by Hantz (1977) more than 30 years ago, the native role of KduD in *E. coli* has not been studied in detail. It was shown to catalyze the reversible oxidation of KDG into 2,5-diketo-3-deoxygluconate DKII with a concomitant reduction of NAD⁺ (**Fig. 4.1a**) (Hantz 1977). Putative KduD orthologs in other bacterial species are implicated in the degradation of polygalacturonate (Condemine et al. 1984). The polygalacturonate, a component of the plant cell wall, is degraded by enzymes secreted by these bacterial species into oligogalacturonates, which are then transported into the cell and further metabolized. In the last step of polygalacturonate catabolism, DKII is converted by KduD to KDG, which after phosphorylation by KDG kinase enters the Entner-Doudoroff pathway (Condemine et al. 1984). Comparative genomics analysis performed by Rodionov *et al.* (2000 and 2014) revealed that *E. coli* K-12 strain, in contrast to the polygalacturonate metabolizing bacterium *E. chrysanthemi*, lacks most of the enzymes of polygalacturonate degradation pathway (such as methyltransferases, pectate lyases, and oligogalacturonate lyases) as well as transporters for oligogalacturonates. Recently Rothe *et al.* (2013) showed that KduD is involved in the metabolism of hexuronates in *E. coli* under osmotic stress conditions. It was proposed that KduD catalyzes the reduction of tagaturonate and fructuronate (**Fig. 4.1 b**) into altronate and

mannonate, respectively, in *E. coli* cells exposed to the high osmolality environment. The *in vitro* activity of recombinant KduD as prepared here against tagaturonate and fructuronate remains to be investigated.

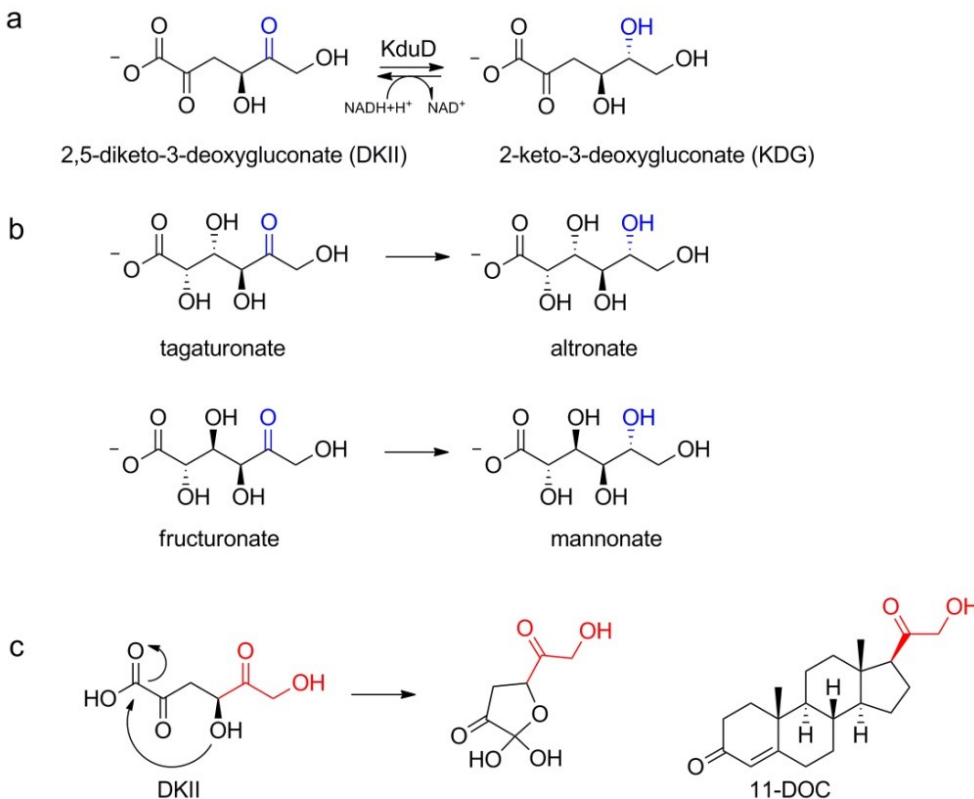


Fig. 4.1 Substrates of KduD. (a) Reversible reduction of DKII into KDG catalyzed by KduD. Carbonyl group reduced by KduD is shown in blue. (b) KduD catalyzed reduction of two novel substrates of KduD (tagaturonate and fructuronate) as proposed by Rothe *et al.* (2013). Carbonyl group that was proposed to be reduced by KduD is shown in blue. (c) Structural similarities between KduD substrates: carbohydrate derivative DKII and steroid 11-DOC. A molecule fragment that is identical in both substrates and contains carbonyl group that is reduced by KduD is shown in red.

The present study showed for the first time that KduD from *E. coli* catalyzes the reduction of 5-keto-D-gluconate and oxidation of D-gluconate. Two enzymes from *E. coli* are already known to reduce 5-keto-D-gluconate: gluconate 5-dehydrogenase (IdnO, EC 1.1.1.69) and L-idonate-5-dehydrogenase (IdnD, EC 1.1.1.264) catalyze the reversible reduction of 5-keto-D-gluconate into D-gluconate and L-idonate, respectively (Bausch et al. 1998). In the present work it was not identified which of these two compounds was the product of KduD catalyzed reduction of 5-keto-D-gluconate. Further work is required before a biological role of

KduD in this conversion can be speculated. The affinity of recombinant KduD towards D-gluconate (K_M 544.8 mM) and 5-keto-D-gluconate (K_M 184.5 mM) is significantly lower than the affinity of the enzyme to KDG (30 mM) (Hantz 1977). It is therefore unlikely that KduD is involved in the metabolism of D-gluconate and 5-keto-D-gluconate *in vivo*. Surprisingly, the K_M values of KduD of *E. coli* for the steroid substrates 11-DOC (0.230 mM) and RSS (0.190 mM) were found to be ~130 and ~158-fold lower than the K_M for its proposed natural substrate KDG (Hantz 1977). This suggests that the *in vitro* binding affinity of KduD is significantly higher for steroids than sugars, despite the fact that sugar molecules are suggested to be the native substrates for this enzyme. This raises the question: are steroid compounds indeed the natural substrates of KduD *in vivo*? *E. coli* is found in the gastrointestinal tract of the warm-blooded organisms. These organisms produce glucocorticoids and mineralocorticoids (Black 1988, Taves et al. 2011). However, the physiological concentration of the steroid hormones (in the range of 10^{-9} - 10^{-12} M) is much lower than the K_M of KduD for steroid substrates. This suggests that the 20-ketosteroid reductase activity of KduD does not convey any fitness advantage to *E. coli in vivo*.

4.4 KduD is a short-chain dehydrogenase/reductase with a broad substrate spectrum

E. coli KduD belongs to the short-chain dehydrogenase/reductase (SDR) protein superfamily. There is currently no crystal structure available for KduD from *E. coli*, but a protein sequence alignment of KduD with two microbial SDRs with available crystal structures reveals that KduD has a conserved GxxxGxG cofactor binding region and a conserved YxxxK active site motif (**Fig. 4.2**). This suggests KduD belongs to the “classical” SDR subfamily (Kavanagh et al. 2008). Classical SDRs typically have a protein length of about 250 amino acid residues, and are known to catalyze NAD(P)(H)-dependent oxidoreduction of hydroxyl/keto groups within a large array of small molecules such as steroids, alcohols, polyols, growth factors, xenobiotics and secondary metabolites (Kavanagh et al. 2008). Many SDRs were shown to have a broad spectrum of substrates (Asada et al. 2009, Powell et al. 2000, Wu et al. 2007). KduD from *E. coli*, however, appears to be a sole example of a SDR that is capable to convert both steroids and polyols (carbohydrate derivatives and 1,2-propanediol) with relatively high efficiency.

```

KduD      ----MILSAFSLGKVAVVVTGCDTGLGQGMALGLAQAGCDIVG--INIVEPTETIEQVTA 54
Ga5DH     MNQQFSLDQFSLKGGKIALVTGASYGIGFAIASAYAKAGATIVFNDINQELVDRGMAAYKA 60
20-HSD    -----MNDLSGKTVIITGGARGLGAEEARQAVAAGARVVL---ADVLDEEGAATARE 49

KduD      LGRRFLSLTADLRKIDGIPALLDRAVAEFGHIDILVNNAGLIRREDALEFSEKDWDVVMN 114
Ga5DH     AGINAHGYVCDVTDEDGIQAMVAQIESEVGIIDILVNNAGIIRRVPMIEMTAAQFRQVID 120
20-HSD    LGDAARYQHLDVTIEEDWQRVVAYAREEFGSVDGLVNNAGISTGMFLETESVERFRKVVD 109

KduD      LNIKSVFFMSQAAAKHFIAQNGGGKTIINIASMLSFQGGIRVPSYTASKSGVMGVTRLMAN 174
Ga5DH     IDLNAPFIVSKAVIPSMIKKGGH-KIINICSMSELGRETVSAYAAAKGGLKMLTKNIAS 179
20-HSD    INLTGVFIGMKTVI PAMKDAGGG-SIVNISSAAGLMGLALTSSYGASKWGV RGLSKLAAV 168
                                         *           *           *

KduD      EWAKHNIINVNAIAPGYMATNNTQQLRADEQR-----SAEILDRI PAGRWG-LPSDLMGP 227
Ga5DH     EYGEANIQCNGIGPGYIATPQTAPLRELQKDGSRHPFDQFIIAKTPAARWG-EAEDLMGP 238
20-HSD    ELGTDRI RVNSVHPGMTYTPMTAETGIRQEGE-----NYPNTPMGRVGNPEGEIAGA 220

KduD      IVFLASSASYVNGYTI AVDGGWLAR----- 253
Ga5DH     AVFLASDASN FVNGHILYVDGGILAYIGKQPEA-- 271
20-HSD    VVKLLSDTSSYVTGAELAVDGGWTTGPTVKYVMGQ 255

```

Fig. 4.2 Multiple amino acid sequence alignment of 2-dehydro-3-deoxy-D-gluconate 5-dehydrogenase (KduD) from *E. coli*, gluconate 5-dehydrogenase (Ga5DH) from *Streptomyces suis* (UniProt: A4VVQ2) and 20 β -hydroxysteroid dehydrogenase (20-HSD) from *Streptomyces hydrogenans* (UniProt: P19992). Residues conserved in all three enzymes are shown in grey background, glycine-rich cofactor binding motif is boxed, and residues forming conserved catalytic triad are marked by asterisks. Sequences were aligned using CLUSTALW.

All KduD substrates share a common alpha-hydroxy ketone functional group which is reduced by the enzyme, or in the reverse reaction, a 1,2-dihydroxy functional group that is oxidized by the enzyme. Despite that, steroids and polyols are divergent substrates, thus KduD needs to be regarded as a substrate promiscuous enzyme. Even though KduD has a higher catalytic efficiency (k_{cat}/K_M) for 20-ketosteroids in comparison to polyols (5-keto-D-gluconate and D-gluconate), its activity towards 20-ketosteroids, unlike activity towards polyols, should be considered promiscuous because it is not a part of the *E. coli* physiology. In contrast to the 20-ketosteroid reductase activity of KduD, role of which in *E. coli* is still unclear, another steroid converting enzyme from this microorganism, 7 α -hydroxysteroid dehydrogenase (7 α -HSD), was found to play an important role in the bile acid metabolism in the human intestinal tract (Ridlon et al. 2006).

The substrate spectrum of KduD is not limited to polyols and steroids. In this work, it was shown that KduD can also catalyze the reduction of doxorubicinone. Thus, this bacterial oxidoreductase could be also an attractive enzyme for the biocatalytic preparation of expensive metabolites of doxorubicin.

The high affinity of KduD to the steroid substrates 11-DOC and RSS could be explained by the structural similarities of these molecules to the proposed natural substrate DKII. The molecule fragment comprising C5-C6 of DKII can be superimposed on C20-C21 of the steroid molecule (4.1 c). In addition to that, DKII might be bound in a substrate binding pocket of KduD in a conformation that facilitates the intramolecular cyclization of this molecule (by attack of C4-OH group on C1) resulting in the formation of a five-membered lactone that resembles a cyclopentane ring of the steroid molecule (4.1 c).

4.5 Control of expression of *kduD* gene in *E. coli*

Most strains of *E. coli* do not exhibit 20-ketosteroid reductase activity against steroid substrates such as 11-DOC, despite containing a full-length *kduD* gene. In this study, the detectable 20-ketosteroid reductase activity was not observed in *E. coli* strains, including the expression strains BL21 (DE3) and UT5600 (DE3). Previous studies revealed that the transcription of *kduD* gene in *E. coli* is under control of KdgR repressor (Rodionov et al. 2000, Rodionov 2004). A unique feature of the DH5 α strain, a derivative of K-12, is the disruption of the *kdgR* gene by an insertion element (IS5 disruption), a feature that is not found in the K-12 wild type strain W3110 (Xia et al. 2011). The disruption of the *kdgR* gene leads to the constitutive expression of KduD in *E. coli* DH5 α (Xia et al. 2011). It is proposed that this constitutive overexpression is the reason why KduD-mediated steroid metabolism was detectable in DH5 α , and not in the other *E. coli* strains tested, such as *E. coli* K-12 derivative UT5600 (DE3). Interestingly, the expression strain *E. coli* BL21 (DE3) has an IS150 disruption directly in the *kduD* gene that most likely results in the expression of inactive KduD enzyme (Jeong et al. 2009), making it a good candidate for the recombinant expression and purification of untagged KduD in further studies.

This study indicates that 11-DOC is not involved in the regulation of the expression of *kduD* gene in *E. coli*. The measured specific activities of 20-ketosteroid reductase in the cell-free extracts of *E. coli* DH5 α cells that were cultured in LB medium in the presence of 11-DOC and in the absence of this steroid were similar. Moreover, the steroid reductase activity was not detected in the cell-free extracts of *E. coli* UT5600 (DE3) cells that were grown in LB medium with 11-DOC.

4.6 Biochemical properties of KduD from *E. coli*

The KduD oxidoreductase has a higher pH optimum for the oxidation of D-gluconate (pH 9.5) than for the reduction of 11-DOC (pH 7.0). A similar effect has previously been shown for the KduD of *Erwinia chrysanthemi*, where the pH optimum for the oxidation of KDG (pH 10) was significantly higher than for the reduction of DKII (7.0-7.5) (Condemine et al. 1984). The pH optimum of *E. coli* KduD for the oxidation of KDG was previously reported as 9.3 (Hantz 1977). This correlates with the pH optimum that was measured for the oxidation of D-gluconate in this study.

The K_M of KduD for NAD^+ was ~7.4-fold lower (0.285 mM) than the previously reported K_M for the native *E. coli* enzyme (2.1 mM) (Hantz 1977). This difference could be due to the different substrates used (D-gluconate rather than KDG) or due to the presence of the 6xHis tag. Using KDG as a substrate, the KduD from *E. chrysanthemi* has previously been shown to have a K_M for NAD^+ of 0.4 mM (Condemine et al. 1984), a value that closely corresponds to that found in this study for the *E. coli* KduD. The KduD oxidoreductases from *E. chrysanthemi* and *E. coli* have an amino acid sequence identity of 80%. The K_M values of KduD of *E. coli* for NADH (0.037 mM) was similar to the value previously reported for the putative ortholog from *E. chrysanthemi* (0.03 mM, determined with DKII) (Condemine et al. 1984).

As shown in this study, KduD oxidoreductase from *E. coli* like the majority of short-chain dehydrogenases/reductases does not require metal ions for the activity. Only few SDRs were reported to be dependent on the metal cofactors. One example is the R-specific alcohol dehydrogenase from *Lactobacillus brevis*, which was shown to be strictly dependent on the presence of Mg^{2+} in its active site (Niefind et al. 2003). The second example is a gluconate 5-dehydrogenase from *Streptococcus suis* serotype 2 which has a Ca^{2+} ion bound in its active site (Zhang et al. 2009). Interestingly, the pairwise amino acid alignment of KduD from *E. coli* and gluconate 5-dehydrogenase from *S. suis* revealed that KduD has four conserved amino acid residues (Ser145, Met146, Pro188, Gly189) which were shown to be involved in the coordination of Ca^{2+} in the crystal structure of gluconate 5-dehydrogenase (Zhang et al. 2009). It was proposed that Ca^{2+} ion is important for the active site formation in gluconate 5-dehydrogenase (Zhang et al. 2009). In this study, the profound stimulating effect of Ca^{2+} on the activity of KduD was not observed as well as incubation of KduD with EDTA did

not decrease enzyme's activity, therefore, it is very unlikely that Ca^{2+} ions are crucial for the active site formation of KduD.

Some SDRs such as glucose dehydrogenase from *Bacillus megaterium* are known to be unstable and loose activity at pH above 9.0 without presence of high concentration of NaCl (2 M). NaCl stabilizes the active homotetrameric form of this enzyme by preventing its dissociation into inactive monomers (Maurer and Pfleiderer 1985). In order to find out if NaCl has a stabilizing effect on KduD, the activity of this oxidoreductase was investigated in the presence of varying concentrations of NaCl. The increasing concentrations of NaCl did not increase the activity of KduD. In contrast, in the presence of high concentrations of NaCl (1-3 M) the activity of KduD oxidoreductase was completely inhibited.

The sequence analysis of KduD revealed that this oxidoreductase contains two cysteine residues (Cys18 and Cys35) at the N-terminal part of the protein. These cysteine residues are unlikely to form the intramolecular disulfide bond as predicted by the DISULFIND server (Ceroni et al. 2006). In addition, in the homology model of KduD predicted by SWISS-MODEL (Arnold et al. 2006) these cysteine residues were found to be located at the distance (12.5 Å) which does not favor the formation of the intramolecular disulfide bond (**Fig. 4.3**). Cys18 is found in the conserved GXXXGXG cofactor binding motif of KduD (**Fig. 4.2**). This cofactor binding motif is found in all classical-type SDRs (Kavanagh et al. 2008). Besides KduD, the cysteine residue within the cofactor binding region, analogous to Cys18 in KduD, is present in human 17 β -HSD type 1 (Cys10) (Nashev et al. 2013) and human 11 β -HSD type 2 (Cys90) (Atanasov et al. 2003). The cysteine residue in the cofactor binding region was shown to be essential for the activity of 11 β -HSD type 2 (Atanasov et al. 2003), and turned out to be important for the stability of 17 β -HSD type 1 (Nashev et al. 2013). The point mutation of Cys18 residue into Ser did not abolish the activity of KduD (data not shown), indicating that the Cys residue present in the cofactor binding site of KduD is not essential for the activity of KduD.

Reducing agents such as DTT, 2-ME and GSH as well as oxidizing agent GSSG had no stimulating effect on the activity of KduD. This result gave no clue about the importance of the oxidative state of the cysteine residues for the activity of KduD. In contrast, in the presence of high concentrations of these agents (10 mM DTT, 0.1-10 mM 2-ME and 7 mM of GSH or GSSG) inhibition of KduD activity was observed which was likely resulting from the

competitive binding of these molecules at the active site of KduD. Further studies are required to explain the mechanism of observed inhibition of KduD.

The activity of KduD was also inhibited in the presence of fatty acids. Lauric acid inhibited KduD oxidoreductase completely at 1 mM, whereas 50 % inhibition of KduD activity was already observed with 0.01 mM of myristic acid. Similarly, fatty acids were reported to inhibit activity of SDR, carbonyl reductase from rabbit heart (Imamura et al. 1999). Further studies are required to find out the inhibition mechanism of KduD with fatty acids.

4.7 Design of the KduD whole-cell biocatalyst using Autodisplay

4.7.1 Expression

The Autodisplay technology emerged as an attractive tool for the generation of the whole-cell biocatalysts in the Gram-negative bacteria. For an efficient expression of recombinant proteins on the surface of *E. coli* cell, Autodisplay utilizes a simple secretion mechanism of autotransporter proteins. In the typical Autodisplay construct, the gene encoding a protein of interest (a passenger) which is desired to be displayed on the surface of *E. coli* cell, is placed between two DNA sequences, encoding Sec signal peptide and translocator unit of the autotransporter protein, at 5' and 3', respectively. Thus, in the typical Autodisplay plasmid encoded fusion protein the C-terminus of a passenger protein is fused to a linker region of the translocator unit, whereas, the N-terminus is fused to the Sec signal peptide, which is normally removed by the signal peptidase during transport to the periplasm of the cell.

In this work two Autodisplay fusion proteins based on the two homologous autotransporter proteins (EhaA and AIDA-I, amino acid sequence identity 27.3 %, amino acid identity of translocator units – 36.5 %) were probed for the expression of functional KduD oxidoreductase in *E. coli*.

With AIDA-I based Autodisplay technology two fusion proteins FP and FP $\Delta\beta$ 1, which differ in the length of the linker region of AIDA-I translocator unit, were successfully expressed in various strains of *E. coli*. The surface exposure of FP in several strains of *E. coli*, such as JK321 (DE3) and BL21 ClearColi (DE3) could not be confirmed by the protease K accessibility test due to the observed damage of the outer membrane of the cells indicated by the noticeable degradation of OmpA protein. Moreover, when *E. coli* JK321 (DE3) cells overexpressing FP

protein were incubated with the specific protease IgA1, which has a cleavage site at the linker region of FP protein, specific release of passenger domain was not observed. This result suggested that either the FP protein was not expressed on the surface of *E. coli* cell or it was translocated to the surface of the cell but the IgA1 cleavage site was not accessible to the protease. In contrast to FP, the results of the protease K accessibility test indicated the surface exposure of FP $\Delta\beta$ 1 in *E. coli* JK321 (DE3) strain. Nevertheless, additional alternative methods, such as whole-cell ELISA or FACS are required to confirm the surface exposure of FP $\Delta\beta$ 1 as well as FP in *E. coli* unequivocally.

When the EhaA-based Autodisplay technology was used, the successful expression of FP1 and FP2 proteins, which differ in the length of a linker region, was achieved in several different strains of *E. coli*. The incomplete digestion of FP1 and FP2 in protease accessibility assay, suggested that only ~60 % of the overexpressed FP1 and FP2 were likely localized at the surface of the cell, whereas the rest of the recombinant protein was most probably forming the inclusion bodies within a periplasm or cytosol.

4.7.2 Activity

The expression of KduD oxidoreductase fused to the translocator unit of either AIDA-I or EhaA autotransporter using Autodisplay technology resulted in inactive enzyme. KduD oxidoreductase is a cytosolic, metal-ion independent enzyme, which does not require any additional cofactors except NADH/NAD⁺ for its activity. Thus, in contrast to membrane anchored enzymes or enzymes that require the additional prosthetic groups for the activity, KduD oxidoreductase was not assumed to be a challenging passenger for the Autodisplay technology. If the KduD oxidoreductase is able to adopt its native functional structure on the surface of *E. coli* cell, it should be able to transform its substrates, such as 11-DOC or D-gluconate, in the presence of respective cofactor, NADH or NAD⁺.

Although the crystal structure of *E. coli* KduD oxidoreductase is not available, the homology model of KduD predicted by SWISS-MODEL (Arnold et al. 2006) suggests that KduD adopts the α/β fold, which is highly conserved among other SDR enzymes (**Fig. 4.3**). The results of a gel filtration experiment suggested that the native form of KduD is a homotetramer. Many other SDRs were shown to form homotetramers (Ghosh et al. 1994, Tanaka et al. 1996, Zhang et al. 2009, Pampa et al. 2014). A recently solved crystal structure of KduD oxidoreductase from

T. thermophilus (33 % sequence identity in comparison to the KduD from *E. coli*) provides a clue of a probable tetrameric organization of KduD from *E. coli* (Pampa et al. 2014). The KduD oxidoreductase from *T. thermophilus*, likewise other SDRs, such as the 20 β -HSD from *S. hydrogenans* (Ghosh et al. 1994) and gluconate-5 dehydrogenase from *S. suis* (Zhang et al. 2009) forms a homotetramer in which each monomer is interacting with the two neighboring subunits in an inverse orientation. Several conserved structural elements are involved in oligomerization of subunits. The respective protein segments that are predicted to be involved in the oligomerization of KduD from *E. coli* are shown in **Fig. 4.3**. It was reported that the tetrameric form is crucial for the activity of 20 β -HSD from *S. hydrogenans* (Pasta et al. 1980, Carrea 1989) and was suggested to be important for the activity of KduD from *T. thermophilus* (Pampa et al. 2014). Thus, it is very likely that formation of the tetramer is also crucial for the activity of KduD from *E. coli*.

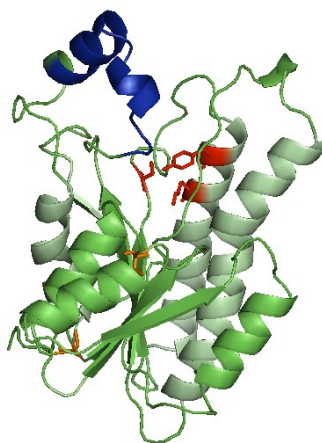


Fig. 4.3 Homology model of KduD from *E. coli* as predicted by SWISS-MODEL (Arnold et al. 2006). Following elements are depicted: predicted substrate binding loop (194-210 aa, blue), two cysteine residues Cys18 and Cys35 (orange), predicted catalytic triad Ser145, Tyr158 and Lys162 (red), structural elements predicted to be involved in subunit interaction: α -helices (106-132, 156-177 and 221-232 aa) and β -strand (243-246 aa) are depicted in pale green. The substrate binding loop, catalytic triad and structural elements involved in oligomerization were predicted based on the alignment of *E. coli* KduD protein sequence with two short-chain dehydrogenases/reductases: *E. coli* 7 α -HSD and *S. hydrogenans* 20 β -HSD for which annotated 3D structures are available (Tanaka et al. 1996, Ghosh et al. 1994).

The length of the linker region in AIDA-I based Autodisplay construct encoding FP protein should be sufficient for the proper oligomerization of the passenger domains as shown by the successful surface display of functional sorbitol dehydrogenase (SDH) from *Rhodobacter*

sphaeroides (Jose and von Schwichow 2004). The SDH from *R. sphaeroides* is a homodimeric SDR in which the dimerization of subunits occurs in the inverse orientation in a similar manner as predicted for the KduD from *E. coli*.

The linker region of the translocator unit of AIDA-I autotransporter has an extracellular β 1-domain, which was predicted to interact with the extracellular part of the β -barrel (Gawarzewski 2013, Gawarzewski et al. 2014). As shown by the autodisplay of Δ FP protein, which lacks the β 1-domain in comparison to FP, the deletion of this domain did not help to obtain the active KduD passenger. Thus, it is unlikely that the presence of this domain could somehow interfere with the assembly of the functional KduD or inhibit the activity of this enzyme on the surface of *E. coli* cell.

When KduD oxidoreductase was fused to the translocator unit of the EhaA autotransporter, the produced FP1 protein was expressed by the Autodisplay in an inactive form. Furthermore, introduction of a flexible glycine-serine spacer between the C-terminus of the KduD oxidoreductase and the N-terminus of the linker region of EhaA translocator did not produce functional FP2 protein. Taken all together, these results strongly indicate that the KduD oxidoreductase is inactive when fused to the translocator unit of either AIDA-I or EhaA autotransporter most probably not due to the suboptimal length of the linker region, which could prevent a proper assembly of a KduD tetramer.

The conserved interaction interface of oligomeric (dimeric or tetrameric) SDR enzymes involves extensive hydrophobic and ion-ion contacts between the two neighboring subunits. The presence of these hydrophobic and charged regions within the polypeptide chain of SDR subunit might complicate the correct folding of the enzyme in the absence of the assisting cytosolic chaperons. Furthermore, the protein sequence of KduD oxidoreductase contains a set of possible amyloidogenic segments, which are characteristic for the proteins that form insoluble amyloid fibrils, as predicted by the AMYLPRED tool (Frousios et al. 2009). A misfolding of KduD oxidoreductase driven by these hypothetical amyloidogenic segments might be one of the reasons why KduD is inactive when expressed on the surface of the *E. coli* cell.

The substrate binding pocket of SDR enzymes is located at the C-terminal part of the protein in the close proximity to the C-terminus. It was shown for several SDRs that the C-terminus of the

enzyme as well as the substrate-binding loop, which is localized at the C-terminal part of the enzyme, undergoes conformational changes upon binding of the substrate molecule (Hwang et al. 2013, Tanaka et al. 1996). In the Autodisplay technology used in this work, the KduD oxidoreductase was fused via C-terminus to the translocator unit of the autotransporter protein. As a result, the flexibility of the C-terminus of the KduD oxidoreductase could have been significantly restrained. Moreover, the polypeptide fused to the C-terminus of KduD oxidoreductase might have covered the substrate entrance to the active site of the enzyme. The significant reduction in activity was observed for the surface displayed dimeric SDR, SDH from *R. sphaeroides*. It was only 5 % in comparison to the free enzyme (Jose and Meyer 2007). Furthermore, the change in the substrate specificity was reported for the autodisplayed SDH in comparison to the free enzyme (Jose and von Schwichow 2004). Therefore, it should not be excluded that KduD expressed with Autodisplay technology was inactive against its classical substrates, such as 11-DOC, RSS or D-gluconate, due to the extreme change of the substrate specificity of the autodisplayed enzyme. It might as well be possible that fusion of the translocator unit of autotransporter protein to the C-terminus of KduD has a deleterious effect on oxidoreductase activity of this enzyme.

The surface of *E. coli* cell is covered by the complex LPS layer, consisting of lipids and complex polysaccharide. The carbohydrate components of LPS, such as 3-deoxy-D-manno-oct-2-ulosonic acid (KDO), D-glucose, D-mannose or D-galactose can theoretically act as the competitive inhibitors of sugars converting enzymes, such as KduD oxidoreductase from *E. coli* or SDH from *R. sphaeroides*. When KduD oxidoreductase was expressed with Autodisplay technology in several *E. coli* strains which have reduced amounts of sugars in LPS layer (F470, F515), or contain LPS made only of lipid IVa (BL21 ClearColi (DE3)), the activity of KduD was not detected. Thus, it is very unlikely that the polysaccharide of LPS layer plays a role in inactivation of KduD oxidoreductase.

5 Conclusions

The following conclusions were drawn from the current study:

- An enzyme that possesses 20-ketosteroid reductase activity in *E. coli* is encoded by the *kduD* gene.
- KduD oxidoreductase is a NADH-dependent and metal ion independent broad substrate spectrum short-chain dehydrogenase/reductase that converts steroids and carbohydrate derivatives *in vitro*.
- The expression of KduD oxidoreductase fused to the translocator unit of either AIDA-I or EhaA autotransporter protein using Autodisplay technology in *E. coli* host yields inactive KduD whole-cell biocatalyst. Thus, an Autodisplay technology is unsuitable for the design of a functional KduD whole-cell biocatalyst in *E. coli*.

6 References

- Abul-Hajj YJ, Qian XD (1986) Transformation of steroids by algae. *J Nat Prod* 49:244-8.
- Al-Awadi S, Afzal M, Oommen S (2001) Studies on *Bacillus stearothermophilus*: Part I. Transformation of progesterone to a new metabolite 9,10-seco-4-pregnene-3,9,20-trione. *J Steroid Biochem Mol Biol* 78:493-498.
- Al-Awadi S, Afzal M, Oommen S (2002) Studies on *Bacillus stearothermophilus*: Part II. Transformation of progesterone. *J Steroid Biochem Mol Biol* 82:251-256.
- Allner R, Eggstein M (1976) Untersuchungen über die Substratspezifität eine 3 α , 20 β -Hydroxysteroid: NAD⁺-oxidoreductase. *J Clin Chem Clin Biochem* 14:59-64.
- Altschul SF, Madden TL, Schäffer AA, Zhang J, Zhang Z, Miller W, Lipman DJ (1997) Gapped BLAST and PSI-BLAST: a new generation of protein database search programs. *Nucleic Acids Res* 25:3389-3402.
- Andersson S, Moghrabi N (1997) Physiology and molecular genetics of 17 β -hydroxysteroid dehydrogenases. *Steroids* 62:143-147.
- Arifuzzaman M (2006) Large-scale identification of protein-protein interaction of *Escherichia coli* K-12. *Genome Res* 16:686-691.
- Arinbasarova AY, Medentsev AG, Akimenko VK, Koshcheyenko KA, Skryabin GK (1985) Redox reactions in hydrocortisone transformation by *Arthrobacter globiformis* cells. *J Steroid Biochem* 23:307-312.
- Arnold K, Bordoli L, Kopp J, Schwede T (2006) The SWISS-MODEL workspace: a web-based environment for protein structure homology modelling. *Bioinformatics* 22:195-201.
- Arora A, Abildgaard F, Bushweller JH, Tamm LK (2001) Structure of outer membrane protein A transmembrane domain by NMR spectroscopy. *Nat Struct Mol Biol* 8:334-338.
- Asada Y, Endo S, Inoue Y, Mamiya H, Hara A, Kunishima N, Matsunaga T (2009) Biochemical and structural characterization of a short-chain dehydrogenase/reductase of *Thermus thermophilus* HB8. *Chem Biol Interact* 178:117-126.
- Askonas LJ, Ricigliano JW, Penning TM (1991) The kinetic mechanism catalysed by homogeneous rat liver 3 α -hydroxysteroid dehydrogenase. Evidence for binary and ternary dead-end complexes containing non-steroidal anti-inflammatory drugs. *Biochem J* 278:835-841.
- Atanasov AG, Tam S, Röcken JM, Baker ME, Odermatt A (2003) Inhibition of 11 β -hydroxysteroid dehydrogenase type 2 by dithiocarbamates. *Biochem Biophys Res Commun* 308:257-262.

Atta FM, Zohri AA (1995) Transformation reactions of progesterone by different species of *Streptomyces*. J Basic Microbiol 35:1–7.

Barski OA, Tipparaju SM, Bhatnagar A (2008) The aldo-keto reductase superfamily and its role in drug metabolism and detoxification. Drug Metab Rev 40:553–624.

Bausch C, Peekhaus N, Utz C, Blais T, Murray E, Lowary T, Conway T (1998) Sequence analysis of the GntII (subsidiary) system for gluconate metabolism reveals a novel pathway for L-idonic acid catabolism in *Escherichia coli*. J Bacteriol 180:3704–3710.

Begley M, Gahan CGM, Hill C (2005) The interaction between bacteria and bile. FEMS Microbiol Rev 29:625–651.

Benz I, Schmidt MA (1989) Cloning and expression of an adhesin (AIDA-I) involved in diffuse adherence of enteropathogenic *Escherichia coli*. Infect Immun 57:1506–1511.

Benz I, Schmidt MA (2011) Structures and functions of autotransporter proteins in microbial pathogens. Int J Med Microbiol 301:461–468.

Beranič N, Gobec S, Rižner TL (2011) Progestins as inhibitors of the human 20-ketosteroid reductases, AKR1C1 and AKR1C3. Chem Biol Interact 191:227–233.

Bethesda Research Labs (1986) BRL pUC host: *E. coli* DH5 α competent cells. Focus 8:9.

Betz G, Warren JC (1968) Reaction mechanism and stereospecificity of 20 β -hydroxysteroid dehydrogenase. Arch Biochem Biophys 128:745-52.

Black HE (1988) The Effects of Steroids Upon the Gastrointestinal Tract. Toxicol Pathol 16:213–222.

Blomquist CH (1973) The molecular weight and substrate specificity of 20 β -hydroxysteroid dehydrogenase from *Streptomyces hydrogenans* Arch Biochem Biophys 159:590–595.

Bokkenheuser VD, Suzuki JB, Polovsky SB, Winter J, Kelly WG (1975) Metabolism of deoxycorticosterone by human fecal flora. Appl Microbiol 30:82–90.

Bokkenheuser VD, Winter J, Morris GN, Locascio S (1986) Steroid desmolase synthesis by *Eubacterium desmolans* and *Clostridium cadavaris*. Appl Environ Microbiol 52:1153–1156.

Brändén CI, Eklund H, Nordström B, Boiwe T, Söderlund G, Zeppezauer E, Ohlsson I, Akeson A (1973) Structure of liver alcohol dehydrogenase at 2.9-Å resolution. Proc Natl Acad Sci 70:2439–2442.

Bryndova J, Klusonova P, Kucka M, Mazancova-Vagnerova K, Miksik I, Pacha J (2006) Cloning and expression of chicken 20-hydroxysteroid dehydrogenase. J Mol Endocrinol 37:453–462.

Carius Y, Christian H, Faust A, Zander U, Klink BU, Kornberger P, Kohring GW, Giffhorn F, Scheidig AJ (2010) Structural insight into substrate differentiation of the sugar-metabolizing enzyme galactitol dehydrogenase from *Rhodobacter sphaeroides* D. J Biol Chem 285:20006–20014.

Carrea G, Longhi R, Mazzola G, Pasta P, Vecchio G (1989) Denaturation by urea and renaturation of 20 β -hydroxysteroid dehydrogenase studied by high-performance size exclusion chromatography. Anal Biochem 180:181-5.

Caspi E (1956) The synthesis of 20 β ,21-dihydroxy-4-pregnen-3-one and 3,5-pregnadiene-20 β ,21-diol. J Org Chem 21:729–732.

Celik N, Webb CT, Leyton DL, Holt KE, Heinz E, Gorrell R, Kwok T, Naderer T, Strugnell RA, Speed TP, Teasdale RD, Likić VA, Lithgow T (2012) A bioinformatic strategy for the detection, classification and analysis of bacterial autotransporters. PLoS ONE 7:e43245.

Ceroni A, Passerini A, Vullo A, Frasconi P (2006) DISULFIND: a disulfide bonding state and cysteine connectivity prediction server. Nucleic Acids Res 34:W177–W181.

Chen Q, Nancarrow CD, Sweet F (1987) Isolation of 3 β , 20 α -hydroxysteroid oxidoreductase from sheep fetal blood. Steroids 49:477–496.

Chen Q, Rosik LO, Nancarrow CD, Sweet F (1989) Fetal lamb 3 β ,20 α -hydroxysteroid oxidoreductase: dual activity at the same active site examined by affinity labeling with 16 α -(bromo[2'-¹⁴C] acetoxy)progesterone. Biochemistry 28:8856–8863.

Chetrite GS, Thole HH, Philippe JC, Pasqualini JR (2004) Dydrogesterone (Duphaston®) and its 20-dihydro-derivative as selective estrogen enzyme modulators in human breast cancer cell lines. Effect on sulfatase and on 17 β -hydroxysteroid dehydrogenase (17 β -HSD) activity. Anticancer Res 24:1433–1438.

Choudhry S, Halos S, Krischenowski D, Schmeda-Hirschmann G (1993) Two new 17 α -hydroxyprogesterone transformation products from *Nocardia* DSM 43298. World J Microbiol Biotechnol 9:56–58.

Condemine G, Hugouvieux-Cotte-Pattat N and Robert-Baudouy J (1984) An enzyme in the pectinolytic pathway of *Erwinia chrysanthemi*: 2-keto-3-deoxygluconate oxidoreductase. J Gen Microbiol 130:2839-2844.

Cremonesi P, Carrea G, Ferrara L, Antonini E (1975) Enzymatic preparation of 20 β -hydroxysteroids in a two-phase system. Biotechnol Bioeng 17:1101–1108.

Csaba G (2012) The hormonal system of the unicellular *Tetrahymena*: A review with evolutionary aspects. Acta Microbiol Immunol Hung 59:131–156.

Davies HG, Gartenmann TCC, Leaver J, Roberts SE, Turner MK (1986) Reduction of 7-chlorobicyclo[3.2.0]hept-2-en-6-ones catalyzed by 3 α , 20 β -hydroxysteroid dehydrogenase. *Tetrahedron Lett* 27:1093-1094.

De Amici M, De Micheli C, Molteni G, Pitre D, Carrea G, Riva S, Spezia S, Zetta L (1991) Chemoenzymic synthesis of the eight stereoisomeric muscarines. *J Org Chem* 56:67–72.

De Rosa M, Gambacorta A, Sodano G, Trabucco A (1981) Transformation of progesterone by *Caldariella acidophila*, an extreme thermophilic bacterium. *Experientia* 37:541–542.

Desvaux M, Hébraud M, Talon R, Henderson IR (2009) Secretion and subcellular localizations of bacterial proteins: a semantic awareness issue. *Trends Microbiol* 17:139–145.

Detzel C, Maas R, Tubeleviciute A, Jose J (2013) Autodisplay of nitrilase from *Klebsiella pneumoniae* and whole-cell degradation of oxynil herbicides and related compounds. *Appl Microbiol Biotechnol* 97:4887–4896.

Donova MV (2007) Transformation of steroids by Actinobacteria: A review. *Appl Biochem Microbiol* 43:1–14.

Donova MV, Egorova OV (2012) Microbial steroid transformations: current state and prospects. *Appl Microbiol Biotechnol* 94:1423–1447.

Dubendorf JW, Studier FW (1991) Controlling basal expression in an inducible T7 expression system by blocking the target T7 promoter with *lac* repressor. *J Mol Biol* 219:45–59.

Dufort I, Rheault P, Huang XF, Soucy P, Luu-The V (1999) Characteristics of a highly labile human type 5 17 β -hydroxysteroid dehydrogenase. *Endocrinology*. 1999 Feb;140:568-74.

Earhart CF, Lundrigan M, Pickett CL, Pierce JR (1979) *Escherichia coli* K-12 mutants that lack major outer membrane protein a. *FEMS Microbiol Lett* 6(5):277-280

Edwards DP (2005) Regulation of signal transduction pathways by estrogen and progesterone. *Annu Rev Physiol* 67:335–376.

Elkins CA, Mullis LB (2006) Mammalian steroid hormones are substrates for the major RND- and MFS-type tripartite multidrug efflux pumps of *Escherichia coli*. *J Bacteriol* 188:1191-5.

Endo S, Arai Y, Hara A, Kitade Y, Bunai Y, El-Kabbani O, Matsunaga T (2013) Substrate specificity and inhibitor sensitivity of rabbit 20 α -hydroxysteroid dehydrogenase. *Biol Pharm Bull* 36:1514-8.

Endo S, Matsunaga T, Arai Y, Ikari A, Tajima K, El-Kabbani O, Yamano S, Hara A, Kitade Y (2014) Cloning and characterization of four rabbit aldo-keto reductases featuring broad substrate specificity for xenobiotic

and endogenous carbonyl compounds: relationship with multiple forms of drug ketone reductases. *Drug Metab Dispos* 42:803–812.

Faramarzi MA, Adrangi S, Yazdi MT (2008) Microalgal biotransformation of steroids. *J Phycol* 44:27–37.

Faramarzi MA, Yazdi MT, Shafiee A, Zarrini G (2002) Microbial transformation of hydrocortisone by *Acremonium strictum* PTCC 5282. *Steroids* 67:869–872.

Faramarzi MA, Tabatabaei Yazdi M, Amini M, Zarrini G, Shafiee A (2003) Microbial hydroxylation of progesterone with *Acremonium strictum*. *FEMS Microbiol Lett* 222:183–186.

Favia AD, Nobeli I, Glaser F, Thornton JM (2008) Molecular docking for substrate identification: the short-chain dehydrogenases/reductases. *J Mol Biol* 375:855–874.

Fernandes P, Cruz A, Angelova B, Pinheiro H., Cabral JM. (2003) Microbial conversion of steroid compounds: recent developments. *Enzyme Microb Technol* 32:688–705.

Filling C, Berndt KD, Benach J, Knapp S, Prozorovski T, Nordling E, Ladenstein R, Jörnvall H, Oppermann U (2002) Critical residues for structure and catalysis in short-chain dehydrogenases/reductases. *J Biol Chem* 277:25677–25684.

Filloux A (2013) The rise of the type VI secretion system. *F1000prime Rep.* 5:52.

Fokina VV, Sukhodolskaya GV, Baskunov BP, Turchin KF, Grinenko GS, Donova MV (2003) Microbial conversion of pregna-4,9(11)-diene-17 α ,21-diol-3,20-dione acetates by *Nocardioides simplex* VKM Ac-2033D. *Steroids* 68:415–421.

Friedrich T, Scheide D (2000) The respiratory complex I of bacteria, archaea and eukarya and its module common with membrane-bound multisubunit hydrogenases. *FEBS Lett* 479:1-5.

Frousios KK, Iconomidou VA, Karletidi CM, Hamodrakas SJ (2009) Amyloidogenic determinants are usually not buried. *BMC Struct Biol* 9:44.

García-Gómez E, González-Pedrajo B, Camacho-Arroyo I (2013) Role of sex steroid hormones in bacterial-host interactions. *BioMed Res Int* 2013:1–10.

Garcia-Rodriguez LK, Korobova YN, Medvedeva IV, Shner VF, Messinova OV (1978) Microbiological hydroxylation of steroids. III. Study of side reactions occurring in the hydroxylation of cortexolone in cultures of *Cunningamella blakesleeana* and *Curvularia lunata*. *Pharm Chem J* 12:1199–1201.

Gawarzewski I (2013) Determination of the AIDA-I beta-barrel crystal structure: getting the clue to the autotransporter secretion pathway. Dissertation, Heinrich-Heine University Duesseldorf.

Gawarzewski I, Smits SH, Schmitt L, Jose J (2013) Structural comparison of the transport units of type V secretion systems. *Biol Chem* 394:1385–1398.

Gawarzewski I, DiMaio F, Winterer E, Tschapek B, Smits SH, Jose J, Schmitt L (2014) Crystal structure of the transport unit of the autotransporter adhesin involved in diffuse adherence from *Escherichia coli*. *J Struct Biol*, DOI: 10.1016/j.jsb.2014.05.003.

Ghosh D, Pletnev VZ, Zhu DW, Wawrzak Z, Duax WL, Pangborn W, Labrie F, Lin SX (1995) Structure of human estrogenic 17 beta-hydroxysteroid dehydrogenase at 2.20 Å resolution. *Structure* 3:503-13.

Ghosh D, Vihko P (2001) Molecular mechanisms of estrogen recognition and 17-keto reduction by human 17β-hydroxysteroid dehydrogenase 1. *Chem Biol Interact* 130:637–650.

Ghosh D, Wawrzak Z, Weeks CM, Duax WL, Erman M (1994) The refined three-dimensional structure of 3α,20β-hydroxysteroid dehydrogenase and possible roles of the residues conserved in short-chain dehydrogenases. *Structure* 2:629-40.

Ghosh D, Weeks CM, Grochulski P, Duax WL, Erman M, Rimsay RL, Orr JC (1991) Three-dimensional structure of holo 3α,20β-hydroxysteroid dehydrogenase: a member of a short-chain dehydrogenase family. *Proc Natl Acad Sci U S A* 88:10064-8.

Gibb W, Jeffery J (1973) 3-Hydroxy steroid dehydrogenase activities of cortisone reductase. *Biochem J* 135:881–888.

Godula K (2006) C-H bond functionalization in complex organic synthesis. *Science* 312:67–72.

Göndös G, Gera L, Bartók M, Orr JC (1989) Homogeneous and heterogeneous catalytic asymmetric reactions: II. Asymmetric hydrogenation of steroid ketones. *J Organomet Chem* 373:365–375.

Göndös G, Orr JC (1982) Stereoselective and regioselective reduction of steroid ketones by potassium tri(*R,S*-butyl) borohydride. *J Chem Soc Chem Commun* 1239–1240.

Han CA, Monder C (1982) Asymmetric reduction of 20-steroidal ketone: synthesis of corticosteroid derivatives containing the 20α-ol-21-al side chain. *J Org Chem* 47:1580–1584.

Han CA, Monder C (1983) Asymmetric reduction of steroidal 20-ketones: Chemical synthesis of corticosteroid derivatives containing the 20α, 21-diol and 17α, 20α, 21-triol side chains. *Steroids* 42:619–626.

Handel S (2003) Entwicklung eines Ganzzell-Biokatalysators durch Autodisplay von Sorbitol Dehydrogenase. Dissertation. University of Saarland.

Hannemann F, Bernhardt R, Jose J (2007) Biocatalytic synthesis of 4-pregnen-20,21-diol-3-one, a selective inhibitor of human 5α-reductase type II. *J Enzyme Inhib Med Chem* 22:570–576.

Hantke K (1981) Regulation of ferric iron transport in *Escherichia coli* K-12: isolation of a constitutive mutant. *Mol Gen Genet* MGG 182:288–292.

Hantz O (1977) La voie dégradative secondaire du 2-céto-3-desoxygluconate chez *Escherichia coli*. Oxydation enzymatique du 2-céto-3-desoxygluconate. Dissertation, Claude Bernard University.

Hara A, Nakagawa M, Taniguchi H, Sawada H (1989) 3(20) α -Hydroxysteroid dehydrogenase activity of monkey liver indanol dehydrogenase. *J Biochem (Tokyo)* 106:900–903.

HersHKovitz L, Beuschlein F, Klammer S, Krup M, Weinstein Y (2007) Adrenal 20 α -hydroxysteroid dehydrogenase in the mouse catabolizes progesterone and 11-deoxycorticosterone and is restricted to the X-zone. *Endocrinology* 148:976–988.

Hickman J, Ashwell G (1960) Uronic acid metabolism in bacteria II. Purification and properties of D-altronic acid and D-mannonic acid dehydrogenases in *Escherichia coli*. *J Biol Chem* 235:1566–1570.

Hoffmann F, Maser E (2007) Carbonyl reductases and pluripotent hydroxysteroid dehydrogenases of the short-chain dehydrogenase/reductase superfamily. *Drug Metab Rev* 39:87-144.

Hogg JA (1992) Steroids, the steroid community, and Upjohn in perspective: a profile of innovation. *Steroids* 57:593–616.

Horinouchi M, Hayashi T, Yamamoto T, Kudo T (2003) A new bacterial steroid degradation gene cluster in *Comamonas testosteroni* TA441 which consists of aromatic-compound degradation genes for seco-steroids and 3-ketosteroid dehydrogenase genes. *Appl Environ Microbiol* 69:4421–4430.

Hubener HJ, Sahrholz FG, Schmidt-Thome J, Nesemann G, Junk R (1959) 20 β -Hydroxy-Steroid-Dehydrogenase, ein neues kristallines Enzym. *Biochim Biophys Acta* 35:270-272.

Hwang CC, Chang YH, Lee HJ, Wang TP, Su YM, Chen HW, Liang PH (2013) The catalytic roles of P185 and T188 and substrate-binding loop flexibility in 3 α -hydroxysteroid dehydrogenase/carbonyl reductase from *Comamonas testosteroni*. *PLoS ONE* 8:e63594.

Imamura Y, Migita T, Anraku M, Otagiri M (1999) Inhibition of rabbit heart carbonyl reductase by fatty acids. *Biol Pharm Bull* 22:731-3.

Inazu A, Sato K, Nakayama T, Deyashiki Y, Hara A, Nozawa Y (1994) Purification and characterization of a novel dimeric 20 α -hydroxysteroid dehydrogenase from *Tetrahymena pyriformis*. *Biochem J* 297:195–200.

Ismail W, Chiang YR (2011) Oxidic and anoxic metabolism of steroids by bacteria. *J Bioremed Biodegrad* S1:001.

IUPAC commission on the nomenclature of organic chemistry (CNOC) and IUPAC-IUB commission on biochemical nomenclature (CBN). The nomenclature of steroids. Revised tentative rules (1969). *Eur J Biochem* 10:1-19.

Yagen B, Gallili GE, Mateles RI (1978) Progesterone biotransformation by plant cell suspension cultures. *Appl Environ Microbiol* 36:213–216.

Yamazawa R, Nakajima Y, Mushiake K, Yoshimoto T, Ito K (2011) Crystal structure of serine dehydrogenase from *Escherichia coli*: important role of the C-terminal region for closed-complex formation. *J Biochem* 149:701–712.

Yazdi M (2004) Biotransformation of hydrocortisone by a natural isolate of *Nostoc muscorum*. *Phytochemistry* 65:2205–2209.

Yoshimoto T, Higashi H, Kanatani A, Lin XS, Nagai H, Oyama H, Kurazono K, Tsuru D (1991) Cloning and sequencing of the 7 α -hydroxysteroid dehydrogenase gene from *Escherichia coli* HB101 and characterization of the expressed enzyme. *J Bacteriol* 173:2173–2179.

Jayasekara WS, Yonezawa T, Ishida M, Yamanouchi K, Nishihara M (2004) Molecular cloning of goat 20 α -hydroxysteroid dehydrogenase cDNA. *J Reprod Dev* 50:323-31.

Jarabak J, Adams JA, Williams-Ashman HG, Talalay P (1962) Purification of a 17 β -hydroxysteroid dehydrogenase of human placenta and studies on its transhydrogenase function. *J Biol Chem* 237:345–357.

Jeong H, Barbe V, Lee CH, Vallenet D, Yu DS, Choi SH, Couloux A, Lee SW, Yoon SH, Cattolico L, Hur CG, Park HS, Ségurens B, Kim SC, Oh TK, Lenski RE, Studier FW, Daegelen P, Kim JF (2009) Genome Sequences of *Escherichia coli* B strains REL606 and BL21(DE3). *J Mol Biol* 394:644–652.

Jez J, Bennett M, Schlegel B, Lewis M, Penning T (1997) Comparative anatomy of the aldo–keto reductase superfamily. *Biochem J* 326:625–636.

Jin Y, Penning TM (2007) Aldo-keto reductases and bioactivation/detoxication. *Annu Rev Pharmacol Toxicol* 47:263–292.

Jörnvall H, Persson M, Jeffery J (1981) Alcohol and polyol dehydrogenases are both divided into two protein types, and structural properties cross-relate the different enzyme activities within each type. *Proc Natl Acad Sci* 78:4226–4230.

Jose J, Bernhardt R, Hannemann F (2001) Functional display of active bovine adrenodoxin on the surface of *E. coli* by chemical incorporation of the [2Fe-2S] cluster. *ChemBiochem* 2:695-701.

Jose J, Krämer J, Klauser T, Pohlner J, Meyer TF (1996) Absence of periplasmic DsbA oxidoreductase facilitates export of cysteine-containing passenger proteins to the *Escherichia coli* cell surface via the Iga beta autotransporter pathway. *Gene* 178:107-10.

Jose J, Maas RM, Teese MG (2012) Autodisplay of enzymes—molecular basis and perspectives. *J Biotechnol* 161:92–103.

Jose J, Meyer TF (2007) The autodisplay story, from discovery to biotechnical and biomedical applications. *Microbiol Mol Biol Rev* 71:600–619.

Jose J, von Schwichow S (2004) Autodisplay of active sorbitol dehydrogenase (SDH) yields a whole cell biocatalyst for the synthesis of rare sugars. *ChemBioChem* 5:491–499.

Kallberg Y, Oppermann U, Jörnvall H, Persson B (2002) Short-chain dehydrogenases/reductases (SDRs): coenzyme-based functional assignments in completed genomes. *Eur J Biochem* 269:4409–4417.

Kallberg Y, Oppermann U, Persson B (2010) Classification of the short-chain dehydrogenase/reductase superfamily using hidden Markov models. *FEBS J* 277:2375–2386.

Kavanagh KL, Jörnvall H, Persson B, Oppermann U (2008) Medium- and short-chain dehydrogenase/reductase gene and protein families: the SDR superfamily: functional and structural diversity within a family of metabolic and regulatory enzymes. *Cell Mol Life Sci* 65:3895–3906.

Kavanagh KL, Klimacek M, Nidetzky B, Wilson DK (2002) The structure of apo and holo forms of xylose reductase, a dimeric aldo-keto reductase from *Candida tenuis*. *Biochemistry* 41:8785–8795.

Khersonsky O, Malitsky S, Rogachev I, Tawfik DS (2011) Role of chemistry versus substrate binding in recruiting promiscuous enzyme functions. *Biochemistry* 50:2683–2690.

Kisiela M, Skarka A, Ebert B, Maser E (2012) Hydroxysteroid dehydrogenases (HSDs) in bacteria – a bioinformatic perspective. *J Steroid Biochem Mol Biol* 129:31–46.

Konieczny MP, Benz I, Hollinderbäumer B, Beinke C, Niederweis M, Schmidt MA (2001) Modular organization of the AIDA autotransporter translocator: the N-terminal β 1-domain is surface-exposed and stabilizes the transmembrane β 2-domain. *Antonie Van Leeuwenhoek* 80:19–34.

Kozma E, Brown E, Ellis EM, Laphorn AJ (2002) The crystal structure of rat liver AKR7A1. A dimeric member of the aldo-keto reductase superfamily. *J Biol Chem* 277:16285–16293.

Krafft AE, Hylemon PB (1989) Purification and characterization of a novel form of 20 α -hydroxysteroid dehydrogenase from *Clostridium scindens*. *J Bacteriol* 171:2925–2932.

Krafft AE, Winter J, Bokkenheuser VD, Hylemon PB (1987) Cofactor requirements of steroid-17-20-desmolase and 20 α -hydroxysteroid dehydrogenase activities in cell extracts of *Clostridium scindens*. J Steroid Biochem 28:49-54.

Kranen E, Detzel C, Weber T, Jose J (2014) Autodisplay for the co-expression of lipase and foldase on the surface of *E. coli*: washing with designer bugs. Microb Cell Fact 13:19.

Lacy WR, Washenick KJ, Cook RG, Dunbar BS (1993) Molecular cloning and expression of an abundant rabbit ovarian protein with 20 α -hydroxysteroid dehydrogenase activity. Mol Endocrinol Baltim Md 7:58–66.

Leyton DL, Rossiter AE, Henderson IR (2012) From self sufficiency to dependence: mechanisms and factors important for autotransporter biogenesis. Nat Rev Microbiol 10:213–225.

Leu YL, Wang PH, Shiao MS, Ismail W, Chiang YR (2011) A novel testosterone catabolic pathway in bacteria. J Bacteriol 193:4447–4455.

Li C, Zhu Y, Benz I, Schmidt MA, Chen W, Mulchandani A, Qiao C (2008) Presentation of functional organophosphorus hydrolase fusions on the surface of *Escherichia coli* by the AIDA-I autotransporter pathway. Biotechnol Bioeng 99:485–490.

Ma H, Penning T (1999) Characterization of homogeneous recombinant rat ovarian 20 α -hydroxysteroid dehydrogenase: fluorescent properties and inhibition profile. Biochem J 341:853–859.

Madyastha KM (1994) Preparatively useful transformations of steroids and morphine alkaloids by *Mucor piriformis*. Proc Indian Acad Sci 106:1203-1212.

Mahato SB, Banerjee S (1986) Metabolism of 17-hydroxyprogesterone by a *Bacillus* species. Biochem J 239:473–476.

Mahato SB, Banerjee S, Podder S (1988) Oxidative side-chain and ring fission of pregnanes by *Arthrobacter simplex*. Biochem J 255:769–774.

Mao J, Duan RW, Zhong L, Gibori G, Azhar S (1997) Expression, purification and characterization of the rat luteal 20 α -hydroxysteroid dehydrogenase. Endocrinology 138:182-90.

Maser E (1995) Xenobiotic carbonyl reduction and physiological steroid oxidoreduction: The pluripotency of several hydroxysteroid dehydrogenases. Biochem Pharmacol 49:421–440.

Maurer E, Pfeleiderer G (1985) Reversible pH-induced dissociation of glucose dehydrogenase from *Bacillus megaterium* I. Conformational and functional changes. Biochim Biophys Acta 827:381–388.

Maurer J, Jose J, Meyer TF (1997) Autodisplay: one-component system for efficient surface display and release of soluble recombinant proteins from *Escherichia coli*. J Bacteriol 179:794–804.

Maurer J, Jose J, Meyer TF (1999) Characterization of the essential transport function of the AIDA-I autotransporter and evidence supporting structural predictions. *J Bacteriol* 181:7014–7020.

Merino E, Barrientos A, Rodríguez J, Naharro G, Luengo JM, Olivera ER (2013) Isolation of cholesterol- and deoxycholate-degrading bacteria from soil samples: evidence of a common pathway. *Appl Microbiol Biotechnol* 97:891–904.

Mindnich RD, Penning TM (2009) Aldo-keto reductase (AKR) superfamily: genomics and annotation. *Hum Genomics* 3:362-70.

Miura R, Shiota K, Noda K, Yagi S, Ogawa T, Takahashi M (1994) Molecular cloning of cDNA for rat ovarian 20 α -hydroxysteroid dehydrogenase (HSD1). *Biochem J* 299:561–567.

Mukherjee A, Mahato SB (1984) Metabolism of steroid acetates by *Streptomyces albus*. *J Steroid Biochem* 20:781–784.

Nagahama Y (1997) 17 α ,20 β -dihydroxy-4-pregnen-3-one, a maturation-inducing hormone in fish oocytes: mechanisms of synthesis and action. *Steroids* 62:190-6.

Naidansuren P, Park CW, Kim SH, Nanjidsuren T, Park JJ, Yun SJ, Sim BW, Hwang S, Kang MH, Ryu BY, Hwang SY, Yoon JT, Yamanouchi K, Min KS (2011) Molecular characterization of bovine placental and ovarian 20 α -hydroxysteroid dehydrogenase. *Reproduction* 142:723–731.

Nakajin S, Ohno S, Shinoda M (1988) 20 β -hydroxysteroid dehydrogenase of neonatal pig testis: purification and some properties. *J Biochem* 104:565–569.

Nashev LG, Atanasov AG, Baker ME, Odermatt A (2013) Cysteine-10 on 17 β -hydroxysteroid dehydrogenase 1 has stabilizing interactions in the cofactor binding region and renders sensitivity to sulfhydryl modifying chemicals. *Int J Cell Biol* 2013:1–8.

Naumann JM, Messinger J, Bureik M (2010) Human 20 α -hydroxysteroid dehydrogenase (AKR1C1)-dependent biotransformation with recombinant fission yeast *Schizosaccharomyces pombe*. *J Biotechnol* 150:161–170.

Naumann JM, Zöllner A, Drăgan CA, Messinger J, Adam J, Bureik M (2011) Biotechnological production of 20 α -dihydroprogesterone at pilot scale. *Appl Biochem Biotechnol* 165:190–203.

Niefind K, Müller J, Riebel B, Hummel W, Schomburg D (2003) The crystal structure of R-specific alcohol dehydrogenase from *Lactobacillus brevis* suggests the structural basis of its metal dependency. *J Mol Biol* 327:317–328.

Nobeli I, Favia AD, Thornton JM (2009) Protein promiscuity and its implications for biotechnology. *Nat Biotechnol* 27:157–167.

Noda K, Shiota K, Takahashi M (1991) Purification and characterization of rat ovarian 20 α -hydroxysteroid dehydrogenase. *Biochim Biophys Acta* 1079:112–118.

Norymberski JK, Woods GF (1955) Partial reduction of steroid hormones and related substances. *J Chem Soc* 3426–3430.

Ohno S, Nakajin S, Shinoda M (1991) 20 β -hydroxysteroid dehydrogenase of neonatal pig testis: 3 α / β -hydroxysteroid dehydrogenase activities catalyzed by highly purified enzyme. *J Steroid Biochem Mol Biol* 38:787-94.

Oppermann U (2007) Carbonyl Reductases: The complex relationships of mammalian carbonyl- and quinone-reducing enzymes and their role in physiology. *Annu Rev Pharmacol Toxicol* 47:293–322.

Oppermann U, Filling C, Hult M, Shafqat N, Wu X, Lindh M, Shafqat J, Nordling E, Kallberg Y, Persson B (2003) Short-chain dehydrogenases/reductases (SDR): the 2002 update. *Chem Biol Interact* 143:247–253.

Pajic T, Vitas M, Zigon D, Pavko A, Kelly SL, Komel R (1999) Biotransformation of steroids by the fission yeast *Schizosaccharomyces pombe*. *Yeast* 15:639–645.

Pakkianathan BC, Singh NK, Krishnan M, König S (2012) A proteomic view on the developmental transfer of homologous 30 kDa lipoproteins from peripheral fat body to perivisceral fat body via hemolymph in silkworm, *Bombyx mori*. *BMC Biochem* 13:5.

Pampa KJ, Lokanath NK, Kunishima N, Rai RV (2014) The first crystal structure of NAD-dependent 3-dehydro-2-deoxy-D-gluconate dehydrogenase from *Thermus thermophilus* HB8. *Acta Crystallogr D Biol Crystallogr* 70:994–1004.

Pasta P, Carrea G, Longhi R, Antonini E (1980) Renaturation and urea-induced denaturation of 20 β -hydroxysteroid dehydrogenase studied in solution and in the immobilized state. *Biochim Biophys Acta* 616:143–152.

Pedruzzi I, Rivoire C, Auchincloss AH, Coudert E, Keller G, de Castro E, Baratin D, Cuche BA, Bougueleret L, Poux S, Redaschi N, Xenarios I, Bridge A, UniProt Consortium (2013) HAMAP in 2013, new developments in the protein family classification and annotation system. *Nucleic Acids Res* 41:D584–D589.

Penning TM (1997) Molecular endocrinology of hydroxysteroid dehydrogenases. *Endocr Rev* 18:281–305.

Penning TM (2003) Hydroxysteroid dehydrogenases and pre-receptor regulation of steroid hormone action. *Hum Reprod Update* 9:193–205.

Penning TM (2004) Introduction and overview of the aldo-keto reductase superfamily. In: Penning TM, Petrash JM Aldo-keto reductases and toxicant metabolism, ACS Symposium Series, American Chemical Society, Washington, DC, 865: 3-20.

Persson B, Hedlund J, Jörnvall H (2008) Medium- and short-chain dehydrogenase/reductase gene and protein families: The MDR superfamily. *Cell Mol Life Sci* 65:3879–3894.

Persson B, Kallberg Y, Bray JE, Bruford E, Dellaporta SL, Favia AD, Duarte RG, Jörnvall H, Kavanagh KL, Kedishvili N, Kisiela M, Maser E, Mindnich R, Orchard S, Penning TM, Thornton JM, Adamski J, Oppermann U (2009) The SDR (short-chain dehydrogenase/reductase and related enzymes) nomenclature initiative. *Chem Biol Interact* 178:94–98.

Persson B, Kallberg Y, Oppermann U, Jörnvall H (2003) Coenzyme-based functional assignments of short-chain dehydrogenases/reductases (SDRs). *Chem Biol Interact* 143-144:271-8.

Persson B, Krook M, Jörnvall H (1991) Characteristics of short-chain alcohol dehydrogenases and related enzymes. *Eur J Biochem* 200:537–543.

Petersen TN, Brunak S, von Heijne G, Nielsen H (2011) SignalP 4.0: discriminating signal peptides from transmembrane regions. *Nat Methods* 8:785–786.

Peterson DH, Murray HC, Eppstein SH, Reineke LM, Weintraub A, Meister PD, Leigh HM (1952) Microbiological transformations of steroids. I. Introduction of oxygen at carbon-11 of progesterone. *J Am Chem Soc* 74:5933–5936.

Plesiat P, Nikaido H (1992) Outer membranes of Gram-negative bacteria are permeable to steroid probes. *Mol Microbiol* 6:1323-33.

Pohlner J, Halter R, Beyreuther K, Meyer TF (1987) Gene structure and extracellular secretion of *Neisseria gonorrhoeae* IgA protease. *Nature* 325:458-62.

Pollio A, Pinto G, Della Greca M, de Maio A, Fiorentino A, Previtiera L (1994) Progesterone bioconversion by microalgal cultures. *Phytochemistry* 37:1269–1272.

Poos GI (1955) The C-20 epimers of 4-pregnene-11 β ,17 α ,20-triol-3-one. *J Am Chem Soc* 77: 4932–4935.

Powell AJ, Read JA, Banfield MJ, Gunn-Moore F, Yan SD, Lustbader J, Stern AR, Stern DM, Brady RL (2000) Recognition of structurally diverse substrates by type II 3-hydroxyacyl-CoA dehydrogenase (HADH II)/amyloid- β binding alcohol dehydrogenase (ABAD). *J Mol Biol* 303:311–327.

Prabha V, Ohri M (2006) Review: bacterial transformations of bile acids. *World J Microbiol Biotechnol* 22:191–196.

Preiss J, Ashwell G (1963) Polygalacturonic acid metabolism in bacteria. II. Formation and metabolism of 3-deoxy-D-glycero-2,5-hexodiulosonic acid. *J Biol Chem* 238:1577-83.

Puranen T, Poutanen M, Ghosh D, Vihko P, Vihko R (1997) Characterization of structural and functional properties of human 17 β -hydroxysteroid dehydrogenase type 1 using recombinant enzymes and site-directed mutagenesis. *Mol Endocrinol* 11:77-86.

Purdy GE, Fisher CR, Payne SM (2007) IcsA surface presentation in *Shigella flexneri* requires the periplasmic chaperones DegP, Skp, and SurA. *J Bacteriol* 189:5566-5573.

Rath A, Glibowicka M, Nadeau VG, Chen G, Deber CM (2009) Detergent binding explains anomalous SDS-PAGE migration of membrane proteins. *Proc Natl Acad Sci* 106:1760-1765.

Restaino OF, Marseglia M, Castro C, Diana P, Forni P, Parrilli M, Rosa M, Schiraldi C (2014) Biotechnological transformation of hydrocortisone to 16 α -hydroxy hydrocortisone by *Streptomyces roseochromogenes*. *Appl Microbiol Biotechnol* 98:1291-1299.

Ridlon JM, Kang DJ, Hylemon PB (2006) Bile salt biotransformations by human intestinal bacteria. *J Lipid Res* 47:241-259.

Ridlon JM, Ikegawa S, Alves JMP, Zhou B, Kobayashi A, Iida T, Mitamura K, Tanabe G, Serrano M, De Guzman A, Cooper P, Buck GA, Hylemon PB (2013) *Clostridium scindens*: a human gut microbe with a high potential to convert glucocorticoids into androgens. *J Lipid Res* 54:2437-2449.

Ried G, Koebnik R, Hindennach I, Mutschler B, Henning U (1994) Membrane topology and assembly of the outer membrane protein OmpA of *Escherichia coli* K-12. *Mol Gen Genet* MGG 243:127-135.

Rimsay RL, Murphy GW, Martin CJ, Orr JC (1988) The 20 α -hydroxysteroid dehydrogenase of *Streptomyces hydrogenans*. *Eur J Biochem* 174:437-442.

Rodionov DA, Gelfand MS, Hugouvieux-Cotte-Pattat N (2004) Comparative genomics of the KdgR regulon in *Erwinia chrysanthemi* 3937 and other gamma-proteobacteria. *Microbiology* 150:3571-3590.

Rodionov DA, Mironov AA, Rakhmaninova AB, Gelfand MS (2000) Transcriptional regulation of transport and utilization systems for hexuronides, hexuronates and hexonates in gamma purple bacteria. *Mol Microbiol* 38:673-683.

Rossiter AE, Leyton DL, Tveen-Jensen K, Browning DF, Sevastyanovich Y, Knowles TJ, Nichols KB, Cunningham AF, Overduin M, Schembri MA, Henderson IR (2011) The essential β -barrel assembly machinery complex components BamD and BamA are required for autotransporter biogenesis. *J Bacteriol* 193:4250-4253.

Rothe M, Alpert C, Loh G, Blaut M (2013) Novel insights into *E. coli*'s hexuronate metabolism: KduI facilitates the conversion of galacturonate and glucuronate under osmotic stress conditions. PLoS ONE 8:e56906.

Sato F, Takagi Y, Shikita M (1972) 20 α -Hydroxysteroid dehydrogenase of porcine testes: purification and properties. J Biol Chem 247:815–823.

Schlegel BP, Jez JM, Penning TM (1998) Mutagenesis of 3 α -hydroxysteroid dehydrogenase reveals a "push-pull" mechanism for proton transfer in aldo-keto reductases. Biochemistry 37:3538-48.

Schmidt G, Jann B, Jann K (1970) Immunochemistry of R lipopolysaccharides of *Escherichia coli*. Eur J Biochem 16:382–392.

Schneider KH, Jäkel G, Hoffmann R, Giffhorn F (1995) Enzyme evolution in *Rhodobacter sphaeroides*: selection of a mutant expressing a new galactitol dehydrogenase and biochemical characterization of the enzyme. Microbiology 141:1865-73.

Schultheiss E, Paar C, Schwab H, Jose J (2002) Functional esterase surface display by the autotransporter pathway in *Escherichia coli* J Mol Catal B Enzym 18:89–97.

Schultheiss E, Weiss S, Winterer E, Maas R, Heinzle E, Jose J (2008) Esterase autodisplay: enzyme engineering and whole-cell activity determination in microplates with pH sensors. Appl Environ Microbiol 74:4782–4791.

Schumacher SD, Hannemann F, Teese MG, Bernhardt R, Jose J (2012) Autodisplay of functional CYP106A2 in *Escherichia coli*. J Biotechnol 161:104–112.

Schumacher SD, Jose J (2012) Expression of active human P450 3A4 on the cell surface of *Escherichia coli* by Autodisplay. J Biotechnol 161:113–120.

Sedlacek L, Smith LL (1988) Biotransformations of steroids. Crit Rev Biotechnol 7:187–236.

Shah SA, Sultan S, Hassan NB, Muhammad FK, Faridz MA, Hussain FB, Hussain M, Adnan HS (2013) Biotransformation of 17 α -ethynyl substituted steroidal drugs with microbial and plant cell cultures: a review. Steroids 78:1312–1324.

Sharaf MA, Sweet F (1982) Dual activity at an enzyme active site: 3 β ,20 α -hydroxysteroid oxidoreductase from fetal blood. Biochemistry 21:4615–4620.

Sreenivasulu G, Senthilkumaran B (2009) New evidences for the involvement of 20 β -hydroxysteroid dehydrogenase in final oocyte maturation of air-breathing catfish. Gen Comp Endocrinol 163:259-69.

Staels B, Fonseca VA (2009) Bile Acids and Metabolic Regulation: Mechanisms and clinical responses to bile acid sequestration. Diabetes Care 32:S237–S245.

Stastná E, Cerný I, Pouzar V, Chodounská H (2010) Stereoselectivity of sodium borohydride reduction of saturated steroidal ketones utilizing conditions of Luche reduction. *Steroids* 75:721-5.

Strickler RC, Tobias B, Covey DF (1981) Human placental 17 β -estradiol dehydrogenase and 20 α -hydroxysteroid dehydrogenase. Two activities at a single enzyme active site. *J Biol Chem* 256:316–321.

Studier FW, Moffatt BA (1986) Use of bacteriophage T7 RNA polymerase to direct selective high-level expression of cloned genes. *J Mol Biol* 189:113-30.

Sweet F, Samant BR (1980) Bifunctional enzyme activity at the same active site: study of 3 α and 20 β activity by affinity alkylation of 3 α ,20 β -hydroxysteroid dehydrogenase with 17-(bromoacetoxy) steroids. *Biochemistry* 19:978–986.

Tanaka M, Nakajin S, Kobayashi D, Fukada S, Guan G, Todo T, Senthilkumaran B, Nagahama Y (2002) Teleost ovarian carbonyl reductase-like 20 β -hydroxysteroid dehydrogenase: potential role in the production of maturation-inducing hormone during final oocyte maturation. *Biol Reprod* 66:1498-504.

Tanaka M, Ohno S, Adachi S, Nakajin S, Shinoda M, Nagahama Y (1992) Pig testicular 20 β -hydroxysteroid dehydrogenase exhibits carbonyl reductase-like structure and activity. cDNA cloning of pig testicular 20 β -hydroxysteroid dehydrogenase. *J Biol Chem* 267:13451–13455.

Tanaka N, Nonaka T, Tanabe T, Yoshimoto T, Tsuru D, Mitsui Y (1996) Crystal structures of the binary and ternary complexes of 7 α -hydroxysteroid dehydrogenase from *Escherichia coli*. *Biochemistry* 35:7715-30.

Taves MD, Gomez-Sanchez CE, Soma KK (2011) Extra-adrenal glucocorticoids and mineralocorticoids: evidence for local synthesis, regulation, and function. *AJP Endocrinol Metab* 301:E11–E24.

Templeton JF, Kumar VS, Marat K, Kim RS, Labella FS, Cote D (1987) New hydroxylation products of progesterone with *Mucor griseocyanus*. *J Nat Prod* 50:463–467.

Terada T, Sugihara Y, Nakamura K, Mizobuchi H, Maeda M (2003) Further characterization of Chinese hamster carbonyl reductases (CHCRs). *Chem Biol Interact* 143:373–381.

Terada T, Sugihara Y, Nakamura K, Sato R, Sakuma S, Fujimoto Y, Fujita T, Inazu N, Maeda M (2001) Characterization of multiple Chinese hamster carbonyl reductases. *Chem Biol Interact* 130:847–861.

Thatcher DR (1980) The complete amino acid sequence of three alcohol dehydrogenase alleloenzymes (*Adh*^{N-11}, *Adh*^S and *Adh*^{UF}) from the fruitfly *Drosophila melanogaster*. *Biochem J* 187:875–883.

Tokarz J, Mindnich R, Norton W, Möller G, Hrabé de Angelis M, Adamski J (2012) Discovery of a novel enzyme mediating glucocorticoid catabolism in fish: 20 β -hydroxysteroid dehydrogenase type 2. *Mol Cell Endocrinol* 349:202–213.

Tokarz J, Norton W, Möller G, Hrabé de Angelis M, Adamski J (2013) Zebrafish 20 β -hydroxysteroid dehydrogenase type 2 is important for glucocorticoid catabolism in stress response. PLoS One 8:e54851.

Ueda S, Oda M, Imamura S, Ohnishi M (2004) Transient-phase kinetic studies on the nucleotide binding to 3 α -hydroxysteroid dehydrogenase from *Pseudomonas sp.* B-0831 using fluorescence stopped-flow procedures. Eur J Biochem 271:1774–1780.

Van Ulsen P, Rahman SU, Jong WSP, Daleke-Schermerhorn MH, Luirink J (2013) Type V secretion: From biogenesis to biotechnology. Biochim Biophys Acta: DOI: 10.1016/j.bbamcr.2013.11.006.

Wadhwa L, Smith KE (2000) Progesterone side-chain cleavage by *Bacillus sphaericus*. FEMS Microbiol Lett 192:179–183.

Warren JC, Murdock GL, Ma Y, Goodman SR, Zimmer WE (1993) Molecular cloning of testicular 20 α -hydroxysteroid dehydrogenase: identity with aldose reductase. Biochemistry 32:1401–1406.

Wells TJ, Sherlock O, Rivas L, Mahajan A, Beatson SA, Torpdahl M, Webb RI, Allsopp LP, Gobius KS, Gally DL, Schembri MA (2008) EhaA is a novel autotransporter protein of enterohemorrhagic *Escherichia coli* O157:H7 that contributes to adhesion and biofilm formation. Environ Microbiol 10:589–604.

Westman EL, Canova MJ, Radhi IJ, Koteva K, Kireeva I, Waglechner N, Wright GD (2012) Bacterial inactivation of the anticancer drug doxorubicin. Chem Biol 19:1255–1264.

Wiest WG, Wilcox RB (1961) Purification and properties of rat ovarian 20 α -hydroxysteroid dehydrogenase. J Biol Chem 236:2425-8.

Wilson MR, Gallimore WA, Reese PB (1999) Steroid transformations with *Fusarium oxysporum* var. *cubense* and *Colletotrichum musae*. Steroids 64:834-43.

Winter J, Cerone-McLernon A, O'Rourke S, Ponticorvo L, Bokkenheuser VD (1982) Formation of 20 β -dihydrosteroids by anaerobic bacteria. J Steroid Biochem 17:661-7.

Winter J, Morris GN, O'Rourke-Locascio S, Bokkenheuser VD, Mosbach EH, Cohen BI, Hylemon PB (1984) Mode of action of steroid desmolase and reductases synthesized by *Clostridium scindens* (formerly *Clostridium* strain 19). J Lipid Res 25:1124–1131.

Wintergalen N, Thole HH, Galla HJ, Schlegel W (1995) Prostaglandin-E2 9-reductase from corpus luteum of pseudopregnant rabbit is a member of the aldo-keto reductase superfamily featuring 20 α -hydroxysteroid dehydrogenase activity. Eur J Biochem 234:264–270.

Wu L, Einstein M, Geissler WM, Chan HK, Elliston KO, Andersson S (1993) Expression cloning and characterization of human 17 β -hydroxysteroid dehydrogenase type 2, a microsomal enzyme possessing 20 α -hydroxysteroid dehydrogenase activity. *J Biol Chem* 268:12964–12969.

Wu X, Knapp S, Stamp A, Stammers DK, Jörnvall H, Dellaporta SL, Oppermann U (2007) Biochemical characterization of TASSELSEED 2, an essential plant short-chain dehydrogenase/reductase with broad spectrum activities. *FEBS J* 274:1172–1182.

Xia XX, Qian ZG, Lee SY (2011) Comparative proteomic and genetic analyses reveal unidentified mutations in *Escherichia coli* XL1-Blue and DH5 α : proteomic and genetic analyses reveal unknown mutations. *FEMS Microbiol Lett* 314:119–124.

Zhang Y, Dufort I, Rheault P, Luu-The V (2000) Characterization of a human 20 α -hydroxysteroid dehydrogenase. *J Mol Endocrinol* 25:221-8.

Zhang Q, Peng H, Gao F, Liu Y, Cheng H, Thompson J, Gao GF (2009) Structural insight into the catalytic mechanism of gluconate 5-dehydrogenase from *Streptococcus suis*: Crystal structures of the substrate-free and quaternary complex enzymes. *Protein Sci* 18:294–303.

Zhang W, Cui L, Wu M, Zhang R, Xie L, Wang H (2011) Transformation of prednisolone to a 20 β -hydroxy prednisolone compound by *Streptomyces roseochromogenes* TS79. *Appl Microbiol Biotechnol* 92:727–735.

7 Supplemental material

7.1 Abbreviations

11-DOC – 11-deoxycorticosterone

2-ME – 2-mercaptoethanol

AKR – aldo-keto reductase

bla – a gene encoding beta-lactamase

BSA – bovine serum albumin

CtxB – cholera toxin B subunit

DKII – 2,5-diketo-3-deoxygluconate

DTT – dithiothreitol

hdhA – gene encoding 7 α -hydroxysteroid dehydrogenase (HdhA)

HPLC – high-performance liquid chromatography

IPTG – isopropyl β -D-1-thiogalactopyranoside

KDG – 2-keto-3-deoxy-D-gluconate

KduD – 2-dehydro-3-deoxy-D-gluconate 5-dehydrogenase

kduD – a gene encoding 2-dehydro-3-deoxy-D-gluconate 5-dehydrogenase (KduD)

lacI – gene encoding lactose operon repressor

LC-MS – liquid chromatography-mass spectrometry

MW – molecular weight

ORF – open reading frame

PMSF – phenylmethylsulfonylfluorid

RBS – ribosomal binding site

RSS – 11-deoxycortisol

SDR – short-chain dehydrogenase/reductase

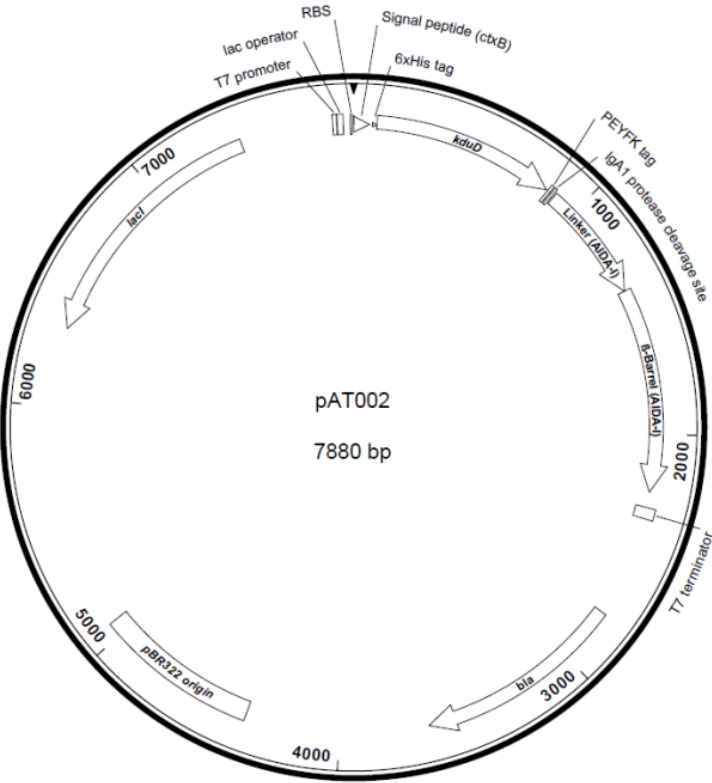
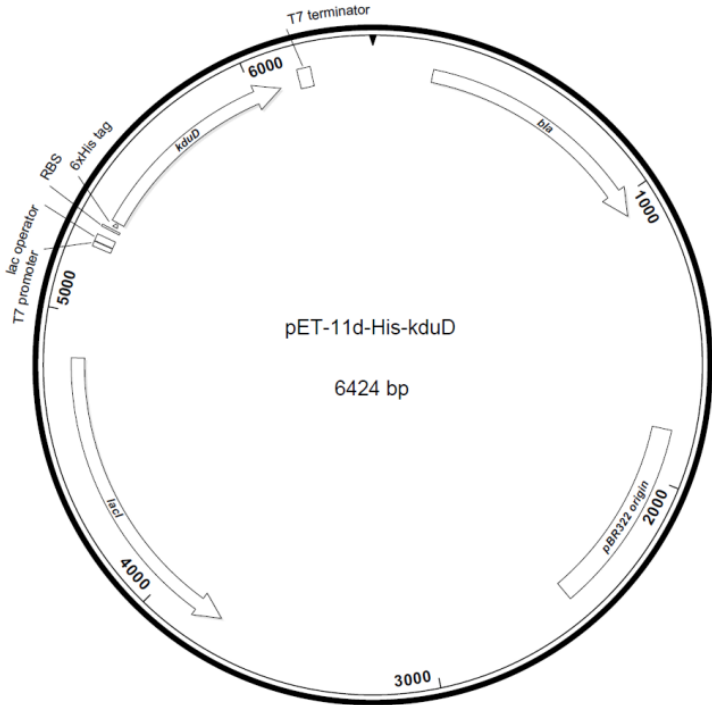
SDS-PAGE - sodium dodecyl sulfate polyacrylamide gel electrophoresis

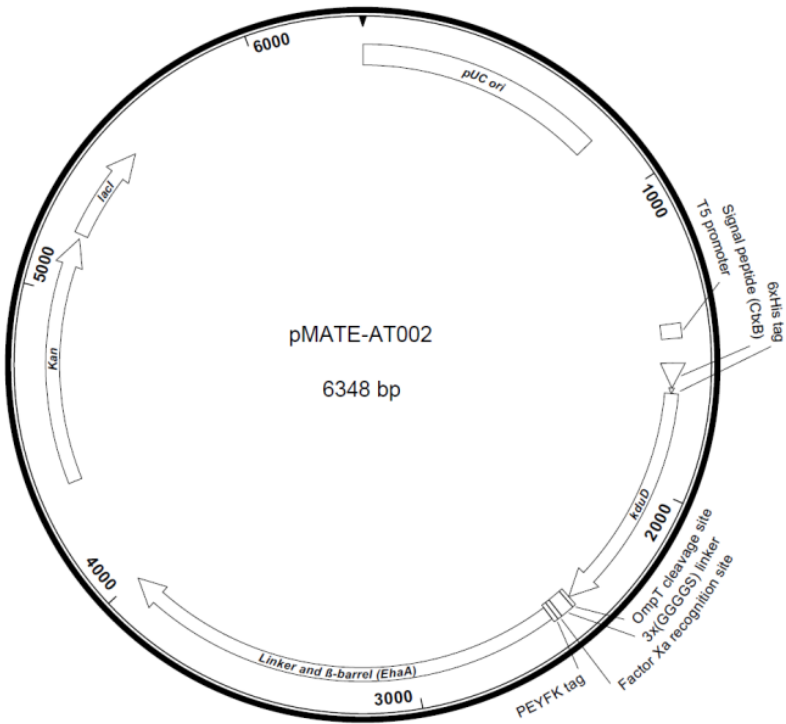
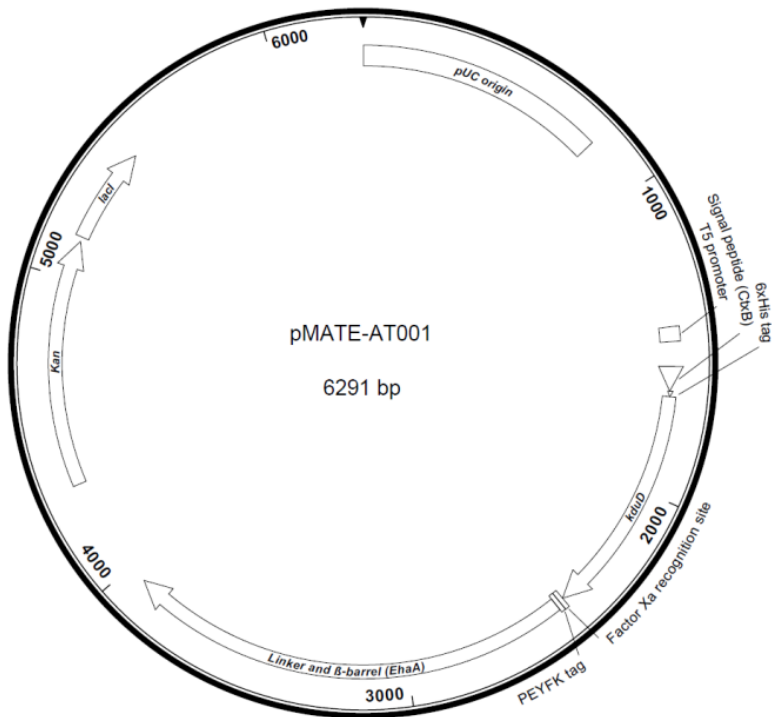
uxuB – gene encoding D-mannonate oxidoreductase (UxuB)

ydbC – gene encoding putative oxidoreductase YdbC

FPLC - fast protein liquid chromatography

7.2 Plasmid maps





7.3 Supplementary tables

Table S1. List of proteins identified by mass spectrometry in the sample of partially purified 20-ketosteroid reductase of *E. coli* DH5 α .

UniProt ID	Protein name
P0A6F9	10 kDa chaperonin
P0A6Y8	Chaperone protein DnaK
P0A850	Trigger factor
P0A6M8	Elongation factor G
P0A6P1	Elongation factor Ts
P0CE47	Elongation factor Tu 1
P0CE48	Elongation factor Tu 2
P23909	DNA mismatch repair protein mutS
P0AB78	Putative 8-amino-7-oxononanoate synthase/2-amino-3-ketobutyrate coenzyme A ligase
P0A825	Pyridoxal-phosphate-dependent serine hydroxymethyltransferase
P27302	Transketolase 1
P33570	Transketolase 2
P0A9D8	2,3,4,5-tetrahydropyridine-2,6-dicarboxylate N-succinyltransferase
P0AB77	2-amino-3-ketobutyrate coenzyme A ligase
P0A953	3-oxoacyl-[acyl-carrier-protein] synthase 1
P37647	2-dehydro-3-deoxygluconokinase
P0A6A3	Acetate kinase
P0A6F3	Glycerol kinase
P0A763	Nucleoside diphosphate kinase
P76015	PTS-dependent dihydroxyacetone kinase, dihydroxyacetone-binding subunit dhaK
P00509	Aspartate aminotransferase
P06986	Histidinol-phosphate aminotransferase
P23721	Phosphoserine aminotransferase
P0ABP8	Purine nucleoside phosphorylase deoD-type
P12758	Uridine phosphorylase
P37769	2-dehydro-3-deoxy-D-gluconate 5-dehydrogenase
P0AET8	7-alpha-hydroxysteroid dehydrogenase
P39160	D-mannonate oxidoreductase
P00350	6-phosphogluconate dehydrogenase, decarboxylating
P0A9Q9	Aspartate-semialdehyde dehydrogenase
Q46856	Alcohol dehydrogenase YqhD
P06715	Glutathione reductase
P69924	Ribonucleoside-diphosphate reductase 1 subunit beta
P0AE08	Alkyl hydroperoxide reductase subunit C
Q46938	4-deoxy-L-threo-5-hexosulose-uronate ketol-isomerase
P0A6T1	Glucose-6-phosphate isomerase
P0AG07	Ribulose-phosphate 3-epimerase
P0A858	Triosephosphate isomerase
P09147	UDP-glucose 4-epimerase
P0A8G3	Uronate isomerase
P0A9L3	FKBP-type 22 kDa peptidyl-prolyl cis-trans isomerase
P25516	Aconitate hydratase 1
P36683	Aconitate hydratase 2
P0A6L2	Dihydrodipicolinate synthase
P37759	dTDP-glucose 4,6-dehydratase 1
P0AB71	Fructose-bisphosphate aldolase class 2
P0A9G6	Isocitrate lyase
P24215	Mannonate dehydratase

P0A853	Tryptophanase
P69908	Glutamate decarboxylase alpha
P69910	Glutamate decarboxylase beta
P0ABK5	Cysteine synthase A
P0A7D4	Adenylosuccinate synthetase
P21888	Cysteine-tRNA ligase
P0A7A9	Inorganic pyrophosphatase
P15288	Cytosol non-specific dipeptidase
P04825	Aminopeptidase N
P27298	Oligopeptidase A
P21165	Xaa-Pro dipeptidase

8 Scientific output

Publications

Tubeleviciute A, Teese MG, Jose J (2014) *Escherichia coli kduD* encodes an oxidoreductase that converts both sugar and steroid substrates. *Appl Microbiol Biotechnol* 98(12):5471-5485.

Detzel C, Maas R, Tubeleviciute A, Jose J (2013) Autodisplay of nitrilase from *Klebsiella pneumonia* and whole-cell degradation of oxynil herbicides and related compounds. *Appl Microbiol Biotechnol* 97(11):4887-96.

Patent application

Tubeleviciute A, Teese MG, Jose J (2012) An enzyme for the reduction of keto groups and oxidation of hydroxyl groups in steroids and carbohydrate derivatives. Submitted to European Patent Office (application no. 12006199.9).

Poster presentations

Tubeleviciute A, Teese M, Jose J (2013) An oxidoreductase from *Escherichia coli* catalyzes the regioselective reduction of mineralocorticoids and glucocorticoids *in vitro*. DPhG annual conference, Freiburg, MC.59.

Tubeleviciute A, Teese MG, Jose J (2012) Discovery of a novel bacterial steroid dehydrogenase. 6th International Congress on Biocatalysis, Hamburg, P383

Poster presentations and oral presentations within CLIB-Graduate Cluster

4th Annual Retreat of the CLIB-Graduate Cluster, Lünen, Germany (2013): Autodisplay of an *E. coli* steroid C-20 dehydrogenase for regioselective reduction of steroidal compounds (oral presentation and poster presentation).

3rd Annual CLIB-Graduate Cluster Retreat, Bergisch Gladbach, Germany (2012): Autodisplay of an *E. coli* steroid C-20 dehydrogenase for regioselective reduction of steroidal compounds (poster presentation).

2nd internal CLIB-GC Retreat HHU Düsseldorf, Mülheim an der Ruhr, Germany (2012):
Discovery of *Escherichia coli* steroid C-20 dehydrogenase (oral presentation).

2nd Annual CLIB-Graduate Cluster Retreat, Bonn, Germany (2011): Autodisplay of an *E. coli*
steroid C-20 dehydrogenase for regioselective reduction of steroidal compounds (poster
presentation).

1st internal CLIB-GC Retreat HHU Düsseldorf, Mülheim an der Ruhr, Germany (2011):
Autodisplay of an *E. coli* steroid C-20 dehydrogenase for regioselective reduction of steroidal
compounds (oral presentation).

Acknowledgements

The current work was accomplished in the frame of the program of the CLIB-Graduate Cluster Industrial Biotechnology and was financed by the Ministry of Innovation of North Rhine-Westphalia.

I would like to show my gratitude to people who supported me during my PhD studies:

- Prof. Dr. Joachim Jose for an opportunity to join his research group in 2010, for an interesting topic of my PhD thesis, scientific advices, and support
- My PhD project advisors Prof. Dr. Jörg Pietruszka and Prof. Dr. Holger Gohlke
- Dr. Mark Teese for a great mentoring and motivating scientific discussions
- CLIB Graduate School coordinators Dr. Sonja Meyer zu Berstenhorst and Dr. Jessica Hilbig for the nice welcome in Germany, support and help during doctorate studies
- Scholars of CLIB Graduate School for the great time spent in retreats, support, and exchange of international experiences
- Prof. Dr. Simone König, Dr. Jörk Fabian and the research group of Prof. Dr. Peter Proksch for the help with mass spectrometry
- My supervised students who helped me on this project: Juliane Brüggem, Katharina Penner, Johanna Piernikarczyk, Verena Brokamp, Sally Lüßing, Imke Meißner, and Ann-Kathrin Ridder
- My colleagues from HHU Düsseldorf and WWU Münster: Prof. Dr. Samer Haidar, Dr. Dagmar Aichele, Dr. Min Park, Dr. Andreas Gratz, Dr. Claas Hundsdörfer, Dr. Tanja Völker, Dr. Michael Goblirsch, Dr. Iris Gawarzewski, Dr. Sarah Thömmes, Dr. Claudia Reicheneder, Dr. Stephanie Schumacher, Dr. Eva Kranen, Dr. Christian Detzel, Dr. Alia Al-Sarraj, Dr. Karsten Rose, Dr. Tatjana Brossette, Dr. Beate Walter, Petra Nordlohne, Irina Altendorfer, Andre Bollacke, Bertan Bopp, Achim Braukmann, Indra Finger, Cristina Gisbert, Christian Nienberg, Isabelle Olschewski, Uta Meidt, Zoya Orlando, Paul Quehl, Ilka Rauch, Kristina Lang, Annika Meyers, Winni Scherlitzki, Catharina Holtschulte, Jana Stracke, Claudia Lindemann, Thorsten Saenger, Shanna Sichwart, Jan Schüürmann, Philipp Tozakidis, Tamara Tahan, and Wilhelmine Weckenbrock.
- My family and my friend Ümit Aydin for your support and care during the time when I was writing my thesis.